Assessing the Use of Geochemical Modelling in Supporting Mine Site Remediation

Marlese Elizabeth Fairgray

July 2019

A thesis submitted in partial fulfilment of the requirements for the degree of Doctor of Philosophy

If my people, which are called by my name,
shall humble themselves and pray; …
then I will hear from heaven, and will forgive their sins
and will heal their land

2 Chronicles 7:14

Abstract

The extraction of minerals through mining activities often results in the generation of acid mine drainage (AMD) due to the exposure of sulfidic minerals to oxygen and water at a rate faster than would have occurred naturally. In order to operate at best practice, the effects of mining and AMD on the natural environment need to be mitigated or prevented. In this thesis water and sediment chemistry of three historic mine sites at various stages in the post-closure process in New Zealand were assessed. Changes in water and sediment chemistry due to the precipitation of Fe, Mn and Al precipitates and the adsorption of trace elements to freshly formed precipitates were modelled in PHREEQC. The modelled results were compared to measured results in order to evaluate the effectiveness of PHREEQC in modelling post-remediation water and sediment chemistry at mining sites.

The remedial works carried out at Tui Mine have resulted in an increased pH and decreased concentration of dissolved trace elements (Fe, Cu, Pb, Zn, Cd, As) in Tui Stream and in Tunakohoia Stream. The remedial works have been more effective in mitigating the effects of AMD in Tui Stream than in Tunakohoia Stream due to the difference in the pre-remediation pH of these two streams. PHREEQC was used to show that the concentrations of Zn^{2+} and Cd^{2+} remain above ecologically relevant guidelines even after remedial works have been completed. PHREEQC was also used to show that the addition of limestone to these streams is unlikely to reduce the concentration of these two elements by either formation of mineral precipitates or adsorption to Fe (oxy)hydroxide precipitates to a concentration suitable for supporting healthy ecosystem function in the streams draining Tui Mine. The use of Tui Mine to assess the reliability of PHREEQC modelling found that it is possible to use PHREEQC to reliably model a system where the elements of concern are cationic metals such as Cu, Pb, Zn and Cd. In fact, it is possible that the remediation works carried out between 2010 and 2013 could have achieved a better outcome had PHREEQC been used to model the post-remediation water chemistry expected in the Tui and Tunakohoia Streams following the addition of limestone to the tailings dam and mine adits at Tui Mine. However, adsorption of Pb to HFO was underestimated and adsorption of As to HFO was overestimated by PHREEQC.

Historic mining operations to produce mercury, the surfacing of roads with aggregate containing Hg and As and the presence of sinter outcrops containing Hg and As have resulted in elevated concentrations of sediment-bound Hg and As, above ISQG-high guidelines, in the streams draining the Puhipuhi area. This has led to depauperate macroinvertebrate communities at the sites higher up in this catchment where sediment-bound Fe and Hg is greatest. Additionally, this has also lead to the bioaccumulation of Hg in eels which is of concern to human health, should these be consumed as part of a regular diet and the cultural value of eel harvesting for consumption. PHREEQC could be used to reliably model the speciation of cationic trace elements (Cu, Zn and Ni), the formation of Fe (oxy)hydroxides and the consequent adsorption of Cu, Zn and Ni to Fe (oxy)hydroxides. However, these elements were not the elements of concern in this catchment. PHREEQC could not be used to reliably model the speciation of dissolved Hg and the formation of methylmercury, the form of Hg which bioaccumulates, because the

process of methylation is outside the capacity of the PHREEQC model. It could not be used to reliably predict the adsorption of Hg and As to Fe (oxy)hydroxides and it could not be used to model the stability of HgS found within the quartz sinter matrix as this mineral consists of components not able to be measured in natural waters and therefore cannot be input into PHREEQC. Arsenic was associated with residual FeS_2 for which the stability again could not be reliably predicted in PHREEQC due to S^{2-} not being present in natural waters and therefore it was not able to be input into PHREEQC. Therefore, it is not recommended that PHREEQC be used to model systems where Hg and As are the elements of most environmental concern as the thermodynamic data required by PHREEQC to make accurate predictions of the behaviour of these elements is not yet known and the adsorption of As to HFO is not reliably predicted by PHREEQC.

The water chemistry of Cannel Creek prior to and following the installation of a sulfate-reducing bioreactor treatment system at Bellvue Mine was measured. The treatment system resulted in >80% less Fe, Al and Ni and a 66% less of Zn on average in Cannel Creek downstream of the AMD discharge point. Additionally, the treatment system increased the pH of AMD entering Cannel Creek sufficiently that Fe- and Al-rich precipitates were able to form and adsorption of trace elements to HFO became favourable. PHREEQC was used to develop a model predicting water chemistry in Cannel Creek following the installation of the treatment system and was validated by comparing the predicted water quality to measured water quality. The model that was developed predicted water quality in the upper reaches of the stream very well but the measured concentrations of dissolved Fe and Al deviated from those predicted in the lower reaches of the stream as there had not been sufficient time for the Fe (oxy)hydroxysulfates and Al oxides to precipitate out of solution in between sampling sites.

PHREEQC is a geochemical modelling program suitable for predicting the speciation of trace elements in AMD solutions and the attenuation of trace elements by mineral formation and adsorption to HFO. However, there are certain situations where PHREEQC cannot reliably predict trace element attenuation quantifiably. These include adsorption of dissolved Cd to HFO where solution pH is in the range of greatest change for the Cu adsorption edge, adsorption of Pb and As to HFO and methylation of Hg. In these situations PHREEQC models can provide guidance as to what processes are likely to occur but should not be depended on to set remediation targets for water quality.

Deputy Vice-chancellor's Office

Postgraduage Office

UNIVERSITY OF CANTERBURY
Te Whare Wānanga o Waitaha
CHRISTCHURCH NEW ZEALAND

Co-Authorship form

This form is to accompany the submission of any thesis that contains research reported in co-authored work that has been published, accepted for publication, or submitted for publication. A copy of this form should be included for each co-authored work that is included in the thesis. Completed forms should be included at the front (after the thesis abstract) of each copy of the thesis submitted for examination and library deposit.

Please indicate the chapter/section/pages of this thesis that are extracted from co-authored work and provide details of the publication or submission from the extract comes:

Partially reproduced in Chapter3

Fairgray, M., Webster-Brown, J. and Pope, J. (Submitted 2019). Testing geochemically modelled predictions of trace element toxicity and bioavailability at a rehabilitated mine site Mine Water and the Environment. Mine Water and the Environment.

Fairgray, M. and J. Webster-Brown (2017). Release of toxic trace elements from contaminated stream sediment at Tui Mine, Te Aroha, New Zealand. Proceedings of the 2017 AusIMM New Zealand Branch Annual Conference. Christchurch, New Zealand, AusIMM. Pp 8.

Fairgray, M., Webster-Brown, J., Harding, J. and Waters, S. (2016). Geochemical Modelling of Metal Toxicity in the Tui Mine Catchment, Te Aroha, NZ. Proceedings of the 2016 AusIMM New Zealand Branch Annual Conference. Wellington, New Zealand. AusIMM. Pp 9.

Please detail the nature and extent (%) of contribution by the candidate:

The candidate carried out data collection (90%), data analyses (90%) and led manuscript writing (95%). Co-authors were involved in conception of the research idea, accompanied the candidate on data collection field trips, contributed data from manuscripts independent of the candidates work and were involved in manuscript edition.

Certification by Co-authors:
If there is more than one co-author then a single co-author can sign on behalf of all.
The undersigned certifies that:

- The above statement correctly reflects the nature and extent of the PhD candidate's contribution to this co-authored work.
- In cases where the candidate was the lead author of the co-authored work he or she wrote the text.

Name: Jenny Webster-Brown

Signature:  Date: 25/07/19

Acknowledgements

This work would not have been possible without the input and support from many people, whom I will attempt to thank in the next two pages.

Firstly, to my supervisors Prof. Jenny Webster-Brown and Dr. James Pope.

Jenny: Thank you for taking a chance on me in awarding me this PhD project, thank you for your support and guidance as I made my way through this project, thank you for your scribbled comments all through the written work I gave you. I appreciate the time you spent reading through my brain dumps and providing constructive feedback on how to pull out something meaningful. Thank you for inspiring me to enter the world of aqueous geochemistry.

James: Thank you for letting me join the CRL team "one day a week" and setting me up with a workspace at the CRL Christchurch office. Thank you for taking the time to read through my work and for giving me the head-space to think critically about the significance of this work.

Next, thank you to the people who helped with this work:

- Technical staff at both Lincoln University and the University of Canterbury (John Revell, Roger Cresswell, Lynne Clucas, Rob Stainthorpe and Mike Flaws) who assisted with lab work and completed HPIC, ICP-OES, ICP-MS and SEM-EDS analysis on samples.
- Phil White from Panda Geosciences who carried out XRD analysis on samples.
- Dave Trumm from CRL Energy Ltd. who was instrumental in getting the remedial work at Bellvue Mine to go ahead and provided water chemistry data to supplement my own data.
- All those who accompanied me on field trips (Jon Harding, Justin Pomeranz, Kevin Simon, Rose Gregersen, Katrina Hansen, Kerry Webster, Aaron Dutton, Kerry Gordan, Emma MacKenzie, Abbie Ryan). Special thanks to Aaron Dutton and Kerry Gordan from CRL Energy Ltd. who completed stream flow analysis at Bellvue Mine while I collected my water samples. Emma, sorry about the injury sustained whilst on a field trip with me!
- Emma Mackenzie and Anna Henderson who completed macroinvertebrate identification on samples collected from Puhipuhi Mine.

Thank you to the Ministry of Business, Innovation and Employment (MBIE) for the funding to carry out this research through contract CRLE 1403 – The Mine Lifecycle Environment Guide from the Endeavour Fund.

Thank you to Pauline Clarkin from the Iwi Advisory Group at Tui Mine and Allan Halliday from Ngati Hau at Puhipuhi for their cultural advice and for being the face of the communities who will benefit from this work around

mine site remediation. I hope with all my heart that you are able to harvest tuna and mahinga kai from your streams in the future.

Thank you to all the people who provided me with emotional support during the undertaking of this PhD.

- Staff and thesis students at Waterways and Gateway Antarctica for contributing to the warm, friendly atmosphere on Level 7 of the Biology Building at UC and the Soil and Water Building at LU. Special shout out to Suellen Knopick for being my Waterways "mom". Thank you for your encouragement and advice over the last 4 years. Thank you for being my sugar mama and organising social events for us. Thank you for giving me tough love and letting me know when it's time to "put on my big girl pants". Thank you for listening to me and providing me with support when the dark clouds rolled in.
- Staff at CRL Energy Christchurch and Greymouth. Thank you for making me feel welcome at your office space and for letting me borrow equipment for field work. I especially enjoyed the Friday afternoon drinks and hallway cricket with you guys.
- My flatmates and friends from Latimer Church, Grace Vineyard and Riccarton Toastmasters. Thank you for coming on this 4 year journey with me and seeing me through to the end of it.

Finally, thank you to my family for getting me to this place.

Dad: Thank you for instilling in me a curiosity and a passion for the scientific world.

Mum: Thank you for teaching me to read and write, and more recently for your financial support, care packages and for being just a phone call away.

Laura: Thank you for your encouragement and support.

Elle: Thank you for joining me in the post-graduate life. Thank you for all the phone calls discussing how great freshwater systems are and how important it is to have healthy aquatic ecosystems that people can enjoy and utilise. #morethanjustaprettyface.

Thank you all

♥

Table of Contents

List of Figures

Chapter 1

Chapter 2

Chapter 3

Chapter 4

Chapter 5

Chapter 6

List of Tables

Chapter 2

Chapter 3

Chapter 4

Chapter 5

Appendix

List of Symbols and Acronyms

Acronyms and Abbreviations:

ALD	Anoxic Limestone Drain
AMD	Acid Mine Drainage
ARD	Acid Rock Drainage
AVS	Acid Volatile Sulfide
BLM	Biotic Ligand Model
CCU	Cumulative Criterion Unit
CRS	Chromium Reducible Sulfur
DO	Dissolved Oxygen
DIC	Dissolved Inorganic Carbon
DOC	Dissolved Organic Carbon
DOM	Dissolved Organic Matter
EDS	Energy Dispersive Spectroscopy
EPT	Ephemeroptera, Plecoptera, Tricoptera
FIAM	Free Ion Activity Model
HDPE	High-Density Polyethylene
HFO	Hydrous Ferric Oxide
HPIC	High Pressure Ion Chromatography
ICP-MS	Inductively Coupled Plasma Mass Spectrometry
ICP-OES	Inductively Couples Plasma Optical Emission Spectroscopy
NMD	Neutral Mine Drainage
OLC	Open Limestone Channel
ORP	Oxidation Reduction Potential
PHREEQC	pH – Redox Equilibrium modelling in C code
RAPS	Reducing and Alkalinity Producing System
RETRASO	Reactive Transport of Solutes model
SEM	Scanning Electron Microscope
SEP	Sequential Extraction Procedure
SI	Saturation Indices
SRB	Sulfate Reducing bacteria
SRBR	Sulfate Reduction Bio-Reactor
VFW	Vertical Flow Wetland
XRD	X-Ray Diffraction

Chemical Elements (including Cations and Anions):

Al	Akuminium
Ag	Silver
As	Arsenic
Au	Gold
Ca	Calcium
Cd	Cadmium
Co	Cobalt
CO_3^{2-}	Carbonate
Cu	Copper
Fe	Iron
Fe^{2+}	Ferrous Iron – Fe(II)
Fe^{3+}	Ferric Iron – Fe(III)
H^+	Hydronium ion, Proton
HCO_3^-	Bicarbonate
Hg	Mercury
M^+	Metal ion
Mg	Magnesium
Mn	Manganese
Na	Sodium
Ni	Nickel
Pb	Lead
S	Sulfur
S^{2-}	Sulfide
SO_4^{2-}	Sulfate
Sb	Anitmony
Sr	Strontium
Zn	Zinc

Minerals (including Metal Precipitates and Ions)

$Al(OH)_3$	Gibbsite
$Al_4(OH)_{10}SO_4.5H_2O$	Basaluminite
$AlSO_4(OH)\cdot 5H_2O$ or $AlOHSO_4$]	Jurbanite
CuO	Copper oxide
$CuFeS_2$	Chalcopyrite
FeAsS	Arsenopyrite
$Fe(OH)_3$	Ferrihydrite
FeO(OH)	Geothite
$Fe_8O_8(OH)_6SO_4$	Schwertmannite
FeS_2	Pyrite
$(Fe,Ni)_9S_8$	Pentlandite
(Fe,Zn)S	Sphalerite
HgS	Cinnabar
$KAl_3(SO_4)_2(OH)_6$]	Alunite
Mn_2O_4	Birnessite,
Mn_3O_4	Hausmannite
$MnCO_3$	Rhodochrosite
MS	Metal Sulfide
ZnS	Sphalerite
PbS	Galena

List of Publications and Outcomes

Peer-reviewed journal publications

Fairgray, M., et al. (Submitted 2019). "Testing geochemically modelled predictions of trace element toxicity and bioavailability at a rehabilitated mine site Mine Water and the Environment." Mine Water and the Environment.

Conference papers

Fairgray, M. and J. Webster-Brown (2017). Release of toxic trace elements from contaminated stream sediment at Tui Mine, Te Aroha, New Zealand. 2017 AusIMM New Zealand Branch Annual Conference. Christchurch, New Zealand, AusIMM. Pp 8.

Fairgray, M., et al. (2016). Geochemical Modelling of Metal Toxicity in the Tui Mine Catchment, Te Aroha, NZ. 2016 Australian Institute of Minerals and Mining New Zealand Branch Annual Conference, Wellington, New Zealand. Pp 9.

Conference presentations

Fairgray, M., et al. (2018). Changes to the water chemistry of Cannel Creek following remedial work of Bellvue Mine New Zealand Freshwater Sciences Society Annual Conference, Nelson, New Zealand, New Zealand Freshwater Sciences Society.

Fairgray, M., et al. (2018). Changes to the water chemistry of Cannel Creek following remedial work of Bellvue Mine Waterways Postgraduate Student Conference, Lincoln, New Zealand, Waterways Centre for Freshwater Management.

Fairgray, M., et al. (2018). Water chemistry changes in Cannel Creek following remedial work of Bellvue Mine AMD. 2018 AusIMM New Zealand Branch Annual Conference, Tauranga, New Zealand, AusIMM.

Fairgray, M., et al. (2017). The impact of historical mining activity on aquatic macroinvertebrates at Puhipuhi, Northland, New Zealand. Integrating Multiple Aquatic Values (IMAV), Hamilton, New Zealand, New Zealand Freshwater Sciences Society (NZFSS).

Fairgray, M. and J. Webster-Brown (2017). The Fate of Toxic Trace Elements at Tui Mine. Waterways Postgraduate Student Conference, Lincoln, New Zealand.

Fairgray, M., et al. (2017). The impact of historical mining activity on aquatic macroinvertebrates at Puhipuhi, Northland, New Zealand. The International Society for Environmental Biogeochemistry (ISEB) 23rd International Symposium, Palm Cove, Australia.

Fairgray, M. and J. Webster-Brown (2017). Release of toxic trace elements from contaminated stream sediment at Tui Mine, Te Aroha, New Zealand. 2017 AusIMM New Zealand Branch Annual Conference. Christchurch, New Zealand, AusIMM.

Fairgray, M. and J. Webster-Brown (2016). Spatial distribution and bioavailability of Mercury and other toxic trace elements in the Puhipuhi catchment, Northland. New Zealand Freshwater Sciences Society (NZFSS) Annual Conference - Freshwaters On The Edge, Invercargill, New Zealand, New Zealand Freshwater Sciences Society.

Fairgray, M. and J. Webster-Brown (2016). Spatial distribution and bioavailability of Mercury and other toxic trace elements in the Puhipuhi catchment, Northland. Waterways Postgraduate Student Conference, Lincoln, New Zealand, Waterways Centre for Freshwater Management.

Fairgray, M., et al. (2016). Geochemical Modelling of Metal Toxicity in the Tui Mine Catchment, Te Aroha, NZ. 2016 Australian Institute of Minerals and Mining New Zealand Branch Annual Conference, Wellington, New Zealand. Pp 9.

Conference posters

Fairgray, M., et al. (2018). Water chemistry changes in Cannel Creek following remedial work of Bellvue Mine AMD. 2018 AusIMM New Zealand Branch Annual Conference, Tauranga, New Zealand, AusIMM.

Fairgray, M., et al. (2018). The use of redox pairs to model bioreactor processes in the treatment of acid mine drainage. Goldschmidt, Boston, USA, Geochemical Society and European Association of Geochemistry.

Fairgray, M. and J. Webster-Brown (2017). Release of toxic trace elements from contaminated stream sediment at Tui Mine, Te Aroha, New Zealand. 2017 AusIMM New Zealand Branch Annual Conference. Christchurch, New Zealand, AusIMM.

Fairgray, M., et al. (2016). Geochemical Modelling of Metal Toxicity in the Tui Mine Catchment, Te Aroha, NZ. 2016 Australian Institute of Minerals and Mining New Zealand Branch Annual Conference, Wellington, New Zealand

CHAPTER 1

INTRODUCTION

Figure 1. A stream affected by acid mine drainage showing orange-brown iron oxyhydroxide formation, characteristic of acid mine waters. Cannel Creek at Bell11 (Chapter 5) Photo: Jenny Webster-Brown

Mining involves the extraction of minerals from the earth's crust. This can either be through opencast mine pits, underground workings or a combination of both surface mining and underground mining (Cooke and Johnson 2002, Blowes et al. 2003). A mining operation will also involve the construction of mining related infrastructure such as processing plants, buildings, transport paths, overburden piles and tailings dams. A mining operation can have severe impacts on an ecosystem through excavation, processing of ore and generation of waste products which can release elevated concentrations of components to the environment (Lottermoser et al. 1999, Cooke and Johnson 2002, Blowes et al. 2003). Environmental impacts of mining can be physical as well as chemical. The impact that is most relevant to this thesis is the release of trace element-rich acid mine drainage.

1.1 Acid mine drainage

Acid mine drainage (AMD) is a term used to describe the environmental phenomenon of low pH mine drainage water with high concentrations of sulfate ions, iron and other trace elements (Nordstrom and Alpers 1999). AMD occurs when rocks containing iron sulfide minerals are exposed to oxygen and water (Singer and Stumm 1970, Evangelou 1995, Blowes et al. 2003), causing the dissolution of iron sulfide as shown in Equations 1.1 - 1.4.

Immediate oxidation of iron sulfide (pyrite) occurs by the following equation:

$$2FeS_{2(s)} + 7O_{2(g)} + 2H_2O_{(l)} \rightarrow 2Fe^{2+}_{(aq)} + 4SO^{2-}_{4(aq)} + 4H^{+}_{(aq)} + energy \qquad \text{(Eqn. 1.1)}$$

Complete oxidation of iron sulfide then occurs by an additional three interconnected reactions which proceed by the following equations:

$$FeS_{2(s)} + 14Fe^{3+}_{(aq)} + 8H_2O_{(l)} \rightarrow 15Fe^{2+}_{(aq)} + 2SO^{2-}_{4(aq)} + 16H^{+}_{(aq)} + energy \qquad \text{(Eqn. 1.2)}$$

$$4Fe^{2+}_{(aq)} + O_{2(g)} + 4H^{+}_{(aq)} \rightarrow 4Fe^{3+}_{(aq)} + 2H_2O_{(l)} + energy \qquad \text{(Eqn. 1.3)}$$

$$Fe^{3+}_{(aq)} + 3H_2O_{(l)} \rightarrow Fe(OH)_{3(s)} + 3H^{+}_{(aq)} \qquad \text{(Eqn. 1.4)}$$

Equation 1.1 describes the oxidation of molecular pyrite by oxygen; Equation 1.2 describes the oxidation of pyrite at low pH (<3.5) whereby soluble ferric iron acts as the oxidant; Equation 1.3 describes the oxidation of ferrous iron to ferric iron; and Equation 1.4 describes the hydrolysis of ferric iron to iron hydroxide (ferrihydrite).

Iron sulfide oxidation can be either an abiotic process, or a faster biotic process if microorganisms, such as *Acidithiobacillus ferrooxidans,* are present (Temple and Colmer 1951, Blowes et al. 2003). If conditions are favourable for microbial activity by bacteria such as *A. ferrooxidans*, which oxidizes Fe(II) to Fe(II) in acidic, sulfate-rich environments (Silverman 1967, Nemati et al. 1998). In the first phase of the AMD generation process, the conditions are at a moderate pH (>4.5), the concentration of sulfate ions is high but concentration of iron is low (Salomons 1995). The reaction prescribed by Equation 1.1 proceeds abiotically as well as through bacterial oxidation. The oxidation of Fe^{2+} and subsequent hydrolysis proceeds abiotically but becomes less energetically favourable as the pH decreases. In the second phase of AMD generation the pH is between 2.5 and 4.5, sulfate

concentrations are high and total iron concentration is increasing. In this phase dissolution of iron sulfide occurs abiotically as well as biotically. In the final stage, the pH is low (<2.5), sulfate and total iron concentrations are high. The oxidation of ferrous iron occurs solely through bacterial oxidation and the oxidation of iron sulfide by the ferric ion is determined by the reaction rate of bacterially mediated iron oxidation (Salomons 1995, Johnson and Hallberg 2005).

These mechanisms of iron sulfide oxidation generate hydrogen ions (Equation 1.1). The generation of hydrogen ions, and the associated lowering of the solution pH, causes dissolution of other minerals in the host rock (Blowes et al. 2003). Other sulfide-containing minerals oxidise and contribute sulfate ions and trace elements to AMD include chalcopyrite [$CuFeS_2$], galena [PbS], sphalerite [(Fe,Zn)S], pentlandite [$(Fe,Ni)_9S_8$], arsenopyrite [FeAsS] and cinnabar [HgS] (Blowes et al. 2003, Gore et al. 2007, Lindsay et al. 2009). The dissolution of auxillary sulfide minerals releases additional trace elements into the AMD solution (Saria et al. 2006). The lower concentration of oxidising ferric iron in non-pyritic minerals results in the oxidation of other sulfide-containing minerals at a slower rate than would occur during the oxidation of iron sulfides (Blowes et al. 2003, Lottermoser 2003). Additionally, generation of acidity is much lower when oxidation of the sulfide mineral occurs with oxygen as the electron acceptor compared to ferric iron (Nordstrom and Alpers 1999, Plumlee 1999, Dold 2017). For example, monosulfide minerals which do not contain Fe, such as sphalerite and galena, do not generate proton acidity if oxidation occurs via oxygen but generate 8 mols of H^+ when oxidation occurs via ferric iron (Equations 1.5-1.8; Equations 1.5-1.8; Nordstrom and Alpers 1999, Plumlee 1999, Dold 2017). However, the protons produced by this reaction can then be used up re-oxidising the ferrous iron back to ferric iron (Equation 1.4). Additionally, trace elements such as arsenic (As) and antimony (Sb) which are commonly found within sulfides can be released to the AMD solution (Craw et al. 2000a, Craw et al. 2000b, Lindsay et al. 2015).

Oxidation of sphalerite [ZnS]:

$$ZnS + 2O_2 \rightarrow Zn^{2+} + SO_4^{2-} \quad \text{(Eqn 1.5)}$$

$$ZnS + 8Fe^{3+} + H_2O \rightarrow Zn^{2+} + 8Fe^{2+} + SO_4^{2-} + 8H^+ \quad \text{(Eqn 1.6)}$$

Oxidation of galena [PbS]:

$$PbS + 2O_2 \rightarrow Pb^{2+} + SO_4^{2-} \quad \text{(Eqn 1.7)}$$

$$PbS + 8Fe^{3+} + H_2O \rightarrow Pb^{2+} + 8Fe^{2+} + SO_4^{2-} + 8H^+ \quad \text{(Eqn 1.8)}$$

Oxidation of non-ferrous sulfides, such sphalerite or galena, which produce less acidity than iron sulfide results in solutions with a circum-neutral or basic pH but high concentrations of sulfide ions and trace elements (Banks et al. 1997, Warrender et al. 2011, Ciszewski et al. 2012, Iavazzo et al. 2012, Kovács et al. 2012). This is known as neutral mine drainage (NMD) or alkaline/basic mine drainage depending on the pH (Nordstrom et al. 2015). NMD can also form as a result of iron sulfide oxidation in the presence of minerals, such as carbonates, which are able to neutralise the acidity (Banks et al. 1997).

Remediation of NMD can be challenging because low ferrous ion concentrations limits Fe(II) mineral precipitates, such as ferrihydrite and/or schwertmannite, that naturally adsorb trace elements (Carlson et al. 2002, Warrender et al. 2011). Trace elements, such as Zn, Mn, Cd, Pb and Cu, can remain soluble over a wide pH range under suitable redox conditions further confounding remediation of NMD (Lindsay et al. 2009, Warrender et al. 2011).

Such solutions with a low pH, high concentration of sulfate ions and a high concentration of trace elements are defined as "acid rock drainage" (ARD) if occurring naturally and "acid mine drainage" (AMD) if the generation of such waters has occurred due to mining activities (Nordstrom et al. 2015). The process of iron sulfide oxidation is often accelerated by mining activities as the rock is being exposed to oxygen and water faster than would occur naturally (Powell 1988, Akcil and Koldas 2006) hence the need to differentiate between the natural process of ARD generation and anthropogenic process of AMD generation.

1.1.1 Effects of AMD on aquatic ecosystems

AMD can exert both chemical and physical stressors on aquatic biota (Hogsden and Harding 2011). Chemical stressors include shifts in pH and toxic concentrations of trace elements (Lottermoser et al. 1999). Physical stressors include turbid waters due to high amounts of suspended particulate matter (eg. Coal fines, mineral precipitates, clays or sediment) and smothering of the stream bed as mineral precipitates settle out of the water column (Hogsden and Harding 2011).

pH

Changes in pH can directly impact on biota because most aquatic organisms have a restricted pH tolerance range and indirectly as changes in pH can affect the speciation of trace elements in solution (Fromm 1980, Harding and Boothroyd 2004). Low pH increases the permeability of the cell membrane (Havas and Advokaat 1995), resulting in less uptake of Na^{2+} (Camargo 1995, Havas and Advokaat 1995), and dissolves the shell of molluscs, oligochaetes and crustaceans (Havas and Advokaat 1995, Gerhardt et al. 2004).

pH also has the following effects on the solubility of trace elements:

- Trace element-bearing minerals, such as feldspars, carbonates are more soluble at low pH, releasing bound trace elements into solution (Cravotta and Trahan 1999).
- Cationic trace elements desorb from charged surfaces, such as organic matter and metal-oxides at low pH. However, anionic trace elements adsorb to such surfaces at low pH and desorb at higher pH.
- Elements are more likely to be in a free ion state at low pH (Paquin et al. 2002)

At low pH (4.5-6) the buffering capacity of a stream is reduced due to protons combining with HCO_3^- in solution to form carbonic acid which can then dissociate to form H_2O and CO_2 (Fromm 1980). At lower pH (<4.5), HCO_3^- is completely exhausted. Therefore when further acid mine effluents are added, the pH will drop more rapidly or the H^+ concentration will increase more rapidly (Harding and Boothroyd 2004, Freund and Petty 2007).

Toxic concentrations of trace elements

Trace elements can be ingested by organisms directly from the water column or sediment pore water through respiratory organs, through intake of food containing trace elements or through intake of contaminated sediment (Batty et al. 2010, Byrne et al. 2012). Some trace elements result in negative effects on the organism due to their toxicity. The toxicity of a trace element will depend on the type of element, the trace element species present and the environmental conditions. Additionally, some species are more tolerant to trace element pollution than others. These factors mean that when a trace element is at an acutely toxic concentration a species cannot survive under such conditions and a flux of trace elements through a system at such a concentration will result in species mortality. Trace elements can also exhibit chronic toxicity. This can affect the growth, reproduction and behaviour of a species, and can be fatal in the longer term (Moreira-Santos et al. 2008).

Some trace elements, such as Fe, Zn and Cu, are micronutrients and are beneficial for growth at low concentrations but become toxic above a threshold concentration (Powell 1988, Smith and Huyck 1999). However, other elements, such as As, Hg, Pb and Cd, have no known physiological benefit and are detrimental to survival and growth at elevated concentrations (Comber et al. 2008, Batty et al. 2010). Even low concentrations of these elements can be toxic. In an AMD solution, multiple trace elements are present, and the different combinations can interact and have synergistic, antagonistic or additive effects. Therefore, assessing metal toxicity is complicated and no single representative value for toxicity is available for natural systems (Byrne et al. 2012). The combination of several difference trace elements in an AMD solution can be taken into account by using a cumulative criterion unit (CCU) to account for additive effects of metals in a solution (Clements et al. 2010).

The toxicity of a trace element is also dependent on the chemical speciation of the element. Different species of trace elements have differing mobility and ecotoxicity (Batley et al. 2004, Byrne et al. 2012). It has been found that toxicity of an element can be poorly correlated with the total trace element concentration (Di Toro et al. 2001, Paquin et al. 2002). Instead, toxicity is related to the concentration of the trace element which is available for uptake by biota (Paquin et al. 2002) and this proportion of the total concentration is determined by the environmental conditions. For example, salinity, hardness, and alkalinity or acidity impacts speciation and affects toxicity. Particulate organic matter and metal (oxy)hydroxides can reduce toxicity by providing additional binding sites to which trace elements can adsorb to, thus reducing the concentration of the free ion in solution. The hardness of the water can also affect toxicity by providing Ca^{2+} and Mg^{2+} ions to compete with trace elements for these binding sites. The pH of a solution is a major factor in determining the toxicity of metals to biota as it will influence both sorption and complexation processes. The interactions between a trace element, other aqueous constituents and an aquatic organism are encapsulated by the free ion activity model (FIAM) and the biotic ligand model (BLM).

Free ion and biotic ligand models

The FIAM and BLM are both conceptual models which show the interactions between a free metal ion in solution, other constituents in the solution and a “site of action” on an aquatic organism (Figure 1.1; Campbell 1995, Di Toro

et al. 2001). These models grew out of research that showed that the toxicity of a trace element was poorly correlated with the total concentration of the element in solution but is often more strongly related to the concentration of the free, un-complexed, trace element (Di Toro et al. 2001). This stronger correlation with the free ion is because the free trace element is in a bioavailable form and is able to be transported across the cell membrane whereas the total concentration includes complexes and adsorbed species which cannot pass through the cell membrane (Lottermoser et al. 1999, Paquin et al. 2002, Batley et al. 2004). For example, Cu and Ag can be taken up into aquatic organisms through Na^+ transport pathways while Zn, Cd, Pb and Co can be taken up through Ca^{2+} transport pathways (Niyogi and Wood 2004). Once inside the cell, these trace elements can disrupt normal cell function causing harm to the organism (Simkiss and Taylor 1995, Lander 2004).

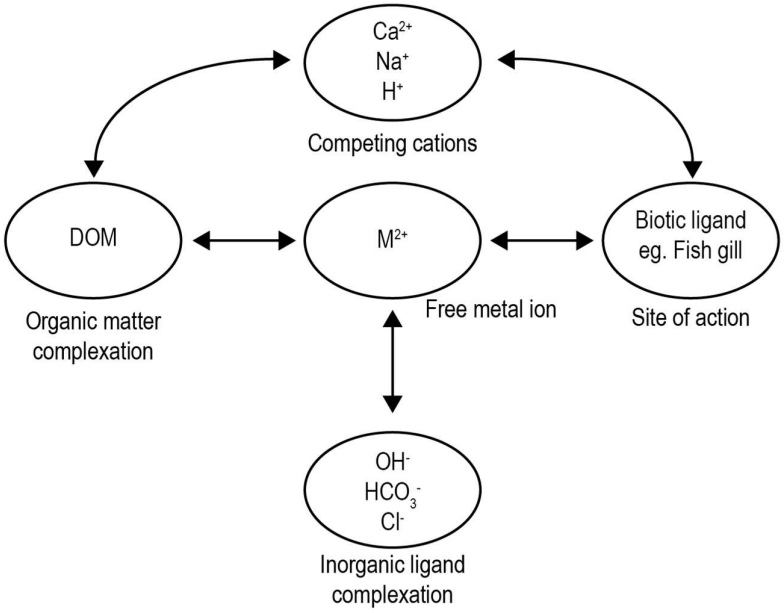

Figure 1.1 The interactions between a trace element, M^{2+}, the biotic ligand, competing cations, inorganic ligands and competing surfaces. Adapted from Paquin et al. (2002) and Di Toro et al. (2001)

The FIAM and BLM use complexation theory to explain the interactions between the trace element, other aqueous constituents and the site of action on the organism (Figure 1.1). The site of action was originally conceptualised as the gills of a fish but has since been generalised to be a nonspecific "biotic" ligand with which the trace element can form a complex (Brown and Markich 2000, Di Toro et al. 2001, Niyogi and Wood 2004). The interactions between the components of the model are assumed to be at equilibrium with each other (Campbell 1995).

The other cations present in the water, such as Ca^{2+}, Mg^{2+}, Na^+ and H^+, compete with the trace element for the biotic ligand binding site (Paquin et al. 2002). Therefore the toxicity of an element is a dependent on the hardness or salinity of the water (Brown and Markich 2000, Paquin et al. 2002, Wang et al. 2010, Smith et al. 2015). Organic matter provides other binding sites that the trace element and competing cations can complex with, thus reducing the toxicity of the trace element (Brown and Markich 2000, Paquin et al. 2002). Other organic and inorganic ligands

can form complexes with the trace element, rendering it non-bioavailable and preventing it from binding to the biotic ligand. Notable exceptions to the FIAM and BLM are Cu-hydroxide complexes which have been shown to be bioavailable to aquatic organisms and contribute to the toxicity of Cu (Chakoumakos et al. 1979, Wagemann and Barica 1979, de Schamphelaere and Janssen 2002) and oxyanions of elements such as As and Sb which are present and toxic in natural waters as oxyanions, not free ions (Jennette 1981, Sundar and Chakravarty 2010).

Although similar to the BLM, the FIAM is based on measurements of the activity of free metal ion in solution, while the BLM is based on measurements of the metal adsorbed to the site of action (Brown and Markich 2000, Hassler et al. 2004). Additionally, the BLM places a greater emphasis on link between the element complexed to biotic ligand and the effect that it has on the organism.

Because the FIAM and BLM s are based on reactions for which thermodynamic equilibrium data can be obtained, the concentration at which a response in the organism is observed can be calculated for specific trace elements and organisms (Santore et al. 2001, Santore et al. 2002, Hassler et al. 2004); Toxicity calculations for these models, however, focus on acute toxicity rather than chronic toxicity.

Precipitation of metal oxides

When reduced AMD, with high concentrations of Fe, Mn or Al, has oxygen or a neutralizing agent added Fe-, Mn- or Al-oxides and hydroxides will form. These precipitates can adsorb trace element and reduce their toxicity because they have charged and chemically active surfaces. This particulate matter will settle out of the water column and onto the stream bed and this can have adverse effects on aquatic ecosystems.

The settling of mineral precipitates can clog up the spaces between stream bed substrate and coat detrital matter which grazing macroinvertebrates would feed on (Letterman and Mitsch 1978, Harding and Boothroyd 2004, Gray and Harding 2012). The decreased processing of detrital matter by shredder macroinvertebrates and microbes reduces leaf litter breakdown rates preventing energy from passing up the food chain (Barnden and Harding 2005). Additionally, deposited iron oxide precipitate has been shown to damage the internal organs of benthic macroinvertebrates (Gerhardt 1992).

The accumulation of trace elements on the surface of metal oxide and hydroxide precipitates and the settling of these precipitates onto the stream bed results in stream sediment with elevated concentrations of trace elements (Cravotta et al. 2010, Ciszewski et al. 2012). As with dissolved trace elements, the toxicity of sediment-bound trace elements will dependent on the bioavailability of the trace elements, and this depends on how the trace element is bound to the sediment (Simpson and Batley 2007). Sediment-bound trace elements can generate high concentrations of trace elements in the sediment pore water, or not depending on sediment and pore water chemistry. Particle-feeding organisms more susceptible to intake of sediment-bound metals (Byrne et al. 2012)

and benthic organisms are slower to recover from the effects of a sediment contamination event than more mobile organisms in the water column (Clements et al. 2010).

Once deposited, trace elements can remain in a stream bed for long periods of time (Byrne et al. 2012). A "slug" of contaminated sediment can be transported or dispersed downstream if the stream bed gradient and flow rates are high enough (Byrne et al. 2012). Trace elements and acidity can also be re-released into the environment from the sediment if conditions in the stream change (Lottermoser et al. 1999, Gore et al. 2007, Ciszewski et al. 2012, Kovács et al. 2012). In addition, an increase in suspended solids due to precipitation of metal oxides and hydroxides reduces light penetration through the water column and lower rates of photosynthesis in plants (Ranville and Schmiermund 1998). Suspended sediment can also affect the visibility between prey and predators.

Effects on food web structure

Under AMD conditions, algal communities shift from being a diverse community to one dominated by filamentous green algae and periphyton (Lottermoser et al. 1999, Bray et al. 2009, Hogsden and Harding 2011). Such algae and other plant species can either take up trace elements into their biomass in a similar concentration to the surrounding environment or at a higher or lower concentration. Some plants that take up trace elements and concentrate the trace elements in the shoots and leaves (hyperaccumulate) and can be useful for incorporating into a constructed wetland to remove trace elements from the water column. Other plants, excluders, do not take up trace elements into the biomass of the plant and instead form plaques of iron oxide precipitates around the roots of the plant (Otte and Jacob 2006). Additionally, low pH, low nutrients or low water holding capacity of soils can make it difficult for plants to survive in AMD affected environments (Lottermoser et al. 1999).

The benthic dwelling, sedentary nature of macroinvertebrates means that the overall structure of a macroinvertebrate community present in a stream is representative of the environmental conditions in the stream (Batty et al. 2010, Byrne et al. 2012). By measuring parameters and calculating metrics of macroinvertebrate community, such as species abundance, number of taxa, %Ephemeroptera, Plecoptera and Tricoptera (EPT) and % chironimidae, the macroinvertebrate community structure can be used to measure stream health to indicate the level of AMD impact on the aquatic ecosystem or to measure the progress of recovery at a remediated site (Gerhardt 1993, Clements et al. 2010). A variety of physiological and behavioural changes have been observed in macroinvertebrates due to mine contamination (Byrne et al. 2012). However, the variation in tolerance to acidic and trace element contamination is highly variable for different species. For the macroinvertebrate species, sensitivity to metal mine contamination usually follows the order Ephemeroptera > Tricoptera > Plecoptra > Diptera but some variation within taxa and species is present (David 2003, Byrne et al. 2012). For example, it has been observed that certain EPT species in areas with naturally acidic streams have adapted to be tolerant of acidity (O'Halloran et al. 2008, Gray and Harding 2012). The tricopteran species hydropsyche and chironomidae are most tolerant of AMD contamination (Letterman and Mitsch 1978). Snails, which are typically considered to be tolerant of pollution, are not commonly found in AMD affected streams as the acidity reacts with their shell (Batty et al.

2010). Therefore, a macroinvertebrate community in a stream impacted by AMD will undergo changes in community composition as sensitive species become absent. This results in a lowered diversity, number of taxa, number of EPT taxa and abundance of species in streams affected by AMD (David 2003, Gunn et al. 2010, Gray and Harding 2012).

The survival, growth and reproduction of fish and shellfish can be affected by AMD contamination of stream environments (Haines and Baker 1986, Moreira-Santos et al. 2008), as well as the behaviour of these organisms, such as avoidance of contaminated areas (Moreira-Santos et al. 2008). The fish/shellfish community composition can be affected in a similar way to macroinvertebrate communities with a reduction in fish population density, number of taxa and loss of sensitive taxa. As noted previously, trace elements can have a toxic effect on species when the trace element is taken up by cells. Al exhibits a unique toxicity mechanism in fish whereby the pH gradient across the gills results in the formation of Al colloids on fish gills. This leads to the suffocation of fish in high Al waters (Nordstrom 1982, Cravotta et al. 2010). These higher trophic level organisms are also capable of bioaccumulating trace elements in their organs and flesh.

Bioaccumulation of trace elements

Bioaccumulation occurs where the mechanism for excreting the trace element is slower than uptake of the trace element. Bioaccumulation of trace elements can occur in the roots and shoots of terrestrial and aquatic plants (Smith and Huyck 1999). Plants that have a capacity for taking up trace elements are called metallophytes and can be used for phytoremediation of an area contaminated with trace elements (Sheoran and Sheoran 2006). Macroinvertebrates can bioaccumulate trace elements without negative impacts (Farag et al. 1998, Goodyear and McNeill 1999). Fish and shellfish are particularly susceptible to bioaccumulation of trace elements (Bryan et al. 1983, Regoli and Principato 1995). Shellfish can take up trace elements directly from the sediment due to their benthic dwelling nature (Hoggins and Brooks 1973). Fish can take up trace elements from their environment or from their food (Robertson et al. 1975, Safran 20177). Bioaccumulation of trace elements in fish and shellfish is particularly important due to its risk as a human health hazard as shellfish and fish are commonly consumed by humans.

1.2 Natural trace element attenuation processes

There are a variety of naturally occurring biotic and abiotic processes that reduce the negative impacts AMD can have on the environment, the aquatic ecosystem and human health. These processes involve the neutralisation of solution acidity and lowering the concentration of free ion trace elements to a non-toxic level, either by dilution, complexation of the free ion, precipitation of trace element-bearing particulates or the adsorption of trace elements to a surface.

1.2.1 Neutralization of acidity

One of the most important steps, and often the first step, in reducing the toxicity of AMD is to neutralize high acidity (Hedin et al. 1994, Younger et al. 2002). This can occur where carbonate minerals are present in the host rock at a concentration sufficient to neutralise solution acidity (Powell 1988, Lindsay et al. 2015). As well as reducing the effect of high acidity on acid sensitive biota, a pH increase also reduces the solubility of trace elements and trace element bearing minerals (Salomons 1995, Watzlaf et al. 2004, Byrne et al. 2012, Skousen et al. 2016).

1.2.2 Precipitation of minerals phases

The next step in reducing the toxicity of AMD is to change the oxidation state of an element to one that will easily react with counter-ions in the solution and form an insoluble precipitate. Precipitates form when the solubility of a mineral is exceeded by either a changing pH or changing redox conditions. The solubility of a trace element bearing mineral precipitate controls the concentration of the trace element in the solution

Oxygenated aqueous conditions will usually oxidise ferrous iron to ferric iron (Equation 1.9) which can then react with water to form iron (oxy)hydroxides (Equation 1.10). Manganese can also undergo oxidation and form oxides or (oxy)hydroxides (Skousen et al. 2016) whereas Aluminium undergoes hydrolysis to form (oxy)hydroxides.

$$Fe^{2+} \rightarrow Fe^{3+} + e^{-} \quad \text{(Eqn 1.9)}$$

$$Fe^{3+} + 3H_2O \rightarrow Fe(OH)_{3(s)} + 3H^{+} \quad \text{(Eqn 1.10)}$$

It should be noted that these reactions generate protons, so the solution must contain sufficient alkalinity in order to neutralise the generated acidity and maintain a circum-neutral pH or further acidity will result (Smith 1999, Johnson and Hallberg 2005).

Ferrihydrite [$Fe(OH)_3$], also known as hydrous ferric oxide (HFO) or amorphous iron hydroxide, is the first hydrolysis product of iron to form in natural waters with a pH>5.5 (Nordstrom and Alpers 1999). Ferrihydrite forms when ferrous iron is oxidised and hydrolysed rapidly, ie. When a sudden pH change occurs in AMD waters (Blowes et al. 2003). Ferrihydrite can recrystallize and transform into goethite [FeO(OH)] a more stable iron oxyhydroxide. Another common Fe precipitate in AMD waters is schwertmannite [$Fe_8O_8(OH)_6SO_4$] (Bigham et al. 1996). Schwertmannite is an iron hydroxysulfate that forms in AMD waters with intermediate pH (3.5-5.5). Schwertmannite converts to goethite at pH>2.5 or to jarosite [$KFe_3(OH)_6(SO_4)_2$] at pH<2.5 (Nordstrom et al. 2015).

$$8Fe^{3+}_{(aq)} + SO^{2-}_{4(aq)} + 14H_2O_{(l)} \rightarrow Fe_8O_8(OH)_6(SO_4)_{(s)} + 22H^{+}_{(aq)} \quad \text{(Eqn 1.11)}$$

Mn is more soluble than Fe under most conditions, especially those found in natural riverine environments (Hem 1963). Oxides or hydroxides of manganese will only precipitate in solutions with a high pH (Sobolewski 1999), ie. in neutral mine drainage or where an alkaline product has been added to increase the pH. Additionally, Mn oxides

can be reduced by ferrous iron, so formation of Mn oxides is only possible once iron has been removed from the solution (Sobolewski 1999). Formation of Mn oxides can also be enhanced by bacterial oxidation of Mn (Christenson et al. 2019). Mn oxides formed in mine drainage waters are birnessite, [Mn_2O_4] and hausmannite, [Mn_3O_4]. Mn carbonate, rhodochrosite [$MnCO_3$], can also form in solutions with a high concentration of bicarbonate if pH>7 (Hem 1963).

The solubility of Al is controlled by amorphous aluminium hydroxide[$Al(OH)_3$] or hydrous aluminium oxide (HAO) in waters with pH>4.5 (Nordstrom and Alpers 1999). However, the crystalline form of HAO, gibbsite [$Al(OH)_3$], is unstable at pH <5.5. Al-sulfates and hydroxysulfates, such as basaluminite [$Al_4(OH)_{10}SO_4.5H_2O$], jurbanite [$AlSO_4(OH)\cdot 5H_2O$] and alunite [$KAl_3(SO_4)_2(OH)_6$] are more stable in AMD environments than common soil minerals such as gibbsite and kaolinite (Nordstrom and Alpers 1999, Espana et al. 2005).

A circum-neutral pH is not usually high enough to cause hydroxides of Cu, Cd, Ni and Zn to form in AMD (Pérez-López et al. 2011), although higher pH conditions can lead to the formation of metal carbonates provided that the concentrations of metals are sufficient (Sobolewski 1999).

Reducing conditions can result in the reduction of the sulfate ion to sulfide (Equation 1.12) which can then react with cationic trace elements to form metal sulfides (Equation 1.13) (Neculita et al. 2007).

$$2CH_2O_{(s)} + SO_{4(aq)}^{2-} \rightarrow H_2S_{(aq)}^0 + 2HCO_{3(aq)}^- \quad \text{(Eqn 1.12)}$$

$$M_{(aq)}^{2+} + H_2S_{(aq)} \rightarrow MS_{(s)} + 2H_{(aq)}^+ \quad \text{(Eqn 1.13)}$$

In this way, divalent trace elements (eg. Fe, Zn, Pb, Cd, Cu, Ni) can be removed by precipitation as sulfide minerals (Equation 1.13; Dvorak et al. 1992, Sobolewski 1999, Doshi 2006, Skousen et al. 2016). However this reaction will reverse under oxidising conditions (Skousen et al. 2016).

The bicarbonate ions produced by sulfate reduction can react with protons to form carbon dioxide and water, therefore removing acidity from the solution and raising the pH of the solution (Equation 1.14) (Dvorak et al. 1992).

$$HCO_{3\,(aq)}^- + H_{(aq)}^+ \rightarrow CO_{2\,(g)} + H_2O_{(l)} \quad \text{(Eqn 1.14)}$$

1.2.3 Trace element adsorption

The charged nature of oxide and hydroxide precipitates provides a surface to which trace elements in the AMD solution can adsorb to (Figure 1.2). Iron (oxy)hydroxide surfaces are the most abundant surface within AMD environments (Smith 1999) so adsorption to Fe (oxy)hydroxide surfaces is a significant trace element removal process, particularly for divalent trace elements such as Cu, Zn, Pb, Ag, Mn and Sr (Benjamin and Leckie 1981, Filipek et al. 1981, Dzomback and Morel 1990, Webster et al. 1998, Lottermoser et al. 1999, Langley et al. 2009,

Skousen et al. 2016) and for trace elements which form oxyanions, such as As and Sb (Haffert and Craw 2008, Rait et al. 2010). For adsorption to an Fe (oxy)hydroxide surface to be a viable natural attenuation process for these trace elements, there must be a high concentration of Fe sulfides in the ore as compared to other metal sulfides (Haffert and Craw 2008). Additionally, where Fe-rich precipitates contain significant quantities of sulfate, the sulfate ion can adsorb/co-precipitate with iron (oxy)hydroxide forming an Fe hydroxysulfate such as schwertmannite (Bigham et al. 1996). Adsorption of Cu, Cd and Zn to the Fe oxyhydroxy sulfate precipitate is enhanced by ternary complexes between the trace element, sulfate ion and the oxyhydroxy sulfate surface (Webster et al. 1998, Swedlund and Webster 2001, Swedlund et al. 2003). The degree of adsorption of Cu and Zn has been shown to be greater for Fe(III) precipitates collected from an AMD-affected site than for synthetic schwertmannite which in turn was greater than for adsorption onto two line ferrihydrite (Webster et al. 1998).

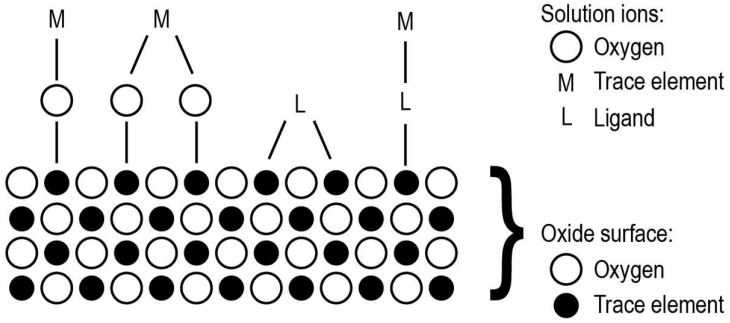

Figure 1.2 The ways in which a charged trace element can interact with an oxide surface and ligand (Smith 1999, Warren and Haack 2001).

Adsorption of trace elements to Fe (oxy)hydroxide is controlled strongly by pH (Benjamin and Leckie 1981, Lottermoser et al. 1999). At low pH cationic trace elements will show low adsorption. As pH increases cationic trace elements will transition from a low adsorption percentage to being almost completely adsorbed within a few pH units (Figure 1.3). The pH at which this adsorption transition occurs depends on the iron oxide surface and the solution but generally follows the trend: Pb < Cu < Zn < Cd (Benjamin and Leckie 1981). Arsenic occurs in natural waters as an oxyanion so has the opposite behaviour to cationic trace elements (Goldberg and Johnston 2001, Smedley and Kinniburgh 2002, Bowell et al. 2014). Arsenic is most strongly adsorbed at low pH and undergoes desorption as pH increases. Adsorption to Fe (oxy)hydroxides is not a permanent attenuation process for trace elements in AMD waters as they can be released from the (oxy)hydroxide surface if different pH or redox conditions occur (Craw 2005).

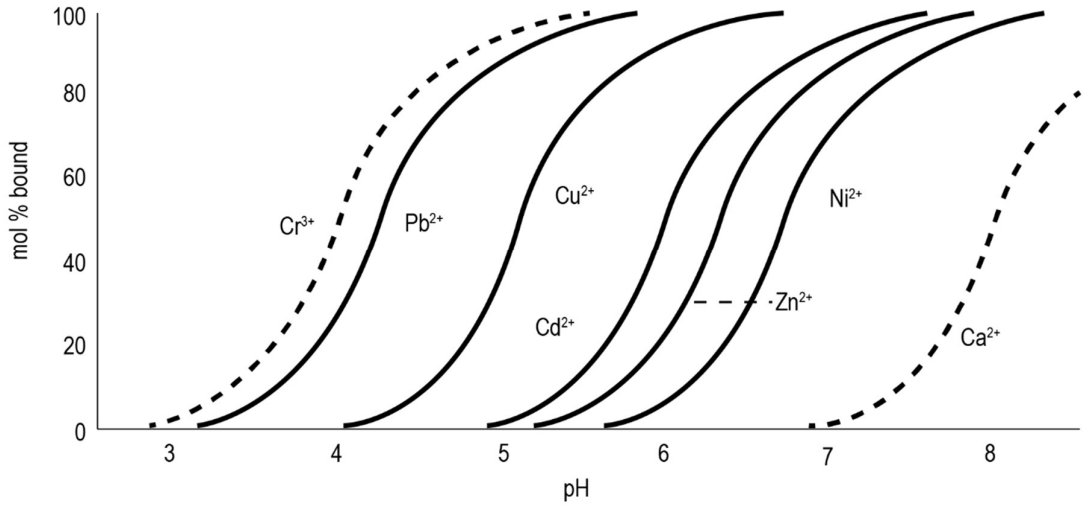

Figure 1.3 The extent of adsorption (through surface complexation) of cationic trace elements as a function of pH (trace element concentration 5 x 10-7, ferrihydrite concentration 10-3 M, ionic strength 0.1mol/L; trace element concentration 5 x 10-7, ferrihydrite concentration 10-3 M, ionic strength 0.1mol/L; Stumm 1992).

Adsorption of trace elements, particularly Pb and Co, to Mn oxide surfaces is important in some environments (McKenzie 1980, Smith 1999, Kumpiene et al. 2008, Della Puppa et al. 2013, Ghaly et al. 2016). However, adsorption to Mn oxide surfaces is a less important attenuation process for most trace elements due to the lower abundance of Mn oxide surfaces in comparison to Fe oxide surfaces. Adsorption of trace elements onto Al oxide surfaces is minor, especially in AMD systems where Fe oxide surfaces are usually much more abundant (Balistrieri et al. 2007).

In addition to Fe and Mn oxide surfaces, natural organic matter also provides sites to which trace elements can adhere to (Sobolewski 1996, Skousen et al. 2016). Adsorption to natural organic matter is of importance for Cu and Ni (Sobolewski 1996).

1.2.4 Co-precipitation

Adsorption of trace elements to the (oxy)hydroxide surface can occur simultaneously with the precipitation reaction so adsorbed trace elements can become included as impurities within (oxy)hydroxide precipitates (Karthikeyan et al. 1997, Sheoran and Sheoran 2006, Lu et al. 2011). This process is called co-precipitation. Co-precipitation and adsorption are different but very closely linked processes. Co-precipitation involves adsorption of trace elements on freshly formed mineral surface (eg. HFO) in addition to solid solution formation of a mineral with trace elements incorporated into the mineral lattice, and the encapsulation of aqueous trace elements by the precipitate (Karthikeyan et al. 1997).

1.2.5 Uptake by plants and other biota

A number of terrestrial and aquatic plants have been found to take up trace elements from the soil or pore-water in which they are rooted (Denny 1980, Alford et al. 2010, Baker et al. 2010). These plants which have the ability to survive and reproduce on soils with a high concentration of trace elements are called metallophytes (Baker et al. 2010). Metallophytes can accumulate trace elements, such as Cd, Cu, Pb, Ni, Zn and As in their roots and leaves to remarkably high levels (Batty 2003, Baker et al. 2010), even to the extent that these plants can be used to indicate ore deposits (Brooks et al. 1977, Morrison et al. 1979). Although aquatic plants aren't as good at accumulating trace elements within biomass as terrestrial plants (Sobolewski 1999), they can still facilitate trace element removal from solution through phytostabilisation (Mendez and Maier 2007). This is where the trace elements are held in a chemically stable form around the roots of a plant and occurs due to oxidation of iron in solution by oxygen released by the plant roots leading to the formation of iron oxyhydroxide plaques in the root rhizosphere. As iron oxyhydroxides are especially good at removing trace elements to their surface, trace elements such as As and Zn also accumulate within the rhizosphere (Otte et al. 1995). The concentration of trace elements in plant tissue usually follows the order root> rhizome> leaf tissue (Mays and Edwards 2001). However, a disadvantage of trace element attenuation via plant uptake is the release of trace elements from the organic material during decomposition of the plant (Sobolewski 1999).

1.3 Mine remediation techniques

AMD treatment systems are designed to optimise natural removal processes. They may include engineered water treatment plants, such as anaerobic and aerobic wetlands and various limestone-based systems including anoxic or oxic limestone drains, open limestone channels, limestone diversion wells, and vertical flow compost wetlands (Figure 1.4; Hedin et al. 1994, Watzlaf et al. 2004, Skousen et al. 2016).

Remediation techniques have traditionally been categorised as being active and passive treatment systems but a biological and geochemical division may be more useful (Johnson and Hallberg 2005, Neculita et al. 2007, Trumm 2010b). Active treatment consists of continual dosing of AMD with an alkaline reagent, at a rate proportional to the flow of AMD through the system. Passive treatment consists of installing a treatment system with enough reactive material to treat AMD emanating from a point source for a long period of time (eg. 25years). Passive treatment makes use of natural chemical and biological processes to treat AMD (Watzlaf et al. 2004, Skousen et al. 2016). Although passive treatment systems generally require more land, they are often less costly in terms of the reagents used and maintenance costs (Watzlaf et al. 2004). Additionally, passive treatment systems don't require a power supply or regular human intervention (Skousen et al. 2016).

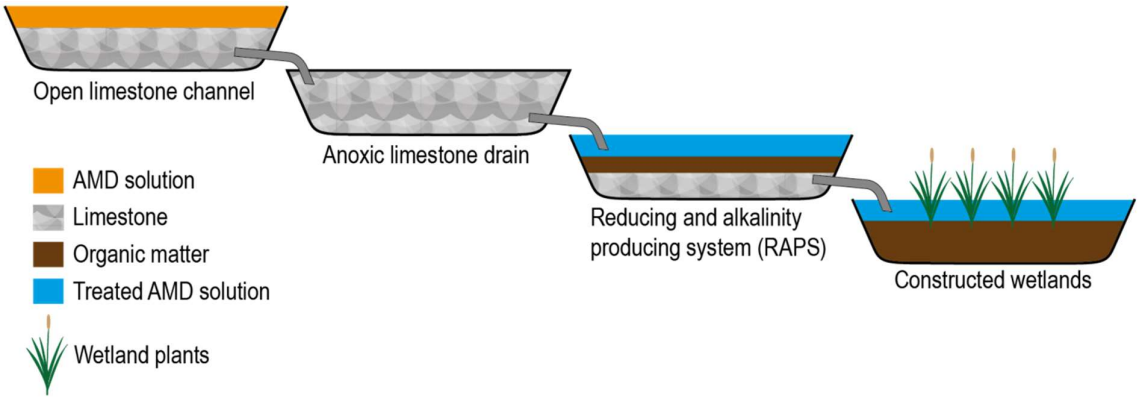

Figure 1.4 A typical passive AMD treatment system with an open limestone channel, an anoxic limestone drain, a RAPS and a constructed wetland in series. An AMD treatment system may include more than one type of treatment system or several cells of the same treatment system type in series. (Skousen 1998, White 2006, McCauley et al. 2008, Zipper et al. 2014)

1.3.1 Neutralizing pH

The simplest type of remediation is to add a neutralizing agent to the AMD to increase the pH and alkalinity of the solution as shown in Equations 1.15 and 1.16 (Blowes et al. 2003, Skousen et al. 2016).

$$CaCO_3 + H^+ \rightarrow Ca^{2+} + HCO_3^- \quad \text{(Eqn. 1.15)}$$

$$CaCO_3 + 2H^+ \rightarrow Ca^{2+} + CO_2 + H_2O \quad \text{(Eqn 1.16)}$$

Common neutralizing agents use are limestone, hydrated lime, soda ash, sodium hydroxide, ammonia, calcium peroxide, kiln dust and fly ash (Skousen et al. 1993, Watzlaf et al. 2004, Akcil and Koldas 2006, Trumm 2010b). The increased pH and alkalinity of the AMD solution accelerates the rate of oxidation ferrous iron and the manganous ion can cause trace elements to precipitate as oxides or carbonates (Hedin et al. 1994, Johnson and Hallberg 2005). The solution then needs to then be passed through a settling tank where ferric oxide precipitates form and settle out of solution (Akcil and Koldas 2006). This type of treatment generates large amounts of sludge waste (Johnson and Hallberg 2005).

a) *Open limestone channel*

An open limestone channel (OLC) consists of a drainage channel lined with limestone pieces which AMD can flow down and react with the limestone (Ziemkiewicz et al. 1997, Trumm 2010b). This adds alkalinity to the solution and therefore increases the pH under oxidising conditions (Trumm 2010b). Reaction can be inhibited by coating of limestone by iron hydroxides, calcium sulfate and biological growth (Akcil and Koldas 2006). This is most likely to occur in OLC's with a shallow gradient, <10%, where the flow of AMD is not strong enough to prevent the sedimentation of precipitates (Ziemkiewicz et al. 1997). It is estimated that armouring of limestone in an OLC reduces the reactivity of limestone to 20% that of unarmoured limestone (Ziemkiewicz et al. 1997). Therefore, if

armouring is anticipated, an OLC should be constructed to be 5x longer than would be necessary to treat the AMD with unarmoured limestone. The solubility of limestone is low under atmospheric conditions as reaction with limestone can be buffered by $CO_{2(g)}$ so alkalinity can be limited in channels open to the atmosphere (Hedin et al. 1994, Akcil and Koldas 2006).

b) Anoxic limestone drain

An anoxic limestone drain (ALD) consists of a drainage channel which contains limestone but is sealed off from oxygenated water and the atmosphere, often by burying the channel (Hedin et al. 1994, Cravotta and Trahan 1999, Johnson and Hallberg 2005). Mine water flows through the drain and dissolved CO_3^{2-} is added to the solution, increasing the alkalinity of the AMD (Hedin et al. 1994, Johnson and Hallberg 2005). The anoxic conditions ensure that iron is kept as reduced ferrous iron, Fe^{2+}, to avoid the hydrolysis of ferric iron and formation of iron oxides which can then armour limestone, reducing its reactivity (Hedin et al. 1994, Johnson and Hallberg 2005). The partial pressure of $CO_{2(g)}$ is also increased in ALDs so dissolution of limestone is accelerated and a higher alkalinity can be achieved (Hedin et al. 1994, Johnson and Hallberg 2005). ALDs can be used as a first step, upstream of a constructed wetland where iron and manganese oxides are then able to precipitate and be removed from the solution (Hedin et al. 1994). Placement of an ALD before a constructed wetland has been shown to improve the performance of a constructed wetland (Hedin and Watzlaf 1994). ALD's are however not suitable for AMD which has high concentrations of ferric iron, Al or oxygenated waters as hydroxide precipitates will form and coat the limestone (Ziemkiewicz et al. 1997, Johnson and Hallberg 2005).

c) Reducing and alkalinity producing system

A reducing and alkalinity producing system (RAPS), also known as a successive alkalinity producing system (SAPS) or vertical flow wetland (VFW) consists of a layer of waste organic matter (compost) on top of a layer of limestone (Kepler and McCleary 1994, Jage et al. 2001, Johnson and Hallberg 2005, Trumm 2010b). The AMD solution moves down through the compost where microbial reactions remove oxygen and promote reduction of iron and sulfate (Jage et al. 2001, Trumm 2010b). The AMD then flows through the limestone layer where alkalinity is added to the solution and the pH is neutralised (Johnson and Hallberg 2005). The effluent is then re-oxidised and discharged into a settling pond where precipitates form and settle out of the water column (Jage et al. 2001).

1.3.2 Constructed wetlands

Constructed wetlands consist of a shallow excavated area, which is flooded to create a pond, with emergent wetland plant species growing within the wetland area (Sheoran and Sheoran 2006, Trumm 2010b, Skousen et al. 2016). Constructed wetlands may have a layer of limestone at the bottom of the pond if oxidising conditions are desired or compost if reducing conditions are desired (Trumm 2010b). Wetlands are unique in the fact that both oxidising and reducing reaction and processes can occur simultaneously within a wetland environment (Sobolewski 1999). Treatment of AMD with a constructed wetland aims to emulate natural processes occurring in wetlands, such as sedimentation, adsorption of dissolved chemicals to the substrate, formation of hydrolysed metal oxides,

microbially-mediated oxidation or reduction processes and uptake of chemicals by plants (Figure 1.5; Akcil and Koldas 2006, Sheoran and Sheoran 2006, Skousen et al. 2016).

Slow-moving water and a long retention time allows for sedimentation of particles (Sheoran and Sheoran 2006). Trace element removal can occur through adsorption to charged surfaces in the wetland substrate such as organic matter, clays or metal hydroxides (Sheoran and Sheoran 2006). Pb and Cu are typically adsorbed to wetland substrates more strongly than Zn, Ni and Cd (Sobolewski 1999, Sheoran and Sheoran 2006). Removal of Fe, Mn and Al can occur in constructed wetlands through the formation of oxides, hydroxides and oxyhydroxides (Akcil and Koldas 2006, Skousen et al. 2016). Ferric iron forms a variety of hydrolysis products which can precipitate above pH 3.5 while Al hydroxides can precipitate at a pH of 4.5. Mn oxides can form but first require Mn^{2+} to be oxidised to Mn^{4+} which requires a pH of 8 and typically only occurs after Fe has been removed (Skousen et al. 2016). The formation of iron oxide plaques and rhizospheres around plant roots, which are effective at removing As and Zn from solution, is an important trace element attenuation process occurring in wetlands (Otte et al. 1995, Batty 2003). Oxygen released through plant roots can enhance ferrous iron oxidation (Johnson and Hallberg 2005).

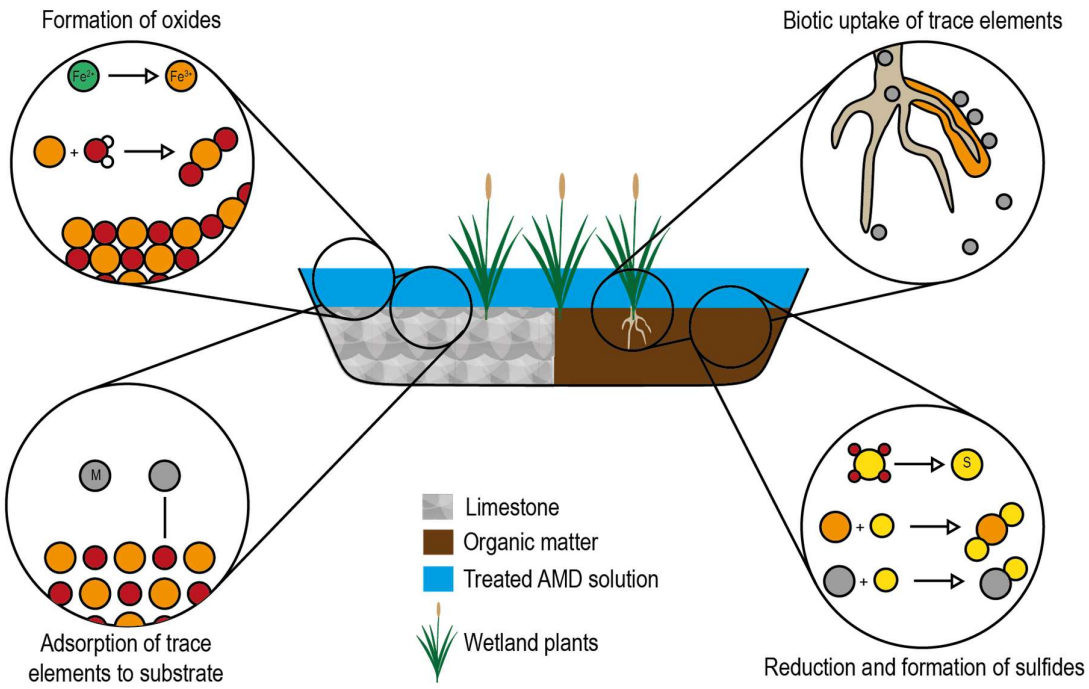

Figure 1.5 Trace element attenuation processes that can occur within a constructed wetland. a) The formation of oxide surfaces, for example, through the reduction and hydrolysis of iron (Equations 1.9 and 1.10). b) The adsorption of trace elements (M^+) to a surface in the substrate, for example, an iron oxide surface. c) The uptake of trace elements through plant roots or the retention of trace elements to an iron plaque around the plant roots. d) The formation of pyrite or metal sulfides through the reduction of sulfate to sulfide and the combination of sulfide with cationic metals (Equations 1.11 and 1.12).

1.3.3 Sulfate-reducing bioreactors

Sulfate-reducing bioreactors (SRBR's) are an adaptation of the RAPS/VFW with the specific aim of utilizing the function of sulfate-reducing bacteria to catalyse the reduction of sulfate to sulfide. The subsequent formation of sulfide mineral precipitation thereby removes sulfate and trace elements from the AMD solution. SRBR's consist of a substrate which contains simple carbon molecules and an alkalinity source (Dvorak et al. 1992, Gusek 2002, Neculita et al. 2007). A key advantage of SRBR's is the use of waste material as the substrate medium (Gusek 2002). This can include wood chips, sawdust, hay and straw, mushroom compost, animal manure (Gusek 2002, Neculita et al. 2007). Additionally, simple carbon sources, such as methanol and lactate can be added to enhance bacterial activity (Gusek 2002, Neculita et al. 2007). Bacterial activity is limited at low pH so an alkalinity source is required to raise the pH to a suitable level in order for sulfate reduction via microbial activity to be sufficient (Dvorak et al. 1992). For some systems the substrate can be a mixture of organic carbon and alkalinity producing media (eg. compost and limestone mixture), or the substrate can be a material which contains both an organic carbon source and produces alkalinity on reacting with the AMD (e.g. mussel shells. Jacob et al. 2008, Uster et al. 2015). Both bacterial sulfate reduction and the dissolution of limestone generate alkalinity and raise the pH of an influent AMD solution (Equations 1.17 and 1.18; Dvorak et al. 1992).

$$2CH_2O + SO_4^{2-} \rightarrow 2HCO_3^- + H_2S \quad \text{(Eqn 1.17)}$$

$$CaCO_3 + CO_2 + H_2O \rightarrow Ca^{2+} + 2HCO_3^- \quad \text{(Eqn. 1.18)}$$

SRBR's enable the reduction of sulfate and removal of several trace elements through the formation of insoluble sulfides (Equation 1.12; Johnson and Hallberg 2005, Neculita et al. 2007). Removal of Al by bioreactors is not well understood. Gusek (2002) indicates that the formation of Al hydroxides such as gibbsite is avoided in SRBR's whereas Dvorak et al. (1992) found that Al could be successfully removed through the formation of $Al(OH)_3$ in an SRBR presumably, as Al does not form a stable sulfide. Sulphur removal occurs via three different mechanisms: acid volatile sulfide (AVS) formation of mono-sulfide precipitates, conversion to FeS_2 or S^0 (CRS – chromium reducible sulfur) and removal in effluent as unreacted H_2S (Dvorak et al. 1992). It is noted that H_2S released in the effluent of the SRBR can have a toxic effect on the receiving environment due to its direct toxicity to aquatic life and ability to re-oxidise to H_2SO_4 (Dvorak et al. 1992). It is necessary to completely neutralise the acidity of the solution to prevent H_2S from forming (Dvorak et al. 1992). This can be done by passing the solution through an alkalinity source such as limestone. Microbial activity decrease with temperature but can continue to function in temperatures approaching freezing (Kepler and McCleary 1994, Gusek 2002).

1.4 The role of geochemical modelling in mine remediation

A model is a simplified version of reality which can help to explain why phenomena occur and be used to make predictive assessments of a system. Models can be conceptual, based on empirical results or numerical. Numerical and empirical models can be written into equations and computer code. However, as a model is reality simplified

it will not be accurate in all situations. Improved understanding of a system can be achieved through constructing a conceptual model of the system then testing the model against further empirical data in order to assess its limitations.

In aquatic geochemistry, the chemical processes occurring in a system such as that of a mining site have been modelled and codified into geochemical modelling programs such as PHREEQC (Parkhurst and Appelo 2013),. The PHREEQC code as applied to the conceptual model of a mining site has be used to quantify trace element speciation and mobility (Watten et al. 2005, Rötting et al. 2008, Bäckström and Sartz 2011). Processes than can be modelled with the PHREEQC code included calculating the speciation of elements in a solution, the saturation index of minerals that can be formed by the solution constituents, and the degree of sorption of trace elements onto a mineral surface provided that the required data is input into the program (Figure 1.6).

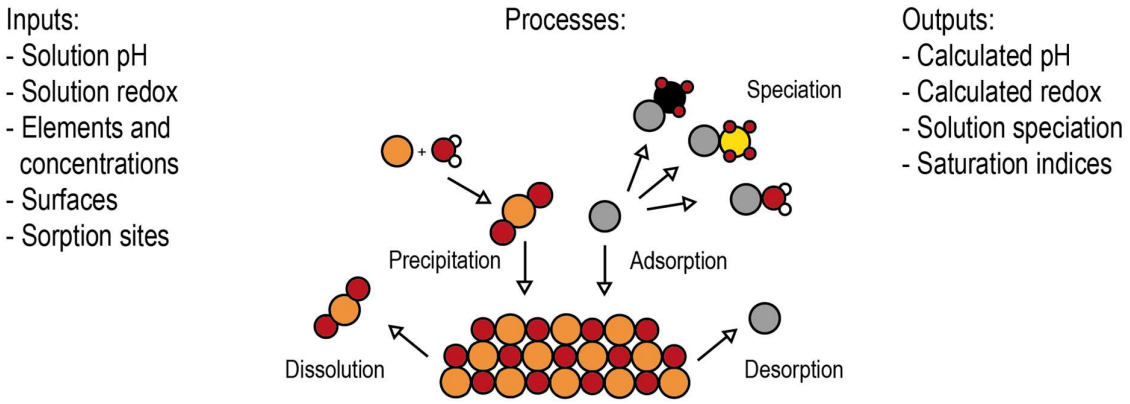

Figure 1.6 Inputs, processes and outputs of an AMD system modelled by the PHREEQC code.

1.4.1 Processes modelled with PHREEQC code

Speciation and toxicity

Speciation modelling in PHREEQC calculates the distribution of dissolved species a trace element may be present as. A trace element can be present as the free ion or many different complexes that are stable under a specific set of physicochemical conditions. As postulated in the Free Ion Activity Model (Campbell 1995, Brown and Markich 2000) and the Biotic Ligand Model (Di Toro et al. 2001, Santore et al. 2001), the free ion is the species which is usually most toxic to aquatic organisms. Therefore, as shown by Waters and Webster-Brown (2013) PHREEQC speciation modelling can be successfully used to predict the degree of toxicity of trace elements such as Al in water bodies receiving AMD. This can be useful for mine remediation planning and environmental impact assessment. For example, Park et al. (2013) identified typical pH ranges where Cu, Zn and Ni transition from being present mainly as free ions to being complexed by carbonate, oxide or hydroxide ligands.

Geochemical modelling carried out with PHREEQC assumes that the system is at thermodynamic equilibrium. However, when modelling systems at dis- or pseudo-equilibrium (eg. in moving water systems) the metal speciation may be influenced by non-thermodynamically stable species which persist due to slow reaction kinetics (Batley et al. 2004). It is therefore, important to treat any models with caution and test out the model in a real world situation.

Saturation with respect to mineral phases

Geochemical modelling programs such as PHREEQC are commonly used to calculate the saturation indices of minerals in mine water in an AMD system (Brown et al. 1998, Balistrieri et al. 2007, Robles-Arenas and Candela 2010) or during treatment (Navarro and Martínez 2010, Bäckström and Sartz 2011, Navarro et al. 2011, Freitas et al. 2013). The saturation index of a trace element-bearing mineral indicates whether the trace element in question is thermodynamically favoured to be mobile in the solution (saturation index < 0.0) or immobilised due to its incorporation into a mineral precipitate (saturation index ≥ 0.0), and the likelihood of reactive materials dissolving when coming into contact with AMD waters. These calculations can be used to identify optimal treatment by promoting the formation of trace element-bearing precipitates (Bäckström and Sartz 2011, Navarro et al. 2011, Freitas et al. 2013). Conversely, a treatment that causes a trace element-bearing mineral phase to dissolve may also cause other trace elements that were adsorbed/co-precipitated with the mineral to also be mobilised (Navarro and Martínez 2010). However, not all phases with a positive saturation index will actually form, some may be prevented from proceeding by the reaction kinetics (Nordstrom 1999, Malmström et al. 2004)

Many studies have used saturation index modelling to predict and understand AMD neutralization processes. For example Rötting et al. (2008) found that due to armouring of limestone, mainly by gypsum and to a lesser extent Fe precipitates, the reactive surface area of calcite had to be decreased in modelling so that output solution predicted matched the effluent chemistry pH and dissolved Ca concentrations. Brown et al. (1998) used saturation indices calculated by PHREEQC to determine that a groundwater AMD plume was neutralised by carbonates in the aquifer to form a transition zone. However, behind the transition zone was an acidic zone where calcite was undersaturated indicating that supply in the aquifer had been exhausted by the AMD plume. Similarly, Pérez-López et al. (2011) used modelling of saturation indices to find the optimal solid:liquid ratios in an AMD treatment system so that as little as possible alkaline reagent was left over. Modelling of saturation indices was used by Watten et al. (2005) were used to show that for the hydraulic retention time used in trials, equilibrium between limestone and sulfuric acid was not reached and the maximum alkalinity able to be added to the solution was not achieved with such a short retention time.

Saturation index calculations have also been used to predict which mineral phases may precipitate in AMD systems, both iron oxyhydroxides and other secondary minerals. For example, gypsum [CaSO4] may be formed as secondary mineral following calcite dissolution by sulfidic waters (Brown et al. 1998); jurbanite [$AlOHSO_4$] may be formed by reaction between Al and sulfate (Brown et al. 1998); basalumnite may form in an “Al precipitate zone” but re-dissolve and precipitate below dissolving calcite as an AMD treatment system ages (Rötting et al. 2008).

Analysis of solid phase samples by XRD and SEM-EDS can be used in parallel with PHREEQC calculations to confirm the formula of freshly-formed trace element-bearing phases (Tonkin et al. 2002, Pérez-López et al. 2011). For example, Tonkin et al. (2002) found that although there was good agreement between the amount of Fe and Al particulates predicted to form in fractions of river water mixed with mine drainage water with measured results, the particulates were highly amorphous in nature, especially at higher pH (~6). Therefore, when predicting adsorption of Cu, Pb, As, Mo and Sb to the freshly formed particulates, XRD data is less important for determining which iron oxide phase should be used as the sorbing surface. However, even with matching the surface used in sorption modelling with that determined by XRD, predicting the degree of adsorption of As, Mo and Sb to the iron oxide surface was poor and the predicted degree of adsorption of Cu and Pb was better predicted (Tonkin et al. 2002).

PHREEQC saturation index modelling also has proved useful for predicting changes in AMD chemistry during oxidation by atmospheric oxygen. The degree of saturation of trace element bearing phases can change when groundwater seepage from an AMD site emerges and becomes oxygenated (Robles-Arenas and Candela 2010). Significant precipitation of trace element-bearing phases was predicted where AMD waters emerge from underground. In areas with a large seasonal fluctuation in rainfall, saturation index calculations in PHREEQC have predicted high concentrations of dissolved AMD trace elements during seasons of high rainfall, but high rates of mineral precipitation during seasons of low rainfall and high evaporation (Lachmar et al. 2006). Hiller et al. (2013) noted than PHREEQC modelling of mine water emanating from tailings impoundments showed no Cu-bearing minerals with a positive saturation index indicating that the concentration of Cu in the mine drainage water was controlled instead by adsorption. Park et al. (2013) found that Cu precipitated from a synthetic AMD solution as CuO at a pH of 5.2 while Zn and Ni precipitated from solution as $Zn_5(CO_3)_2(OH)_6$ and $NiCO_3$ at pH 6.6. Therefore, Cu could be selectively precipitated from a mixed solution but Zn and Ni could not be separated due to their co-precipitation at the same pH.

The prediction of secondary mineral phases that precipitate in an AMD system is limited by the availability of thermodynamic data and the inclusion of data that is emerging and improving with time (Pérez-López et al. 2011).

Adsorption to oxyhydroxide AMD precipitates

The degree of sorption of trace elements to phases, such as iron (oxy)hydroxide [$Fe(OH)_3$] (ferrihydrite or hydrous ferric oxide ("HFO")) is modelled using PHREEQC surface complexation calculations. Ferrihydrite is the major mineral surface that trace elements can adsorb to in AMD systems and a comprehensive set of adsorption constants for trace elements adsorption to HFO has been determined (Dzomback and Morel 1990). These constants are incorporated into the PHREEQC code and this includes the heterogeneous (strong and weak) binding sites of HFO (Benjamin and Leckie 1981).

Adsorption modelling has been used to determine whether adsorption is likely to occur along a pH gradient observed in the mixing zone between mine water and a surface water body (Balistrieri et al. 2007, Bäckström and Sartz 2011). Comparisons between field measurements and computer modelling of trace element adsorption to iron-rich suspended sediment have helped to improve the reliability of adsorption modelling. Better agreement between modelled adsorption and field measurements is found when it is assumed that only adsorption to suspended sediment, not to bed sediment, occurs (Smith 1999). Additionally, the presence of sulfate in AMD systems alters the adsorption of trace elements to HFO through the formation of ternary surface complexes. Cu and Zn adsorption to HFO is underestimated, by up to 40% in the presence of SO_4 (Webster et al. 1998, Swedlund and Webster 2001). Similarly, modelled adsorption of Pb, Cu, As, Mo and Sb on goethite [FeOOH] by Tonkin et al. (2002) did not agree well with measured trace element reduction, even though predicted Fe removal through the formation of goethite agreed with measured Fe removal. Tonkin et al. (2002) concluded that the published surface parameters for goethite did not accurately describe the precipitate formed in the mixing solution. The sorption of As, Sb and various heavy metal ions onto Fe oxyhydroxides predicted by PHREEQC were in good agreement with mineralogical data and field data obtained by Hiller et al. (2013). However, Webster-Brown and Lane (2005) found that As adsorption to HFO was overestimated and better agreement between modelled data and measured data was found when it was assumed that only 4-5% of the HFO was available to As for adsorption.

Modelling with PHREEQC code has been used to predict trace element attenuation processes occurring downstream of mining areas and within AMD treatment systems. However, there are no studies that predict the attenuation processes in a receiving environment when remedial works, such as the installation of a treatment system, have been completed. These kinds of study are the topic of this thesis.

Such discrepancies between measured adsorption data and modelled adsorption can lead to improved modelling methods but may also indicate that trace elements are adsorbing to additional surfaces that are not taken into account (Tonkin et al. 2002). Where Al or Mn are present in high concentrations, and there is a pH change sufficient to cause the precipitation of hydrous oxides of Al or Mn, adsorption to these surfaces may account for some trace element removal. Similarly, natural organic matter may act as an adsorbing surface. Some data on the adsorption of trace elements onto these surfaces have been published (Markich and Brown 1999) and can be manually added to the PHREEQC database.

1.4.2 Improving the reliability of modelling with PHREEQC in AMD systems

As new thermodynamic data for mineral surfaces and complex formation becomes available, this can be incorporated into the PHREEQC model. The formation of schwertmannite is a major control on Fe and SO_4 concentrations in AMD environments and therefore it can be useful to add the schwertmannite solubility constant into a model of an AMD system. There are two solubility constants published for schwertmannite (Bigham et al. 1996, Yu et al. 1999) and both have been used to model Fe solubility in AMD environments (Malmström et al. 2004, Balistrieri et al. 2007, Malmström et al. 2008, Rötting et al. 2008, Robles-Arenas and Candela 2010,

Bäckström and Sartz 2011). The adsorption of trace elements onto schwertmannite was found to be enhanced relative to adsorption onto HFO, leading to the discovery of ternary surface complexes on SO_4-rich iron oxides (Webster et al. 1998).

The hydrolysis and solution complexation constants for Co from Turner et al. (1981) was used by Balistrieri et al. (2007). Adsorption constant sets for Cd, Co, Cu, Ni, Pb and Zn of Tonkin (2002) and Swedlund and Webster (2001) were used by Balistrieri et al. (2003) and Balistrieri et al. (2007) to model the adsorption of these trace elements to Fe precipitates formed during the mixing of AMD with ambient river water. Surface complexation reactions developed for Al_2O_3 by Paulson and Balistrieri (1999), were also used by Balistrieri et al. (2007) to show that adsorption of trace elements to freshly formed Al particulates was not a major attenuation process where Fe particulates were abundant. Additionally, the interactions between trace elements and natural organic matter, such as that of Markich and Brown (1999) can be incorporated into PHREEQC (Waters and Webster-Brown 2013).

Many of the processes modelled with PHREEQC can occur within a moving water system and so 1D transport models have been used to determine how the modelled reactions evolve during transport. The simple 1D transport model available in PHREEQC was successfully used by Brown et al. (1998) to model groundwater transport in an AMD environment. Malmström et al. (2004 & 2008) coupled PHREEQC to another program to create the LaSar-PHREEQC reactive transport model for AMD groundwater transport. Similarly, Rötting et al. (2008) used the RETRASO reactive transport model from Saaltink et al. (2004) in conjunction with PHREEQC to model the transport of AMD through a dispersed alkaline substrate treatment system.

Given the drive to improve model reliability in both natural and experimental systems involving AMD discharge, and the common use of PHREEQC in predicting AMD discharge chemistry and the processes affecting trace element mobility and toxicity, it is surprising that few predictions of mine remediation efficacy appear to have been checked for accuracy on a remediated site.

1.5 Research rationale and objectives

The overall aim of this research project is to investigate the effectiveness and reliability of geochemical modelling, using PHREEQC code, in the prediction of the chemistry and toxicity of contaminant trace elements released by mining, on past (present and future) mine sites in New Zealand.

Three case study sites were used in this research and were chosen to be representative of the types of mines found in NZ and the risks associated with different types of mines. At each of these sites the impacts of mining on ecological health were investigated and the trace elements involved in degrading the aquatic ecosystem were determined. The processes attenuating toxic trace elements in mine drainages were determined through both analysis of collected samples and geochemical modelling. Through the comparison between measured and

modelled data, the efficiency of remediation works and the accuracy and reliability of the geochemical models in PHREEQC were evaluated.

New Zealand has a temperate climate, in contrast to warmer more arid regions where mining and mine remediation techniques have usually been developed and geochemical models tested. In addition, New Zealand topography, particularly in mining areas, is steep with sudden changes in land form. There is also a social aspect to mining and mine remediation, as mining often occurs close to small communities or within relatively pristine environments. As a country New Zealand takes pride in a "clean green" image and growth of the New Zealand economy, through tourism, is based on promoting that image. Pride in this image drives professionals in the mining industry to perform to best practises and be leaders in global mining ethics.

1.6 Thesis overview

This thesis is presented as six chapters. The first chapter outlines the context in which this research has been undertaken. The second chapter outlines the methods used in this research. This includes the selection of the sites used in this research, the methods employed during field work to collect samples and in-field data, the analytical methods used to obtain data from samples and how the analytical data was used to construct geochemical models. Chapters' three to five are research chapters, each focussed on a case study site, and seek to answer the research questions outlined in section 1.5. Each research chapter contains an introduction to the site, a short description of the methods used to collect and analyse data from the site, the results of the research and a discussion of the results.

Chapter 3 describes the geochemical processes occurring at Tui Mine, an epithermal mineral deposit mine that was remediated five years prior to this study. The results of water and sediment analysis are presented along with geochemical modelling of the metal removal processes that have occurred at the site since remedial work was completed. This chapter seeks to answer the following research questions:

- What is the current state of the streams draining Tui Mine, encompassing stream water chemistry, sediment chemistry, and ecology of the streams?
- How does the current state of the streams compare to the pre-remediation state?
- Can geochemical modelling reliably predict the attenuation processes occurring in these streams, particularly that of Fe, Cu, Pb and Zn?
- Could geochemical modelling have been used to predict the post-remediation water and sediment quality to achieve a better post-remediation result?

Sections of this chapter have been published in the conference proceedings of the 2016 and 2017 Australian Institute of Minerals and Mining (AusIMM) new Zealand branch annual conference ("Geochemical Modelling of Metal Toxicity in the Tui Mine Catchment, Te Aroha, NZ." (Fairgray et al.

2016), "Release of toxic trace elements from contaminated stream sediment at Tui Mine, Te Aroha, New Zealand" (Fairgray and Webster-Brown 2017b)), the in conference proceedings of the 2017 Waterways Postgraduate Student Conference ("The Fate of Toxic Trace Elements at Tui Mine" (Fairgray and Webster-Brown 2017a)) and Mine Water and the Environment "Testing geochemically modelled predictions of trace element toxicity and bioavailability at a rehabilitated mine site Mine Water and the Environment." Fairgray, M., et al. (Published online 2019). Mine Water and the Environment.

In Chapter 4 the geochemical processes occurring at Puhipuhi Mine, an epithermal mineral deposit mine which has not had any remedial work carried out are described. The results of water and sediment chemistry analysis are presented. The metal removal processes occurring in streams draining the area are constructed from the data. From the model, the problem areas for remedial work are highlighted. This chapter seeks to answer the following research questions:

- What is the current state of the streams in the Puhipuhi area, encompassing stream water chemistry, sediment chemistry, and ecology of the streams?
- How does historic mining of Hg continue to affect stream water and sediment quality and impact biota in the affected streams?
- Can geochemical modelling reliably predict how trace elements, in particular Hg, are attenuated downstream of the mine?

Sections of this chapter have been published in the conference proceedings of the 2016 Waterways Postgraduate Student Conference ("Spatial distribution and bioavailability of Mercury and other toxic trace elements in the Puhipuhi catchment, Northland" (Fairgray and Webster-Brown 2016b)), in the conference proceedings of the 2016 and 2017 New Zealand Freshwater Sciences Society (NZFSS) annual conference ("Spatial distribution and bioavailability of Mercury and other toxic trace elements in the Puhipuhi catchment, Northland" (Fairgray and Webster-Brown 2016a), " The impact of historical mining activity on aquatic macroinvertebrates at Puhipuhi, Northland, New Zealand" (Fairgray et al. 2017a)) and in the conference proceedings of the International Society for Environmental Biogeochemistry (ISEB) 23rd International Symposium ("The impact of historical mining activity on aquatic macroinvertebrates at Puhipuhi, Northland, New Zealand" (Fairgray et al. 2017b))

Chapter 5 describes the geochemical processes occurring at Bellvue Mine, an acid forming coal mine that was remediated during the course of this research. The results of water chemistry analysis both before and after the installation of sulfate-reducing bioreactors at the site are presented. Through these results the efficacy of the treatment tanks is assessed in terms of the geochemistry of the treatment effluent as it enters Cannel Creek.

Geochemical modelling was used to predict metal removal processes taking place in the bioreactors and in Cannel Creek where the bioreactor effluent enters the stream. This chapter seeks to answer the following research questions:

- What is the pre-remediation state of the streams in the Cannel Creek catchment, in terms of stream water and sediment chemistry of the streams?
- How does water and sediment quality in Cannel Creek change following the installation of a mine drainage water treatment system in the upper section of the catchment?
- How do conditions in Cannel Creek, following the installation of a treatment system compare to the conditions predicted by geochemical modelling?
- Can geochemical modelling reliably predict how trace elements, particularly that of Fe, Al, Zn and Ni, are attenuated in the treatment system and downstream of the treatment system?

Sections of this chapter have been published in the proceedings of Goldschmidt 2018 ("The use of redox pairs to model bioreactor processes in the treatment of acid mine drainage" (Fairgray et al. 2018b)), the conference proceedings of the 2018 AusIMM New Zealand branch annual conference ("Water chemistry changes in Cannel Creek following remedial work of Bellvue Mine AMD" (Fairgray et al. 2018d)), the conference proceedings of the 2018 Waterways Postgraduate Student Conference ("Changes to the water chemistry of Cannel Creek following remedial work of Bellvue Mine" (Fairgray et al. 2018a)), and the conference proceedings of the 2018 NZFSS annual conference ("Changes to the water chemistry of Cannel Creek following remedial work of Bellvue Mine" (Fairgray et al. 2018c))

The research chapters are followed by a synthesis chapter where the results from each site are compared and contrasted to draw out useful outcomes for the use of PHREEQC. Chapter 6 integrates the findings of the previous three research chapters and compares the reliability of the PHREEQC geochemical model in the different situations in order to make recommendations on how PHREEQC can be best used to optimise mine remediation. This chapter also presents suggestions for future work to further test the modelling reliability in AMD site assessment and remediation.

CHAPTER 2

METHODOLOGY

Figure 2. Sample collection at Bell11. Photo: Jenny Webster-Brown

This chapter provides information on the selection of study sites to be used in this research, the sampling procedure, the analytical methods used to determine water and sediment chemistry and a description of the geochemical modelling procedure. More detailed information about the individual study sites is given in subsequent chapters relating to each study site.

2.1 Study site selection

This research was completed as part of the Centre for Minerals Environmental Research (CMER) project entitled "The New Zealand Mine Environment Lifecycle Guide" (MELG). The MELG project put together a series of guides structured around different mineral deposits mined in New Zealand including epithermal gold deposits, mesothermal and alluvial gold, potentially acid forming (PAF) and non-acid forming (NAF) coal deposits (Cavanagh et al. 2015a, Cavanagh et al. 2018a, Cavanagh et al. 2018b, Cavanagh et al. 2018c). These MELG's focus on gold and coal mining as this encompasses the majority of current mining operations in NZ (Cavanagh et al. 2015a), although elements besides gold are currently mined, have been mined in the past (White 1986, Sabti et al. 2000, Wilson et al. 2004a) and different elements can be expected to be mined in the future (Durance et al. 2018, Morgenstern et al. 2018). From these mineral deposit types, case study sites can be selected to represent the types of mines that commonly occur in New Zealand.

2.1.1 Epithermal mineral deposits

Epithermal mineral deposits are found in geothermally active areas or areas with fossil geothermal activity (Henley et al. 1985). They are formed through the transport of elements to the upper sections of the earth's crust by hot water flow paths related to volcanic activity (Ellis and Mahon 1964, 1967, Craw et al. 2005, Cavanagh et al. 2015a).

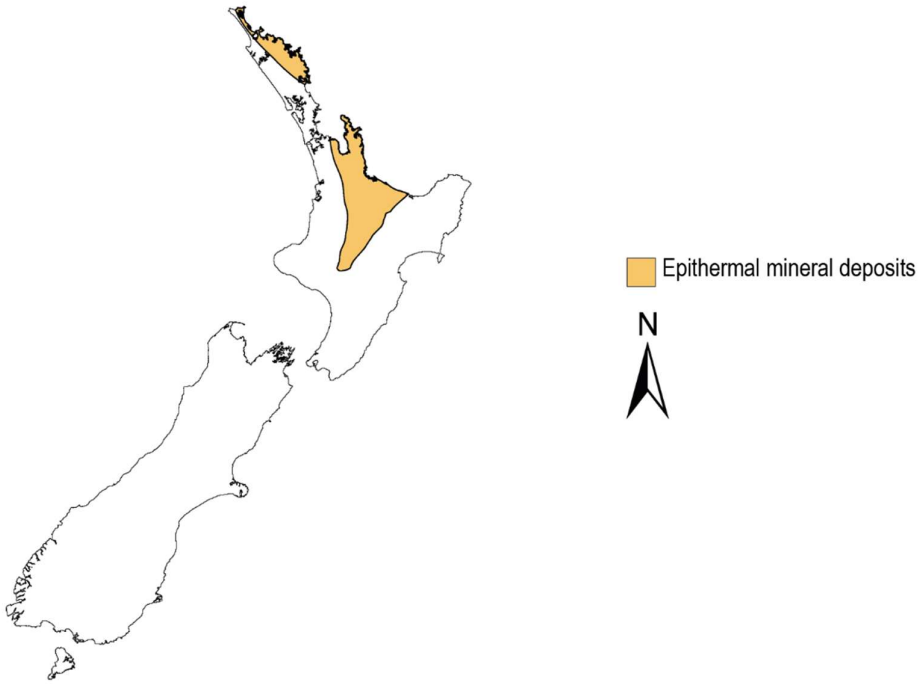

Figure 2.1 The location of epithermal mineral deposits in New Zealand (Cavanagh et al. 2015a).

Epithermal mineral deposits form in the top 1.5km of the crust and may contain elements such as Au, Ag, Zn, Cu, Pb, As, Sb, Cd, Hg, or Mn (Cavanagh et al. 2018a). They commonly include veins or stockworks of new minerals compared to surrounding host rock, as well as alteration zones where host rock minerals change composition and

recrystallize. Common minerals associated with epithermal mineral deposits include quartz, carbonates, clay minerals and sulfides such as pyrite, chalcopyrite, sphalerite and galena (Cavanagh et al. 2018a). These types of deposits are found in the Northland, Waikato and Bay of Plenty regions of New Zealand (Figure 2.1).

In Northland, epithermal mineral deposits are found within the Purua beds and are Hg-rich (Edbrooke and Brook 2009, Cavanagh et al. 2015a). The northland mineral deposits have been mined for mercury and silver at Puhipuhi. This area has also been prospected for gold (Christie and Brathwaite 1995, McLean 2016, Hobbins 2018) but as yet no gold mine has been opened. Mercury is also found at Ngawha hot springs but has not been mined (Davey and Van Moort 1986).

In the Waikato and Bay of Plenty regions, epithermal mineral deposits are found in the Coromandel area, and extend down toward the Taupo Volcanic Zone (TVZ, Figure 2.1; Leonard et al. 2010, Cavanagh et al. 2015a). The Waikato epithermal mineral deposits are found within the Whitianga group, Waiwawa group and Kuaotunu group deposits. The Coromandel area has been extensively mined for gold, both historically and curently, and historically for base metals. Coromandel goldfield mines include the active Martha Mine (including the Favona, Trio and Correnso extensions) at Waihi, Golden Cross Mine, Tui Mine and many other smaller historic mines (Brathwaite and Christie 1996, Cavanagh et al. 2018a). In the TVZ, no active mining of hard minerals has taken place but geothermal energy from the active epithermal system is used to generate power (Cavanagh et al. 2015a).

Northland

Mining of alluvial silver at Puhipuhi occurred between 1890 and 1901 and mining of mercury began in 1910 and continued until 1946 (White 1986, Locke et al. 1999, Hampton et al. 2004). Mercury in stream waters and sediments downstream from Puhipuhi Mine and uptake of Hg by shellfish was discovered in 1973 (Hoggins and Brooks 1973) and the mobility of Hg and As from mineralized rock was assessed out in 2000-2005 (Craw et al. 2000a, Craw et al. 2002, Craw 2005). Pathways for Hg contamination were identified (Gionfriddo et al. 2015) but no remediation work has been completed to address the environmental impacts of historic mining in Northland.

Coromandel

Many gold mines operated around the Coromandel peninsula and Karangahake Gorge at the peak of production in the Hauraki goldfields between 1880-1950 (Brathwaite and Christie 1996). As well as these early mines, there are three major modern mines, Golden Cross Mine, Martha Mine and Tui Mine in the Coromandel area for which the environmental effects of the mining and outcomes of rehabilitation works are known.

Golden Cross Mine operated between 1892 and 1917, and again between 1991 - 1998 to produce gold and silver (Boothroyd et al. 2005). At the end of the most recent mining operations a three phase closure plan was implemented (Boothroyd et al. 2005). This included the development of a closure plan, consenting and implementing of the plan followed by monitoring of environmental parameters. Site specific water quality criteria

were developed to ensure that even the most sensitive aquatic species in downstream receiving waters would not be significantly impacted by mine discharge water following closure (Boothroyd et al. 2005). Sediment-bound trace elements with the exception of Mn, including As, Cu, Pb, Zn and Ni, in the Waitekauri River sediments downstream of the Golden Cross mine, cannot be attributed to the most recent mining operations because the concentration of these elements has in fact decreased between 1986 and 2002 (Bogue et al. 2002). The site was revegetated and used for pastoral grazing however, the water treatment plant remains in operation to treat elevated concentrations of Fe and Mn and significant concentrations of Zn and Cu (Whelan 2007). A vertical flow bioreactor was found to be effective at removing Fe, Zn and Cu but had a limited effect on Mn concentrations. Trials of wetland plant efficacy to attenuate trace elements found significant uptake of Fe into plants at the site receiving mine water while moderate uptake of Mn by plants was observed at the bioreactor sites. However, the wetland plants showed less uptake of Zn and Cu (Whelan 2007). Manganese removal was investigated through trial systems consisting of an oxidising system and slag leaching bed at the site (Trumm and Pope 2015). Oxygenation removed 82-96% of Fe and 10% of Mn while the slag leaching bed removed 99% of the remaining Mn. Modelling of this system using PHREEQC indicates that Fe(II) and Mn are limited by saturation with siderite [$FeCO_3$] and rhodochrosite [$MnCO_3$] (Trumm and Pope 2015).

Martha mine at Waihi was operational between 1893-1952 and from 1988 to present to produce gold and silver (Brathwaite and Christie 1996). The mine consists of the Martha open pit and three underground extensions: Favona, Trio and Correnso (Trumm 2016b). The tailings from both the open pit and underground mine workings are contained within two storage facilities (TSF-1A and TSF-2) while the waste rock from the open pit is used to construct embankments around the tailings storage facilities (TSFs). Water collected from within the TSFs contains high concentrations of Fe and Mn and elevated concentrations of other trace elements (Co, Cu, Ni, Zn, Al). This water is currently treated at a water treatment plant before being discharged to the environment but plans to treat this water passively are in development (Trumm 2016b).

Tui Mine operated briefly in the 1880's as a gold mine and then again between 1966 and 1973 as a lead-zinc mine (Brathwaite and Christie 1996, Morrell 1997, Webster-Brown and Craw 2005). The effects of Tui Mine on the surrounding environment were first studied shortly after the closure of the mine (Ward et al. 1976, Ward et al. 1977). The concentrations of heavy metals in the soil due to atmospheric deposition were investigated along with heavy metals in stream sediment and uptake of heavy metals by vegetation around the mine (Ward et al. 1976). Concentrations of heavy metals in the sediment and stream waters from Tui Mine have since been documented in several studies (Tay 1980, Hendy 1981, Pang 1995, Webster 1995, Hickey and Clements 1998, Sabti et al. 2000, Harvey and Webster-Brown 2003, Sharplin 2008). Between 2010 and 2013 major rehabilitation works were carried out at Tui Mine. Consistent monitoring of heavy metal concentrations in stream waters has been carried out since 2010 producing a large data set from which the trends in water chemistry can be determined (PDP 2014). Surveys of macroinvertebrate communities carried out at Tui Mine both prior to and after the rehabilitation works indicated that the reduction in trace elements and acidity in Tui Stream has enabled the recolonization of the stream by

aquatic macroinvertebrate species including sensitive taxa (Hickey and Clements 1998, Coffey 2009, PDP 2013, Gregersen 2016, Harding and Simon, in prep).

Comstock and Jubilee Streams in the Karangahake Gorge were identified by Livingston (1987) as tributaries contributing elevated levels of metals to the Ohinemuri River, and Tui Stream contributing metals to the Waihou River. Webster (1995) found that Cu, Mn and Zn were transported from these tributaries in the dissolved form while Fe was predominantly transported downstream in the particulate form, and As was transported in both the dissolved and particulate-bound form (Boothroyd et al. 2005). Sediment concentration of Cu, Zn, Cd, Pb and As are elevated in the Ohinemuri River and Tui and Tunakohoia Streams indicating the influence of mining operations at Martha Mine and Tui Mine on stream sediment quality (Sabti et al. 2000). Additionally, high concentrations of Au were found in the sediments of the Waitekauri River which drains Golden Cross Mine and significant concentrations of Au were found in the biomass of aquatic macrophytes collected from the Ohinemuri and Waitekauri Rivers.

The concentrations of Cd, Cu, Pb and Zn increased in the Waiomu, Tunakohoia and Tararu Streams downstream of discharges from Monowai Mine, Tui Mine and a small abandoned mine (un-named) respectively. In addition, the taxonomic richness and total macroinvertebrate density reduced in these streams downstream of the mine discharge, concomitant with the increase in trace element concentration (Hickey and Clements 1998). Mine wastes from Monowai, Maratoto and Zeehan Mines were found to contain variable concentrations of Cu, Pb, Zn and As (Cu: 11-75000ppm, Pb: 29-104000ppm, Zn: 57-513000ppm, As: <5-5890ppm). Arsenic concentrations were typically 10x lower than Cu, Pb and Zn. In areas with low pH (2-4) flushing of base metals and retention of As in Fe (oxy)hydroxide cements is favoured. In areas with higher pH (circum-neutral) due to high carbonate content in the ore, base metals are retained in the Fe (oxy)hydroxide cements and As is flushed from the system (Craw and Chappell 2000).

Of the Hauraki goldfield mines, only the larger modern mines have received attention regarding their environmental impacts and remedial works have been completed at these sites.

2.1.2 Mesothermal mineral deposits

Mesothermal mineral deposits are formed by the cooling of underground water at moderate depth (10km;Craw et al. 2005). These deposits are usually non-acid forming due to locally abundant calcium carbonate [$CaCO_3$] and ankerite [$(CaMgFe)_2(CO_3)_2$] (Plumlee et al. 1999). As a consequence, these deposits can produce NMD enriched with As, Sb and various other trace elements.

Mesothermal mineral deposits in New Zealand are only found in the South Island in two belts on either side of the alpine fault (Figure 2.2; Craw et al. 2002, Cavanagh et al. 2015a).

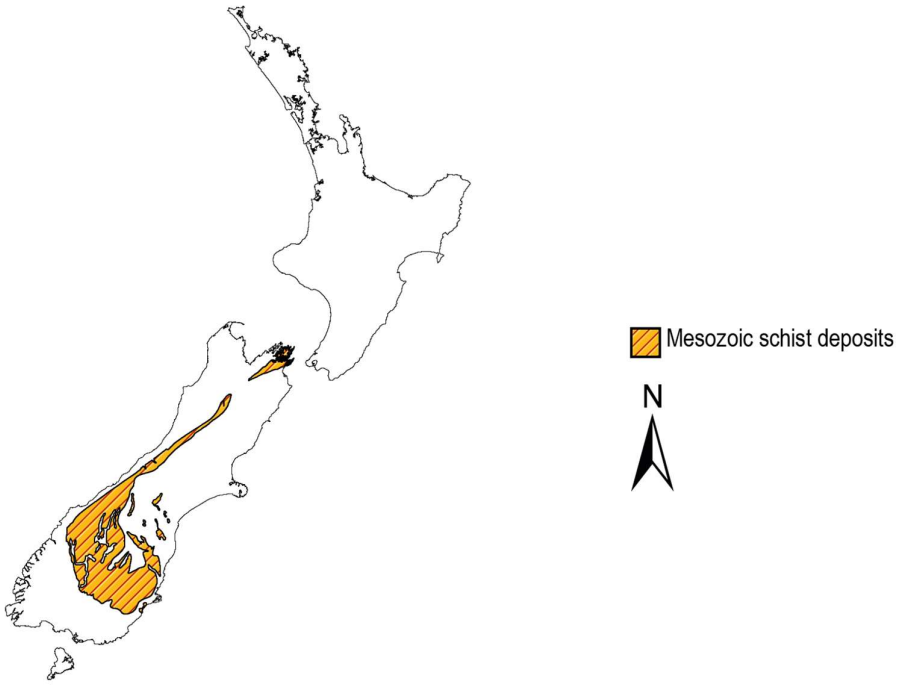

Figure 2.2 The location of mesothermal mineral deposits in New Zealand from Cavanagh et al. (2018b).

Marlborough

In Marlborough, mining and smelting of Sb from Mesozoic schist occurred over a period of almost 30years between 1874 and 1907 at Endeavour Inlet. (Wilson et al. 2004a, b). Most of the sulfide minerals in the tailings had oxidised by 2004 releasing soluble Fe, As and Sb. Dissolved As and Sb are attenuated by adsorption to Fe (oxy)hydroxides within 50m of the smelter and do not entering the adjacent river (Wilson et al. 2004a). Very little Fe (oxy)hydroxide formation occurred in the mine workings so the mine water contains high concentrations of As and Sb but the load of As and Sb from the mine waster is negligible compared to the load from natural weathering of the mineral deposit (Webster-Brown and Craw 2005). No work has been done to treat the mine drainage water at the Endeavour Inlet Antimony smelter.

West Coast gold

Between 1872-1951 around 84 small mines operated in the Reefton goldfields producing a combined total of over 65t Au (Rattenbury and Stewart 2000, Christie and Brathwaite 2003). Gold extracted from these historic mines was mostly coarse-grained free Au from quartz rock rather than Au encapsulated in sulfide minerals as technology to extract Au from sulfides was not available at the time (Milham and Craw 2009).

Exploration resumed in 1980 and 1990 leading to the opening of the modern Globe-Progress Mine in 2007 which encompassed four older mines (Christie and Brathwaite 2003, Madambi and Moore 2013). Water from adits at Globe-Progress Mine contained dissolved As concentrations up to 58.9mg/L and dissolved Sb concentrations up to 19µg/L (Hewlett et al. 2005). Fe-rich precipitates associated with AMD at Globe-Progress Mine contained As in

the range of 10-20 wt%. Because of the abundance of Fe-rich precipitates in AMD from Alborns Coal Mine (discussed in Section 2.1.3) which was hydraulically connected to AMD from Globe-Progress Mine, coal mine AMD could be used to improve the water quality downstream of these two mines through adsorption of As and other trace elements to HFO (Hewlett et al. 2005). The mine ceased production in 2016 and the operators continue to work with regulatory authorities to complete restoration of the site (OceanaGold 2017).

Analysis of As (and Sb) contamination at other smaller mines (Murray Creek, Slab hut Creek, Prohibition Mill, Snowy River battery, Alexander Mine, Golden Lead, Big River) has been carried out (Hewlett et al. 2005, Haffert and Craw 2008, Haffert et al. 2010, Malloch et al. 2017, McLachlan and Craw 2018) and although no effort to remediate these sites has occurred, some natural revegetation of contaminated soils has been observed (Craw et al. 2007a).

Otago gold

Much small-scale mining of alluvial gold has occurred in the Otago region while the major mining of Mesozoic schist occurs at Macraes Mine. Analysis of As and other trace elements around other smaller mine workings (St Bathans, Nenthorn, Barewood, Bullendale, Deepdell Creek) have been investigated (Craw et al. 2000b, Barker et al. 2004, Black et al. 2004b) but no remediation of these sites has been documented.

Macraes Mine, a large-scale modern mine opened in 1990 to extract Au and scheelite [$CaWO_4$] from Otago schist (Webster-Brown and Craw 2005). Arsenic is readily released from the ore during processing and waters on site can have very high concentrations of As. However, due to abundant pyrite in the ore, Fe is also released and Fe (oxy)hydroxides which can scavenge As from solution are present. This enables the discharge water to have low concentrations of As and a neutral pH (Webster-Brown and Craw 2005). Some areas of older tailings at Macraes Mine have been revegetated with pasture grasses (Craw and Rufaut 2017). Macraes Mine has two tailings dams, a concentrated tailings impoundment and a mixed tailings facility (MTF). A core extracted from the MTF in 2017 showed that the deep tailings (77m) contain As associated with sulfide minerals while the shallower tailings (44m) contain As associated with Fe (oxy)hydroxide minerals, a reflection of the ore processing techniques used as the time of tailings deposition (Christenson et al. 2017).

2.1.3 Potentially acid forming and non-acid forming coal

Coal is a combustible sedimentary rock formed through the deposition of plant debris as peat in a swamp environment (Ward et al. 2005). Burial, compaction and heat cause the peat to transform into coal. Coal consists of an organic component and an inorganic (mineral) component (Ward et al. 2005). The organic component is utilised in power generation and steel manufacturing, while the mineral content is an impurity and contains elements that are harmful to the environment. Coal measure rocks usually contain Fe and Al and are commonly enriched with Zn, Ni and Mn plus trace amounts of Cr, Co and Cu, which when oxidised are highly mobile (Cavanagh et al. 2015a). Drainage from coal deposits can range from neutral to highly acidic depending on the

quantities of pyrite and carbonate minerals present in the coal (Pope et al. 2010a, Pope et al. 2010b). ARD can also occur in non-mined areas where coal deposits are exposed.

Coal deposits occur throughout New Zealand in Northland, Waikato, Taranaki, Nelson, Canterbury, West Coast, Otago and Southland Regions (Figure 2.3;Cavanagh et al. 2018c). Of these regions, coal mining currently occurs in the Waikato, Canterbury, West Coast, Otago and Southland regions with the West Coast and Waikato being the most productive region (Barry et al. 1994).

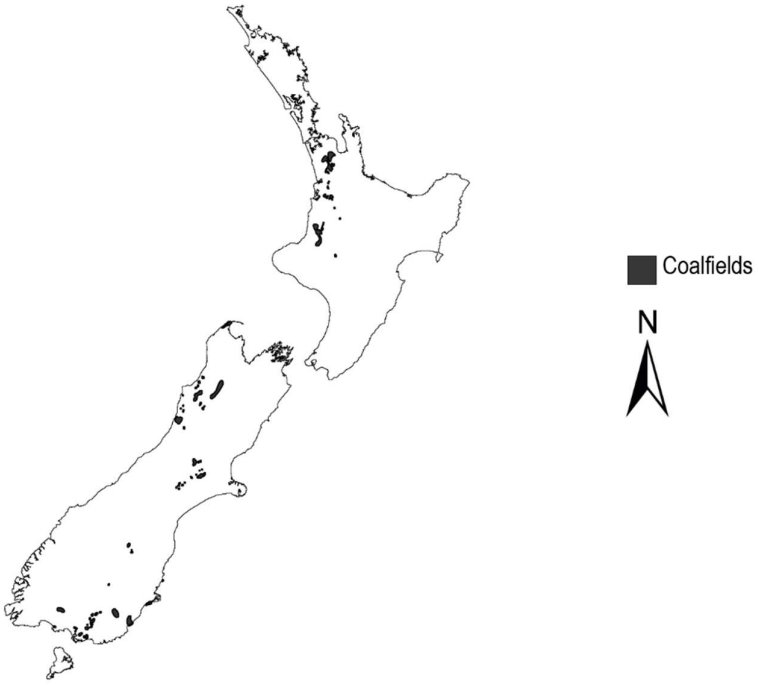

Figure 2.3 The location of coalfields in New Zealand (Cavanagh et al. 2015a).

The Brunner Coal Measures (BCM, West Coast) and some parts of the Gore Lignite Measures (Southland) are potentially acid-forming (PAF) while the Waikato Coal Measures, Paparoa Coal Measures (PCM, West Coast), Morley Coal Measures (Southland) and parts of the Gore Lignite Measures are non-acid-forming (Pope et al. 2010a).

Waikato

The Waikato coalfields cover an area 160km in length and include the Maramarua, Waikare, Huntly, Rotowaro, Kawhia and Tihiroa coalfields (NZPAM 2017). These coalfields are currently mined at Rotowaro and Maramarua for steel production, process heat and power generation (Cavanagh et al. 2015a, NZPAM 2017). Some older areas of these coal mines have been revegetated to pasture and plantation forest (Cavanagh et al. 2018c)

West Coast coal

Mining of coal in the West Coast region occurs within 13 coal fields between Greymouth and Seddonville, north of Westport (Barry et al. 1994). The most productive of these are the Buller, Greymouth, Reefton and Garvey Creek coalfields (Barry et al. 1994). West Coast coal is usually extracted from either the Brunner or Paparoa Coal Measures.

Early mine rehabilitation work focussed on the restoration of terrestrial ecosystems, in particular, the rehabilitation of native forests (Langer et al. 1999, Simcock et al. 1999, Ross et al. 2000, Simcock et al. 2004). In the early 2000's Simcock noted that "coal mining has moved from leaving nature to rehabilitate to establishing forest or plantation forests and using techniques such as DVT." (Simcock et al. 2004). Around this time, some assessments of the extent to which waterways in the West Coast region were affected by AMD were made (Webster and Brown 2001, James 2003, Noble 2003). Methods for assessing AMD impacted sites were developed and protocols for their remediation were embarked upon (Trumm et al. 2003). Additionally, a management strategy to address the environmental impacts of mining on the natural environment was put together (Black et al. 2004a). The first systems to treat AMD were installed at the now closed West Coast Mines: Sullivans Mine and Pike River Mine.

Field trials were carried out with an OLC, VFW and ALD at Sullivans Mine (Trumm et al. 2005a). The VFW, which was constructed with limestone as well as spent mushroom compost, performed better than the limestone only systems (Table 2.1; Trumm et al. 2005a). At Pike River Mine a small-scale VFW containing limestone and spent mushroom compost was constructed and successfully used to treat AMD from the mine (Table 2.1; Trumm et al. 2005b). The efficacy of a limestone column to treat AMD from Blackball Mine was tested also tested but under laboratory conditions (Table 2.1; Trumm et al. 2006). A larger scale reducing system was recommended for Sullivans Mine and Pike River Mine while an oxidising system was recommended to treat AMD at Blackball Mine (Trumm et al. 2005b, 2006). Using the results of the pilot trials, flow charts to determine which system would be best to treat AMD at a particular site were constructed for both passive treatment and active treatment (Trumm 2007, 2008). Another set of field trials with different treatment systems was completed at Herbert Stream, Stockton Mine (Trumm et al. 2007, Trumm et al. 2008). These trials included an OLC, a RAPS and an LLB. The OLC and the LLB consisted of limestone only while the RAPS (VFW) consisted of limestone as well as mushroom compost. All three systems achieved >95% removal of Fe and Al (Table 2.1; Trumm et al. 2007, Trumm et al. 2008).

Analysis of mine drainage chemistry from a selection of West Coast coal mines found that mines extracting PCM coal do no produce AMD whereas mines hosted in BCM coal do produce AMD (Pope et al. 2006, Pope et al. 2010a).

Table 2.1 A summary of the metal removal efficiencies of treatment systems trialled at West Coast coal mines between 2005 and 2008.

Location and System type	Acidity removal (%)	Fe removal (%)	Al removal (%)	Zn removal (%)	Ni removal (%)	Mn removal (%)	pH achieved	Reference
Sullivans Mine								(Trumm et al.
VFW	100	71	59	-	38	26	5.8	2005a)
OLC	0	0	0				<3.0	
ALD	7	12				5	<3.0	
Pike River Mine								(Trumm et al.
VFW	100	99	96	99	95	51	-	2005b)
Blackball Mine*								(Trumm et al.
LC	100	83	82	64	-	8	-	2006)
Herbert Stream, Stockton Mine								(Trumm et al.
RAPS		97	99	80-87		95	6.4-7.4	2008)
LLB		99	99	91		92	7.3-7.9	
OLC		94-95	99			21-74	<5.6	

VFW: Vertical flow wetland, OLC: Open limestone channel, ALD: Anoxic limestone drain, LC: Limestone column, RAPS: Reducing and alkalinity producing system, LLB: Limestone leaching bed.
*Limestone column was trialled using AMD from Blackball Mine under laboratory conditions.

Assessments of the ecology of several mining-impacted stream in the West Coast regions, with a particular focus on tributaries to the Inangahua River (Reefton), was completed (Barnden and Harding 2005, Bray et al. 2009, Gray and Harding 2012, Hogsden 2013). Lower densities of shredder invertebrate species and presence of metal precipitates were found to increase the time taken for organic matter to be processed in AMD-affected streams. (Barnden and Harding 2005). Algal assemblages were found to change across a pH gradient such that AMD-impacted streams contained species of algae that were able to withstand highly acidic environments (Bray et al. 2009). The mayfly species *Deleatidium* spp. was found to be tolerant of dissolved metals and low pH (O'Halloran et al. 2008) and a new metric for determining ecosystem health in AMD-impacted streams was devised (Gray and Harding 2012). However, AMD-impacted streams in the West Coast region were found to contain, in general, partial aquatic invertebrate communities and truncated food webs as compared streams that are not impacted by AMD (Hogsden 2013).

Trials of systems to treat AMD were continued with laboratory-based trials of SRBRs using AMD sourced from Stockton Mine (McCauley 2011). The SRBRs in these trials were constructed with mussel shells, nodulated stack dust (NSD, from cement industry) and limestone as the alkaline material and post peel, pine bark and compost as the organic material. The SRBR's containing mussel shells performed better than those with limestone and a 30% mussel shell composition was found to be optimal for SRBR performance (McCauley 2011).

Laboratory-based trials of systems to treat AMD sourced from Fanny Creek were also completed with an SRBR, a LLB, an OLC and alkaline river water mixing (Mackenzie 2010). The SRBR contained a mix of carbonate and organic carbon sources while the LLB and OLC consisted of limestone only. The SRBR system was found to treat

the AMD most effectively but size requirements and long-term treatment performance were thought to limit the effectiveness of a full-scale treatment system (Mackenzie 2010).

Table 2.2 Summary of metal removal efficiencies of trial treatment systems carried out using mine drainage water from West Coast coal mines between 2014 and 2015.

Location and reactor specifications	Al removal (%)	Fe removal (%)	Mn removal (%)	Cu removal (%)	Zn removal (%)	Ni removal (%)	Reference
Stockton Mine							
Mussel shell down flow reactor	99.7	99.8	-	-	99.6	97.4	(Crombie et al. 2011)
Stockton Mine AMD							
Mussel shell + Organics Short HRT Up-flow reactor	99.5	92.0	29.6	89.6	99.5	83.0	(Uster et al. 2015)
Mussel shell + Organics Long HRT Up-flow reactor	99.7	95.2	55.2	91.8	99.6	95.3	
Limestone + Organics short HRT Upflow reactor	99.0	86.5	19.8	87.4	99.1	81.7	
Limestone + Organics Long HRT Upflow reactor	99.4	91.8	47.1	91.2	96.1	82.7	
Active coal mine (AMD)							
Mussel shell Up-flow reactor	<99	96-<99	0-22	-	98->99	95-<99	(Trumm et al. 2015a)
VFR – Ochre + gravel Down-flow	-	8.3-77	-	-	-	-	(Trumm et al. 2015b) (Sapsford et al. 2015)
Active Coal Mine (NMD)							
VFR – Ochre + gravel Down-flow	-	90-100	-	-	-	-	(Sapsford et al. 2015)
Bellvue Mine							
VFR – Ochre + gravel Down-flow, anoxic AMD	-	0	-	-	-	-	(Trumm et al. 2015b) (Sapsford et al. 2015)
VFR – Ochre + gravel Down-flow, oxidised AMD	-	0-15	-	-	-	-	(Trumm et al. 2015b)
Mussel shell Up-flow, oxidised AMD	99.9	99.8	51	-	98	99	(West 2014)
Mussel shell Up-flow, reduced AMD	86	60	0	-	66	55	
Bioreactor (mussel shell + organics)	86	69	0	-	68	49	
ALD	0	0	0	-	0	0	

Down-flow SRBRs with fresh and weathered mussel shells were trialled at Stockton Mine (Crombie et al. 2011, Weber et al. 2015). Analysis of the substrate after 18 months determined that several zones had formed within the SRBRs. An upper zone where transported sediment was deposited formed at the top of the SRBR. An oxic and transitional zone consisting of Fe then Al precipitates formed in the middle of the SRBR. Finally a zone where sulfate reduction was occurring formed at the bottom of the SRBR on top of the unreacted mussel shell substrate (Weber et al. 2015). Overall the SRBRs resulted in 96-99% removal of Fe, Al, Ni and Zn (Table 2.2; Crombie et al. 2011, Weber et al. 2015).

Vertical flow wetlands (VFR), which contain an ochre layer on top of a gravel bed and a stone bed, were installed at three coal mines (Table 2.2;Sapsford et al. 2015, Trumm et al. 2015b). Removal of Fe from the VFR receiving anoxic mine water from Bellvue Mine was not observed, although a decrease in Fe(II) concentration was observed. Low removal rates of Fe were attributed to the low pH (Trumm et al. 2015b).

Further laboratory-based trials of up-flow SRBRs were completed using AMD sourced from Stockton Mine (Uster 2015). These SRBR's consisted of bark, compost and bark mulch as the organic materials and limestone and mussel shells as the alkaline materials. Removal of Fe, Al, Cu, Zn and Ni was >80% for all systems trialled while removal of Mn was between 19.8 and 55.2% (Table 2.2; Uster et al. 2015). In general, the mussel shell SRBR's resulted in higher metal removal efficiencies and performed better over a longer period of time than the SRBR's containing limestone (Uster 2015). Three mussel shell reactors in series up-flow configuration were constructed at an active coal mine (Trumm et al. 2015a). This treatment system resulted in >95% removal of Fe, Al, Zn and Ni, 0-22% removal of Mn (Table 2.2).Trials using a mussel shell-only SRBR, a mussel shell + organic matter bioreactor and an ALD were also trialled at Bellvue Mine (West 2014). Of these trialled systems, the mussel shell SRBR treating oxidised AMD performed the best (Table 2.2) but permeability of the SRBR was reduced due to precipitation of Fe (oxy)hydroxides within the treatment tank (West 2014). Based on these trials a full-scale mussel shell only SRBR treatment system was developed for Bellvue Mine (Trumm 2016a, Trumm et al. 2016).

Otago and Southland coal

Coal deposits in the Southland and Otago regions are found within the Ohai coalfield and Eastern Southland lignite deposits (Cavanagh et al. 2015a). Characterisation of AMD from Southland and Otago coal mines has been investigated at Kai Point Mine, Newvale Coal Mine, Ohai Coal Mine and Wangaloa Coal Mine (Craw et al. 2006, Craw et al. 2008).

Upon closure of Wangaloa coal mine rehabilitation work was not actively carried out but some natural recolonization of vegetation occurred (Rufaut et al. 2015). The site was revegetated with *Pinus radiata* in the 1980's but acidic drainage water resulted in poor growth (Craw et al. 2006, Rufaut et al. 2015). In 2000-2003, the pine trees were removed and the site was revegetated with native New Zealand species, however, due to high concentrations of Boron (B) and limited soil cover, up to 30% of the plants failed to establish at the site (Craw et al. 2006, Craw et al. 2007b). In spite of this natural colonisation of plant species, which resulted in increased soil pH has allowed for the establishment of ecosystems at the site (Rufaut et al. 2015).

2.1.4 Case study sites chosen

Three historic mine sites at various stages of rehabilitation were chosen as case study sites in this research. These sites were: Tui Mine, Waikato region; Puhipuhi Mine, Northland region; and Bellvue Mine, West Coast region (Figure 2.4). These mines were selected due to the inactive nature of mining operations, contamination of nearby waterways known to be occurring, and there either being remediation work to treat the AMD contamination already

carried out or interest in remedial works taking place at the site (Tay 1980, Craw et al. 2000a, Sabti et al. 2000, Harvey and Webster-Brown 2003, Webster-Brown and Craw 2005, Trumm and Cavanagh 2006, Sharplin 2008). In the case of Bellvue Mine, remedial works were carried out during the course of this research. Details about the history of mining, the impact of mining on the surrounding area and remedial works to address the impacts of mining at these sites can be found in the introduction to the relevant chapters (Chapter 3: Tui Mine, Chapter 4: Puhipuhi Mine and Chapter 5: Bellvue Mine).

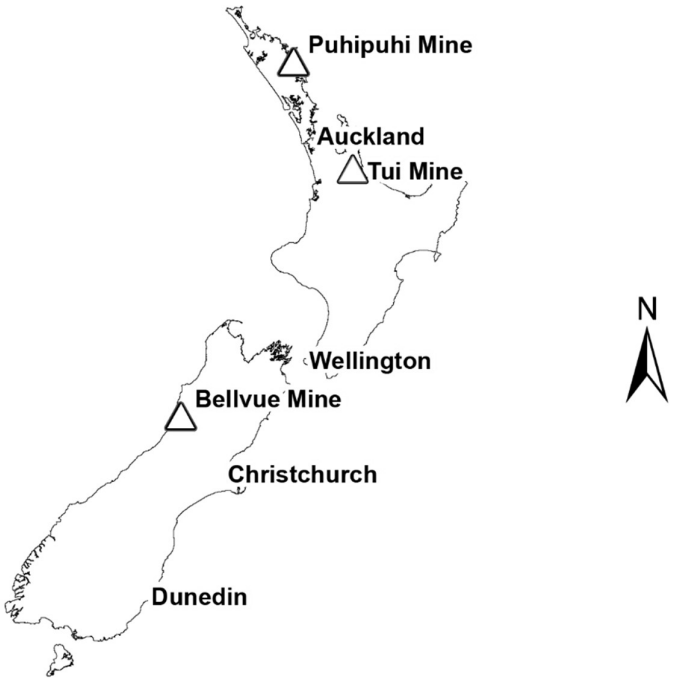

Figure 2.4. Map of New Zealand showing the location of the case study sites used in this research in relation to major cities.

Martha Mine at Waihi and Blackwater Mine at Waiuta were also considered as case study sites. Focus shifted from Blackwater Mine to Bellvue Mine as the plans to install a treatment system at Bellvue Mine developed and funding to complete the installation of the treatment system were secured. Martha Mine was discounted as a case study site as on-site active treatment of AMD was already taking place, and there are low concentrations of trace elements in the discharged mine water.

Within each of these study sites, field data, water samples and sediment samples were collected from 11-16 individual sampling sites. This included control sites either upstream of any mine drainage input, on an un-impacted tributary which feeds into the impacted stream or in a nearby catchment with similar geology. These individual sampling sites were selected based on previous research at the site so that continuity of data was possible and access to the sites was through established routes. Additional, previously untested sites were sometimes included

in between established sites to gain a better understanding of how and where contamination of mine-impacted water occurs within the catchment.

2.2 Sampling methods

Measurements of temperature, pH, conductivity and dissolved oxygen were made *in situ* using either a HACH HQ40d portable multi-parameter meter or a YSI 556 handheld multi-parameter meter. Water samples were collected in sterile high density polyethylene (HDPE) centrifuge tubes. Samples for trace element analysis (one unfiltered and one filtered through a 0.45 µm membrane filter using a handheld syringe) were acidified with 50µL Aristar-grade concentrated nitric acid to achieve a pH of <2. Samples for anion and dissolved inorganic carbon (DIC) analysis were collected in HDPE centrifuge tubes. These samples were refrigerated until analysis. At Bellvue Mine, additional water samples were collected for sulfide analysis, nutrient analysis and dissolved organic carbon (DOC) analysis. Samples for sulfide analysis were filtered through a 0.45µm membrane filter, as for the trace element samples, collected in HDPE centrifuge tubes and preserved by the addition of sodium hydroxide (NaOH) and zinc acetate dihydrate. These samples were also kept refrigerated until analysis. Samples for nutrient analysis were filtered through a 0.45µm membrane filter and collected in a sterile HDPE centrifuge tube. The samples for DOC analysis were collected in a sterile amber glass bottle. Nutrient and DOC samples were kept frozen until analysis. Samples for sediment chemistry analysis were collected in HDPE pottles, from the top 5cm of substrate. The amount of sediment collected varied between sites due to the nature of the streambed substrate but was normally between 100 - 250g.

Flow was measured using a SonTek flow tracker for main channel sites or a bag, fish weighing scales and a stopwatch for small seeps. For sites where flow was measured with the Flow Tracker, a minimum of 10 measurements were made across a transect of the stream, perpendicular to stream flow. Total discharge was calculated by the summation of the depth and water velocity at each station. For small seeps, a thick plastic bag was placed across the entire width and depth of the seep so that all of the flow from the seep flowed into the bag. The bag was held across the seep for a measured time and the amount of water that collected was measured by weight. It was assumed that the bag had a negligible weight as compared to the water collected and that the density of the water was 1kg/L. This process was repeated 3x for each site and the average flow rate was calculated from the readings.

2.3 Analytical Methods - Water

2.3.1 Trace Elements and Major Cations

Water samples were analysed for major cations (Na, Mg, K and Ca) and trace elements (Al, Fe, Mn, Co, Ni, Cu, Zn, As, Cd, Sb, Pb and Hg) by inductively coupled plasma mass spectrometry (ICP-MS). A known volume of aqua regia containing L-cysteine was added to samples for Hg analysis to enhance detection of Hg.

Quality Control and Limits of Detection (LOD)

For each batch of samples tested, six standards were analysed as well as a certified reference material (CRM) at the beginning of each run. A duplicate sample was run for every 10 samples and a 3-point standard check as well as a sample spiked with a 1µg/L solution was tested every 20 samples. Each sample was also spiked with a rhodium internal standard to determine recovery. A deionised water blank was analysed along with each batch of samples. The limit of detection (LOD) for each element was calculated as 3x the standard deviation of the 0.1µg/L standard measurements across all ICP-MS analysis carried out (Table 2.3).

Table 2.3. The average concentration of the deionised water blanks and the limit of detection (LOD) for the elements analysed for using ICP-MS. The number of analyses used to determine the LOD are denoted in parentheses beside each value.

Element	Deionised water blank (µg/L) (n=7)	LOD (µg/L)
Na	8.74	2.22 (n=13)
Mg	1.53	0.33 (n=17)
K	<LOD	2.77 (n=14)
Ca	<LOD	17.9 (n=17)
Al	6.12	0.72 (n=23)
Fe	1.45	1.20 (n=20)
Mn	0.03	0.02 (n=25)
Co	<LOD	0.02 (n=25)
Ni	<LOD	0.04 (n=25)
Cu	<LOD	0.04 (n=24)
Zn	<LOD	0.73 (n=21)
As	<LOD	0.03 (n=25)
Cd	<LOD	0.03 (n=25)
Sb	<LOD	0.17 (n=25)
Pb	<LOD	0.04 (n=25)
Hg	<LOD	0.05 (n=8)

The variability in CRM concentration between runs (n=24) was <10% for most elements, except for Cu (10.7%), Cd (25.2%), Pb (12.5%) and Co (10.8%). The variability of the duplicate samples was within 10% for all elements and samples analysed when above the LOD. Recovery of a 10µg/L spike was >90% for most elements and samples, except for those below the LOD or much greater than 10µg/L. For example, when the spiked sample contained ~500µg/L Fe or Mn, the variability between any two samples was typically greater than 10µg/L, so the %recovery of the spike was masked by the variability of the sample concentration. The average concentration for the deionised water blanks was greater than the LOD for Na, Mg, Al, Mn and Fe, and less than the LOD for all other elements (Table 2.3).

2.3.2 Anions

Water samples were analysed for major anions (Cl, NO_3, SO_4 and PO_4) by high performance liquid chromatography (HPLC) using a Dionex DX-2100 AS-AP Autosampler with an IonPac AS18 ion exchange column (IEC). DIC concentrations were determined by acidifying the sample with ortho-phosphoric acid under a nitrogen gas head

space, generating CO_2 gas from DIC in the sample. The concentration of CO_2 gas in the headspace was then determined with an Infra-red gas analyser (IRGA) then converted to HCO_3 for reporting. The IRGA was calibrated daily before each set of samples was analysed with a calibration curve constructed from 4 standards, made from a stock solution of accurately weighed $NaHCO_3$, and a deionised water blank. For all calibration curves the line of best fit had an R^2 value of >0.97. A deionised water blank was included in each set of samples analysed. This method had a detection limit of 5.23mg/L, as calculated by 3x the standard deviation of the 1mmol/L calibration standard (Table 2.4). The average concentration of the deionised water blanks was 5.79mg/L (Table 2.4).

Quality Control and Limits of Detection (LOD)

A 10ppm standard, a duplicate sample and a deionised water blank were run with each sample batch. Calibration curves were constructed from 8 standards and had an R^2 value of >0.999. The 10ppm standard was within 10% of the nominal value for all anions and analyses. Duplicate samples were all within 5% of each other, except for at concentrations below 1mg/L. The average concentration of the deionised water blanks and the limit of detection (LOD) as calculated by 3x the standard deviation for the lowest standard for each anion is given in Table 2.4.

Table 2.4. The average concentration of the deionised water blanks and the limit of detection (LOD) for anions determined by HPLC and IRGA.

Anion	Deionised water blank (mg/L)	LOD (mg/L)
Cl	0.020	0.005
NO_3	0.096	0.050
SO_4	<LOD	0.150
PO_4	0.020	0.100
DIC	5.79	5.23

2.3.3 Other water constituents

DOC concentrations were determined by high temperature combustion of total and inorganic carbon and subtracting inorganic carbon from total carbon using a Shimadzo TOC analyser (APHA method 5310 B).

Nutrient and sulfide concentrations were determined by UV/Vis spectroscopy. Ammoniacal nitrogen concentrations were determined by the phenate method (APHA method 4500-NH_3 F) where blue indophenol is formed by the reaction of ammonia, phenol and hypochlorite, with nitroprusside added to catalyse the reaction (Eaton et al. 2005). The resulting solution is then analysed spectroscopically at 640nm. Nitrate nitrogen concentrations were determined by the spongy cadmium method where nitrate is reduced to nitrite with spongy cadmium and then reacted with sulphanilamide in acidic conditions to form a diazonium salt (Caspers et al. 1979). The diazonium salt is reacted with N-1-naphthaleneethylenediamine dihydrochloride which produces a pink azo-dye. The resulting solution is analysed spectroscopically at 543nm. Dissolved reactive phosphorous concentrations were determined by the ascorbic acid method (APHA method 4500-P E). Ammonium molybdate and antimony potassium tartrate react under acidic conditions with orthophosphate to form phosphomolybdic acid (Eaton et al. 2005). This acid is

reduced by ascorbic acid to form molybdenum blue. The resulting solution is analysed spectroscopically at 880nm. Sulfide concentrations were determined by the methylene blue method (APHA method 4599-S^{2-} D). N,N-dimethyl-p-phenylenediamine oxalate in sulfuric acid and $FeCl_3$ react with sulfide to produce methylene blue (Eaton et al. 2005). Diammonium hydrogen phosphate is added to the solution to remove the colour of ferric chloride. The resulting solution is analysed spectroscopically at 650nm. Samples with an absorbance greater than 3.5 were diluted 10x before reagents were added and analysis carried out as normal (Dec 2017 samples were diluted 1000x for ammonial nitrogen analysis). Ferrous iron was measured at Belluve Mine, immediately after sampling, by the 1,10-Phenanthroline Method (HACH method DOC316.53.01049).

Quality Control and Limits of Detection (LOD)

The TOC analyser was calibrated before each run using two sets of 5 standards prepared from stock solutions made by dissolving accurately weighed potassium biphthalate (total carbon solution) and sodium carbonate/sodium bicarbonate (inorganic carbon solution) in deionised water. The R^2 value for the calibration curves was >0.995. The detection limit for this method was 0.39mg/L, as calculated by 3x the standard deviation of the deionised water blanks as these had sufficient measurable concentrations of DOC (Table 2.5). The average concentration of the deionised blanks was less than the detection limit.

The spectroscopic methods were calibrated daily before each run with calibration curves of at least 4 points as well as a blank for each set of samples analysed. The calibration curves were constructed from standards of known concentration made from accurately weighed ammonium chloride (ammoniacal nitrogen), potassium nitrate (nitrate nitrogen), Potassium phosphate monobasic (dissolve reactive phosphorous), sodium sulfide (sulfide) which had been dried in an oven overnight and dissolved in a known volume of deionised water in a volumetric flask. The calibration curve for sulfide analysis was constructed from sodium sulfide standards made up in dissolved in deoxygenated deionised water. For these analyses a deionised water blank and at least one standard made up to a known concentration were analysed along with each set of samples analysed. For all calibration curves, the line of best fit had an R^2 value of >0.990 The LOD for these methods, as calculated by 3x the standard deviation of the blanks (Table 2.5). The average concentration for all deionised water blanks were below the LOD (Table 2.5).

Table 2.5. Average concentration of deionised water blanks and LOD for DOC, nutrients and sulfide.

Water Constituent	Average blank concentration (mg/L)	LOD (mg/L)
DOC	<LOD	0.39
NH_4-N	<LOD	0.01
NO_3-N	<LOD	0.05
PO_4-P	<LOD	0.01
S^{2-}	<LOD	0.03

2.4 Analytical Methods - Sediment

Water from wet sediment samples was decanted off while ensuring that no fine sediment was lost. Sediment samples were dried at 40°C until the samples were dry and showed no visible sign of moisture, for very wet

samples this could take up to a week. A temperature of 40°C was used as some samples were thought to contain mercury which could vaporize at higher temperatures. Once dried, the samples were sieved through both a 67µm polyester mesh, supported within a PVC casing, and a 2mm polypropylene sieve, to separate the fine or coarse particulate matter respectively.

2.4.1 Total Sediment Digestions

For total sediment digestions, 0.1g of the sample was accurately weighed into a Teflon beaker which was then digested in hot nitric acid using the method described in Sharplin (2008). One sediment-free blank and one CRM sample (PACS-2 marine sediment) were included in each batch of <67µm samples analysed. A sediment free blank was also included in each batch of <2mm samples analysed. Samples were diluted 10x prior to analysis by ICP-MS. Samples were analysed for major cations (Na, Mg, K and Ca), and trace elements (Al, Fe, Mn, Co, Ni, Cu, Zn, As, Cd, Sb, Pb and Hg). For samples analysed for Hg, a known volume of aqua regia containing L-cysteine was added to enhance detection of Hg (Li et al. 2006).

Quality Control and Limits of Detection (LOD)

As with water samples, a deionised water blank was analysed with each batch of samples, a duplicate sample was analysed for every 10 samples and a sample spiked with a 10µg/L solution was analysed for every 20 samples. Duplicate samples were within 20% of the average value for 92% of samples and elements and within 25% for 98% of samples and elements. For 2 elements and/or samples out of 126 analyses the variability between duplicate samples was 51%-58%, excluding elements that were below the LOD. The LOD was calculated based on 3x the standard deviation of the sediment-free blanks (Table 2.6).

Table 2.6. LOD and measured concentration of trace elements in the CRM samples compared to stated value (Sperling 2010). The number of samples used in the calculation of the LOD is given in parentheses. The measured CRM concentration is given as an average with one standard deviation. Values are in mg/kg except for Al and Fe.

Element	LOD (mg/kg)	CRM stated value (mg/kg)	CRM measured value (mg/kg) (n=4)
Al	120 (n=8)	6.62 ± 0.32 (g/100g)	3.07 ± 3.97 (g/100g)
Fe	360 (n=8)	4.09 ± 0.06 (g/100g)	1.16 ± 0.36 (g/100g)
Mn	19.6 (n=10)	440 ± 19	357 ± 511
Co	0.48 (n=8)	11.5 ± 0.3	11.6 ± 17.0
Ni	1.04 (n=4)	39.5 ± 2.3	44.2 ± 65.4
Cu	1.91 (n=10)	310 ± 12	361 ± 495
Zn	4.20 (n=7)	364 ± 23	368 ± 497
As	9.77 (n=10)	26.2 ± 1.5	28.3 ± 38.9
Cd	0.27 (n=10)	2.11 ± 0.15	2.44 ± 3.36
Sb	1.06 (n=10)	11.3 ± 2.6	3.09 ± 3.96
Pb	2.81 (n=6)	183 ± 8	193 ± 260

All sediment-free blanks were below the LOD. The average concentration (n=4) for the CRM samples was within the certified range for Co and Zn, close to the certified range for all other elements (Table 2.6). Three of the 4 CRM

analyses had a low variability but low accuracy. Homogeneity is only guaranteed by the manufacturer for samples ≥500mg (Sperling 2010). Each sample was only 100mg but the four samples have a combined total of 400mg.

2.4.2 Sequential Extractions

A sequential chemical extraction following the method set out by Leleyter and Probst (1999) and the additional hot nitric acid step of Salvarredy-Aranguren et al. (2008) was used to identify specific phases in the sediment which are accumulating trace elements (Table 2.7). For most steps 10mLs of the extractant was added to the dried sediment, however lower volumes (3-5mLs) were used for reagents in steps 5 and 6. The trace element concentration of fractions 1, 4a, 4b, 4c, 5 and 6 of the sequential extraction were analysed by ICP-MS and fractions 2&3 were analysed by ICP-OES (optical emission spectrometry). The same elements were analysed for in the sequential chemical extraction fractions as for the total sediment digests.

Table 2.7. The sequential extraction scheme of Leleyter and Probst (1999) with an additional final step from Salvarredy-Aranguren et al. (2008). All extractions were undertaken at 20°C, except for Fraction 4c (80°C) and 5 & 6 (85°C).

Target Fraction	Reagent	Reaction time
1. Water soluble	Deionised water	30 min
2. Easily exchangeable	1M magnesium nitrate	2 hours
3. Low pH leachable	1M Sodium acetate at pH=4.50	5 hours
4a. Mn oxides	0.1M hydroxylammonium chloride	30 mins
4b. Amorphous Fe oxides	0.2M ammonium oxalate + 0.2M oxalic acid	4 hours in dark
4c. Crystalline Fe oxides	0.2M ammonium oxalate + 0.2M oxalic acid + 0.1M ascorbic acid	30 mins
5. Organic matter	0.02M HNO_3 + 35% H_2O_2	5 hours
	3.2M ammonium acetate in 20% v/v HNO_3	30 mins
6. Residual (incl. sulfide)	8M HNO_3	3hours

Some sequential extraction fraction labels can have poor specificity for dissolving the targeted mineral phases and the redistribution of elements to other phases during the sequential extraction process is possible (Bacon and Davidson 2008). In this case, the sodium acetate step has been renamed as “low pH leachable” (formerly “bound to carbonates”) to more accurately describe the process occurring during this step and where the elements extracted during this step came from. The nomenclature of target fractions in Table 2.7 is used throughout this thesis.

Quality Control and Limits of Detection (LOD)

Each batch of samples contained a sediment-free blank and either a duplicate sample or a CRM sample (PACS-2 marine sediment). The duplicate sample was consistent to within 30% for all elements and within 10% for all elements except Zn and Cd. The CRM sample was within the range of the total sediment digests. The detection limit for the sequential extraction was the same as for total sediment digests. Agreement between the sum of the sequential extraction fractions and the total sediment digests was variable. For Al, the sum of sequential extract fractions was less than the total sediment digest by up to 50%. For Fe, the agreement between the two values was

within 20% for most samples. For Mn, Cu, Pb, Zn and Cd, the sequential extraction for Tuna2 gave a total concentration significantly higher than the total sediment digest. This is likely a reflection of the heterogeneity of the samples.

2.4.3 Sediment Mineralogy

Sediment samples were also analysed by X-ray diffraction (XRD) and scanning electron microscopy (SEM). XRD was performed by Panda Geoscience on a Philips 1130 diffractometer over a 2θ range from 5° to 62°. SEM was carried out by the author on a JEOL JSM IT-300 variable pressure scanning electron microscope with an Oxford Aztec SDD energy dispersive x-ray analysis system attached.

2.5 Experimental Simulation of Sediment Leaching

Batch leaching experiments were carried out on sediment samples from the Tui Mine area to determine whether the sediment may leach trace elements into overlying water and if so, how rapidly and under what conditions this might occur.

For these experiments, 0.2g of accurately weighed fine sediment (<0.67µm) was added to an acid-washed glass 1L volumetric flask containing deionised water. The volumetric flask was stoppered and the contents mixed by a combination of swirling and inverting the flask. 50mls of the solution was then poured into HDPE centrifuge tubes, swirling the solution between pouring to ensure the sediment remained evenly dispersed through the solution. The tubes containing the solution, together with a deionised water blank were placed on an end-over-end mixer and rotated at a constant speed, then removed from the mixer at predetermined times, ranging from 5mins to 10days. The tubes removed from the mixer were filtered immediately through a 0.45µm membrane filter into clean HDPE tubes. The pH of the leachate solution was measured and recorded. 50µL of ultrapure concentrated nitric acid was added to the filtered leachate to preserve them for analysis of major cations (Na, Mg, K and Ca) and trace elements (Al, Fe, Mn, Co, Ni, Cu, Zn, As, Cd, Sb and Pb) by ICP-MS. Samples were also analysed for calcium (Ca) and carbonate (as HCO_3) to determine whether sedimentary carbonates were being dissolved. Samples for HCO_3 analysis were placed in tubes which had been flushed with nitrogen gas to avoid exchange of CO_2 gas with the atmosphere. Dissolved inorganic carbon (DIC) concentrations were determined by Infra-red gas analysis (IRGA) then DIC concentrations were converted to HCO_3 for reporting. Ca was determined by ICP-MS.

Quality Control

Two sample tubes were removed at each removal time. A sediment-free deionised water blank was also removed after 10days to ensure no contamination from the HDPE tubes occurred. Duplicates of every 10th sample were analysed by ICP-MS. Triplicate samples were not able to be analysed as there was insufficient sample available. The LOD for these analyses were the same as for the water samples. Variability between ICP-MS duplicates were mostly within 10% of each other. Variability between ICP-MS duplicates was greater than 10% for 6 samples and/or elements 6 times out of 84 (7%). Most of the times variability was greater than 10% was for Cu analysis. Variability

between duplicate test samples was within 25% for most samples but was up 100% for Fe analysis for some samples. This variability is shown by error bars on Figure 3.12 in Chapter Three.

2.6 Geochemical Modelling

PHREEQC is a computer program developed by the United States Geological Survey (USGS) to carry out geochemical calculations in aqueous systems. It simulates reactions between aqueous solutions, minerals, gases, solid solutions, ion exchangers and adsorptive surfaces, and calculates the distribution of chemical species between each of the phases present when equilibrium between the reactants is reached (Parkhurst and Appelo 2013). The name PHREEQC is an acronym referring to **pH, re**dox and **eq**uilibrium, the chemistry on which the program is based, in **C** code.

PHREEQC simulates chemical reactions and transport processes that occur in natural waters, polluted waters, laboratory experiments or industrial processes.
PHREEQC can carry out the following calculations:

1. Speciation and saturation index (SI) calculations
2. Batch reactions and 1D transport calculations such as mixing of solutions, surface complexation, dissolution and precipitation of solid phases, and pressure and temperature changes.
3. Inverse modelling, which finds mineral and gas mole transfers which account for changes between an initial solution and a final solution (Parkhurst and Appelo 2013).

Reactions can be thought of as occurring in a beaker. A solution is placed in a beaker, other solutions or phases are added, a reaction occurs between the components in the beaker and a new solution is produced. Such reactions include mixing of solutions, assemblages of pure-phase minerals, solid-solution assemblages, gases, surface assemblages. Transport calculations can be thought of as a series of beakers containing a solution and the solution from the first beaker being added to the second beaker which is then added to the third beaker and so on (Parkhurst and Appelo 2013).

The PHREEQC program comes with six databases of thermodynamic information for different elements, minerals and gases. These databases are ISO, LLNL, MINTEQ.v4, PHREEQC, PITZER, and WATEQ4f (Parkhurst and Appelo 2013). The database files are editable so additional thermodynamic information from other sources can be included in the calculations.

Data for the aqueous system to be modelled is input into the program under headings specifying the water chemistry of a solution and details of any functions to be carried out. Under the “solution” function, the temperature and chemical composition of the initial solution are defined. The concentration of elements in the solution are entered into the program and the electron potential (pE) of the solution is defined using either a set value or

specified to be calculated by the program based on the relative concentrations of two species, that are present in the solution, that make up a redox pair.

Other functions able to be used in PHREEQC, and used in this research, include surface complexation reactions, interactions with other phases at equilibrium with the solution, mixing of two or more solutions and reactions with other chemicals.

The “surface” function in PHREEQC is used for defining the amount and composition of a surface for adsorption. The diffuse double layer (DDL) model, charge distribution multisite complexation (CD-MUSIC) model and Dzombak and Morel surface complexation models are available to be used in PHREEQC. Several different models of surface complexation are available for use including the Dzombak and Morel model, the triple layer model (TLM) and the CD-MUSIC model. The Dzombak and Morel model is based on adsorption of heavy metals to hydrous ferric oxide (HFO, or ferrihydrite; Dzomback and Morel 1990). HFO binds metals and protons to strong and weak sites, and develops a surface charge depending on the ions sorbed (Dzomback and Morel 1990). The “equilibrium phases” function is used to define the amount of a pure phase assemblage (solid phase mineral or gas) that can react reversibly with the aqueous phase. When the solution comes into contact with the phase, the phase will either dissolve or precipitate until equilibrium, or a specified saturation index or log partial pressure is reached. The “reactions” function is used to define irreversible reactions that transfer amounts of elements to or from the aqueous solution during batch reaction calculations. These include reactions that are independent of solution composition or time which are defined independently. The “mixing” function is used to define the solutions to be mixed and the mixing ratio. The database containing the thermodynamic data which is to be used in the modelling is also specified.

When the input code is set to run, PHREEQC first reads database file, then it reads the input file until it reaches the keyword “END” or the end of the file. PHREEQC then processes input data and makes a list of new species, phases and elements. PHREEQC calculates the initial conditions and carries out batch reactions. In these calculations the concentration of elements in the solution are converted to molar concentrations and split into the different valence states. The molar concentrations of elements in the free ion state and complexed with other molecules in the solution are calculated based on the thermodynamic data from the specified database for the solution at equilibrium. Saturation indices of phases able to be formed from the elements in the solution are also calculated.

In this research PHREEQC was used to model dissolved element speciation and potential for mineral formation and adsorption of toxic trace elements onto the newly formed secondary ferrihydrite, as well as expected changes to the element speciation under the regime of change in water quality (i.e. when limestone is added).

2.6.1 Solution speciation

Modelling of aqueous metal speciation, mineral formation or dissolution and adsorption reactions was completed using PHREEQC with either the WATEQ4F or MINTEQ.v4 thermodynamic database (Parkhurst and Appelo 2013) augmented by additional data from Tonkin et al. (2004) and Markich and Brown (1999). pH, temperature and individual element concentrations were input from field measurements or analysis of water samples. For the Tui and Puhipuhi modelling, pE was set to 12 as the waters were fast flowing and well oxygenated. For the Bellvue modelling, redox potential was initially set to 10 for the adit samples as there was less oxygen present in these samples and 12 for the oxygenated stream samples. For subsequent modelling, pE was set to be defined by one of four redox pairs for which the concentration of both species had been determined analytically.

2.6.2 Adsorption modelling

The surface complexation model of Dzomback and Morel (1990) was used for adsorption modelling. This model is based on the complexation of cationic metals to hydrous ferric oxide (HFO), as fresh HFO is abundant at sites affected by AMD. Ferrihydrite was assumed to have the characteristics of HFO given by Dzomback and Morel (1990; 0.005mol strong binding sites/mol Fe, 0.2mol weak binding sites/ mol Fe and a specific surface area of 600m2/g HFO). In addition, manganese oxide adsorption was also assessed assuming MnOOH to have the characteristics typical of hydrous manganese oxide, and adsorb divalent cations with the surface complexation constants for Cu, Pb, Zn and Cd (Tonkin et al. 2004).

2.6.3 Mineral Precipitation

The “reaction” function was used to simulate the effects of AMD treatment using limestone. In this reaction a fixed amount of calcite ($CaCO_3$) was added stepwise to the solution until either the saturation limit (SI=0.0) of calcite was reached or the amount of $CaCO_3$ to be added ran out. The batch reactions were run initially to determine which phases were likely to be supersaturated in the solution, and therefore which minerals were most likely to precipitate. The minerals which had a positive saturation index were then evaluated for their likelihood to precipitate in the environment in which they were collected from. This step discounted the formation of minerals such as hematite, cupricferrite and cuprousferrite which are only formed at high temperatures (Kolta et al. 1981, Gholinejad et al. 2014) and are therefore kinetically hindered from forming at the temperatures observed in the field.

The modelled batch reactions were then run again with the phases likely to precipitate included in the “equilibrium phases” function with an initial amount set to 0.0g so that the phase could not dissolve but only precipitate once a saturation index of 0.0 had been reached.

2.6.4 Modelling accuracy

An acceptable range of error of 10% was used for assessing the reliability of analytical data (Section 2.3) and most data fell within these bounds. However, for analyses involving sediment, the acceptable range of error, importantly between duplicates, was between 20-30% (Sections 2.4 and 2.5). Some elements, such as Cd, Cu and Zn, were observed to exhibit higher variability as noted in Sections 2.3-2.5. By combining these two acceptable ranges of

error for analytical methods and sampling methods the value of 35% results as an acceptable range of variability for predicting concentrations in natural systems. This value is also approximate to half an order of magnitude, an alternative method for determining an acceptable range of variability in natural systems. This acceptable range of variability could then be used as a guide for assessing how reliable the geochemical model described with PHREEQC code was when compared with measured data.

CHAPTER 3

TUI MINE

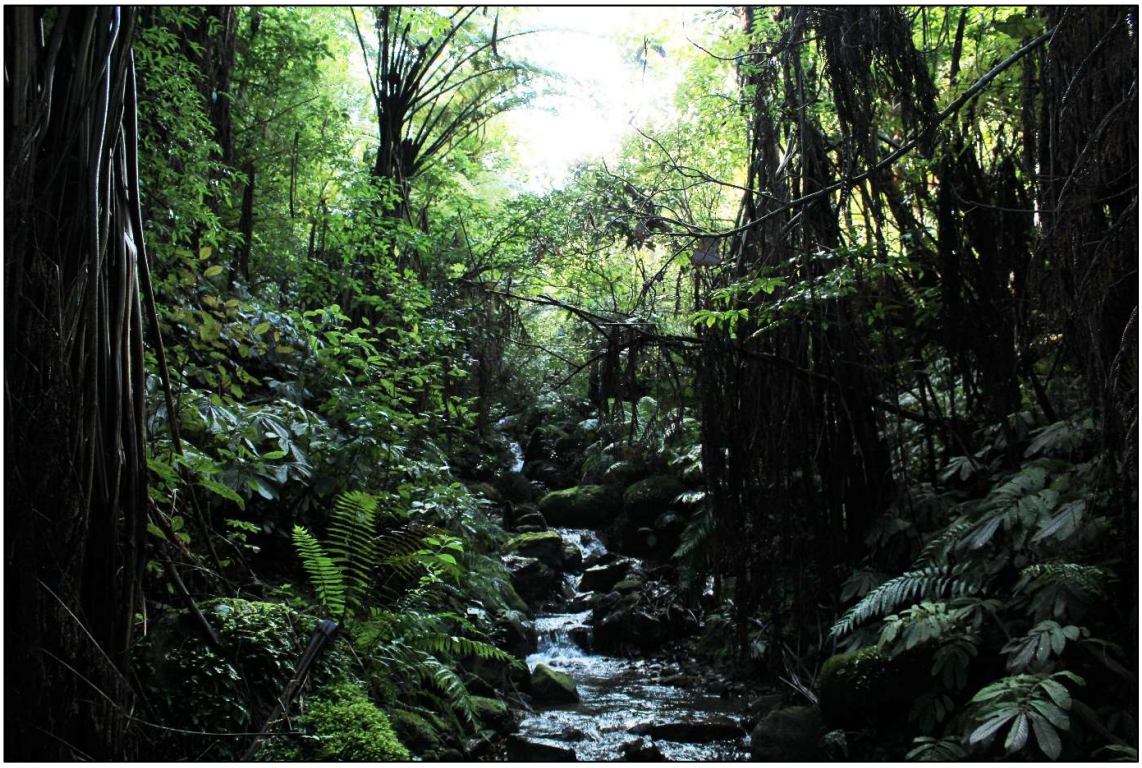

Figure 3. Tui Stream at the Tui1 sampling site. Photo: Rose Gregersen

This chapter reports research into the water and sediment chemistry of streams draining an epithermal mineral deposit mined for galena [PbS] and sphalerite [ZnS] has taken place, but also where remediation through addition of limestone slurry to underground adits and limestone to tailings has been completed The speciation, toxicity and bioavailability of dissolved and sediment-bound trace elements is determined through sample analysis and geochemical modelling. The effects of mining-related trace element contamination and site remediation on macroinvertebrate communities is also assessed. The ability of geochemical modelling to support and optimise site remediation is investigated.

3.1 Introduction

Tui mine is a former base metal mine located on the western slopes of Mt. Te Aroha in the Kaimai Ranges, Waikato region, New Zealand. It is 3km north east of the township of Te Aroha, just below the Coromandel Peninsula. It sits at an altitude of between 300m and 400m above sea level and is surrounded by native bush. Tui Mine is drained by two streams; the Tui Stream on the north side of the mine site and the Tunakohoia Stream on the south side (Figure 3.1). Both streams are tributaries of the Waihou River. The average rainfall is around 2100mm/yr on Mt. Te Aroha (Harvey and Webster-Brown 2003).

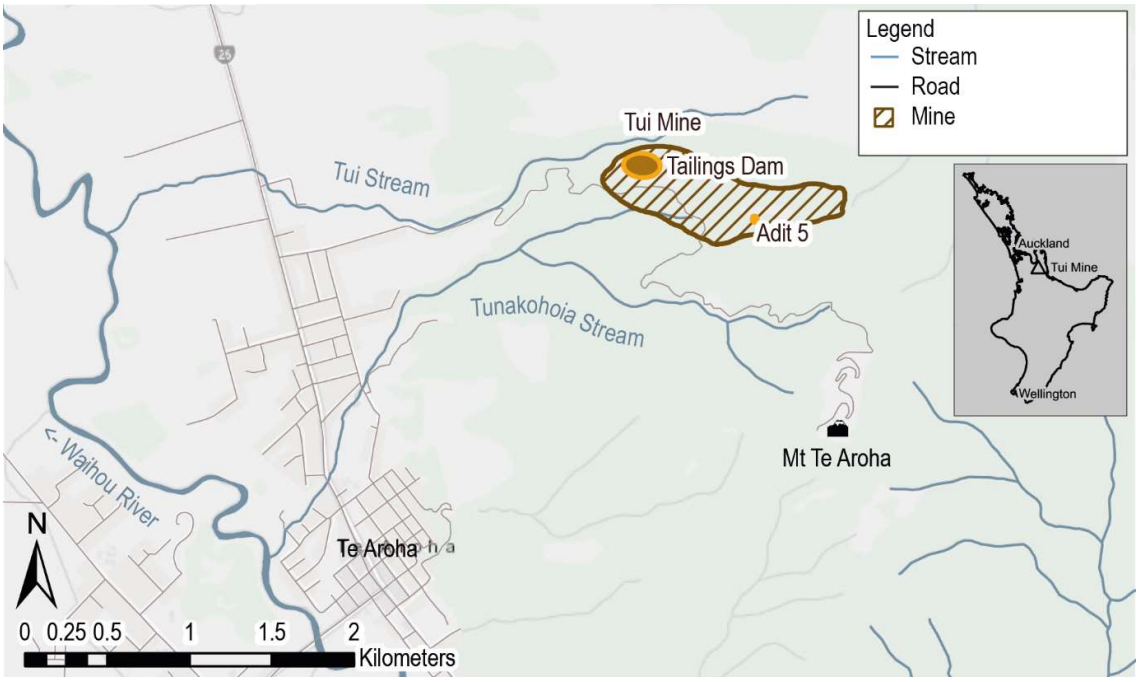

Figure 3.1 The location of Tui Mine and the streams draining the mine area.

3.1.1 Ore geology

The ore extracted at the Tui Mine came from two mineralized quartz reefs, the Champion lode and the Ruakaka lode (Wodzicki and Weissberg 1970). The principal minerals in these lodes were sphalerite [ZnS], galena [PbS], pyrite [FeS_2] and chalcopyrite [$CuFeS_2$] with minor amounts of cinnabar (HgS), marcasite (FeS_2), tetrahedrite ($(Cu, Fe)_{12}Sb_4S_{13}$) and tennantite ($(Cu, Fe)_{12}As_4S_{13}$) (Wodzicki and Weissberg 1970, Tay 1980, Morrell 1997).

3.1.2 History of mining and assessment of impacts

The Champion lode was first mined for Pb, Au and Ag in the 1880's to the early 1900's (Tay 1980, Morrell 1997). The Pb was used as a flux for Au extraction but contained too much Zn to be of much use (Morrell 1997) It was not until 1967 when the mine was operated by Norpac mining that production at the mine intensified dramatically (Morrell 1997). During this time base metals including copper, lead and zinc were extracted from the ore at Tui Mine. However, the mine was closed in 1973 when levels of mercury found in the ore were unacceptable for the

Japanese market and, being unable to find a buyer for the ore, Norpac Mining Ltd. went into receivership (Tay 1980, Morrell 1997). The mine site was not rehabilitated but was left with waste rock dumps, an unstable tailings impoundment at risk of collapse and contaminants leaching from the mine workings, the tailings dam and tailings impoundment into Tunakohoia and Tui Streams.

At the time of closure and for a year after analyses of Cu, Pb, Zn and Cd in soils in a paddock adjacent to the mine were completed. These 4 elements were elevated in the pasture soils at the time of closure but had decreased in the 12 months following closure, presumably by leaching down the soil profile (Ward et al. 1977). Soils, stream waters, stream sediments and vegetation around the Tui Mine were also found to contain high concentrations of Cu, Pb, Zn and Cd (Ward et al. 1976).

Five years after closure of the mine, waters discharging from the mine adits and the tailings dam contained extremely high concentrations of Fe, Cu, Zn and Cd and the discharge from the tailings dam had a very low pH (Tay 1980, Hendy 1981). Downstream measurements found that the concentrations of these elements remained above the World Health Organisation (1971) guidelines for drinking water at the point where water was taken to supply the township of Te Aroha with drinking water. Additionally, Fe-rich precipitates which had formed in Tui Stream had accumulated high concentrations of Zn, Pb, Cu, Cd and Hg (Tay 1980, Hendy 1981). Tui Stream was identified as a significant source of trace elements to the Waihou River Livingston (1987).

Dissolved and acid soluble trace element analysis on water samples from the waters draining Tui Mine and from sediments collected from these streams was completed by Webster (1995). Drainage from the tailings dam was acidic and contained high concentrations of dissolved Fe, Mn, Cu, Pb, Zn and As. In Tui Stream, below the confluence with the drainage from the tailings dam, the pH was circum-neutral (7.03), Fe had precipitated as a hydrous oxide and Cu, Pb and As had adsorbed to the Fe-(oxy)hydroxide. Mn and Zn remained in solution. Further downstream (500m) the Fe (oxy)hydroxide precipitate had settled out of the water column, removing Cu and As from solution (Webster 1995).

In 1995, it was discovered that the tailings dam was leaching Fe, Mn, Cu, Pb, Zn and Cd into the groundwater and that different desorption/adsorption rates had resulted in Cd travelling the furthest from the tailings dam and Fe and Zn travelling the shortest distances from the tailings dam (Pang 1995). Additionally, the mountain streams have some groundwater contribution leading to additional contamination of Tui and Tunakohoia Streams from contaminated groundwater (Pang 1995).

The geochemistry of the tailings impoundment was investigated to determine which techniques could be used to remediate the site (Rumsby 1996). It was found that oxidation and infiltration of rainwater into the tailings had caused three layers within the tailings impoundment to form. The top layer (0-20cm depth) consisted of an oxidised zone which was depleted of sulfide minerals. The middle layer (20-50cm depth) consisted of Fe (oxy)hydroxides

which had accumulated trace elements (Cu, Pb, Zn, Cd and As). The bottom layer (50cm-5m depth) consisted of unoxidised tailings, including sulfide minerals, and Fe- and Mn- oxides with trace elements bound (Rumsby 1996).

The revegetation potential of the Tui Mine tailings dam was investigated and found to be low because of the abundance of Fe-, Cu-, Pb-, Zn- and As- sulfides in the tailings resulted in acidic conditions with high concentrations of these potentially phytotoxic elements (Morrell 1997). This meant that the unmodified tailings were a hostile medium for plant germination and growth but amending the tailings with both agricultural lime and composted sewage sludge could provide a growing medium suitable for revegetation of the tailings to take place (Morrell 1997).

Trace element analysis on water and periphyton samples and statistical analysis of macroinvertebrate samples collected from Tunakohoia Stream found that concentrations of Cu, Pb, Zn and Cd in water samples and periphyton were elevated but not significantly statistically correlated (Hickey and Clements 1998). 100% mortality of *Daphnia magna* was observed in toxicity tests using Tunakohoia Stream water. Macroinvertebrate taxa richness, total abundance, EPT taxa and QMCI were found to be reduced in Tunakohoia Stream as compared to a control stream (Wairongomai Stream) located in a nearby catchment (Hickey and Clements 1998).

Trace element analysis on water and sediment samples collected from both the Tui and Tunakohoia Streams found that 20 years after the mine was closed high concentrations of Pb, Cd, As, Hg, Zn and Cu were still present in stream sediment samples, in particular near the adits which intersected the Champion Reef (Sabti et al. 2000). However, downstream the concentrations became close to background level. Concentrations of trace elements in stream sediments were “unacceptably high” where the Tunakohoia Stream enters the township of Te Aroha (Sabti et al. 2000). Only pyrite was detectable by XRD in sediment from upper reaches of both streams but it was noted that pyrite masks sphalerite (Sabti et al. 2000). Concentrations of Pb, Zn, Cd and As in Tui and Tunakohoia Streams exceeded the Ministry of Health (1995) guidelines for drinking water. Therefore neither of these streams were suitable as a potable drinking water supply source (Sabti et al. 2000).

Trace element analysis of water and sediment samples from around the Tui Mine site found that concentrations of Cu, Zn and Cd exceeded ANZECC (2000) guidelines in streams draining mine site (Harvey and Webster-Brown 2003). Based on flux measurements, the principal pathways for Cu, Zn and Cd contamination to Tui Stream was found to be leachate from the tailings dam and diverted stream water above dam while Adit 5 drainage and a small contribution from waste rock piles below Adit 4 were found to be the principle pathways for Cu, Zn and Cd contamination to Tunakohoia Stream. Flux measurements also showed that removal of Fe, Mn and Zn through precipitation and adsorption processes was occurring in Tui Stream but very little active attenuation is occurring in Tunakohoia Stream (Harvey and Webster-Brown 2003). Dissolved Cd concentrations in the lower Tunakohoia Stream where it passes through township of Te Aroha exceeded Ministry of Health (2000) guidelines for drinking water and ANZECC (2000) recreational health guidelines. The ANZECC (2000) guidelines for aquatic health for

Cu, Zn, and Cd were exceeded in Tunakohoia Stream in early spring when high rainfall resulted in run off from the waste rock piles occurred. In addition to this, sites around the Tui Mine did not comply with (CCME 1999) guidelines for residential/park soils and was therefore not suitable for public access (Harvey and Webster-Brown 2003).

3.1.3 Remediation attempts

After more than 2 decades of study, the Tui Mine became recognised as New Zealand's most contaminated heavy metal site (Sabti et al. 2000). Partial site remediation in the form of replacement of the sediment trap downstream of the tailings dam and the construction of a new spillway at the outlet of the sediment trap was carried out in 2006 after heavy rain caused the former sediment trap to fail (Sharplin 2008). However, the ranking of most contaminated heavy metal site in the country, along with perceived instability of the tailings dam in a major seismic or weather event, prompted the local regional and district councils to begin full rehabilitation of the site in 2010. The 2010-2013 rehabilitation works included plugging the level 5 adit and modifying the level 4 adit in order to control the amount of mine drainage water discharged (Fairgray et al. 2016). The underground workings were allowed to parcially flood and lime slurry was injected into the workings. The tailings dam was stabilized, mixed with lime and cement, and capped with clean fill to prevent oxygen and water from entering the tailings, further oxidising the iron-sulfides. Recent monitoring has shown an improvement in water quality (and ecological health) of the streams, although some discharge from the adits and the tailings dam still occurs (Fairgray et al. 2016). Currently, in Tui Stream the pH is circum-neutral and dissolved Cu and Pb have been reduced to less than 20% of their previous concentrations. A summary of pre- and post-remediation water chemistry for selected sites around the Tui Mine and in the Tui and Tunakohoia Streams is given in Table 3.1.

Little is known about how the toxicity of dissolved trace elements has changed, and whether this decrease in concentration is sufficient to allow the recovery of a healthy aquatic ecosystem. There is also concern that toxic trace elements in the sediments may continue to be released from the sediment over time, providing an ongoing source of contamination. This has implications for the rate of recovery of this rehabilitated mine site. Ecological and water quality monitoring is still being carried out at the site (by consultants to Waikato Regional Council), to evaluate progress towards recovery of the water quality of the Tui and Tunakohoia streams.

The Tui Mine has undergone extensive remediation works and pre-remediation data on water quality downstream of the mine exists. Therefore, the site and associated data can be used to investigate the accuracy of geochemical models by comparing water chemistry predictions to current conditions.

Table 3.1 Historical water quality data from Tui Mine. Dates earlier than 2010 are pre-remedation and dates later than 2013 are post-remediation. Data for during remedial works is also available for some sites.

Location	pH	Cu (mg/L)	Pb (mg/L)	Zn (mg/L)	Cd (mg/L)	Year	Reference
Tailings	3.2-3.7	0.72	-	31-49	-		Tay (1980)
	2.8	2670	1240	44100	-		Webster (1995)
	-	12-570	0.2-649	790-57600	0.1-286		Sabti et al. (2000)
	3.19-6.01	14-1870	0.4-1900	2720-44200	16-330		Harvey and Webster-Brown (2003)
	2.91-3.38	780-4000	1400-2700	44000-46000	160-200		Sharplin (2008)
	3.04-3.36	960-1700	710-890	19000-25000	110-140	2009	PDP (2010)
	6.50-7.95	3.5-136	1.44-5.7	4200-7700	24-76	2013	PDP (2014)
	6.75-7.50	3.5-7.1	5.2-5.9	1690-6400	3.9-25	2014	PDP (2016)
Tui Stream	4.8-5.1	-	-	4.5-5.5	-		Tay (1980)
@ golf course	6.5-6.9	<20	<100-150	40-1010	<50-30		Pang (1995)
	7.03	6.7	0.7	1460	-		Webster (1995)
	-	4	0.03	600	0.7		Sabti et al. (2000)
	6.50-6.71	1-8.45	<dl-2.09	500-780	1-5.74		Sharplin (2008)
	6.99-7.05	7.5-11	2.3-6.1	620-920	3.7-5.4	2009	PDP (2010)
	7.07-7.45	1.3-2.8	0.32-1.58	89-119	0.7-1.31	2013	PDP (2014)
	6.53-7.51	1-3.5	0.11-0.32	63-76	0.43-0.47-	2014	(PDP 2016)
Tui Stream	6.5	<100	<100	100	<20		Pang (1995)
u/s tailings (control)	-	28	51	740	2.0		Sabti et al. (2000)
Adits 4 and 5	7.20-7.84	20-175	<100-40	9840-23800	90-170		Tay (1980)
	-	10-18	0.09-1.00	2740-14000	4.5-23		Sabti et al. (2000)
	6.96-7.67	<dl-85	0.4-13	110-20200	0.8-160		Harvey and Webster-Brown (2003)
	6.79-7.05	0.89-4	<dl	185-595	2.5-5		Sharplin (2008)
	6.31-7.84	0.96-43	0.25-0.49	180-27000	1.6-190	2009	PDP (2010)
	6.66-7.33	<0.5-770	<0.2-104	11100-58000	45-420	2011	PDP (2014)
	6.8-7.42	<10-580	<0.2-33	5900-45000	23-360	2012	PDP (2014)
	6.71-7.69	<0.5-80	<0.2-55	2900-9400	10.4-32	2013	PDP (2014)
	6.9-7.73	<0.5-36	<0.1-57	1740-7800	7-42	2014	PDP (2016)
Tunakohoia Stream	7.59-7.74	<10-30	<100	8680-13300	70-100		Tay (1980)
u/s south branch	7.5	<20-110	110-510	2300-16000	<50-140		Pang (1995)
	-	30.6	12.2	8170	63		Hickey and Clements (1998)
	-	5-310	0.17-24	5600-11300	13-73		Sabti et al. (2000)
	6.43	30	11	6980	68		Harvey and Webster-Brown (2003)
	6.73-7.58	7.6-33	2.8-5	11000-13000	77-98	2009	PDP (2010)
	6.32-6.85	44-52	24-37	6500-15100	45-102	2011	PDP (2014)
	5.43-7.46	6.2-13.9	1.35-4.1	5800-8700	32-59	2012	PDP (2014)
	6.99-7.06	1.6-22	0.5-30	3600-4200	21-24	2013	PDP (2014)
	7.39-7.81	1.9-4.3	0.75-4.2	1710-3300	9.6-18.8	2014	PDP (2016)
Tunakohoia Stream	6.74-7.46	<10-<30	<100	100-500	5-20		Tay (1980)
south branch (control)	6.9	20	<100	<100	<50		Pang (1995)
	-	8	1.00	12	0.1		Sabti et al. (2000)
	6.06-7.93	<0.53-0.63	<0.11	<1.1-1.7	<0.53	2009	PDP (2010)
	6.11-7.63	<0.5-0.8	<0.1-0.27	<1.0-1.9	<0.5	2011	PDP (2014)
	6.93-7.26	<0.5-0.6	<0.1	<1.0	<0.5	2012	PDP (2014)
	7.23-7.77	<0.5	<0.1-0.14	1.1-1.6	<0.5	2013	PDP (2014)
	7.17-7.44	<0.5-1	<0.1-0.14	1.1-3.4	<0.5	2014	PDP (2016)

3.1.4 Aim and objectives of this research

The overall aim of this research is to determine whether geochemical modelling could have predicted past remediation water quality and ecological effects.

The objectives of this research are:

- Determine what the current state of the streams draining Tui Mine is, encompassing stream water chemistry, sediment chemistry, and ecology of the streams.
- Assess the current state toxicity of trace elements, as compared to the pre-remediation state, and the impacts on ecology using modelled toxicity assessments.
- Determine how reliably geochemical modelling can predict the attenuation processes occurring in these streams, particularly that of Fe, Cu, Pb and Zn
- Assess how geochemical modelling could have been used to predict the post-remediation water and sediment quality to achieve a better post-remediation result

3.2 Methods

3.2.1 Study area

Tui Mine was selected for this research because it was a former mine site which had recently undergone remedial works. The site had been extensively researched prior to the major remedial works (2010-2013) and a large dataset of water chemistry is available from before and after remediation.

3.2.2 Sample collection

Water and sediment samples for this study were collected at 10 sites on the Tui and Tunakohoia streams in November 2015; 4 sites on Tui Stream, including a reference site (TuiC) upstream of the mine workings, and 5 sites on Tunakohoia Stream, as well as a reference site (TunaC) on the south branch of the Tunakohoia Stream which is unaffected by mine site drainage (Figure 3.2). Samples had also been collected in early summer (December 2014) by Prof. Jon Harding, augmented by additional sediment samples collected by Prof. Jenny Webster-Brown in May 2015. Sampling times were chosen to avoid the extremes of high rainfall and stream flow during winter, and low stream flow in summer. Samples were collected from the two new sites, Tui3 and Tuna5, during the November 2015 sampling event only.

Measurements of temperature, pH, conductivity and dissolved oxygen were made *in situ* using a HACH HQ40d portable multi parameter meter. Water samples were collected in high density polyethylene (HDPE) centrifuge tubes. One water sample for major ion determination was collected, as well as two water samples (one unfiltered, for “acid soluble” trace element analysis, and one filtered through 0.45 µm membrane, for “dissolved” trace element analysis). Both samples were acidified to 1% HNO_3 with Aristar-grade concentrated nitric acid prior to analysis. Sediment samples were collected in HDPE pottles, from the top 5cm of the stream sediment bed.

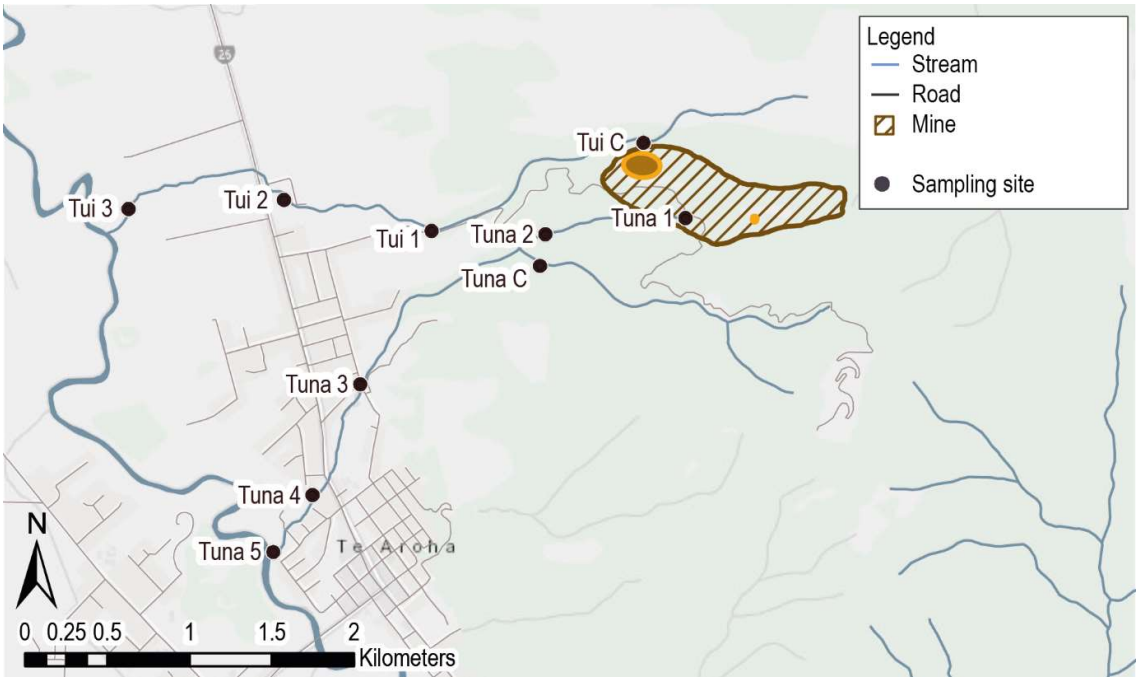

Figure 3.2 Sample sites along the Tui and Tunakohoia Streams

Macroinvertebrate sampling was completed in December 2014 by Prof, Jon Harding (UC) and Dr. Kevin Simon (UoA) alongside the collection of water samples (Harding and Simon, in prep). Macroinvertebrate samples were collected from the sites Tui1-2, TuiC, Tuna1-4 and TunaC using protocol C2 (Stark et al. 2001) and were preserved with 70% ethanol in the field.

3.2.3 Sample analysis

Water

Water samples collected in Nov 2015 were analysed for major cations and trace elements by ICP-MS, for major anions by HPIC, for dissolved inorganic carbon (DIC) by Infra-red gas analysis (IRGA), then reported as HCO_3^+ as all waters were of a neutral pH, as outlined in Section 2.4. Analysis of samples collected in December 2014 was undertaken using the same methods but without the authors involvement.

Sediment

Sediment samples were dried at 40°C and sieved through a 67µm nylon mesh, then digested in hot nitric acid and the digest analysed for trace elements by ICP-MS. Sediment samples were also analysed by X-ray diffraction (XRD) and scanning electron microscopy (SEM) as outlined in Section 2.5. Analysis of the samples collected in December 2014 was completed as above.

Additionally, sediment samples were analysed through a sequential extraction of Leleyter and Probst (1999) and included a final hot nitric acid step (Salvarredy-Aranguren et al. 2008) to identify the specific solid phases in the

sediment which were binding trace elements. The extraction scheme is described in Table 2.7. The trace element concentrations in fractions 1, 4a, 4b, 4c, 5 and 6 of the sequential extraction were analysed by ICP-MS, and in fractions 2 & 3 were analysed by ICP-OES (optical emission spectrometry).

Macroinvertebrates

Macroinvertebrate samples were processed and identification of species to the lowest taxonomic level along with community index values using the key of Winterbourn et al. (2006). This was completed by Prof. Jon Harding and Dr. Kevin Simon. Macroinvertebrate community index parameters were provided (Harding and Simon, in prep) to supplement the work done for this research.

3.2.4 Geochemical modelling

Modelling of dissolved trace element speciation, mineral formation or dissolution and adsorption reactions was completed using PHREEQC version 3.3.2 with the WATEQ4F thermodynamic database (Parkhurst and Appelo 2013). PHREEQC was used in the two ways it is most commonly used to predict mine discharge chemistry by mining companies and their consultants;

1. To model current dissolved trace element speciation to determine free ion concentrations (to assess potential toxicity), and to determine speciation change under a regime of changing water quality.
2. To predict dissolved trace element removal through mineral formation and adsorption onto freshly formed hydrous ferric oxide.

For adsorption modelling in a mine remediation context, the surface complexation model using hydrous ferric oxide (HFO) as the only adsorbing surface, is commonly used. This is based on the adsorption data of Dzomback and Morel (1990) which pertains to freshly-formed HFO, with 0.005 strong binding sites/mol Fe, 0.2 weak binding sites/mol Fe and a specific surface area of 600m2/g. PHREEQC was used with the WATEQ4F database for dissolved speciation modelling and for adsorption modelling. To model dissolved speciation change following the additions of lime (e.g., to the tailings pile and inside Adit 5), 125µmols calcite was added stepwise to the stream water from July 2007 (in the proportions reported by Sharplin 2008) until either the saturation limit (SI=0.0) of calcite was reached or until $CaCO_3$ was no longer available. 125µmols was used because it had been determined that this amount would result in the saturation index of calcite being reached but not exceeded.

Batch reactions were run initially to determine which trace element bearing phases were likely to be supersaturated in the solution, and therefore which minerals were theoretically most likely to precipitate. The minerals which were unlikely to form in a low temperature, freshwater environment were eliminated from consideration. This step discounted the formation of minerals such as hematite, cupric ferrite and cuprous ferrite which are only formed at high temperatures (Kolta et al. 1981, Gholinejad et al. 2014) because precipitation is kinetically hindered at low temperatures. The batch reactions were remodelled with the remaining minerals allowed to precipitate when

saturated and the dissolved ion concentrations reduced accordingly. The resulting pH change was calculated from the ion balance.

3.2.5 Leaching experiments

Leaching experiments were carried out with the fine (<67μm) sediment from sites Tui1 and Tuna1 to determine whether the sediment would release trace elements into the overlying stream water, if the release of trace elements was contributing to ongoing poor water quality (specifically high Zn, Mn and Cd concentrations) in the lower Tui and Tunakohoia streams, and whether this would hinder the re-establishment of a healthy stream ecosystem down stream of Tui Mine.

The leaching experiments were carried out by placing 50mL aliquots of the sediment suspension in HDPE tubes on an end-over-end mixer for periods ranging from 5 minutes to 10 days. At pre-determined times the aliquots were removed from the mixer and immediately filtered. The pH of the final solution was measured and samples for trace element analysis were acidified with Aristar-grade concentrated nitric acid and then analysed by inductively coupled plasma mass spectrometry (ICP-MS) as per Section 2.5.

3.3 Results

3.3.1 Aqueous chemistry

Physiochemical water quality parameters at the sampling sites during the December 2014 and November 2015 sampling events are shown in Table 3.3.1 and Table 3.3.2 respectively.

Water chemistry results show that remediation at the mine site has raised Tui stream water pH to circum-neutral, and lowered conductivity and sulphate concentrations. However, pH was already near neutral in Tunakohoia Stream (Table 3.1) and the addition of lime in Adit 5 has only had a small effect on pH and little effect on conductivity or sulphate concentrations when compared with pre-remediation data (Sharplin 2008). Temperature and dissolved oxygen (DO) levels are sufficient to support a healthy ecology, with the possible exception of the elevated temperature at Tuna 5, a shallow section of this stream where it passes through open farmland.

Acid soluble Hg was consistently below detectable levels, as was Sb at all sites except Tuna 1 (0.25 μg/L) and Tuna 2 (0.13 μg/L). The concentrations of all trace elements were considerably higher in Tunakohoia Stream, which still receives drainage from Adit 5, than in Tui Stream.

Table 3.3.1. Water chemistry for Tui Mine sampling survey, December 2014. Dissolved fraction <0.45µm. Values in bold exceed guidelines for protection of 95% aquatic species (ANZECC 2000).

Site	pH	Temp (°C)	DO (mg/L)	Cond (µS/cm)	Cl^- (mg/L)	NO_3 (mg/L)	SO_4 (mg/L)	HCO_3 (mg/L)	Na (mg/L)	Mg (mg/L)	K (mg/L)	Ca (mg/L)	Fe (µg/L)		Mn (µg/L)		Al (µg/L)	
													Diss	Total	Diss	Total	Diss	Total
Tuna1	7.50	12.8	9.2	805					11.6	16.6	0.61	102	58.2		816		0.60	
Tuna2	7.10	12.3	9.6	457					10.3	10.5	0.95	49.2	33.7		117		15.1	
Tuna3	7.30	15.6	9.3	341					10.3	7.89	0.63	30.3	27.4		1.81		2.91	
Tuna4	6.40	16.7	8.8	279					9.61	6.19	0.60	22.6	34.2		5.96		3.27	
TunaC	7.10	12.1	9.6	104					6.02	1.95	0.11	6.06	12.2		0.45		8.28	
Tui1	6.90	12.7	9.7	149					7.78	3.22	0.44	9.56	6.16		0.33		2.03	
Tui2	7.00	14.1	9.2	148					7.89	3.18	21.5	10.0	27.6		13.4		11.2	
TuiC	7.00	11.7	9.6	129					6.89	2.33	0.20	8.10	3.40		0.08		3.49	
WaiC	7.45	13.6	9.5	144					5.74	3.02	0.26	9.84	30.6		7.06		**67.5**	
ANZECC (2000)														ngv		1900		55

Site	Cu (µg/L)		Pb (µg/L)		Zn (µg/L)		Cd (µg/L)		Ni (µg/L)		Co (µg/L)		As (µg/L)		Sb (µg/L)		Hg (µg/L)	
	Diss	A. S.	Diss	A. S.	Diss	A. S.	Diss	A. S.	Diss	A. S.	Diss	A. S.	Diss	A. S.	Diss	A. S.	Diss	A. S.
Tuna1	**4.22**		2.25		**2630**		**14.8**		**11.4**		3.82		0.45		1.20			
Tuna2	**3.95**		1.26		**1910**		**14.1**		4.68		0.81		0.10		2.20			
Tuna3	**1.20**		2.53		**588**		**6.61**		1.60						1.34			
Tuna4	**1.63**		0.58		**376**		**4.57**		0.93						1.00			
TunaC	0.29		1.83		**19.1**		0.02		0.27						0.58			
Tui1	**1.75**		3.38		**56.5**		**0.44**		0.73				0.19		2.41			
Tui2	1.12		2.85		**79.6**		**5.63**		0.95				0.11		1.44			
TuiC	0.25		0.20		**17.4**		0.07		0.24				0.16		1.01			
WaiC	0.21		0.01		**11.9**		0.18		2.12		0.25				0.78			
ANZECC (2000)		1.4		3.4		8.0		0.2		11		ngv		24/13		ngv		0.6

Table 3.3.2 Water chemistry for Tui Mine sampling survey, November 2015. Dissolved fraction <0.45µm. Values in bold exceed guidelines for protection of 95% aquatic species **(ANZECC 2000)**. nm = not measured

Site	pH	Temp (°C)	DO (mg/L)	Cond (µS/cm)	Cl (mg/L)	NO_3 (mg/L)	SO_4^2 (mg/L)	HCO_3 (mg/L)	Na (mg/L)	Mg (mg/L)	K (mg/L)	Ca (mg/L)	Fe (µg/L)		Mn (µg/L)		Al (µg/L)	
													Diss	Total	Diss	Total	Diss	Total
Tuna1	7.42	13.7	9.69	666	10.2	0.38	285	69.5	13.1	18.1	1.07	109	5.06	360	477	453	3.36	4.75
Tuna2	7.12	12.2	10.1	409	11.8	0.66	154	32.9	13.1	13.7	1.24	50.3	3.14	14.9	75.3	75.3	12.7	49.9
Tuna3	6.84	13.8	9.88	308	12.2	1.03	93.6	34.1	12.7	10.2	1.12	34.6	9.30	11.3	1.75	1.85	3.12	4.65
Tuna4	6.92	15.5	9.39	249	12.7	1.16	65.4	41.7	11.7	7.84	1.04	25.5	13.0	31.3	4.03	5.15	2.90	5.50
Tuna5	7.52	19.6	10.1	252	12.9	0.92	65.6	39.0	11.7	7.52	1.10	24.5	26.1	64.2	20.5	20.9	3.40	9.79
TunaC	7.07	12.1	9.85	102	11.0	0.19	14.6	26.8	7.60	2.81	0.52	8.03	8.29	32.0	0.48	3.58	12.7	31.0
Tui1	7.40	11.9	10.3	150	10.7	0.19	29.2	32.2	9.44	4.38	0.84	12.9	2.88	7.61	0.40	1.13	4.49	7.92
Tui2	7.23	12.9	9.94	150	10.8	0.22	29.6	29.2	9.47	4.37	0.91	12.4	20.2	31.7	10.5	11.8	3.38	5.12
Tui3	7.31	15.9	8.98	150	11.7	0.78	28.6	32.1	10.0	4.65	1.09	11.6	66.7	169	47.8	51.3	2.96	11.2
TuiC	7.21	11.4	9.97	125	10.6	0.31	20.1	31.8	8.90	3.34	0.68	10.8	2.77	38.2	0.20	2.36	4.91	23.6
WaiC	7.28	14.3	9.75	141	9.27	0.04	36.7	18.1	7.20	4.30	0.69	12.5	11.7	24.1	9.75	10.4	**121**	**220**
ANZECC (2000)														ngv		1900		55

Site	Cu (µg/L)		Pb (µg/L)		Zn (µg/L)		Cd (µg/L)		Ni (µg/L)		Co (µg/L)		As (µg/L)		Sb (µg/L)		Hg (µg/L)	
	Diss	A. S.	Diss	A. S.	Diss	A. S.	Diss	A. S.	Diss	A. S.	Diss	A. S.	Diss	A. S.	Diss	A. S.		
Tuna1	**2.77**	**4.94**	2.30	**16.5**	**2470**	**2440**	**15.9**	**15.2**	8.24	7.79	2.09	1.99	1.11	1.52	0.25	0.21	<0.05	<0.05
Tuna2	**3.87**	**5.06**	2.47	**5.04**	**1840**	**1860**	**13.3**	**13.2**	3.75	3.73	0.77	0.77	0.56	0.56	0.13	0.13	<0.05	<0.05
Tuna3	0.92	1.03	0.13	0.19	**647**	**596**	**6.49**	**6.11**	1.35	1.33	0.02	0.02	0.47	0.41	<0.05	<0.05	<0.05	<0.05
Tuna4	0.49	0.94	0.10	0.20	**342**	**352**	**3.89**	**4.13**	0.89	0.88	0.04	0.05	0.39	0.39	<0.05	<0.05	<0.05	<0.05
Tuna5	1.14	**1.54**	0.10	0.68	**181**	**194**	**2.40**	**2.67**	0.66	0.07	0.08	0.10	0.43	0.47	<0.05	0.05	<0.05	<0.05
TunaC	0.33	0.40	<0.03	0.17	0.81	1.03	0.02	0.01	0.17	0.21	<0.02	0.06	0.35	0.26	<0.05	<0.05	<0.05	<0.05
Tui1	0.84	0.95	0.05	0.23	**45.7**	**46.8**	**0.36**	**0.37**	0.59	0.57	<0.02	0.03	0.44	0.44	<0.05	<0.05	<0.05	<0.05
Tui2	0.90	1.01	<0.03	0.11	**53.9**	**55.3**	**0.39**	**0.43**	0.56	0.58	0.08	0.09	0.47	0.49	<0.05	<0.05	<0.05	<0.05
Tui3	0.94	1.26	0.09	0.41	**37.6**	**39.5**	**0.23**	**0.27**	0.60	0.60	0.23	0.26	0.87	0.91	<0.05	<0.05	<0.05	<0.05
TuiC	0.17	0.29	<0.03	0.11	**9.63**	**11.0**	0.06	0.07	<0.04	0.21	<0.02	0.06	0.44	0.48	<0.05	<0.05	<0.05	<0.05
WaiC	0.25	0.33	0.04	0.07	2.57	3.13	0.03	0.03	2.21	2.26	0.40	0.41	0.35	0.42	<0.05	<0.05	<0.05	<0.05
ANZECC (2000)		1.4		3.4		8.0		0.2		11		ngv		24/13		ngv		0.6

Acid-soluble Zn and Cd exceeded ANZECC (2000) trigger values in both streams, but most significantly in Tunakohoia Stream. The Zn trigger value was exceeded (slightly) at the reference site (TuiC), upstream of any tailings drainage input, reflecting natural elevation due to the weathering of host rock. At sites with elevated Zn and Cd, the dissolved concentration is 85-100% of the acid soluble concentration, indicating much of the Zn and Cd in the water column is readily bioavailable.

Of the other trace elements tested, only acid soluble Cu and Pb exceed ANZECC (2000) trigger values, and then only in the upper reaches of the Tunakohoia Stream. The proportion of dissolved (bioavailable) Cu and Pb is also less than for Cd and Zn, with dissolved Cu constituting 56-89%, and Pb 8-68%, of their acid-soluble concentrations. Other trace elements; Fe, Mn, As and Ni did not exceed (ANZECC 2000) trigger values, therefore further assessment of potential toxicity focuses on Zn, Cd, Cu and Pb.

Speciation of dissolved trace elements

PHREEQC was used to determine the proportion of trace element present in free ion form for dissolved trace element concentrations which exceeded ANZECC (2000) trigger values (Cu, Pb, Zn and Cd ;Figure 3.3). All other trace elements were below the ANZECC (2000) trigger values. In the interpretation of modelling results, the free ion is assumed to be the species most toxic to biota as described in the free ion activity model (Campbell 1995). The concentration of trace elements in their free ion state from Figure 3.3 are given in Table 3.4.

The concentrations of free Cu^{2+} and Pb^{2+} ions are modelled to be well below ANZECC (2000) guidelines at all sites, including the upper Tunakohoia Stream, as these metals are complexed by hydroxyl ligands (Figure 3.3a and b; Table 3.4). Maximum free Cu^{2+} concentrations are 40$ of the total dissolved Cu concentration in Tunakohoia Stream and 15% in Tui Stream. Maximum Free Pb^{2+} concentrations are 35% of the dissolved Pb concentration in the Tunakohoia Stream and 20% in the Tui Stream.

Free Cd^{2+} and Zn^{2+} ions are orders of magnitude higher than the ANZECC (2000) guidelines, for all except the reference sites (Table 3.4). The main complexing ligand for Zn and Cd was sulfate ion, although sulfate complexes only made up < 25% of the dissolved Cd and Zn in the Tunakohoia, and < 5% in Tui Stream (Figure 3.3c and d).

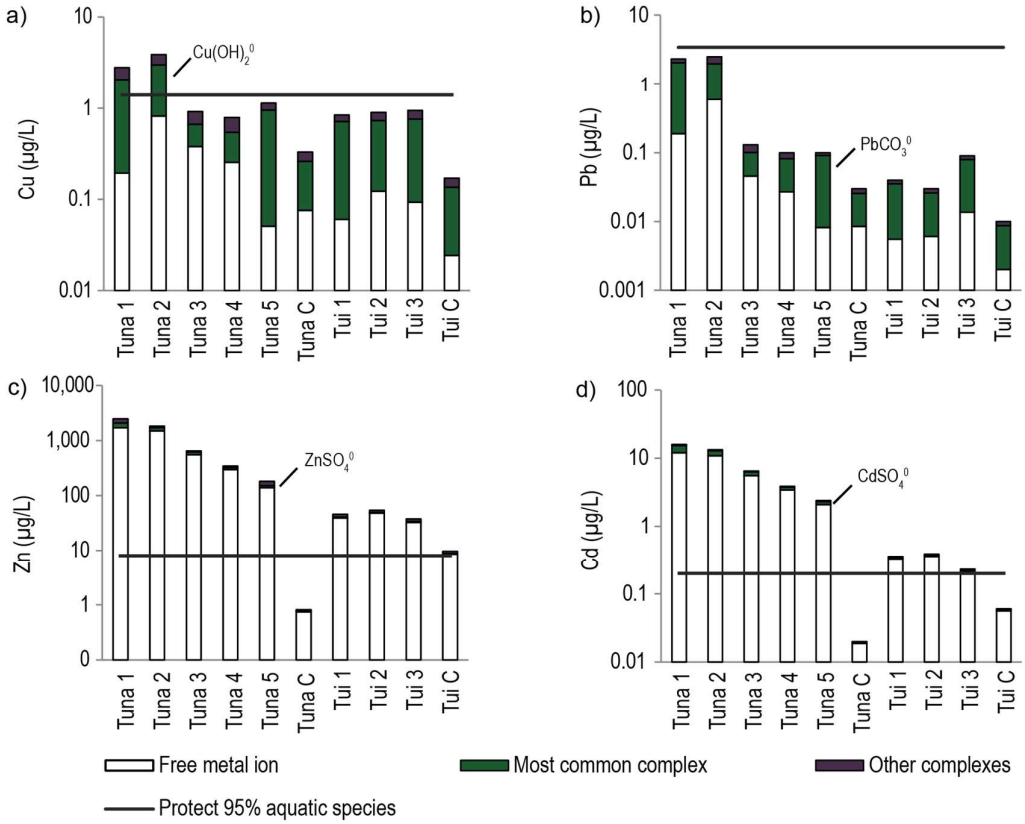

Figure 3.3 Modelled speciation for the trace elements which exceed ANZECC (2000) guidelines for the protection of 95% aquatic species. a) Cu, b) Pb, c) Zn and d) Cd. The most common complex is given in for each element.

Table 3.4 Concentrations of speciated data

Site	Tuna1	Tuna2	Tuna3	Tuna4	Tuna5	TunaC	Tui1	Tui2	Tui3	TuiC
Cu^{2+} (µg/l)	0.19	0.82	0.38	0.26	0.05	0.08	0.06	0.12	0.09	0.02
Pb^{2+} (µg/l)	0.19	0.60	0.05	0.03	0.01	0.01	0.01	0.01	0.01	0.00
Zn^{2+} (µg/l)	1710	1500	557	295	140	0.74	39.1	47.6	32.5	8.58
Cd^{2+} (µg/l)	12.1	10.9	5.57	3.42	2.09	0.02	0.33	0.36	0.21	0.06

Consistency with ecological monitoring data

The modelled concentration of Zn^{2+}, Cd^{2+}, Cu^{2+} and Pb^{2+} free ions were compared to the results of the ecological surveys carried out at these sites (Figure 3.4; Fairgray et al. 2016). There was a strong correlation between macroinvertebrate taxa richness, Zn^{2+} and Cd^{2+} as compared to Cu^{2+} or Pb^{2+} in the Tunakohoia Stream (R^2 for Zn=0.77, Cd = 0.78, compared to Cu=0.45, Pb = 0.47). However, there is no ecological reason for this correlation to exist and the data plotted in Figure 3.4 was not done so to show correlation but to determine a threshold for the concentration of free metal ions which results in a reduced taxonomic abundance of macroinvertebrates.

In the Tunakohoia stream, there was a reduction in ecological taxa at >3.5 µg/L free Cd ion and >300 µg/L free Zn ion. However, as high concentrations of Zn and Cd occur simultaneously, it is not possible to determine which of these metals has the greatest impact on aquatic life. In Tui Stream, ecological impacts occur at a higher concentrations, and may reflect the long-term low pH in this stream prior to mine remediation.

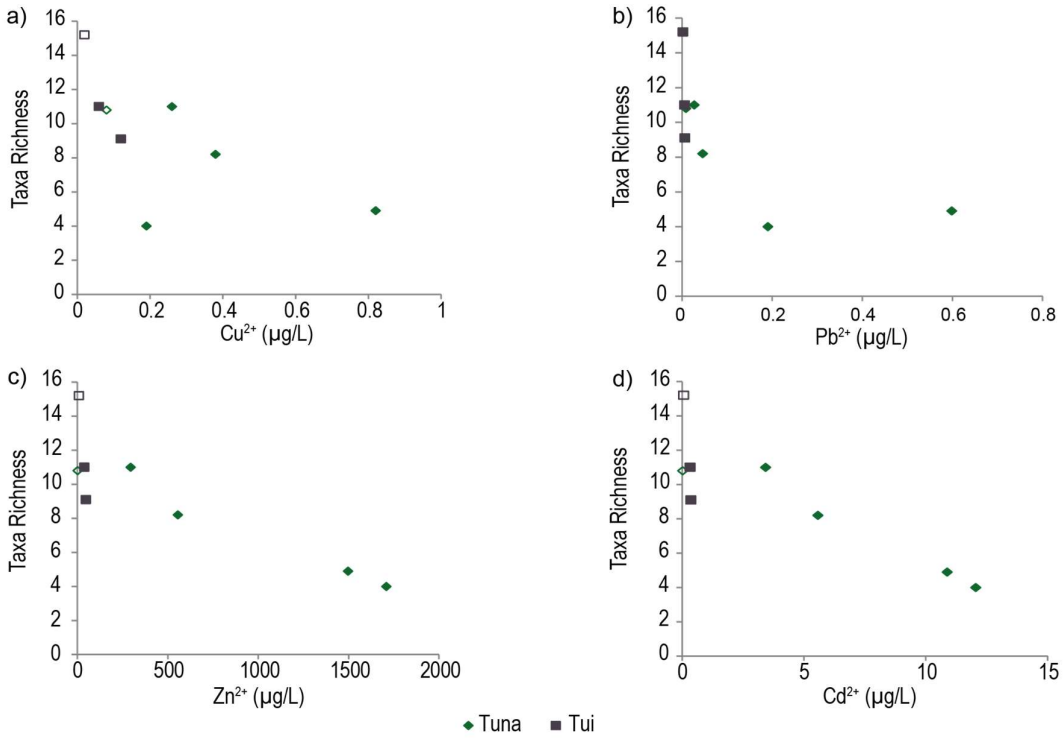

Figure 3.4 The relationship between macroinvertebrate taxa richness and speciated trace elements which exceed ANZECC trigger values; a) Cu, b) Pb, c) Zn and d) Cd. Points with open symbols denote the control sites.

3.3.2 Sediment chemistry

XRD analysis showed the sediment minerals were mostly quartz and plagioclase, with chlorite, smectite, illite and kaolinite clays present as weathering products. No major trace element bearing minerals were identified by XRD. However, SEM analysis revealed a residual Zn-sulfide particle in Tuna1 sediment just below Adit 5 drainage (Figure 3.5a), but no other sulfide minerals. No residual carbonates (such as limestone fragments from the remediation activities) or secondary carbonate phases were observed in the sediments. However, strong mineralogical associations between Fe, Pb and Cu, and between Mn and Zn are present (Figure 3.5).

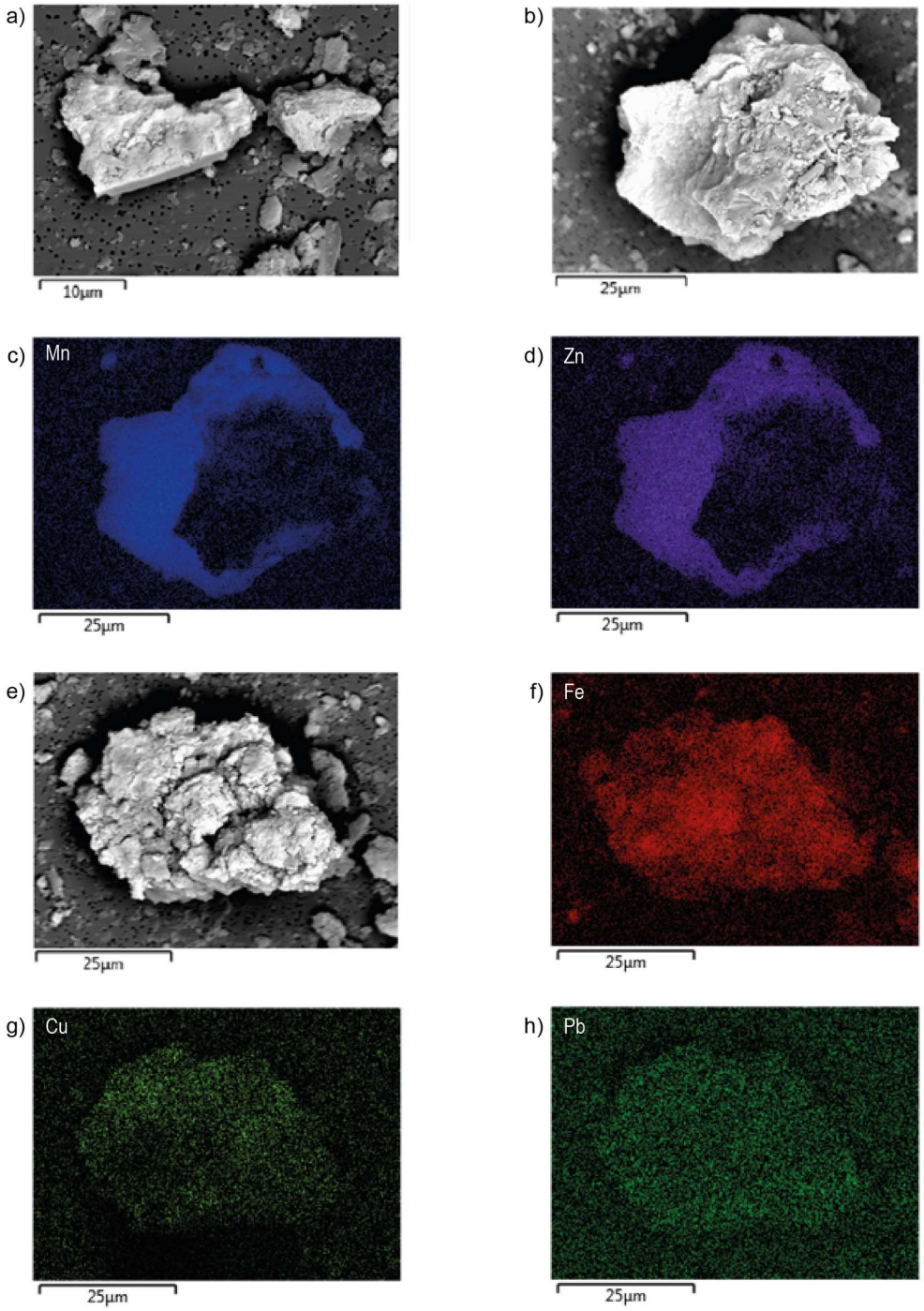

Figure 3.5 SEM-EDS images and elemental maps of particles collected from Tuna1. a) A ZnS particle; b) a quartz particle with a crust showing strong associations between Mn (c) and Zn (d); e) an Fe-rich particle with strong associations between Fe (f), Cu (g) and Pb (h).

Sediment-bound trace element concentrations are shown for the December 2014 and November 2015 sampling events in Table 3.5.1 and Table 3.5.2 respectively. ANZECC (2000) interim sediment quality guidelines (ISQG) for

aquatic life protection are also shown; ISQG-High is the guideline above which a biological impact is frequently observed, and the ISQG-Low is the guideline below which impacts rarely occur. For values between these two guidelines, impacts occur occasionally (Long et al. 1995, ANZECC 2000). ANZECC (2000) sediment quality guidelines are not available for Fe, Mn or Al.

Table 3.5.1 Trace element concentrations in fine sediment (<0.67 µm fraction) in streams receiving AMD from Tui Mine, as measured in December 2014. All concentrations are in mg/kg, except for Fe, Mn and Al in wt%. Concentrations are in bold if exceeding ISQG-Low, or red and bold if exceeding ISQG-High sediment quality guidelines (ANZECC 2000). Nm = not measured.

Site	Fe	Mn	Al	Cu	Pb	Zn	Cd	Ni	As	Sb	Hg
Tuna1	23.4	0.3100		**1740**	**5530**	**51200**	**352**	**77.2**	325	3.97	
Tuna2	6.69	0.1613		**1220**	**5790**	**15200**	**106**	**80.2**	70.3	8.64	
Tuna3	Insufficient sample										
Tuna4	4.41	0.0197		**143**	**412**	**3190**	**20.9**	**44.2**	16.2	0.27	
TunaC	4.37	0.0170		36.1	41.3	117	0.88	**53.5**	14.0	0.07	
Tui1	5.62	0.0420		**227**	**546**	**2790**	**21.7**	**76.4**	38.2	0.24	
Tui2	4.90	0.0213		**141**	**252**	**1640**	**10.4**	**53.0**	38.2	0.31	
TuiC	5.00	0.0145		54.4	35.1	**496**	**3.22**	**52.4**	18.8	0.06	
ISQG-H	-	-	-	270	220	410	10	52	70	25	1.0
ISQG-L	-	-	-	60	50	200	1.5	21	20	2	0.15

Table 3.5.2 Trace element concentrations in fine sediment (<0.67 µm fraction) in streams receiving AMD from Tui Mine, as measured in November 2015. All concentrations are in mg/kg, except for Fe, Mn and Al in wt%. Concentrations are in bold if exceeding ISQG-Low, or red and bold if exceeding ISQG-High sediment quality guidelines (ANZECC 2000).

Site	Fe	Mn	Al	Cu	Pb	Zn	Cd	Ni	As	Sb	Hg
Tuna1	11.4	3.31	3.34	**2160**	**11600**	**45600**	**254**	**112**	**221**	**5.91**	**6.14**
Tuna2	4.69	0.206	5.60	**168**	**611**	**4280**	**22.8**	**49.0**	**26.6**	0.46	<0.01
Tuna3	4.83	0.210	5.89	**149**	**599**	**4230**	**21.8**	**50.3**	**26.2**	0.56	**0.974**
Tuna4	4.24	0.150	4.08	**103**	**397**	**3290**	**14.4**	**45.7**	17.3	0.47	<0.01
Tuna5	3.34	0.119	5.53	29.4	26.7	91.0	0.505	**39.7**	14.5	0.22	<0.01
TunaC	4.83	0.175	4.22	46.2	38.0	120	0.553	**53.7**	16.7	0.10	<0.01
Tui1	7.14	0.338	6.95	**249**	**434**	**3460**	**16.6**	**88.8**	**54.1**	0.78	0.071
Tui2	7.14	0.430	5.76	**277**	**521**	**3320**	**23.5**	**90.4**	**62.3**	0.71	**0.57**
Tui3	4.05	0.145	4.00	**85.2**	**145**	**767**	**4.34**	**38.1**	**22.5**	0.16	<0.01
TuiC	5.18	0.0946	5.63	43.9	35.9	**402**	**1.58**	**49.5**	**30.6**	0.10	<0.01
ISQG-H	-	-	-	270	220	410	10	52	70	25	1.0
ISQG-L	-	-	-	60	50	200	1.5	21	20	2	0.15

Fe concentrations were most elevated in the upper reaches of the streams, closest to mine discharges, up to 23.4wt% in Tunakohoia Stream (Tuna 1) and 7.1wt% in Tui Stream (Tui 1 & 2), but close to background levels elsewhere (3.3 – 5.2wt%). Mn was similarly elevated below Adit 5 (3.3wt%) at Tuna 1 and high immediately below the tailings dam at Tui 1 & 2 (0.34-0.43wt%), but not significantly elevated downstream. Abundant brown Fe (oxy)hydroxide floc occurs in the upper reaches of both streams, however, the dissolved Fe concentration appeared to increase downstream, particularly in Tui Stream. This may be a result of the filtration method as Fe

oxide flocs were not as visible in the lower reaches they were presumably present as smaller particulates, some of which could have passed through a 0.45 µm filter to register as "dissolved" Fe in the stream as has been observed by other researchers (To Bangthanh et al. 1999).

The sediments of Tunakohoia Stream and Tui Stream were severely contaminated with Zn, Pb and Cd, particularly in the upper reaches where concentrations were well above ANZECC (2000) ISQG-High guideline values. Concentrations of up to 4.5wt% Zn and 1.2wt% Pb were present in sediments immediately below Adit 5 drainage (Tuna 1 site) and these sediments also showed high concentrations of Cu, Ni, As, Sb and Hg. Ni was also high immediately below the tailings dam drainage on Tui Stream and at the reference site TunaC.

Modelled trace element precipitation

Modelling carried out using dissolved trace element concentrations indicated that the only trace element-bearing phases that were saturated were oxides of Fe, Mn and Al. No carbonate minerals, such as calcite ($CaCO_3$), rhodochrosite ($MnCO_3$), smithsonite ($ZnCO_3$), otavite ($CdCO_3$), cerrusite ($PbCO_3$), $CuCO_3$, or mixed hydroxycarbonates such as malachite ($Cu_2(OH)_2CO_3$) and azurite ($Cu_3(OH)_2(CO_3)_2$) were saturated at the site. Sulfides of the trace elements, such as sphalerite (ZnS), chalcopyrite ($CuFeS_2$) or galena (PbS), were also not saturated in the stream waters because the redox state of the system favours SO_4 over HS^-. This indicates that the removal of trace elements from the water column is not likely to be due to mineral precipitation for Zn, Cd, Cu or Pb.

Sequential extraction of sediments

Sequential extraction results confirm that Fe and Mn are mostly bound in their respective hydrous oxide phases (Figure 3.6 a and b). For Mn, this relationship is especially strong at Tuna1 and Tuna2 where the total Mn content was elevated compared to the other samples. A higher proportion of Mn was extracted from the "Fe oxide" fractions for the Tui stream and Tuna3 sediment samples. 10-15% of the Fe in Tui sediments was in the residual "sulfide" fraction.

Most of the Cu, Pb and Zn was extracted in either the "pH leachable" or "Fe oxide" fractions (Figure 6c-e). The "Fe oxide" fraction was of greatest importance downstream in the Tunakohoia Stream and in Tui Stream. Pb and Zn also showed some (lesser) affinity for the "Mn oxide" fraction" and Cu and Zn for the "organic" fraction. However, Cu, Zn and Pb in the "sulfide and residual" fraction was <3% for all sites indicating that residual sulfide minerals such as chalcopyrite, sphalerite and galena make an insignificant contribution to sediment chemistry, despite sphalerite being observed with SEM (Figure 3.6a). In contrast to Zn, Cd showed little association with the "Fe oxide" fractions (Figure 3.6f). Cd was instead mainly extracted from the "low pH leachable" fraction in the Upper Tunakohoia Stream sediments, and from the "low pH leachable" and "exchangeable" fractions at Tuna 3 and in the Tui Stream sediments. However, "low pH leachable" can include leaching from iron oxide mineral surfaces at

pH 4.5. As and Sb were principally extracted from the “Fe oxide” fractions (Figure 3.6g-h), almost to the exclusion of all other fractions.

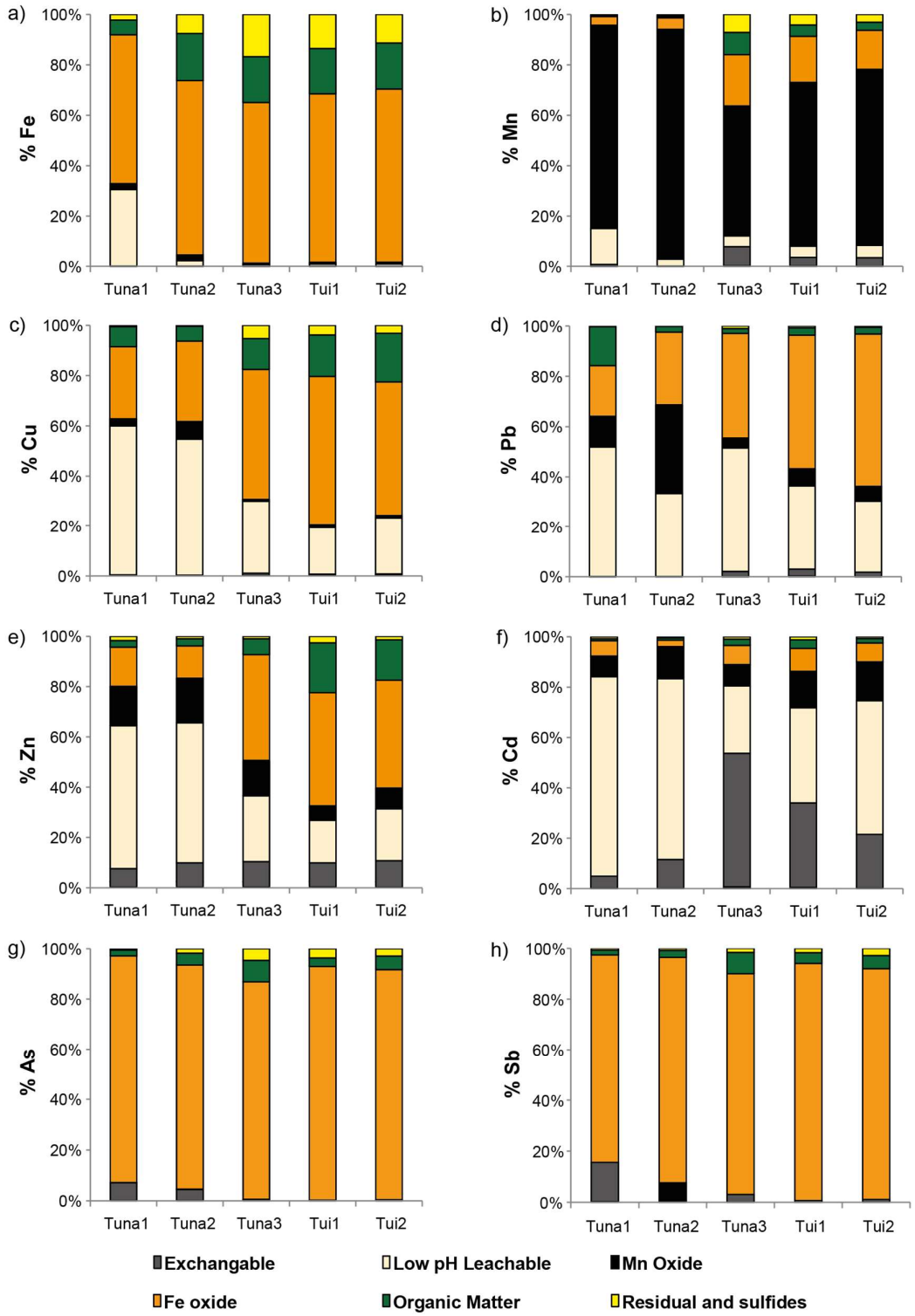

Figure 3.6 The percentage of elements extracted from each fraction during the sequential extraction process for sediments in the upper Tunakohoia Stream and Tui Stream.

Modelled adsorption of trace elements onto HFO

PHREEQC was used to model the degree of adsorption onto fresh hydrous ferric oxide (HFO) present in the water column and surface sediment. To model this process, the concentration of fresh HFO is assumed to equal the particulate Fe concentration in each water sample calculated from the difference between the dissolved and acid soluble Fe concentrations. PHREEQC modelled dissolved trace element concentrations are compared to observed concentrations in Figure 3.7.

PHREEQC reliably predicted the dissolved proportion of Zn, Cd and Ni; trace elements which were all mostly dissolved (Figure 3.7c, d and f). The model also predicted the proportion of dissolved Cu to within 20% of observed dissolved concentrations, although adsorption was generally understimated (Figure 3.7a). PHREEQC underestimated adsorption of Cu to a greater extent at the control sites and the lower catchment waters, indicating additional binding processes (in addition to HFO adsorption) may be important for Cu in these waters.

The model was less reliable when predicting the proportion of dissolved Pb and As (Figure 3.7 b and e). For Pb, PHREEQC modelling overestimated the proportion of dissolved Pb for all sites except the control sites and Tui 3. Although little of the Zn was predicted to adsorb to the HFO, the high concentration of this trace element in the stream water meant that it still occupied a large proportion of HFO binding sites and inhibits adsorption of other trace elements. When Zn adsorption was removed from the model, more Pb bound to the strong binding sites on HFO and the proportion of dissolved Pb decreased. The reliability of Pb modelling is likely to be sensitive to competition for binding sites Zn adsorption modelling, especially when there are high concentrations of Zn.

For As, PHREEQC consistently modelled a high degree of adsorption to the HFO present, which was not occurring because dissolved As makes up 73-100% of the acid soluble As. Using only 2-3% of the HFO surface actually available in the model provided a better estimate of the amount of As adsorbed, similar to when modelling As adsorption in lowland rivers (Webster-Brown and Lane 2005).

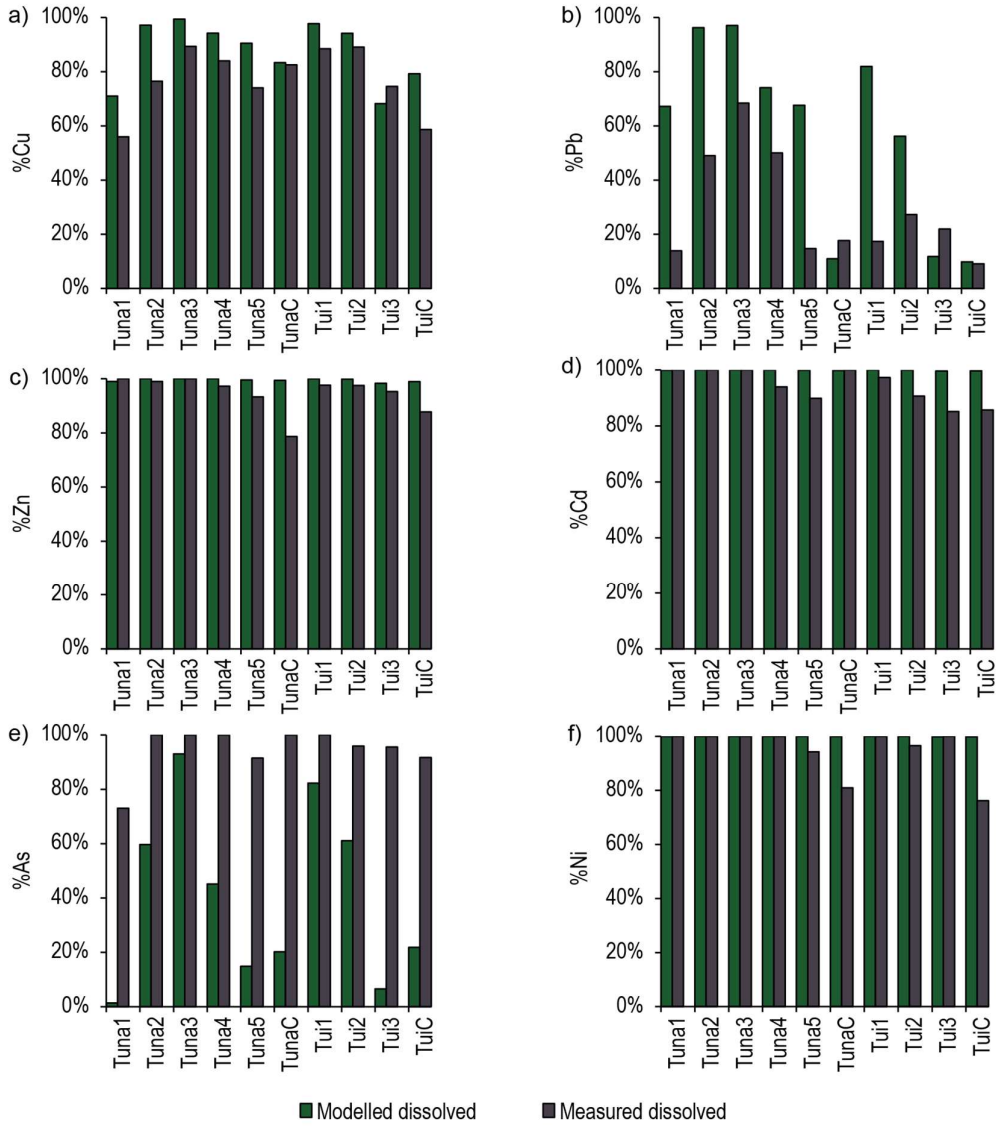

Figure 3.7 The modelled percentage of dissolved trace elements in the water column after adsorption onto freshly-formed HFO, compared to the measured percentage of dissolved trace element at each site. A) Cu, b) Pb, c) Zn, d) As, e) Cd and f) Ni.

As Cu, Pb, Zn and Cd had shown some association with the "Mn oxide" fraction in the sequential extraction, modelling of the predicted dissolved percentage of these elements was carried out with the inclusion of hydrous manganese oxide (HMO) as an adsorbing surface to determine whether this would increase the accuracy of the model. The results of this modelling are shown in Figure 3.8 except for Cd because Cd did not show significant adsorption to HMO. Data from the Tuna1 site is also excluded because no suspended particulate Mn was collected at this site (the dissolved concentration of Mn was equal to the acid soluble Mn concentration) and therefore no aqueous HMO was expected at this site.

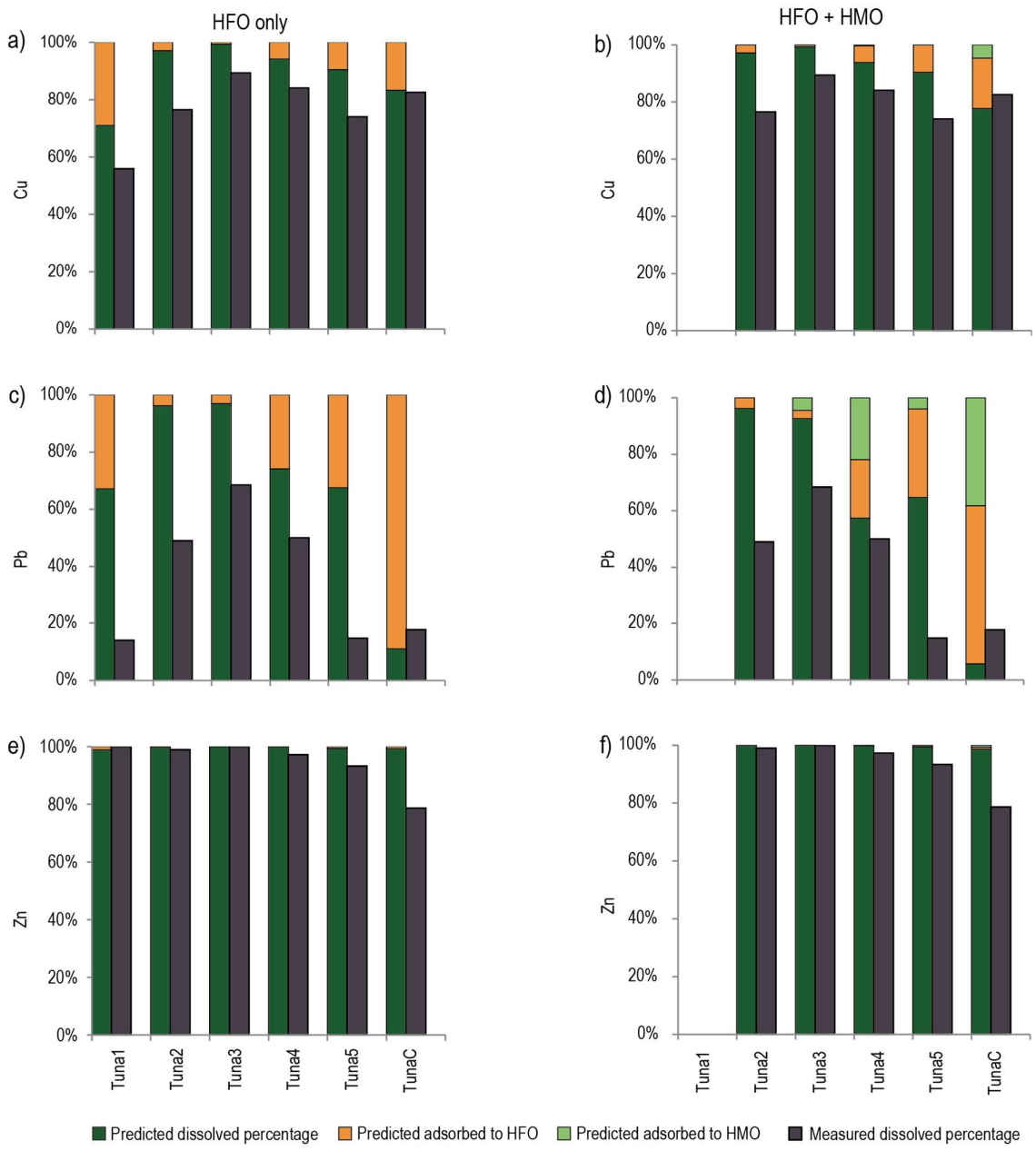

Figure 3.8 Adsorption of Cu, Pb and Zn to HFO and HMO.

Modelling speciation change with limestone addition

The remediation of Tui mine included the addition of crushed limestone and cement to the tailings pile and injection of a limestone slurry to Adit 5, to increase pH. This was anticipated to reduce trace element toxicity through complexation, and to facilitate the removal of dissolved trace elements by precipitation and adsorption. If these changes in trace element speciation can be collectively and reliably modelled with PHREEQC, then the PHREEQC model can be used to support future remediation decisions.

Where the mineral formed is HFO, the adsorption of cationic trace elements, such as Cu, Pb, Zn and Cd, is expected to increase with pH, while the adsorption of anionic trace elements such as As, decreases under the same conditions (Figure 3.9). This shows that where both cationic and anionic trace elements are present in high concentrations, modelling can be used to find the stream pH that will result in the optimum cationic and anionic trace elements adsorption onto HFO.

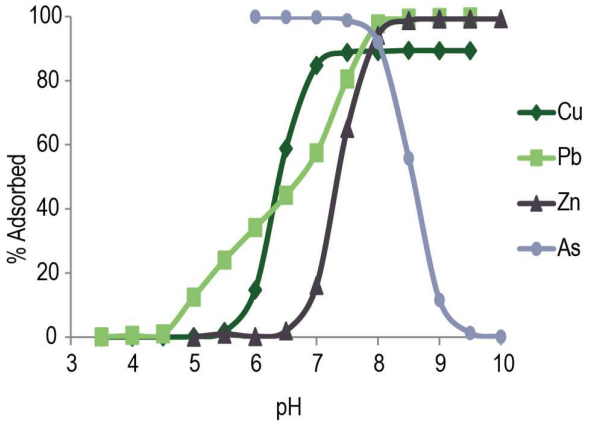

Figure 3.9 Adsorption edges for Cu, Pb, Zn and As onto HFO, under the following conditions: Temperature 13.7°C (Tuna1, Nov 2015), element concentration 0.01mg/L with no competing ions and HFO concentration of 0.68mg/L as calculated from the concentration of suspended particulate Fe (Tuna1, Nov 2015) assumed to be completely present as $Fe(OH)_3$.

The PHREEQC model was used to add calcite ($CaCO_3$) stepwise to pre-remediation stream waters, until saturation with respect to calcite was reached. The pre-remediation composition of water at the Tuna1 and Tui1 sites, as reported for July 2007 (Sharplin 2008), has been used and the electron potential (pe) was set to 12, to reflect the fast flowing, fully oxygenated stream waters.

The results of this modelling are shown in Figure 3.10 for pre-remediation Tui 1 stream water, and Figure 3.11 for pre-remediation Tuna 1 stream water. The same amount of limestone (125µmol $CaCO_3$) added to each stream water yielded quite different results; Tui1, which had a starting pH of 6.5, could be raised to 9.0 before the solution became saturated with $CaCO_3$, whereas Tuna1, which had a starting pH of 7.16, could only be raised to 7.67 with the same amount of $CaCO_3$ and did not reach saturation with respect to $CaCO_3$. This shows the diminished return of trying to achieve a pH increase with limestone addition in a near-neutral, well buffered stream such as Tunakohoia Stream, compared to Tui Stream. The pH actually measured in the streams during this study was around 7.4 for both streams indicating that the reaction had progressed approximately halfway along these modelled trajectory paths.

In both examples, the modelled concentrations of dissolved Fe were well below measured concentrations, due to the solution being saturated with respect to HFO; an effect that became more pronounced in the model at higher pH. The discrepancy between modelled and measured dissolved Fe concentrations in commonly reported and attributed to the ability of fine HFO colloids to pass through 0.45µm filters and be included in a “dissolved” concentration of Fe. Dissolved Fe decreased markedly with increased pH, and was predominantly complexed with hydroxide.

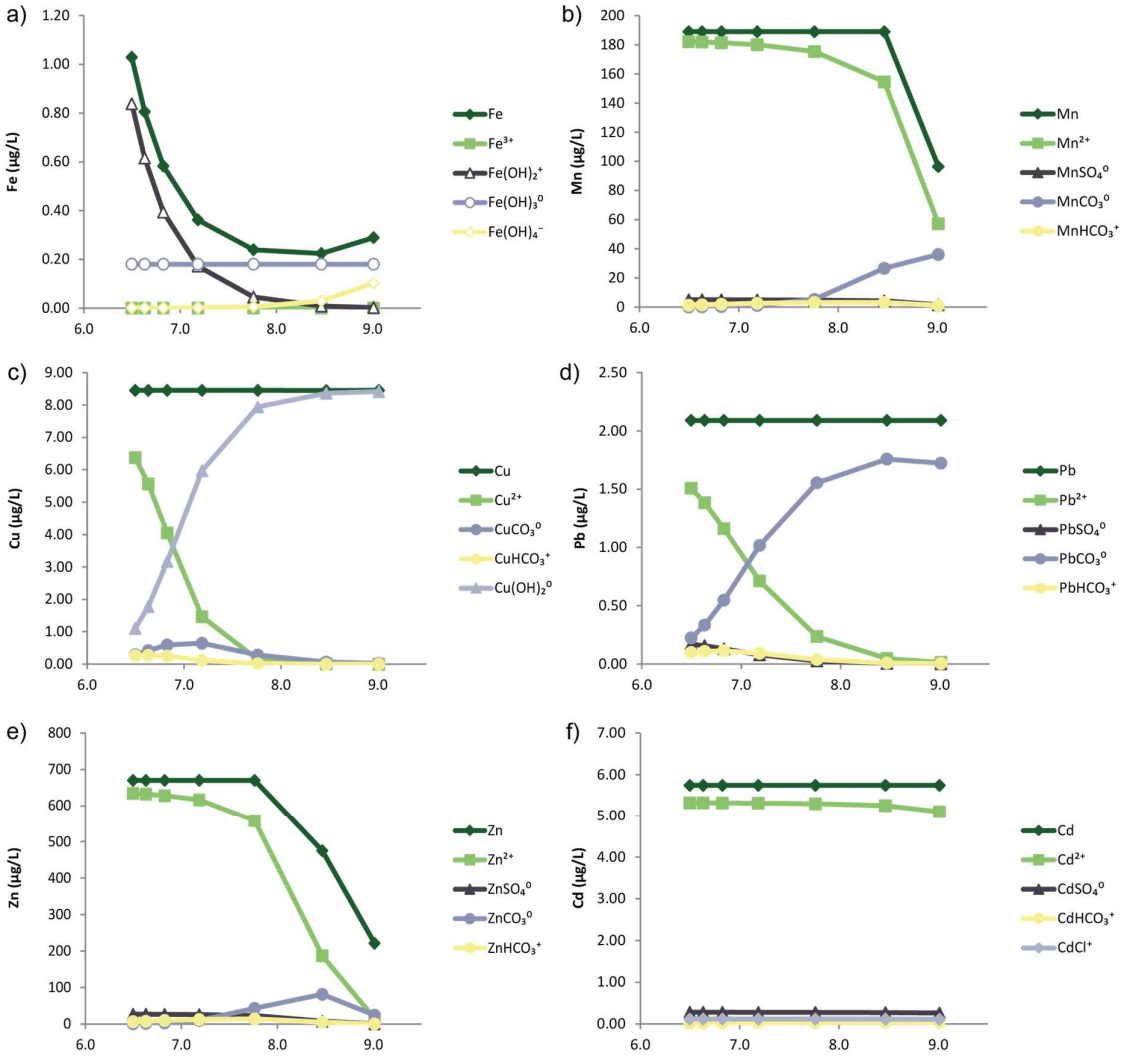

Figure 3.10 Modelled changes in dissolved element speciation when a water from Tui1 (2007 chemistry, 2007 chemistry, Sharplin 2008) is mixed with calcite, simulating the remediation works carried out at Tui Mine between 2010 and 2013.

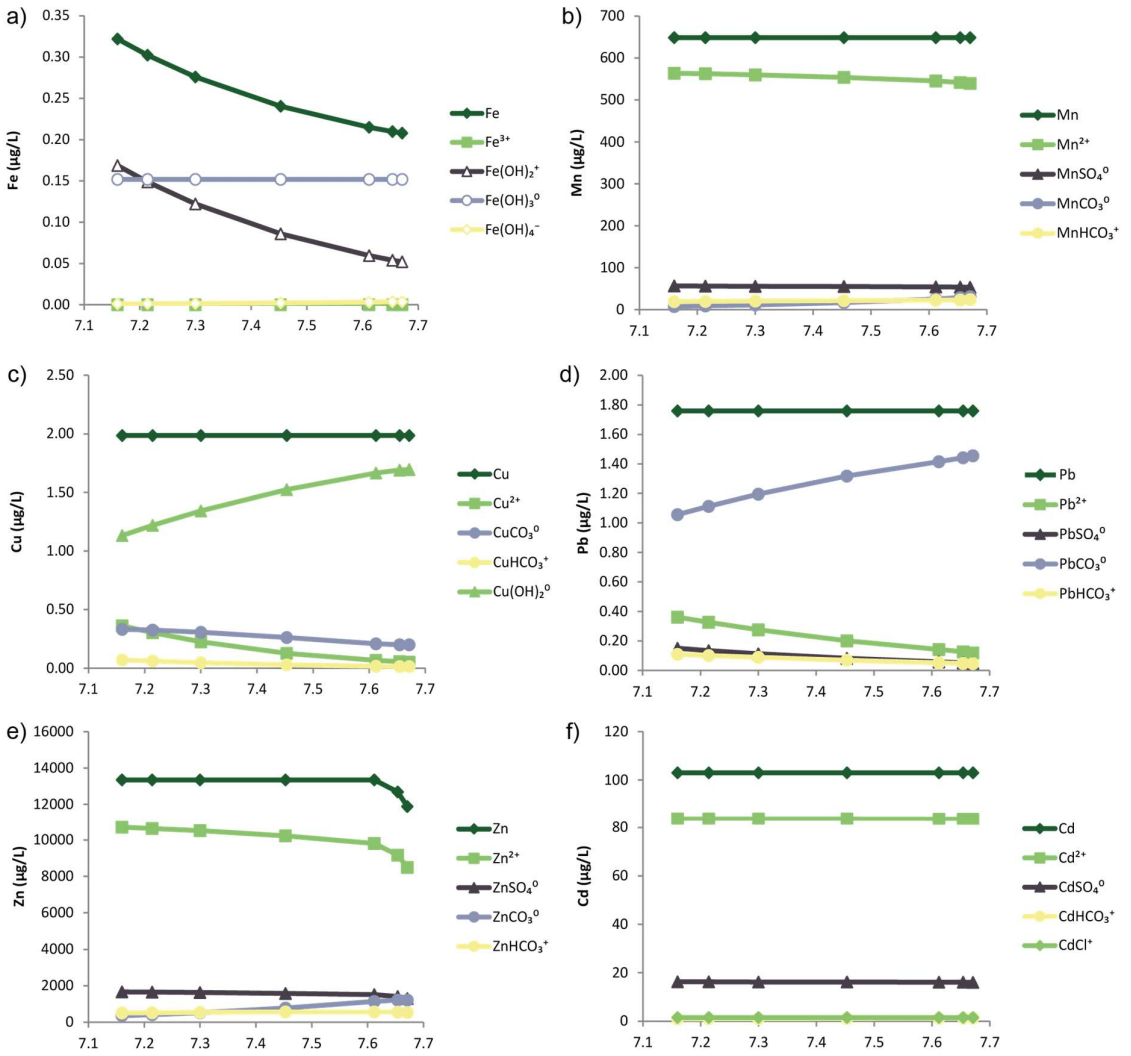

Figure 3.11 Modelled changes in dissolved element speciation when a water from Tuna1 (2007 chemistry, 2007 chemistry, Sharplin 2008) is mixed with calcite, simulating the remediation works carried out at Tui Mine between 2010 and 2013.

Dissolved Mn and Zn were also predicted to decrease significantly, but only above pH 8 (i.e., in Tui Streams only), when water became saturated with respect to rhodocrosite ($MnCO_3$), ZnO and $Zn(OH)_2$. Free Mn^{2+} and Zn^{2+} remained the dominant species. Saturation with respect to rhodochrosite was also achieved in the Tuna1 model, but did not significantly reduce the concentration of Mn or Mn^{2+}. The current Mn and Zn concentrations measured in both streams were much lower than was modelled indicating that additional mineral precipitation reactions (or adsorption reactions) are occurring.

For both streams, no change in dissolved Cd, Cu or Pb concentrations were modelled to occur over the pH range investigated, as no Cd, Cu or Pb-bearing minerals were predicted to reach saturation. However, the concentrations

of Cu^{2+} and Pb^{2+} were predicted to decrease in the Tui1 water, as $Cu(OH)_2^0$ and $PbCO_3^0$ became the dominant dissolved species. In the Tuna1 solution Cu^{2+} and Pb^{2+} were already low as $Cu(OH)_2^0$ and $PbCO_3^0$ were the dominant species at the starting pH. Neither the concentration nor percentage of Cd^{2+} was predicted to decrease significantly in either water. The concentration of Cd, Cu and Pb measured was lower at Tui1, indicating additional mineral precipitation reactions occurring or adsorption reactions occurring. Cd concentrations were lower at Tuna1, but Cu and Pb concentrations were slightly higher than was measured in 2007.

Leaching of trace elements from sediment

In the Tui Stream sediment leaching experiment, the solution pH was initially 5.0 (± 0.2), but increased to 5.6 in the first hour, then remained between 5.5 and 6.0 for the duration of the experiment. In the Tunakohoia Stream sediment leaching experiment, the pH was initially 5.5 (± 0.2), but varied between 5.5 and 6.7 during the first 24hours of the experiment, then stabilised to between 6.0 and 6.5 for the remainder of the experiment. No consistent, ongoing trend in pH was observed. In all solutions, the concentration of HCO_3 was less than detection limit, but Ca concentrations showed a rapid initial increase indicating dissolution of calcite, gypsum or another readily dissolved Ca-mineral. All elements showed a sharp initial increase in dissolved concentration in the first 12 hours when the sediment first became wet (Figure 3.12). Following this rapid initial release one of two trends in concentration occurred.

(a) An apparent "equilibrium" was established and there was little further increase in concentrations. This occurred for Ca, Cu and As leaching from the Tunakohoia sediment, where dissolved Cu and As concentrations after 1hr were >80% of the 10 day concentration. Ca and Cu also showed this trend for the Tui sediment leaching experiment, but As concentrations decreased after peaking in the first 24 hours.

(b) Leaching continued but at a slower rate. This occurred for iron (Fe), Pb, Zn, Mn and Cd. This was most pronounced for Mn and Zn leaching from the Tui Stream sediment, which showed a consistent, increase after the first 24hours.

The concentration of trace elements leached from the Tui sediment was about 10x less than that released from the Tunakohoia sediment, reflecting the much lower concentration of trace elements in the Tui sediment (Table 3.6). When compared with the total sediment concentration, a greater proportion of the bound Cu, Zn, Cd and Mn was released from the Tui sediment.

For the Tunakohoia Stream, the concentration of Fe, Mn, Cu, Pb, Zn, Cd and As after 10 days of sediment leaching was within an order of magnitude or lower, than the total (acid soluble) concentration measured in the stream at the time of sediment collection. For Tui Stream, the concentrations at the end of the leaching experiment were closer to the total (acid soluble) concentration measured in the stream at the time the sediment was collected. In

the case of Fe and Mn, the concentration at the end of the leaching period exceeded the total (acid soluble) concentration measured in the stream (Table 3.6).

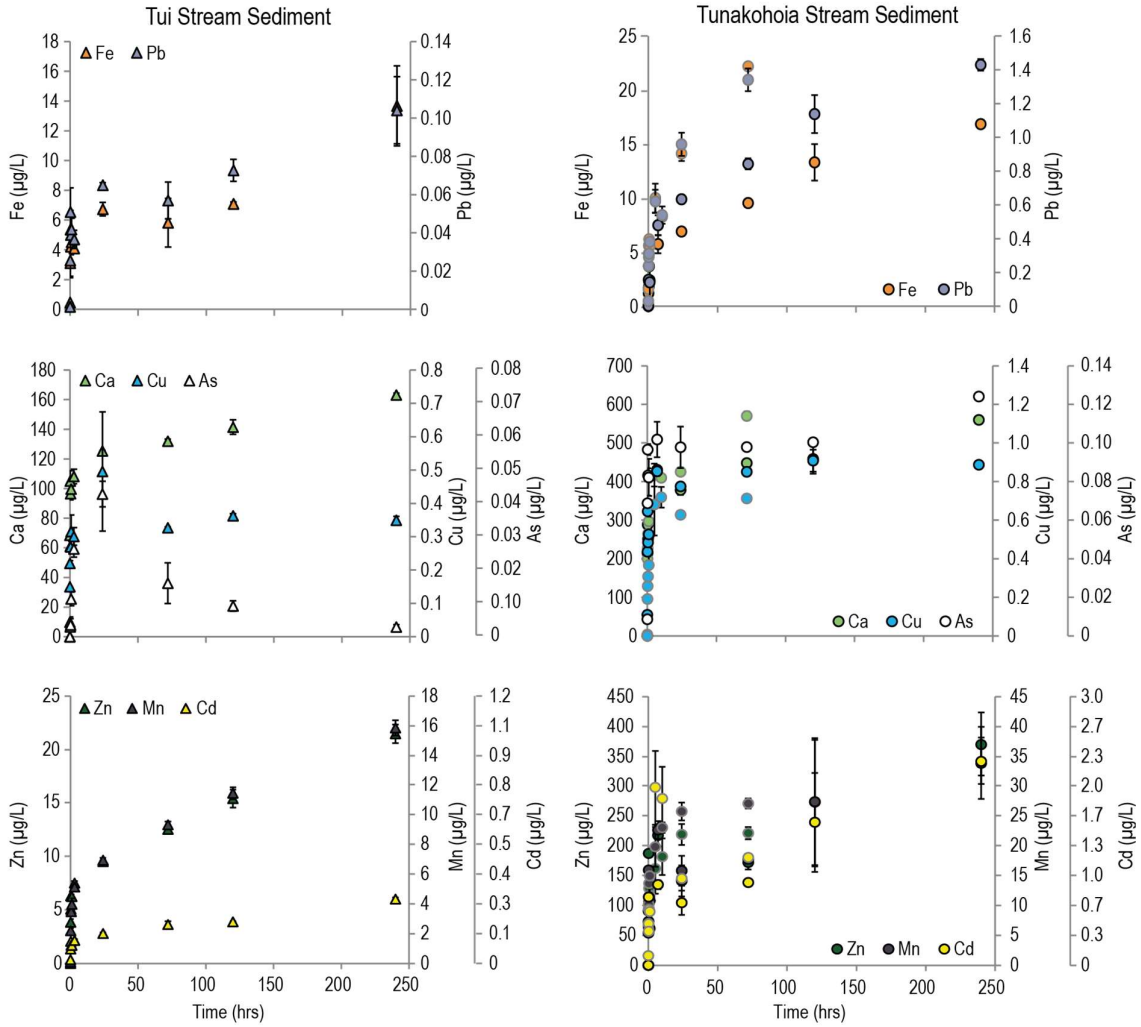

Figure 3.12 The change in dissolved concentration of selected trace elements over the duration of the leaching experiments. Note that the y axis is scaled for Cd (x15) and As (x10). Error bars show the range for duplicate samples. Results for an initial 3 days experiment (Tunakohoia sediment only) are shown with a grey outline. Results for a longer 10day experiments are shown with a black outline.

Table 3.6. The concentration in the leaching solution after 10 days compared to the total (acid soluble) concentration in the stream water at the time the sediment was collected, for Tunakohoia and Tui Stream sediment. Red indicates a higher concentration in the leaching solution compared to the stream water, yellow indicates a similar concentration (within an order of magnitude) and green indicates a lower concentration (<1/10th) in the leaching solution as compared to the stream water.

	Tunakohoia Stream		Tui Stream	
	Leached	Stream	Leached	Stream
Fe	16.8	360	13.7	7.61
Mn	33.9	453	15.9	1.13
Cu	0.89	4.94	0.34	0.95
Pb	1.43	16.5	0.10	0.23
Zn	370	2440	21.5	46.8
Cd	2.28	15.2	0.29	0.37
As	0.12	1.52	<0.01	0.44

3.4 Discussion

The full characterisation of the stream water and sediment geochemistry revealed that following the rehabilitation of the Tui mine site in 2013, there are still high concentrations of some trace elements in the water and sediment of Tunakohoia Stream and upper reaches of the Tui stream. In November 2015, dissolved Zn and Cd were above guidelines for the protection of aquatic life at all sites except the control site on Tunakohoia Stream, and dissolved Cu was above these guidelines in the upper reaches of the stream. The addition of lime slurry to the adits draining to Tunakohoia Stream has therefore not reduced the concentration of either Cd or Zn significantly, and not enough to restore a healthy aquatic ecosystem. Lime addition has not raised the pH of adit drainage from near neutral relative to the more acidic drainage from the tailings dam (Tay 1980, Hendy 1981, Webster 1995, Sharplin 2008). The rehabilitation of the tailings dam has been more effective, increasing pH in Tui Stream to near-neutral and decreasing the concentration of trace elements so that only Cd and Zn remain above ANZECC (2000) guideline values. Ecological surveys indicate an improvement in Tui Stream ecology, but overall a strong negative correlation between macroinvertebrate taxa richness, and the concentration of Zn^{2+} and Cd^{2+} occurs (Fairgray et al. 2016).

Additionally, the concentration of Cu, Pb, Zn, Cd, Ni, As, Sb and Hg in the sediment of these streams is elevated and is likely to be impacting on aquatic life. In the sediment, strong associations with Mn- or Fe-oxide phases occur for Zn, Cu, Pb and Cd, but associations for As and Sb were more exclusively associated with Fe-oxides. The association of Fe, Cu and Pb was confirmed by SEM elemental mapping while evidence of a Mn-Zn association was also seen (Figure 3.5). No carbonate minerals were observed by SEM or XRD. Additionally, although only a small portion of trace elements in the sediment are “exchangeable”, and therefore readily released in a bioavailable form, the sediment is a reservoir for trace elements that are released in favourable geochemical conditions (Fairgray and Webster-Brown 2017b).

The trace elements extracted in step three of the sequential extraction process includes elements that are released at pH 4.5 but not necessarily associated with carbonate minerals. This is why step three of the sequential extraction was renamed from the descriptor given by Leleyter and Probst (1999).

3.4.1 Modelling of dissolved trace element speciation

The PHREEQC model was used to assess the speciation of trace elements to aquatic life by determining the proportion of the element present as the free ion in a similar method to Waters and Webster-Brown (2013). Modelling predicted that the majority of dissolved Zn and Cd is present in the free ion form and therefore mostly likely to be toxic to aquatic life, while the concentration of Cu in the free ion form would be below aquatic protection guidelines (ANZECC 2000). This was supported by ecological data showing that taxa richness is reduced at sites with high Zn^{2+} and Cd^{2+} concentrations (Fairgray et al. 2016), indicating that the model could be reliably used to predict the toxicity of Zn and Cd in these environments.

3.4.2 Modelling of trace element speciation in sediment

PHREEQC has previously been used extensively to understand mine remediation processes (Watten et al. 2005, Rötting et al. 2008, Bäckström and Sartz 2011). The accuracy of the geochemical model, PHREEQC, to predict the precipitation and dissolution behaviour of trace elements has been tested by comparing observed sediment characteristics, with predictions based on modelled processes that could control trace element concentrations and mobility in this catchment system. PHREEQC modelling predicted the precipitation of Fe, Mn and Al oxides, but no trace element bearing minerals under the current water quality conditions. This is consistent with the lack of trace element minerals phases, other than residual primary ZnS (sphalerite) in the sediments. This also supports the conclusion that Pb, Cu, Zn and Cd extracted in the “carbonate” fraction of the sequential extraction were not actually associated with carbonate minerals. Modelling also indicated that increasing pH through the addition of further calcite would not significantly change this scenario for Tunakohoia Stream. In Tui Stream Zn oxide and Mn carbonate precipitation could occur at high pH (>8.0). Enhanced Fe oxide precipitation could be expected in both catchments. Secondary mineral precipitation is therefore not a significant process reducing dissolved trace element concentrations except by adsorption onto the freshly formed secondary Fe, Mn and Al oxides.

The adsorption of trace elements onto HFO was modelled by surface complexation in PHREEQC. Adsorption is likely to be an important removal mechanism for Cu, Pb and As, but less so for Zn, Cd or Ni. Modelling underestimated the removal of Pb (and to a lesser extent Cu) and overestimated removal of As, for which using <5% of available HFO could better simulate the actual degree of adsorption. This indicates that for Cu and Pb, adsorption to HFO is not the only process binding these metals to the sediment, particularly where HFO concentrations are lower at the control sites and in the lower reaches of the catchments.

PHREEQC indicates that precipitation of Mn oxides occurs in the streams, but there was little difference between the Mn concentration in the filtered and unfiltered water samples collected. Where measurable quantities of

particulate Mn were observed, inclusion of a hydrous manganese oxide (HMO) surface into the geochemical model and the PHREEQC input file did little to improve the modelled speciation of Cu, Pb, Zn and Cd (Figure 3.8). When sediment speciation was considered, a large proportion of Mn, Pb and Zn sequentially extracted from the sediment was in the "Mn oxide" fraction. This, combined with the strong association between Mn and Zn observed under SEM supports the presence of Mn oxide in the sediment where Fe oxides can facilitate their formation (Davies and Morgan 1989). It also indicates that adsorption onto and/or co-precipitation with Mn oxides may be an important metal removal process for Zn and Pb. However, this is likely to be of less overall importance than Fe oxide given the relative abundance of HFO and other binding surfaces in an AMD system.

PHREEQC therefore reliably predicts the formation of secondary Fe and Mn oxide phases, and the adsorption of Zn, Cd and Ni, and to a lesser extent Cu, onto HFO. PHREEQC underestimated the adsorption of Pb and overestimated the adsorption of As. A significant limitation of the PHREEQC model is that it assumes that the system is at thermodynamic equilibrium. This may not always be valid when fast moving mine drainage streams allow little time for sediment-water interactions to take place. However, if water and sediment chemistry are constant with time, PHREEQC models can provide useful predictions of AMD processes in aquatic environments. In the case of Tui Mine, PHREEQC modelling indicates that mine remediation through calcite addition alone is unlikely to be more effective.

3.4.3 Contribution of contaminated sediment to ongoing degraded water quality

The leaching results indicated that in fast flowing streams with high concentrations of trace elements, such as the Tui and Tunakohoia Streams, is it unlikely that release of contaminants from the sediment will impact significantly on water quality. If the sediment has sufficient time to equilibrate with the overlying water, the high concentrations of toxic trace elements already in the stream water would suppress the release of sediment-bound trace elements. Leaching of Pb, which could potentially increase Tui Stream water concentrations, would require at least 5 days of contact between the sediment and the water to reach a dissolved concentration greater than that of the stream water. Only Fe and Mn, in Tui Stream could leach rapidly enough to affect water quality in the fast flowing, oxidised stream environments. Neither Fe nor Mn are likely to adversely affect aquatic ecosystems at the concentrations that will be achieved through rapid leaching.

Appreciable concentrations of Zn and Cd are able to leach from the sediment in its current state. However, it is expected that, with time, the contamination coming out of the adits will decrease. With time the contaminated sediment will also flush through the streams in high flow events, and have lower trace element concentrations due to dilution with incoming sediment and desorption processes.

Further work could investigate how fast the sediment is transported downstream and continued sediment monitoring may be able to track a "plug" of contaminated sediment as it moves down the catchment. At this stage

the most contaminated sediment is in the upper-most section of the stream but if contaminant loading is reduced, the most contaminated sediment may move to lower sections of the stream before washing out of the catchment.

3.5 Conclusion

In this research it was found that:

- Remedial works at Tui Mine have reduced the concentration of trace elements (Fe, Mn, Cu, Pb, Zn, Cd, As) compared to pre-remediation concentrations. However, trace element concentrations still exceed ANZECC (2000) guidelines for the protection of 95% aquatic species for dissolved Cu, Zn and Cd. Speciation modelling has shown that the concentration of Cu^{2+} is below the ANZECC (2000) guideline for the protection of 95% aquatic species at all sites but Zn^{2+} and Cd^{2+} still exceed these guidelines.

- The sediment in Tui and Tunakohoia Streams contain trace elements at concentrations exceeding guidelines for ecosystem health. The availability of trace elements from the sediments of these streams may hinder ecosystem recovery when the concentration of dissolved trace elements entering the streams is reduced further.

- Modelling of the trace element attenuation processes that occur after the remedial works were completed at Tui Mine have shown that the pH must be raised above 7.5 before any reduction in Mn and Zn through formation of mineral precipitates will occur. However, a reduction in the concentration of Cu and Pb through adsorption to HFO can occur above pH 6. A reduction in the concentration of Cd and Zn to a concentration suitable for supporting healthy ecosystem functions is unlikely to occur within the pH range able to be achieved by limestone addition at Tui Mine.

- The legacy of trace element contamination in the sediments of Tui and Tunakohoia Streams indicates that the reduction of dissolved trace element concentrations in the overlying water column will be difficult, and Fe, Mn, Pb and Cu can transfer from the sediment into the water column. The concentration of dissolved trace elements in Tui and Tunakohoia Streams is expected to continue to decrease following remedial works at Tui Mine and the contaminated sediment may continue to release trace elements into the water column. At present, the upstream source of trace elements masks the contribution of trace elements from the sediment.

- Modelling of trace element attenuation processes with PHREEQC indicate that the formation of secondary Fe (oxy)hydroxide and Mn oxide phases are reliably predicted by the saturation index function in PHRREQC. Modelling correctly predicts that little adsorption will occur, but has not been tested in a pH range where significant adsorption is likely to occur. The adsorption of Zn, Cd, Ni, and to lesser extent Cu, onto freshly formed Fe (oxy)hydroxides (HFO) is also reliably predicted by PHREEQC. Modelling of attenuation of Pb and As through adsorption to HFO was less reliable. Adsorption of As to HFO was overestimated and adsorption of Pb to HFO was underestimated.

CHAPTER 4

PUHIPUHI MINE

Figure 4. Waikiore Stream at the Puhi3 sampling site. Photo: Justin Pomeranz

This chapter reports research into the water and sediment chemistry of streams draining an epithermal mineral deposit where mining of cinnabar [HgS] and ore processing to produce mercury metal occurred. The speciation, toxicity and bioavailability of dissolved and sediment-bound trace elements are determined through analysis of water and sediment samples and geochemical modelling. The effects of mining and ore processing on macroinvertebrate communities, and the accumulation of mercury into the food chain are assessed. Finally, the ability of geochemical models to accurately predict water quality is tested.

4.1 Introduction

Puhipuhi Mine is located in the Northland Region of New Zealand, 35km north of Whangarei, near Whakapara. The Puhipuhi area is drained by the Waiariki Stream through three main tributaries; Waikiore Stream, Pukekaikiore Stream and Whenuaroa Stream. The Waiariki Stream flows into the Whakapara River which joins the Wairoa River and flows into Kaipara harbour (Figure 4.1). The regional geology consists of greywacke overlain with basalt as well as small areas of lake bed deposits and sinter outcrops (Figure 4.2; Locke et al. 1999). Mineralised ore at Puhipuhi is found within the four areas of silica sinter outcrops aligned in a N-S trend along the Waikiore fault line (White 1986, Christie and Brathwaite 1995). This sinter is the upper zone of an epithermal mineral deposit (Locke et al. 1999, Craw et al. 2000a).

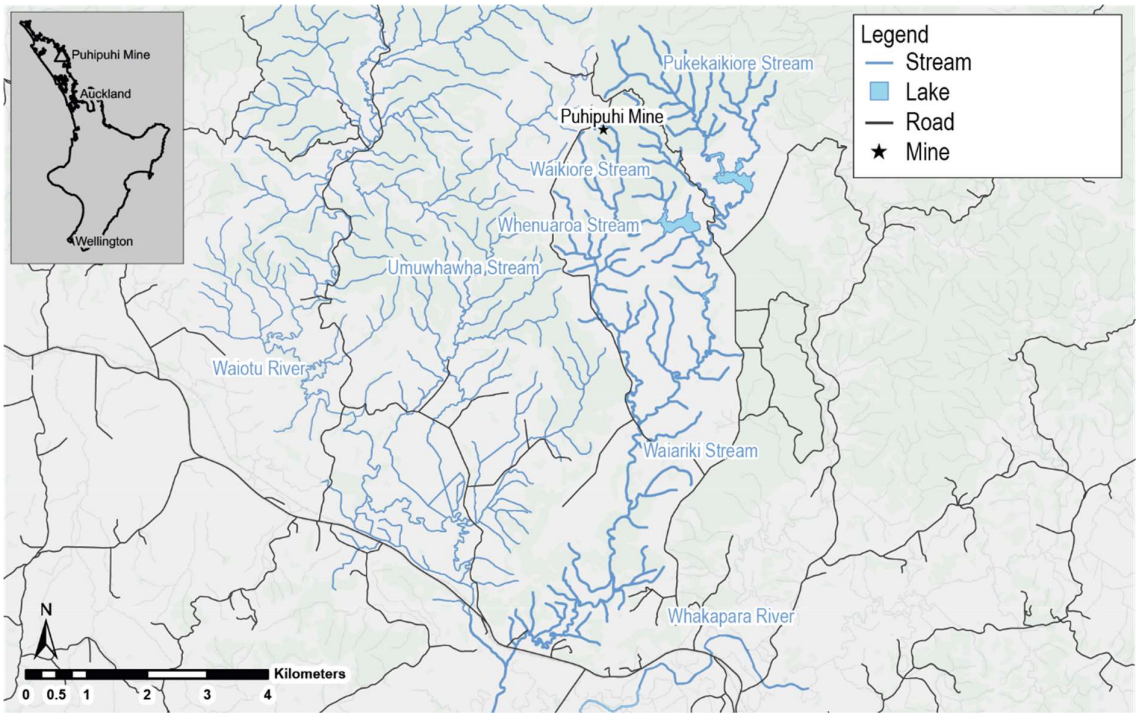

Figure 4.1 The Waiariki Stream catchment where the Puhipuhi Mine and associated deposits are located.

4.1.1 Ore Geology

The most notable trace element-bearing minerals within the deposit are pyrite [FeS_2], marcasite [FeS] and cinnabar [HgS] but several other trace element-bearing minerals are present including chalcopyrite [$CuFeS_2$], covellite [CuS], stibnite [Sb_2S_3], livingstonite [$HgSb_4S_8$], pyrargyrite [$AgSbS_3$], argentite/acanthite [AgS/Ag_2S] and tetrahidrite/freibergite [$Cu_6(Cu_4[Fe,Zn]_2)Sb_4S_{13}/Ag_6(Cu_4Fe_2)Sb_4S_{13-x}$] (White 1986, Craw et al. 2000a, Hampton et al. 2004). Additionally pyrite, marcasite, limonite [FeO(OH)] and phosphate minerals contain Hg and As impurities are present at Puhipuhi (Craw et al. 2000a).

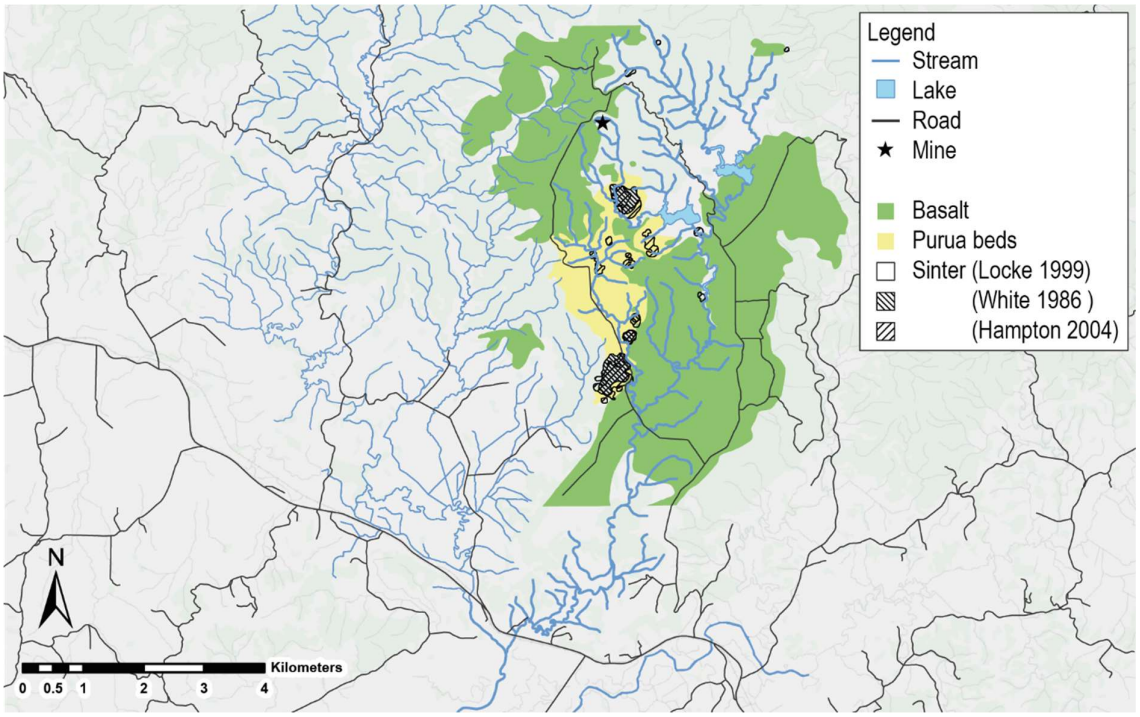

Figure 4.2 Geology of the Puhipuhi area, from Locke et al. (1999)

4.1.2 History of mining at Puhipuhi

The Puhipuhi area was first prospected in 1888 when silver with tracer gold was discovered in the north western part of the Puhipuhi area (Locke et al. 1999). Silver was mined in the Puhipuhi area and around the Pukekaikiore Stream from late 1880's into the early 1900's (White 1986, Locke et al. 1999, Hampton et al. 2004). Alluvial cinnabar, the sulfide ore of mercury, and quartz outcrops containing cinnabar were discovered in the area and the Puhipuhi Mine was opened in 1910 (Christie and Brathwaite 1995). An ore processing area was constructed at the head of the Waikiore Stream with the stream being dammed to create a reliable water supply for the mine (Butcher 2010). Mining of Mt Mitchell sinter, near the Whenuaroa Stream, was carried out during WWII (Locke et al. 1999, Craw et al. 2000a). Several mining companies operated the Puhipuhi mine one after the other until the mine was finally abandoned in 1946 (Butcher 2010). As well as mining, gravel was quarried from the Puhipuhi area and used for construction of roads during the 1960's-1990's (Craw et al. 2002). This practise was stopped due to environmental concerns from residents because of the impacts of acidity of road run-off on roadside vegetation (Craw et al. 2002). In more recent years, several companies have carried out exploration for gold but this interest has not yet progressed into an active mining stage (Christie and Brathwaite 1995, Locke et al. 1999, Craw et al. 2000a, Evolution Mining 2016).

Previous studies identified three main contaminants of concern at Puhipuhi. These are acid load, dissolved mercury (Hg) and dissolved arsenic (As) (Hoggins and Brooks 1973, Craw et al. 2000a, Craw et al. 2002, Craw 2005, Gionfriddo et al. 2015). A pH of as low as 2.8 has been measured in standing water and 1.4 in seeping water at the Puhipuhi Mine site (Craw et al. 2000a, Craw 2005, Gionfriddo et al. 2015). pH as low as 3.1 has been measured

in stream water in the Puhipuhi area (Craw et al. 2000a, Craw et al. 2002). Low pH can dissolve $CaCO_3$ shells of molluscs, oligochaetes, and crustaceans as well as preventing uptake of Na^+ in biota (Camargo 1995, Havas and Advokaat 1995, Gerhardt et al. 2004). Additionally, low pH affects the speciation of trace elements by increasing the solubility of minerals leading to the dissolution of trace element-bearing mineral phases and release of toxic trace elements into solution. Low pH also increases the toxicity of cationic trace elements as they are more likely to being in the free ion (more toxic) form, rather than forming a complex with other water constituents or adhering to a surface such as natural organic matter or hydrous ferric oxide (HFO) (Benjamin and Leckie 1981, Cravotta and Trahan 1999, Brown and Markich 2000, Rytuba 2000, Paquin et al. 2002, Craw 2005). However, at low pH, oxyanions, such as that of As and Sb, are more likely to be adsorbed to a surface such as natural organic matter or HFO (Goldberg and Johnston 2001, Filella et al. 2002, Smedley and Kinniburgh 2002).

Mercury

The concentration of dissolved Hg in the waters draining the Puhipuhi Mine site was 0.5µg/L in 1972, but more recently was in the range of 0.118-0.26µg/L (Table 4.1;Hoggins and Brooks 1973, Gionfriddo et al. 2015, Ropiha and Hansen 2015). The concentration of dissolved Hg decreases downstream of the mine to 0.11µg/L (1972) and <0.05µg/L (2014) where the Waiariki Stream flows under the SH1 bridge (Table 4.1; Hoggins and Brooks 1973, Ropiha and Hansen 2015). The concentration of Hg bound to stream sediment was 28mg/kg at the Puhipuhi Mine site in 1972 but more recently was in the range of 31-83mg/kg L (Table 4.1; Hoggins and Brooks 1973, Ropiha and Hansen 2015). Sediment-bound Hg decreases downstream to 1.0mg/kg (1972) and 1.6-1.8mg/kg (2014) (Table 4.1; Hoggins and Brooks 1973, Ropiha and Hansen 2015).

In humans, Hg is a neurotoxin and causes damage to the brain resulting in behaviour changes, shaking and loss of muscle control, loss of vision, hearing and sensation, and loss of memory (ATSDR 1999). Mercury can also cause damage to other internal organs and has been shown to accumulate primarily in the kidneys but also in the thyroid and pituary glands, and the brain (Kosta et al. 1975, Nylander and Weiner 1991, ATSDR 1999). Methylmercury (MeHg) is a form of Hg that is particularly of concern due to its toxicity to aquatic life and its ability to bioaccumulate in the food chain. It is formed by the methylation of mercury through microbial processes involving sulfate or iron reducing bacteria or methanogenes (King et al. 2002, Parks et al. 2013). Methylmercury is lithophilic so when it is taken up by aquatic organisms, it accumulates in the organism and can then be transferred up the food chain resulting in higher concentrations accumulating in the body of species of a higher tropic level (ATSDR 1999, King et al. 2002). Bioaccumulation of Hg in a food chain can become a human health hazard where aquatic organisms are harvested for human consumption (ATSDR 1999). This aspect is important at Puhipuhi because cultural eel and shellfish harvesting practises of local iwi occur downstream of the Puhipuhi Mine site.

Table 4.1 Previously reported concentrations of dissolved Hg and sediment-bound Hg at four sites in the Puhipuhi area. The Puhipuhi Mine site corresponds to Puhi3 in this research; Pukekaikiore Stream corresponds to Puhi4, and SH1 Bridge corresponds to Puhi1. The Tangiteroria site is further downstream from the sites sampled in this research.

Location	Dissolved Hg (µg/L)	Sediment-bound Hg (mg/kg)	Year	Reference
Puhipuhi Mine site	0.5	28*	1972	Hoggins and Brooks (1973)
	0.118-0.240	-	2013#	Gionfriddo et al. (2015)
	<0.05-0.26	31-83	2014	Ropiha and Hansen (2015)
Pukekaikiore Stream	0.13	4.4	1972	Hoggins and Brooks (1973)
	<0.01	-	1999#	Craw et al. (2002)
	<0.05-0.07	1.9-6.3	2014	Ropiha and Hansen (2015)
SH1 Bridge	0.11	1.0	1972	Hoggins and Brooks (1973)
	<0.05	1.6-1.8	2014	Ropiha and Hansen (2015)
Tangiteroria	-	0.2	1972	Hoggins and Brooks (1973)
Aquatic ecosystem protection†	0.06	0.15		ANZECC (2000)

* Upper-most site for which value is given in Hoggins and Brooks (1973).
# Sampling is assumed to have been carried out in the year in which the paper was received by the journal.
† Protection of 99% aquatic species guideline value used for dissolved Hg. ISQG-low guideline value used for sediment-bound Hg.

Values for acute and chronic concentrations of toxicity of dissolved Hg and MeHg to aquatic fauna span a range of concentrations (Table 4.2). The ANZECC (2000) guideline and maximum acceptable values for the protection of aquatic life and drinking water are also shown in Table 4.2 for comparison. These guideline values for protection of aquatic life are based on toxicity values and do not take into consideration the potential for bioaccumulation of Hg in piscivorous fish or wildlife (Canadian Council of Ministers for the Environment 2003). Ensuring that mercury is not bioaccumulating to the point where it is a human health risk would be preferable however, and so commercial fisheries and food producers must show that their product does not exceed guidelines for food safety. The New Zealand food safety authority limits for non-listed fish (ie. Eels), crustaceans and shellfish is 0.5mg/kg average within a sample with no sample unit greater than 1.5mg/kg (wet weight, wet weight, Food Standards Australia New Zealand 2015).

Table 4.2 Toxicity of dissolved Hg and MeHg to aquatic fauna and relevant guidelines for protection of aquatic ecosystems and drinking water.

Hg Species	Value type	Value	Reference
Hg	Acute toxicity	Invertebrates: 5-5600μg/L Fish: 150-900μg/L	Canadian Council of Ministers for the Environment (2003)
	Chronic toxicity	Invertebrates: 1.28-12.0μg/L Fish: 0.26- >64μg/L	Canadian Council of Ministers for the Environment (2003)
	Aquatic protection guidelines	0.026μg/L	Canadian Council of Ministers for the Environment (2003)
		0.060μg/L*	ANZECC (2000)
		2.4μg/L (acute) 0.77μg/L (chronic)	U.S. EPA (2001)
	Drinking water standard	7.0μg/L	NZ Ministry of Heath (2008)
		2.0μg/L	U.S. EPA (2001)
		6.0μg/L	WHO
MeHg	Acute toxicity	Fish: 24-125μg/L	Canadian Council of Ministers for the Environment (2003)
	Chronic toxicity	Invertebrates: 0.04-1.14 μg/L Fish: 0.93-63μg/L	Canadian Council of Ministers for the Environment (2003)
	Aquatic protection guidelines	0.004μg/L	Canadian Council of Ministers for the Environment (2003)

* Protection of 99% aquatic species guideline value

Arsenic

The concentration of dissolved As is between <1μg/L-140mg/L in run-off water, standing water and seeps at three quarries in the Puhipuhi area, and the concentration of dissolved As was only 1μg/L in stream waters downstream of the Forestry quarry, where standing water with a concentration of 140mg/L (Craw et al. 2002). Dissolved As concentrations between <0.1-0.3μg/L occur at the Puhipuhi Mine site but up to 14μg/L in the other tributaries of the Waiariki Stream (Ropiha and Hansen 2015). Additionally, also measured the
As concentration are up to 600mg/kg in stream sediment downstream of the Forestry quarry (Craw et al. 2002) and between 2.6-170mg/kg within the Puhipuhi area (Ropiha and Hansen 2015).

Arsenic is acutely toxic and a human carcinogen. Lung tumours develop following inhalation of As, skin tumours after oral exposure to As and tumours on internal organs, including bladder, liver and kidneys develop following consumption of As-contaminated drinking water (Hughes 2002). Consensus on whether As is carcinogenic to animals is yet to be reached with some studies showing that it is while others don't (Hughes 2002).

The WHO limit for As in drinking water is 10μg/L (Ministry of Heath 2008, Bowell et al. 2014). ANZECC guideline for protection of 95% of species in aquatic ecosystems are 24μg/L for As(III) and 13μg/L for As(V) (ANZECC 2000).

Aside from these three main contaminants, other trace elements may also be elevated to a level that is toxic to aquatic life or human health.

4.1.3 The environmental effects of the Puhipuhi Mine

The first investigation into the environmental and ecological effects of the mining activities at Puhipuhi found that Hg was detectable in stream water 8km downstream of Puhipuhi Mine and in stream sediment 35km downstream of the mine site (Hoggins and Brooks 1973). Mercury was detected in shellfish 150km downstream of the site but not at levels significantly higher than in shellfish collected from uncontaminated "clean" sites (Hoggins and Brooks 1973).

Electron microprobe analyses of four materials collected from the Puhipuhi area measured Hg and As in ribbons through quartz or dispersed through kaolinite and marcasite at concentrations of around 1% Hg and up to 40ppm As in the sinter sample (Craw et al. 2000a). Measurements of pH and Eh in surface waters and wet soil indicated that at sites with a very low pH (<2), pyrite, elemental sulfur and orpiment [As_2S_3] are stable but at sites with a higher pH, Fe, S, Hg, and As were expected to be dissolved (Craw et al. 2000a). The theoretical stability of Hg- and As-bearing minerals, combined with the concentration of Hg and As within the minerals, were used to show that oxidation of marcasite is the most important process releasing Hg and As into the Puhipuhi environment; while very little Hg is dissolved and released from cinnabar oxidation (Craw et al. 2000a). Samples collected from the Puhipuhi Mine could release up to 20ppm Hg in conditions expected at the site (Craw et al. 2000a).

Investigations into the potential for mineralised rock, which was quarried from three locations in the Puhipuhi area and spread on roads and farm tracks in the area, to contribute acidity, Hg and As contaminants to water courses in the Puhipuhi catchment found that although the mineralised road aggregate had elevated concentrations of As, but the high concentrations of As did not extend beyond the road edge Craw et al. (2002). However, where road run-off entered a watercourse, low pH continued for over 300m from the road. As and Hg were more likely to adsorb to clays or iron oxyhydroxides than to be carried downstream in a soluble form. Although the low pH in these waters enhances the adsorption of Hg and As to HFO. If the iron rich sediment with adsorbed Hg and As was transported to an area with a higher pH, As and Hg would desorb, increasing the mobility of Hg and As. However, the volume of mineralised rock that was spread on roads is much less than exists naturally on forestry and farmland in the Puhipuhi area (Craw et al. 2002).

The mobility of Hg and As in quarry run-off and in nearby soils was examined by Craw (2005). The optimal soil pH for limiting Hg and As mobility was between pH3-4, similar to the nearby forest soils. However, where agricultural soils are amended with lime to increase soil pH, this could lead to mobilisation of Hg and As (Craw 2005).

The concentrations of dissolved trace elements (As, Cd, Cr, Cu, Hg, Ni, Pb and Zn) in the Waiariki Stream catchment were monitored monthly over the course of a year between July 2013 and June 2014 by Northland

Regional Council in collaboration with Ngati Hau representatives (Ropiha and Hansen 2015). The ANZECC (2000) guidelines for ecosystem protection were exceeded for Cr, Cu and Zn but not for Hg during this monitoring program. Sediment samples were also collected from within the Waiariki Stream catchment on two occasions and concentrations of sediment-bound Hg exceeded the ANZECC (2000) ISQG-high guidelines at all sites and the ISQG-low guidelines for Cu and Ni at two sites.

Determination of concentrations of MeHg in water and sediment samples found that the percentage of Hg as MeHg ranged between 0.3-1.6% and was highest in the dam lake where there was a large amount of dissolved organic matter, neutral pH, low sulfate concentration but high nitrate concentration and therefore had a high capacity to methylate Hg (Gionfriddo et al. 2015). Several pathways for Hg contamination of stream water and sediment, soil and plants within the processing plant vicinity were described but more data is needed to assess the pathways by which Hg leaves the site (Gionfriddo et al. 2015).

As interest in the area for further mining may yet progress into an active mine, it is important to determine the current state of the streams, to ascertain how the previous mining operations have affected streams and to model how future mines may affect streams in the catchment.

4.1.4 Aim and objectives of this research

The aim of this research is to assess the current state of the streams in the Puhipuhi area through both chemical and ecological analyses, and to undertake geochemical modelling of trace element attenuation under the different conditions that occur. The objectives of this research are to:

- Determine how historic mining of Hg impacts stream water, sediment quality and biota in the affected streams.
- Determine whether geochemical modelling can reliably predict how trace elements, such as Hg, are attenuated downstream of the mine site.

4.2 Methods

4.2.1 Study area

The Puhipuhi Mine site was selected for this research because it was a former mine site in New Zealand, where trace element contamination of nearby waterways was known to be occurring (Section 2.1). This site was also of interest as it has been explored in the past and was, at the time of this research, undergoing further exploration for mineral deposits which could be safely and economically mined.

Puhipuhi Mine is surrounded by farmland and bush areas consisting of subtropical rainforest, native shrubs and exotic species (Craw et al. 2002). It is at an altitude of 400masl and has an average annual rainfall of 2177m/yr (Northland Regional Council 2016). The Puhipuhi mine is located at the headwaters of the Waikiore Stream, which

was dammed in order to create a reliable water supply for the mine (Butcher 2010). The Pukekaikiore and the Whenuaroa streams drain the catchments adjacent to the mine and they are affected by natural weathering of ore deposits. These streams converge to form the Waiariki Stream which flows into the Whakapara River.

4.2.2 Sample collection

Water and sediment samples were collected from 12 sites within the upper Waiariki River catchment and from two sites in an adjacent catchment, with a similar geology but unaffected by mining activities, which were used as reference sites (Figure 4.3). Samples were collected from sites 1-8 in June 2015 by Prof. Jenny Webster-Brown, and Kerry Webster and Katrina Hansen of Northland Regional Council. Data from this winter sampling event was made available for this study. Samples from these sites, sites 9-11 and the plant site were recollected in January 2016 (summer). Measurement of physiochemical parameters and collection of water and sediment samples was carried out following the methodology outlined in Section 2.2.

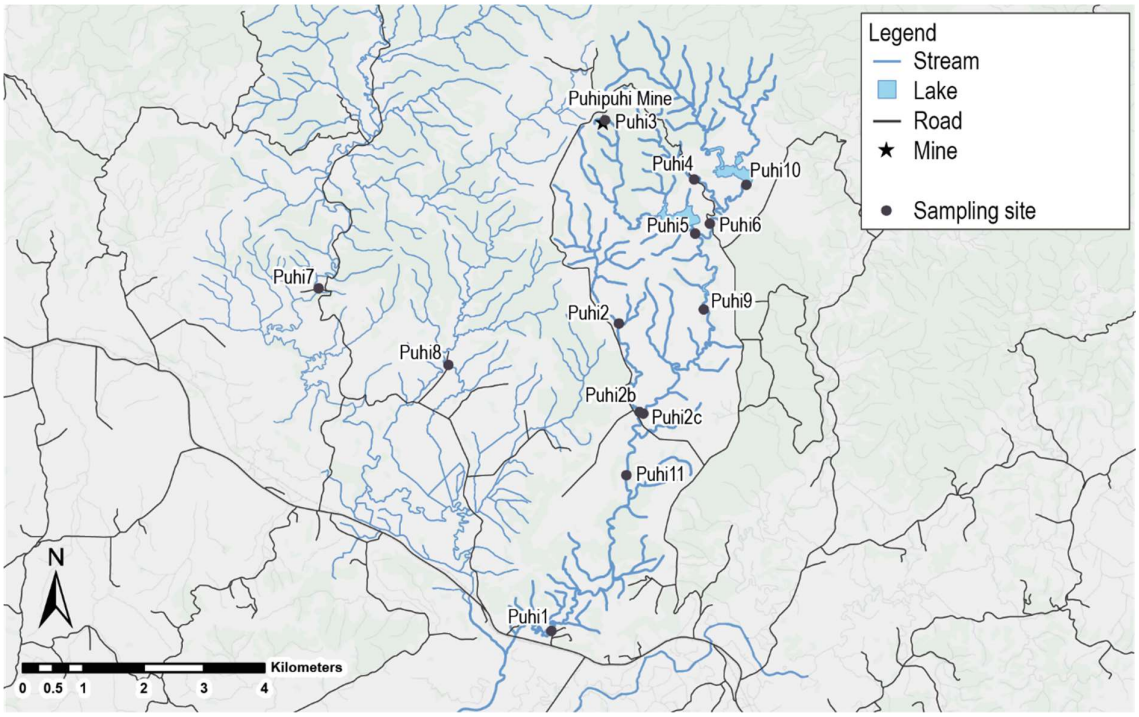

Figure 4.3 Map of Puhipuhi area showing the location of sampling sites based on previous research by Northland Regional Council (Ropiha and Hansen 2015), with the addition of sites Puhi2b, Puhi2c and Puhi9-11.

For ecological assessment, three Surber samples (0.06 m^2, 250 µm mesh) and a qualitative kick net sample (250 µm mesh) were collected. These samples were collected by Justin Pomeranz, Prof. Jon Harding and Dr. Kevin Simon during the January 2016 sampling event. Samples were collected from six impacted sites (Puhi1, 2b, 2c, 3, 4, 6) and the two reference sites (Puhi 7 and 8). The Surber samples were collected from riffle habitats at each site by disturbing the benthic substrate to a depth of approximately 10 cm. Rocks were thoroughly scrubbed in order to remove all individuals. The kick net samples were collected from all habitats present (e.g. riffle, pool, cut

bank margins, submerged large woody debris) in order to gain a complete taxonomic list for each site. All samples were immediately preserved in the field with 70% ethanol.

Samples were collected under flow conditions close to base-flow (1.3m^3/s at Whakapara, just downstream of Puhi1, (Northland Regional Council 2016). Flow at Whakapara during the June sampling was 1.6m^3/s decreasing to 1.5m^3/s. Flow varied between 6.2m^3/s and 4.6m^3/s during the January 2016 sampling event.

During the January 2016 sampling round, two frozen eels were donated by local iwi for analysis. One eel was described as being from the "Hikurangi swamp", a wetland area surrounding the confluence of the Whakapara and Wairua Rivers, and the other from "above Puhipuhi". The "Hikurangi Swamp" eel sample consisted of two pieces of frozen eel flesh; one approximately 20cm long and 4.5 cm in diameter, taken from the mid-section of the eel, and one approximately 14cm long and 3.5cm in diameter, taken from just below the head. The "above Puhipuhi" eel was a complete frozen eel, approximately 84cm long and 5.5cm in diameter. This eel was cut into 3 pieces of roughly equal size in the field, so that it could be transported in a chilly bin of ice back to Christchurch. Samples were kept frozen until analysis could be completed.

4.2.3 Sample analysis and treatment

Water

Water samples were analysed for major cations and trace elements by ICP-MS and for major anions by HPIC (Section 2.3). Dissolved inorganic carbon (DIC) concentrations were determined by infra-red gas analysis of CO_2(g).

Sediment

Total sediment digestions and sequential extraction of trace elements from individual mineral phases were completed (Section 2.4). Due to analytical limitations Hg could not be analysed in the sequential extraction fractions. Samples were also analysed by XRD by Panda Geosciences and by SEM-EDS.

Macroinvertebrates

Macroinvertebrate samples were processed by Emma Mackenzie with identification assistance from Anna Henderson. Samples were sieved through 500µm mesh in the laboratory. Invertebrates were counted and identified to the lowest taxonomic level using identification guides of Winterbourn et al. (2006). AMDI scores were calculated for each site using the tolerance scores of Gray and Harding (2012).

Eel flesh

Three subsamples of approximately 20g were cut from each frozen eel using a clean ceramic knife. The subsamples were forwarded to Hill Laboratories for analysis using a frozen courier service. At Hill Laboratories, the eel samples were digested using a strong acid (HNO_3/HCl) digestion, which was analysed for Sb, As, Cd, Cr,

Co, Cu, Pb, Hg, Ni and Zn using ICP-mass spectrometry. A separate organic (TMAH) digestion was used for determination of Se. The digestion included the skin of the eel, as well as the flesh. Trace element concentrations are given for "wet weight" of sample as received by Hill Laboratories, but an analysis of "dry weight" (after thawing and drying the sample at 65˚C) was also provided.

4.2.4 Geochemical modelling

Geochemical modelling of the speciation of dissolved trace elements, saturation indices of trace element-bearing minerals and binding of trace elements to adsorptive surfaces within the sampled waters was carried out using the PHREEQC geochemical modelling program (Section 2.6). Additional thermodynamic data from the MINTEQv4 database for Hg and Sb was used to supplement the WATEQ4f database.

4.3 Results

4.3.1 Aqueous chemistry

Water chemistry data for sites sampled in June 2015 (Table 4.3.1) and January 2016 (Table 4.3.2). The sites sampled in the Waiariki River catchment had higher concentrations of trace elements compared to the neighbouring Waiotu River catchment, where the reference sites were located.

The total Fe concentration was elevated at Puhi3, downstream of the dam at the ore processing plant, but concentrations decreased downstream (Figure 4.4a). Cu, Zn, As, Sb and Cd had low concentrations downstream of the Waikiore Stream dam (Puhi3) but were elevated with respect to the reference sites in the Pukekaikiore Stream (Puhi4 and Puhi6). Arsenic and Sb are shown in Figure 4.4c and Figure 4.4d respectively. Dissolved concentrations of As, Sb and Cd were also elevated at the Whenuaroa Stream sites (Puhi2 and Puhi2b). Conversely, concentrations of Pb, Ni and Hg were elevated downstream of the Waikiore Stream dam and at the ore processing plant (Puhi3 and Plant site) but lower in the other tributaries (Hg shown in Figure 4.4b). Only Ni concentrations were elevated at a site in a different tributary (Puhi4). ANZECC guidelines for the protection of aquatic ecosystems were exceeded for dissolved Cu, Hg and Zn at several sites and for Al at all sites, including the reference sites, but to a much greater extent for the mine-impacted sites. For most sites, the concentration of dissolved trace elements was higher during summer than winter.

Table 4.3.1 Physiochemical parameters as measured in June 2015. Temperature is measured in °C, pH measured in pH units, conductivity measured in µS/cm, dissolved oxygen (DO) and SO_4 measured in mg/L, trace elements measured in µg/L. ANZECC guidelines for the protection of 95% of aquatic species (99% for Hg), as applied to moderately disturbed systems are also given. Trace elements that exceed the ANZECC guidelines are shown in bold.

Site	Temp	pH	Cond	DO	SO_4	Fe Diss	Fe A.S.	Al Diss	Al A. S.	Mn Diss	Mn A.S.
Puhi1	12.5	6.52	74.0	9.63	6.63	192	310			12.4	13.0
Puhi2	11.5	6.13	82.2	9.60	9.34	162	373			38.9	33.1
Puhi2b	12.6	6.14	84.0	8.78	8.65	172	335			22.2	22.5
Puhi2c	11.9	6.08	70.9	9.81	7.31	206	398			36.7	39.8
Puhi3	11.9	5.38	68.2	8.46	8.31	243	2880			129	161
Puhi4	12.3	5.01	80.5	8.51	11.0	292	241			155	161
Puhi5	12.6	5.66	66.8	9.23	9.33	323	699			73.3	73.5
Puhi6	12.9	5.87	70.5	9.56	8.18	118	271			65.9	70.1
Puhi7	11.7	7.02	73.8	9.53	3.44	309	148			21.6	19.5
Puhi8	11.7	6.99	73.9	10.3	4.09	130	311			23.9	22.5
ANZECC guideline						ngv	ngv		55		1900

Site	Cu Diss	Cu A. S.	Zn Diss	Zn A. S.	Ni Diss	Ni A. S.	As Diss	As A. S.	Sb Diss	Sb A. S.	Hg Diss	Hg A. S.
Puhi1	0.92	1.01	1.98	2.21	0.67	0.67	0.94	1.22	0.75	0.68	<0.001	0.003
Puhi2	0.79	0.91	4.18	4.31	1.17	1.19	2.25	3.11	1.12	1.14	0.008	0.010
Puhi2b	0.67	0.76	3.32	3.95	1.16	1.23	2.02	3.13	1.18	1.20	0.008	0.007
Puhi2c	1.11	1.28	3.54	3.76	0.98	1.02	1.06	1.41	0.76	0.79	0.003	0.005
Puhi3	0.33	**2.25**	1.69	4.15	2.57	3.48	0.08	0.12	0.04	0.04	0.013	0.060
Puhi4	**5.39**	**5.25**	**12.2**	**12.2**	2.75	2.82	2.06	1.82	0.71	0.90	<0.001	0.001
Puhi5	**1.38**	**1.76**	4.55	4.96	1.48	1.50	2.53	3.44	1.37	1.28	0.007	0.008
Puhi6	1.09	**1.44**	3.35	3.42	0.94	0.96	0.77	0.94	0.83	0.81	<0.001	0.004
Puhi7	0.55	0.34	0.73	0.45	0.21	0.19	0.37	0.28	0.12	0.08	<0.001	0.005
Puhi8	0.39	0.49	0.58	0.71	0.26	0.26	0.27	0.32	0.05	0.03	<0.001	<0.001
ANZECC guideline		1.4		8.0		11		13		ngv		0.06

Table 4.3.2 Physiochemical parameters measured in January 2016. Temperature is measured in °C, pH measured in pH units, Conductivity measured in µS/cm, dissolved oxygen (DO) and SO_4 measured in mg/L, trace elements measured in µg/L. ANZECC guidelines for the protection of 95% of aquatic species (99% for Hg), as applied to moderately disturbed systems are also given. Trace elements that exceed the ANZECC guidelines are shown in bold.

Site	Temp	pH	Cond.	DO	SO_4	Fe Diss	Fe A. S.	Al Diss	Al A. S.	Mn Diss	Mn A.S.
Puhi1	20.2	7.03	71.2	8.03	7.11	451	683	**98.5**	**133**	22.3	23.4
Puhi2	20.2	6.31	88.2	7.60	12.0	256	487	**127**	**181**	66.8	65.6
Puhi2b	20.4	6.23	96.4	7.63	12.5	204	358	**88.4**	**119**	48.7	46.6
Puhi2c	21.1	6.55	66.2	8.33	6.57	449	833	**116**	**179**	61.7	60.2
Puhi3	20.0	5.34	71.3	3.76	8.95	990	3830	**134**	**277**	173	171
Plant	16.5	4.18	95.3	6.06	12.1		124		**1020**		83.9
Puhi4	17.2	4.74	80.8	7.72	10.8	225	296	**486**	**493**	163	162
Puhi5	23.6	6.34	66.9	7.96	8.83	447	1316	**136**	**283**	94.8	96.2
Puhi6	18.5	6.25	64.2	8.81	6.85	415	656	**206**	**272**	75.9	76.7
Puhi7	18.5	7.09	68.4	8.24	3.52	242	454	40.9	**80.7**	21.9	26.2
Puhi8	21.0	7.11	74.4	8.19	4.16	137	772	10.2	**72.9**	36.0	37.4
Puhi9	21.9	6.47	64.9	8.02	6.82	426	916	**137**	**228**	79.2	78.5
Puhi10	22.0	6.46	57.5	7.73	6.46	441	745	**142**	**212**	67.3	66.7
Puhi11	21.0	7.00	70.9	8.31	6.80	567	847	**105**	**144**	15.3	20.3
ANZECC guideline						ngv	ngv		55		1900

Site	Cu Diss	Cu A. S.	Zn Diss	Zn A. S.	Ni Diss	Ni A. S.	As Diss	As A. S.	Sb Diss	Sb A. S.	Hg Diss	Hg A. S.
Puhi1	**1.63**	**1.47**	4.32	1.69	0.92	0.78	1.72	2.07	0.81	0.98	0.051	0.039
Puhi2	0.96	1.07	4.68	4.66	1.70	1.69	3.53	4.76	1.50	1.73	0.050	0.048
Puhi2b	1.03	1.10	5.10	4.76	1.68	1.66	3.62	4.36	1.73	1.84	0.051	0.054
Puhi2c	**1.54**	**1.68**	3.26	3.11	1.82	0.97	1.69	2.02	0.72	0.90	0.045	0.055
Puhi3	0.73	**1.44**	3.70	4.40	4.13	4.35	0.40	0.46	0.00	0.20	0.057	**0.093**
Plant		**35.9**		**14.3**		7.82		0.33		0.24		**0.088**
Puhi4	**5.85**	**6.11**	**14.8**	**14.0**	3.16	3.19	1.36	1.63	0.83	0.97	0.053	0.058
Puhi5	1.16	**1.66**	4.03	5.01	1.54	1.66	3.04	4.22	0.94	1.19	0.030	0.059
Puhi6	**2.09**	**2.37**	4.50	5.23	1.19	1.17	1.30	1.48	0.73	0.84	0.053	0.055
Puhi7	0.49	0.56	0.32	2.40	0.20	0.21	0.64	0.73	0.03	0.15	0.037	0.045
Puhi8	0.47	0.66	0.34	1.14	0.21	0.24	0.63	0.78	<0.01	0.08	0.047	0.039
Puhi9	**1.57**	**1.83**	5.13	4.09	1.07	1.10	1.71	2.27	0.72	0.88	0.048	0.038
Puhi10	1.22	**1.55**	2.72	3.34	0.73	0.81	1.53	1.74	0.92	0.97	0.042	0.047
Puhi11	1.26	1.37	2.22	2.23	0.81	0.85	2.04	2.39	0.65	0.78	0.049	0.050
ANZECC guideline		1.4		8.0		11		13		ngv		0.06

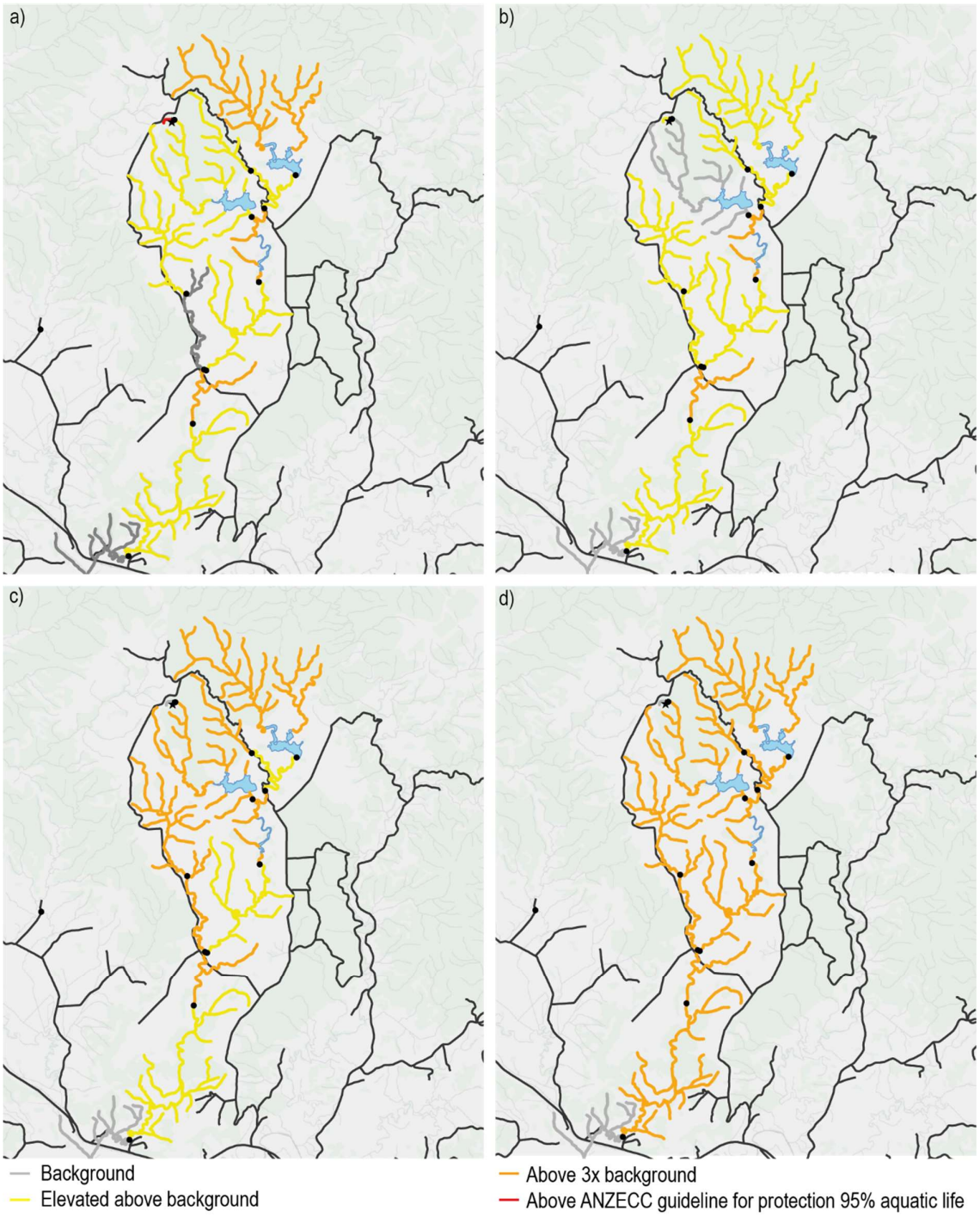

Figure 4.4 Maps showing areas with high concentrations of dissolved trace elements. a) Fe, b) Hg, c) As, d) Sb Values are based on the average between the summer and winter sampling events. For Fe, orange streams are higher than 2x the background concentration and red streams are higher than 3x the background concentration as there is no given value for the protection of aquatic life.

Speciation of dissolved trace elements

PHREEQC modelling predicted that Fe and Al were mostly present as hydroxylated ions such as $Fe(OH)_2^+$, $Fe(OH)_3^0$, $Al(OH)_2^+$and $Al(OH)_4^-$ (Figure 4.5a and b). <0.1% of the Fe concentration was Fe^{3+}. The ore processing plant site and Puhi3 had a large proportion of Al present in the free ion form (50-65% at Plant site and 16% at Puhi3). All other sites had <0.5% Al present as Al^{3+}. Zn and Ni were mostly present as free metal ion (>95%) for all sites including the reference sites (Figure 4.5c and d). Cu was mostly present as Cu^{2+} (>90%) for the impacted sites and between 40-70% as Cu^{2+} for the reference sites and sites 1 and 11 (Figure 4.5e). Arsenic and Sb were mainly predicted to be present as the oxyanions. Mercury was modelled to be present as some combination of $HgCl_2^0$, $HgClOH^0$ and $Hg(OH)_2^0$ (Figure 4.5f). Less than 0.01% of As, Sb and Hg were modelled to be present as free ions (Figure 4.5g and h) as all were present as oxyanions ($H_2AsO_4^-$, $HAsO_4^{2-}$, SbO_3^-, $HgCl_2^0$, $HgClOH^0$ and $Hg(OH)_2^0$).

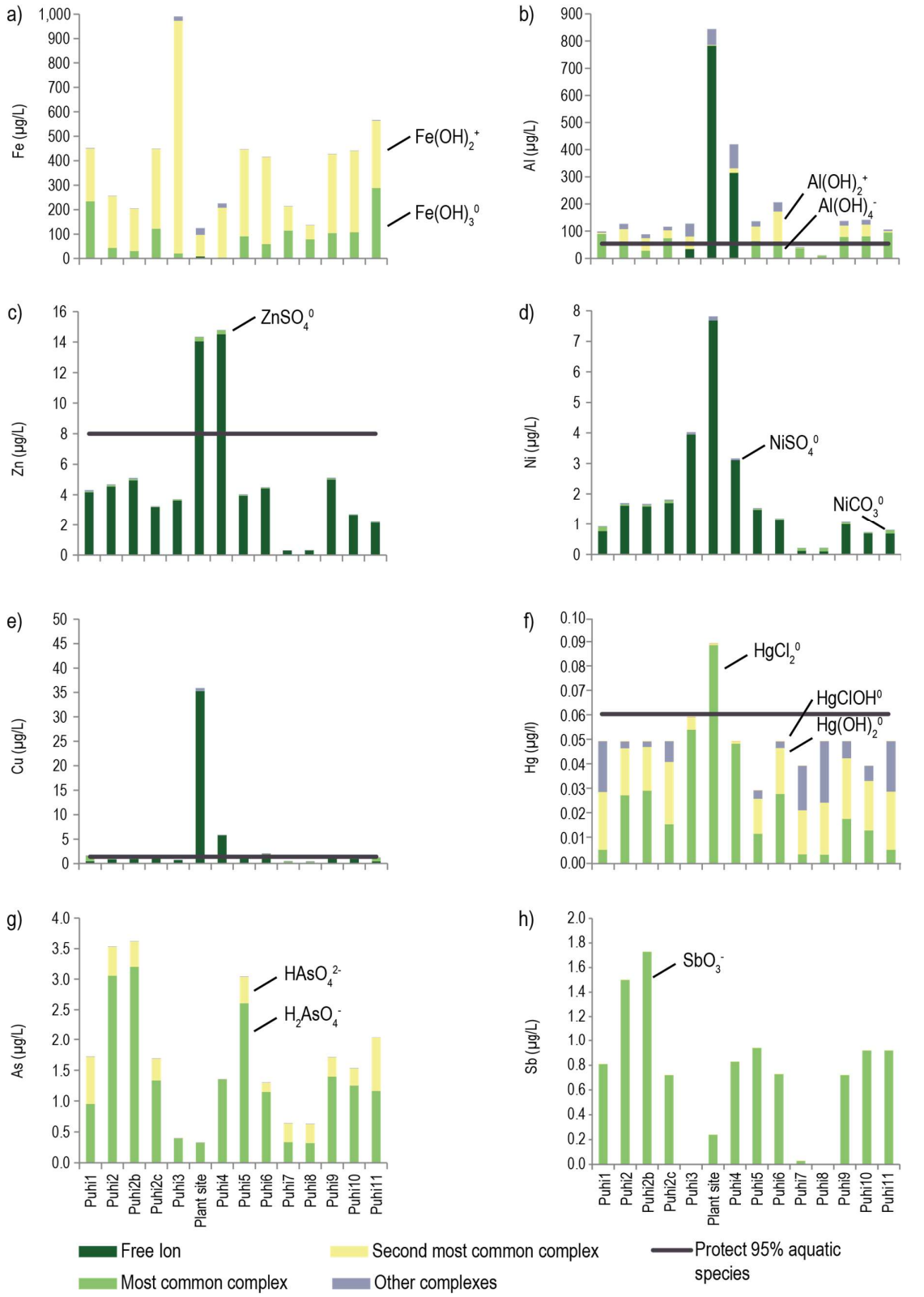

Figure 4.5 PHREEQC modelled speciation of dissolved trace elements at Puhipuhi. a) Fe, b) Al, c) Zn, d) Ni, e) Cu, f) Hg, g) As and h) Sb. Where the ANZECC (2000) guideline for the protection of aquatic life is exceeded, the relevant value is shown as a horizontal brown line.

4.3.2 Sediment chemistry

X-ray diffraction analysis identified the major mineral fraction as quartz with minor kaolinite, smectite, illite and k-feldspars. Sediment chemistry data for sites sampled in June 2015 and January 2016 is shown in Tables .4.4.1 and 4.4.2 respectively. Concentrations of Cu, Zn, As and Sb were low at the head of the Waikiore Stream (Puhi3) but elevated and exceeding the ANZECC (2000) ISQG guidelines for As, Cu and Sb in the Pukekaikiore stream (Puhi4, Puhi6 and Puhi10; Figure 4.6). Sb was elevated in the Whenuaroa Stream (Puhi2 and Puhi2b). Total aqueous Pb was high at the head of the Waikiore Stream but the sediment-bound Pb was not significantly elevated when compared to control sites or ISQG guidelines. Concentrations of sediment-bound Ni and Hg were high at the head of the Waikiore Stream (Puhi3) and were also high, exceeding ISQG guidelines at several other sites further downstream (Figure 4.6).

Table 4.4.1 Trace element concentrations in the fine sediment (<67μm fraction) in Puhipuhi streams, as measured in winter 2015. All concentrations are measured in mg/kg except for Fe and Al which are measured as percentage of weight. The ISQG (high and low) guidelines are given at the bottom of the table. Concentrations that exceed the ISQG-low guidelines are shown in bold and concentrations which exceed the ISQG-high are shown in bold and red.

Site	Al (%)	Fe (%)	Mn	Zn	Ni	Cu	As	Sb	Hg
Puhi1	nm	4.21	739	112	**33.5**	41.3	**37.2**	0.575	0.135
Puhi2		1.72	96	35.2	7.45	17.5	**47.2**	0.156	**0.257**
Puhi2b		4.20	367	60.5	17.4	22.7	**111**	0.758	**0.175**
Puhi2c		5.94	3140	85.5	15.4	42.2	**104**	0.587	**1.165**
Puhi3		8.64	234	69.5	12.1	36.5	1.26	0.141	**7.030**
Puhi4		5.25	100	61.8	2.76	61.6	**221**	0.915	**0.453**
Puhi6		4.02	476	68.9	11.7	49.5	**36.2**	0.385	0.098
Puhi7		2.20	961	83.6	11.2	17.8	5.12	0.022	0.027
Puhi8		2.10	666	63.1	8.14	19.2	4.96	0.024	0.011
ISQG-high				410	52	270	70	25	1
ISQG-low				200	21	65	20	2	0.15

Table 4.4.2 Trace element concentrations in the fine sediment (<67μm fraction) in Puhipuhi streams, as measured in summer 2016. All concentrations are measured in mg/kg except for Fe and Al which are measured as percentage of weight. The ISQG (high and low) guidelines are given at the bottom of the table. Concentrations that exceed the ISQG-low guidelines are shown in bold and concentrations which exceed the ISQG-high are shown in bold and red.

Site	Al (%)	Fe (%)	Mn	Zn	Ni	Cu	As	Sb	Hg
Puhi1	7.36	4.55	946	78.1	**37.0**	38.8	**45.2**	**2.74**	**0.88**
Puhi2	3.48	4.02	69.1	26.9	9.00	13.7	**142**	**9.10**	**1.01**
Puhi2b	5.09	2.53	207	29.7	14.6	14.7	**75.2**	**3.96**	**1.48**
Puhi2c	6.86	3.01	734	55.5	20.6	27.6	**27.4**	**2.55**	**1.91**
Puhi3	3.73	4.99	154	43.3	**34.2**	28.1	3.2	0.20	**26.0**
Puhi4	4.70	7.18	180	28.2	4.97	**70.6**	**307**	**5.80**	**3.29**
Puhi5	4.96	2.99	524	53.8	19.3	22.5	**51.5**	**5.54**	**9.69**
Puhi6	7.72	7.10	1380	84.9	**30.5**	**70.9**	**76.4**	**5.33**	**0.74**
Puhi7	4.28	3.09	1300	56.8	17.0	18.8	3.3	<DL	0.01
Puhi8	3.63	2.74	603	40.3	9.00	16.8	1.9	<DL	0.00
Puhi9	5.91		935	64.9	**27.6**	37.5	19.4	0.66	0.12
Puhi10	4.07		229	42.2	16.1	27.1	**64.7**	**2.29**	**3.10**
Puhi11	4.56		3200	96.6	**37.6**	25.2	**67.0**	**2.27**	**0.19**
ISQG-high				410	52	270	70	25	1
ISQG-low				200	21	65	20	2	0.15

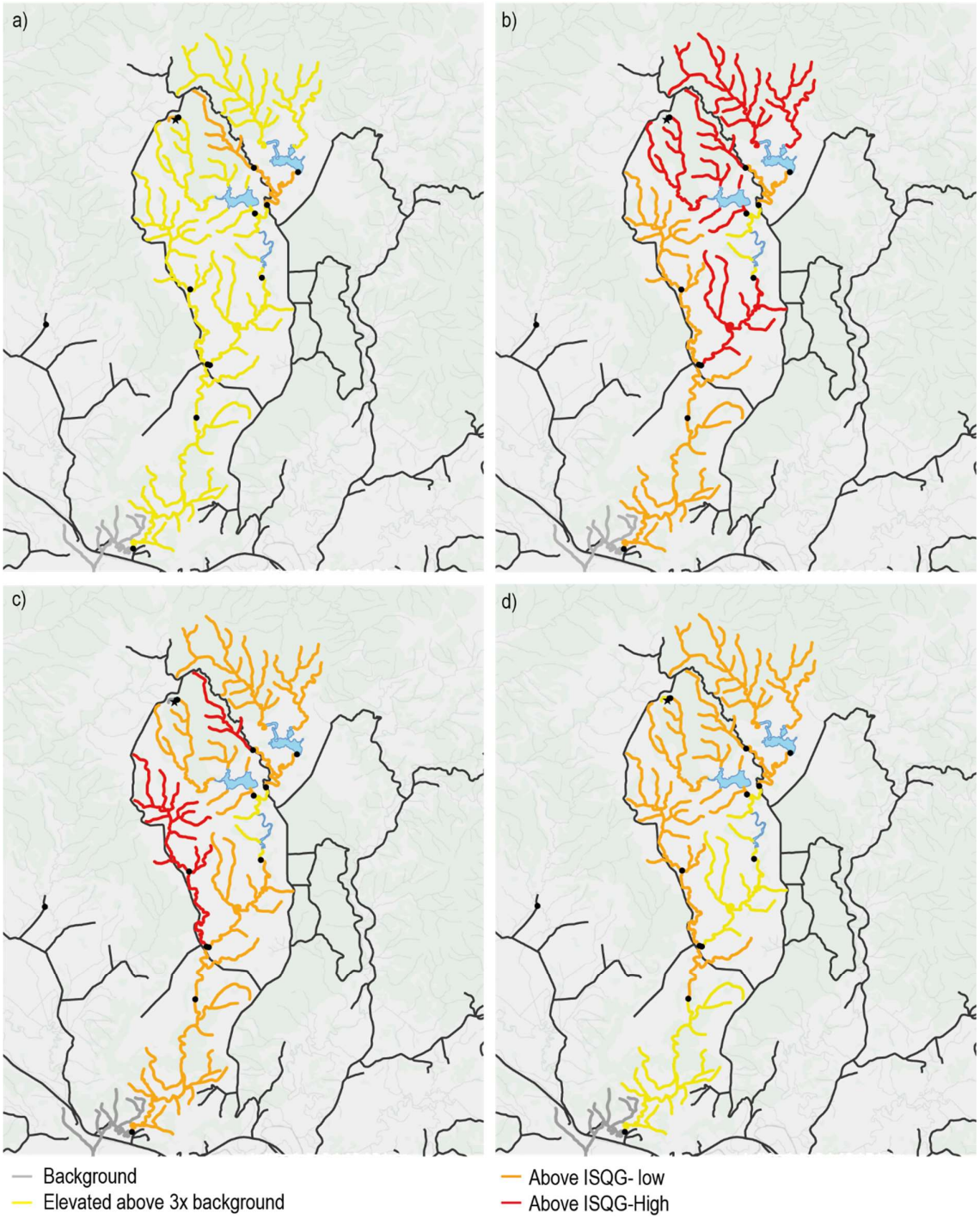

Figure 4.6 Maps showing areas with high concentrations of sediment-bound trace elements. a) Fe, b) Hg, c) As, d) Sb. Values are based on the average of the summer and winter sampling events. For Fe, orange streams are higher than 2x the background concentration and red streams are higher than 3x the background concentration as there is no given value for sediment quality.

Most particles investigated during imaging and elemental mapping by SEM-EDS were Al-Si-O minerals and some Fe-Ti particles were present. Very little Hg, As and Sb were observed in these particles (below detection). Where detectable Hg was present, it was associated with S, Si and Al, but not with Fe as might be expected if it were adsorbed to Fe (oxy)hydroxides minerals (Figures 4.7.1 and 4.7.2). The concentrations of elements adsorbed to Fe (oxy)hydroxide surfaces are often below the detection limit of SEM.

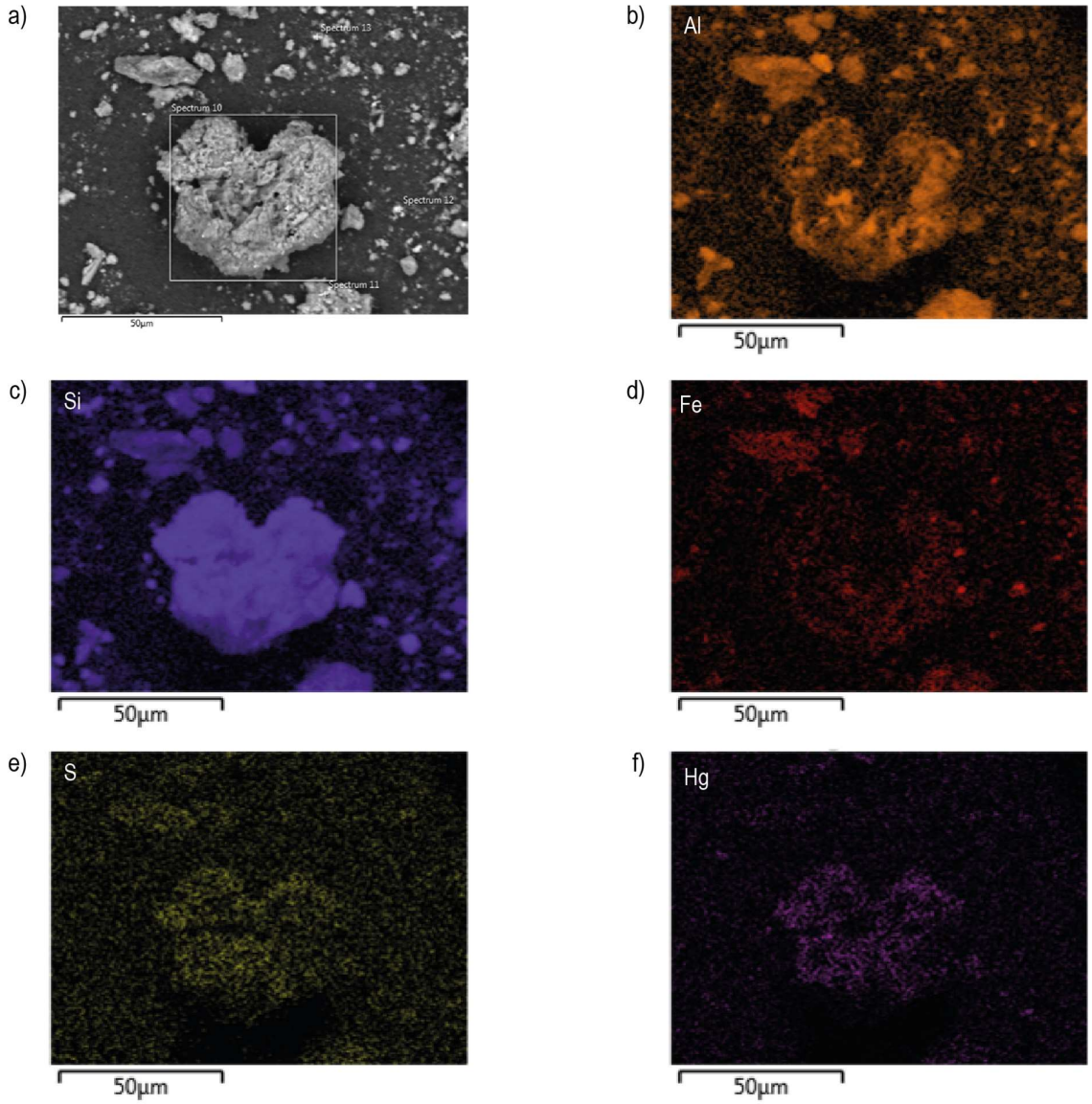

Figure 4.7.1 A SEM-EDS image of a particle collected from Puhi3 (a) with the elemental maps for b) Al, c) Si, d) Fe, e) S and f) Hg. A more intense colour denotes a higher concentration of the element.

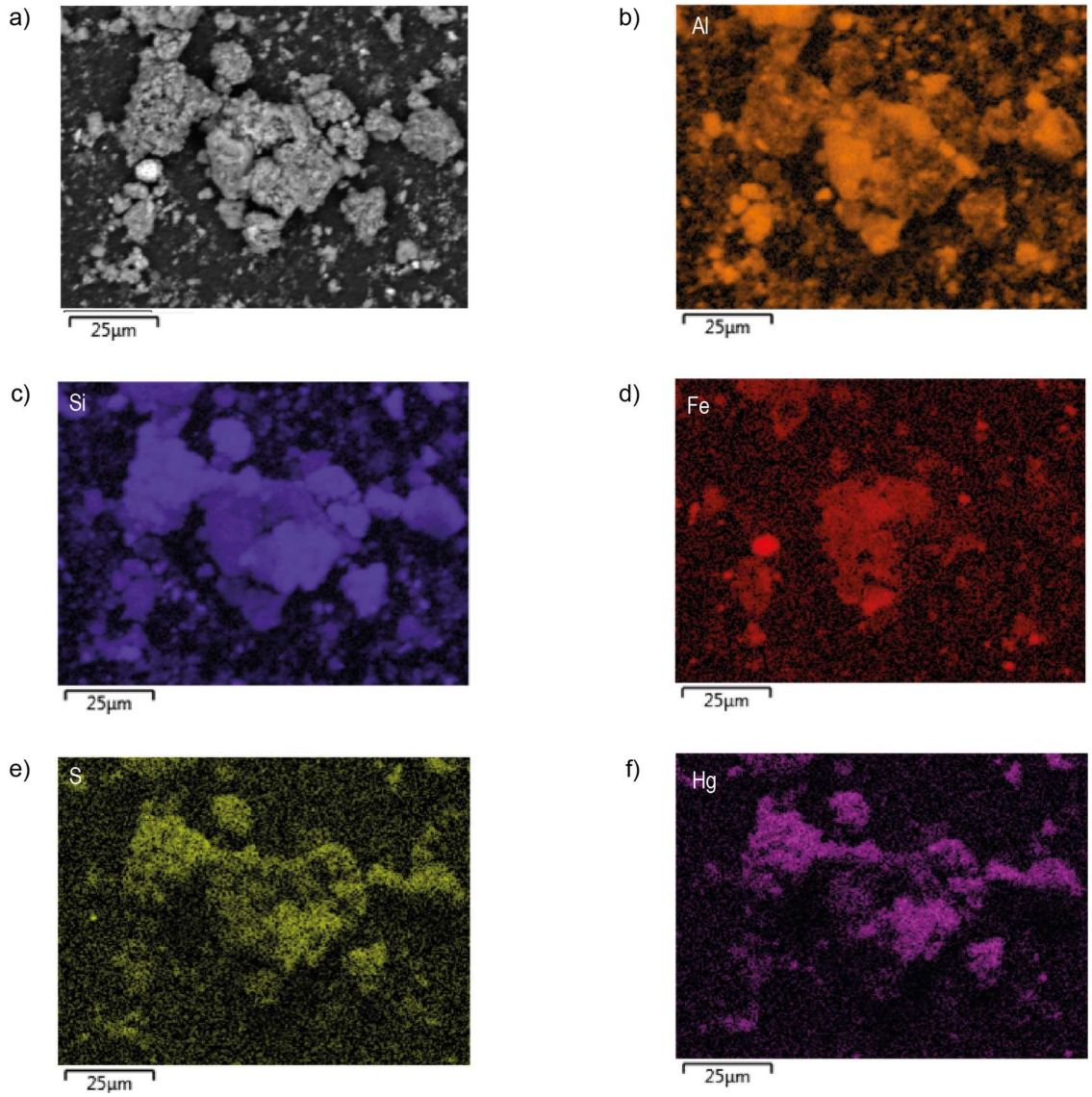

Figure 4.7.2 A SEM-EDS image of a particle collected from Puhi3 (a) with the elemental maps for b) Al, c) Si, d) Fe, e) S and f) Hg. A more intense colour denotes a higher concentration of the element.

The SEM-EDS element maps indicate that HgS is very finely divided within the silica matrix. This is in line with how the quartz sinter was recorded, as discoloured quartz with HgS (Figure 4.8a) and with minor veins of cinnabar (Figure 4.8b).

Figure 4.8 examples of Puhipuhi cinnabar. a) Cinnabar dispersed through the quartz sinter to give a milky pink colour. Photo: Jenny Webster-Brown. b) A cinnabar vein (red) through Fe-rich host rock (orange).

During sequential chemical extraction, Cu and Zn were mostly extracted from the "Fe Oxide" fraction, followed by the "bound to organic matter" and "low acid leachable" fractions (Figure 4.9a and c). Only 15-35% of the Ni was extracted with the "Fe Oxide" fraction while moderate proportions were extracted in exchangeable and "low acid leachable" fractions (Figure 4.9b). Up to 60% of Ni was extracted from the sulfide and residual fraction. The majority of As and Sb was extracted in the "Fe Oxide" fractions except for at Puhi3 (57%) where a significant proportion of As (30%) was extracted in the exchangeable fraction (Figure 4.9e and f). Large proportions of Pb and Cd were extracted from the exchangeable fraction.

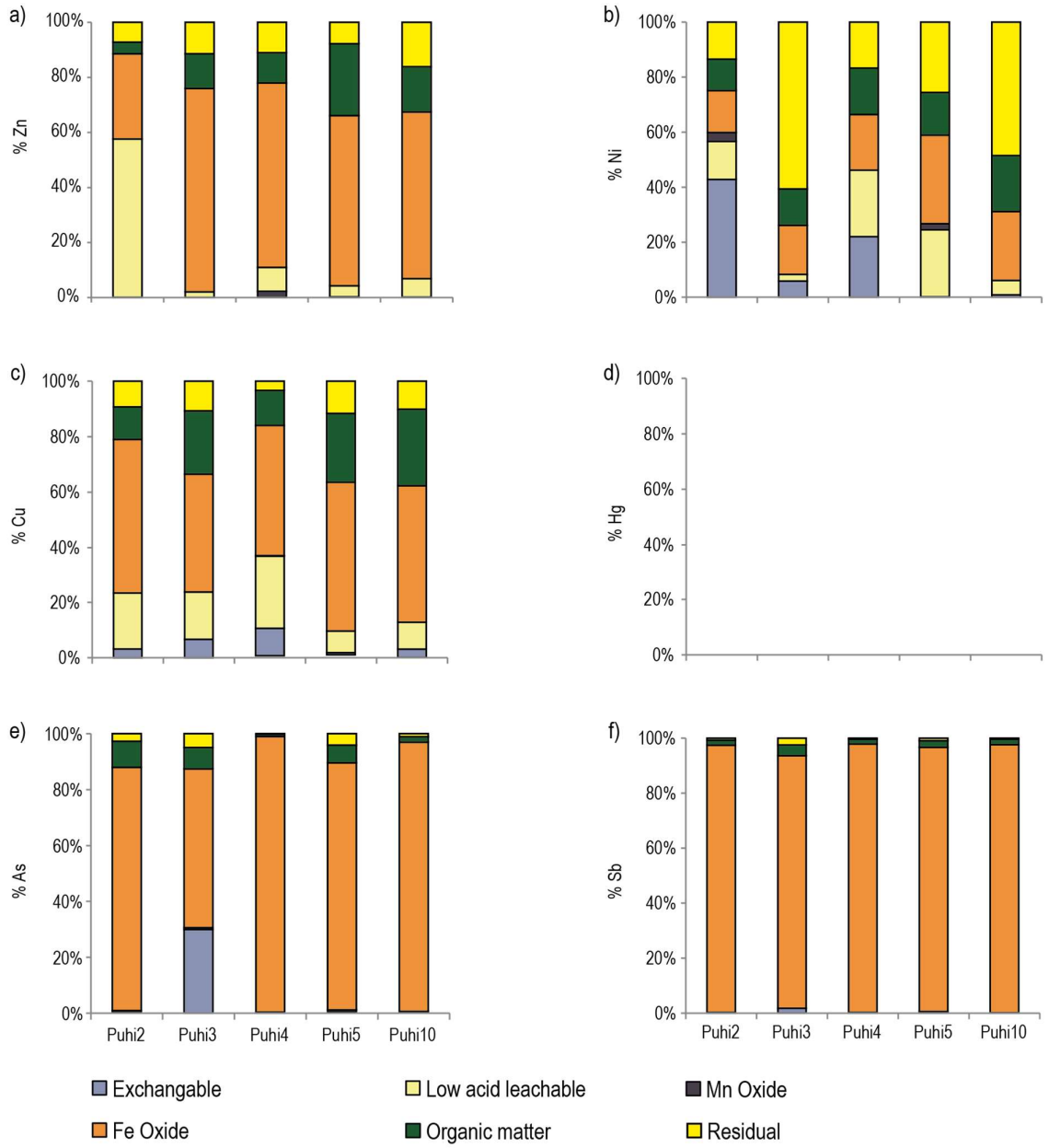

Figure 4.9 Proportions of trace elements extracted from specific mineral phases during the sequential extraction process. a) Zn, b) Ni, c) Cu, e) As and f) Sb. Due to experimental and analytical limitations, analysis of extracts for Hg could not be completed.

Modelling of trace element adsorption to HFO

Modelling of the adsorption of trace elements to HFO with PHREEQC showed that very little Zn, Ni or Hg would adsorb (Figure 4.10a, b and d). This is consistent with what was measured as the percentage of dissolved trace element. The only notable deviations were for Zn at Puhi7 where adsorption was overestimated, and for Hg at the sites with more acidic waters where adsorption was underestimated. Adsorption of Cu and As to HFO was overestimated (Figure 4.10c and e). The only notable exception to this was Puhi4 which was the site with the

lowest pH and consequently the least amount of HFO present. Adsorption of Sb was underestimated at all sites, including control sites and low-pH sites (Figure 4.10f).

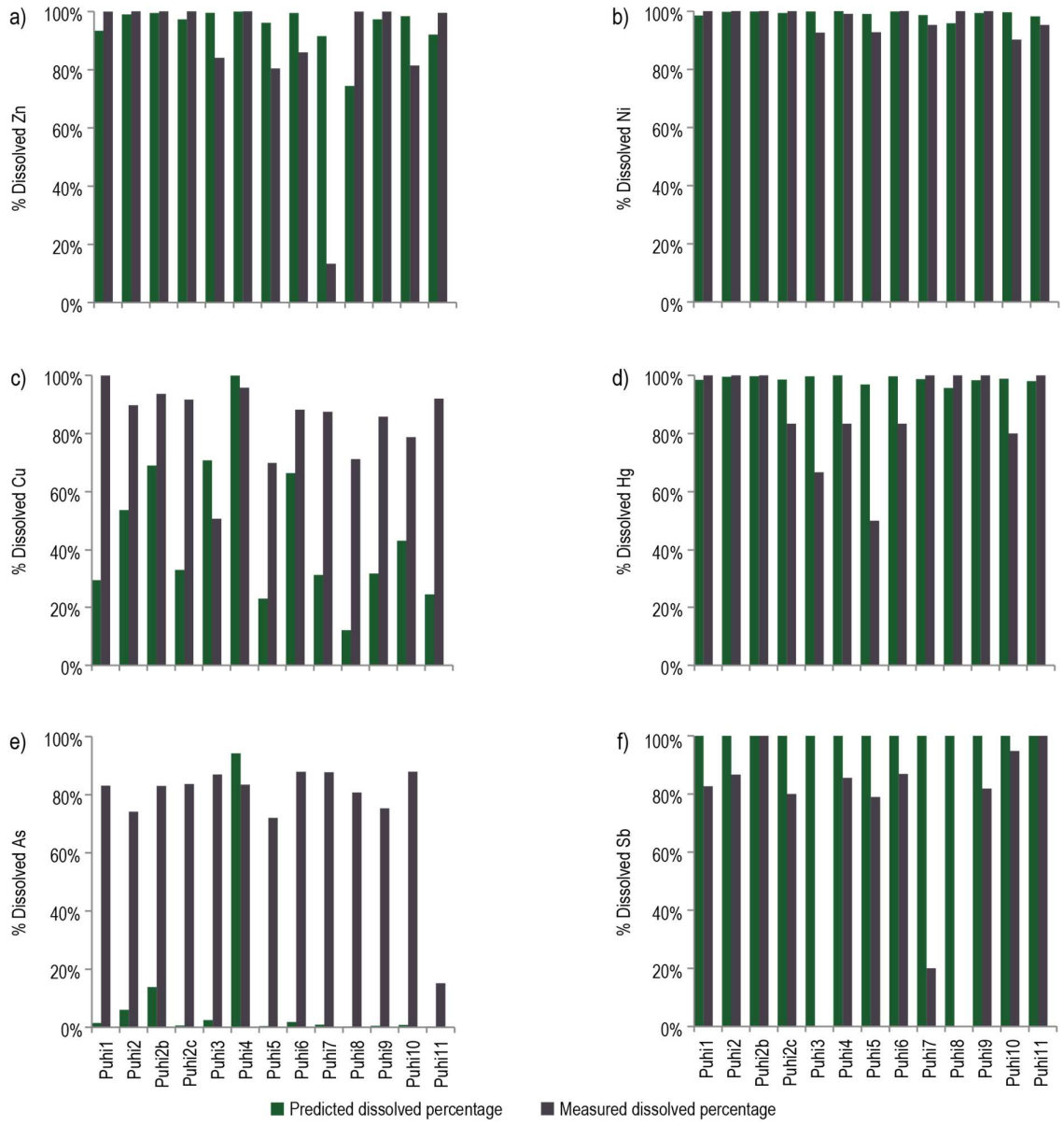

Figure 4.10 A comparison between the percentages of dissolved trace elements predicted to be in solution and measured at the different sites. a) Zn, b) Ni, c) Cu, d) Hg, e)As and f) Sb.

4.3.3 Macroinvertebrate samples

The average denisty of macroinvertebrates was reduced in the streams draining the mined area when compared to the reference sites (Figure 4.11a). The taxa richness was similar for both mine-impacted sites and reference sites with Puhi2b, in the middle of the catchment, having the highest taxa richness (Figure 4.11b). EPT taxa richness was highest at the reference sites and Puhi2b (Figure 4.11c). The number of mayfly taxa was highest at

Puhi7, one of the reference sites. No mayflies were found at Puhi3 and Puhi6, two of the most contaminated sites. The highest number of mayfly individuals, however, was at Puhi1, followed by the reference sites. No stoneflies were found at any of the sites. The highest number of caddis fly taxa was at Puhi2b, followed by the reference sites and Puhi6. The highest number of caddis fly individuals was at Puhi6. Puhi1, Puhi2b and the reference sites were classified as being "impacted sites" following the AMDI classification. Puhi2c and Puhi3-6 were classified as being "severely impacted" by AMD (Figure 4.11d). Puhi1, Puhi2c and the reference sites had a higher proportion of mayflies and beetles compared to the more impacted sites (Figure 4.12). The more impacted sites had a higher proportion of chironomids and caddis flies compared to the reference sites.

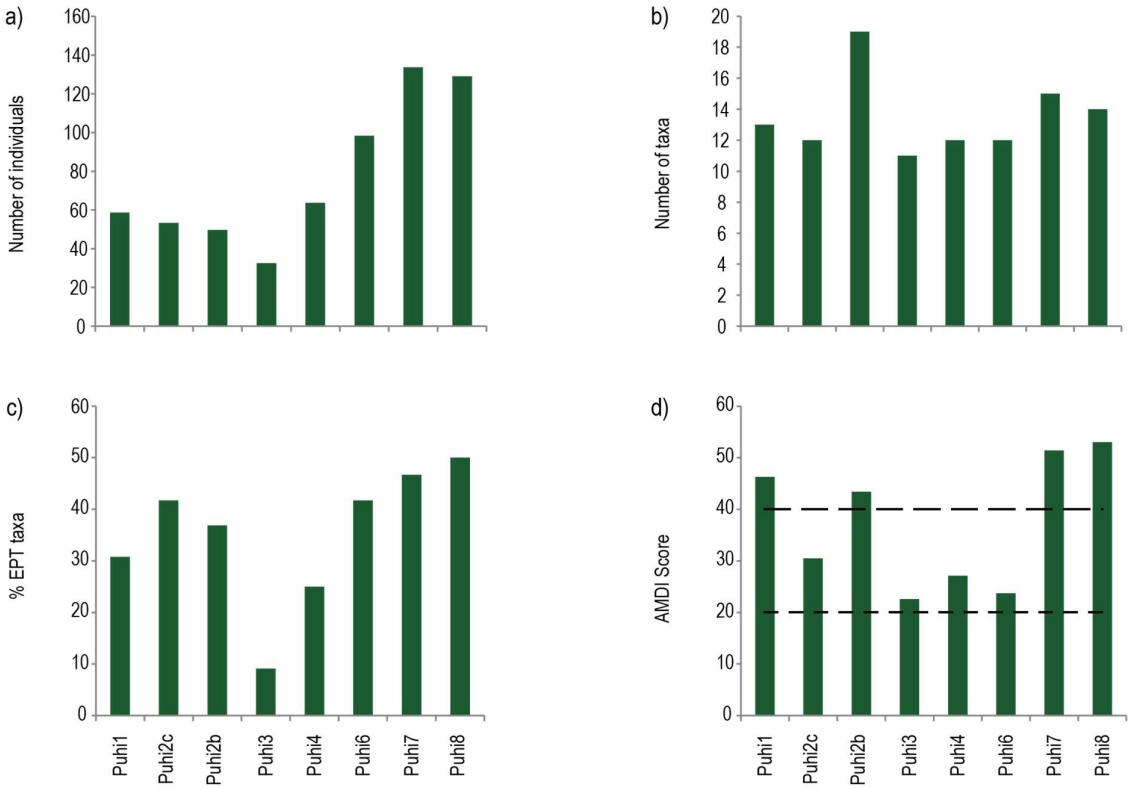

Figure 4.11 Macroinvertebrate community metrics for the sites sampled. a) The average number of individual macroinvertebrates collected from each surber sample, b) The number of macroinvertebrate taxa identified within each sites kicknet sample, c) The percentage of EPT (Ephemeroptera, Plectoptera and Tricoptera) taxa from the kicknet samples, and d) The AMDI score of each site as determined using the tolerance scores of Gray and Harding (2012). Sites with scores below the short dashed line are determined to be highly impacted by AMD and sites above the bottom dashed line but below the top dashed line are determined to be moderately impacted by AMD. Sites with an AMDI score above the top dashed line are determined to be not impacted by AMD.

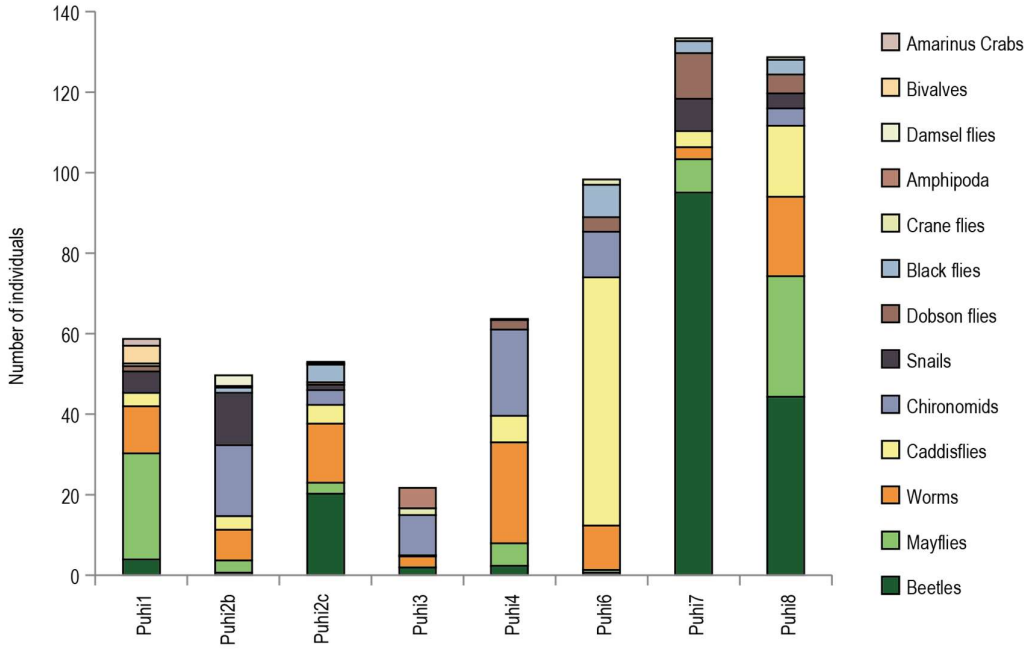

Figure 4.12 The average number of macroinvertebrate species identified from the surber samples.

The correlation values between the macroinvertebrate parameters, water and sediment quality and physical stream parameters is given in Table 4.5. The average macroinvertebrate density showed minor correlations with Na, SO_4, dissolved Ni and dissolved Hg. The number of individuals showed a minor correlation with Cl, dissolved As and stream depth and a moderate correlation with stream width and major cations (Mg, K, Ca). The EPT taxa richness showed a minor correlation with pH, conductivity, dissolved and sediment-bound Hg and stream width. The EPT taxa richness also had a moderate correlation with dissolved Fe, Mn and Ni and sediment-bound Fe. The %EPT taxa was weakly correlated with pH, dissolved Fe and Hg and sediment-bound Fe. A strong correlation between %EPT taxa and dissolved oxygen, dissolved Mn and Ni and sediment-bound Hg occurred. The number of taxa present was weakly correlated with K and sediment-bound Fe, stream width and stream depth. The number of taxa present also showed a strong correlation with dissolved Fe. AMDI was weakly correlated with pH, Na and dissolved Ni and showed a strong correlation with dissolved Mn, sediment-bound Fe and stream width. Overall, macroinvertebrate community metrics were positively correlated with pH, DO and cations. Negative correlations were observed between macroinvertebrate community metrics and dissolved Fe, Mn and Ni (especially nickel for EPT metrics) and with sediment-bound Fe and Hg (especially for EPT metrics). Strong correlations with stream size (depth and width) were present but stream width was also strongly correlated with dissolved Fe and Ni as the streams closer to the sources of contamination were smaller.

Table 4.5 Correlation values between macroinvertebrate community parameters and physicochemical parameters, dissolved trace element concentrations, sediment-bound trace element concentrations and physical parameters. Values greater than 0.75 or less than -0.75 are given in bold. Values greater that 0.8 or less than -0.8 are given in red.

	Density	Number of individuals	EPT taxa richness	%EPT	Number of taxa	AMDI score
pH	0.572	0.340	**0.707**	**0.743**	0.503	**0.772**
Temperature	-0.181	0.206	0.228	0.180	0.056	0.326
Dissolved O_2	0.556	0.270	**0.713**	**0.848**	0.572	0.400
Conductivity	-0.308	**0.750**	0.220	-0.126	0.499	0.213
Major Ions						
Cl	-0.400	**0.758**	0.257	-0.051	0.489	0.191
NO_3	-0.256	0.653	0.441	0.278	0.496	0.238
SO_4	**-0.766**	0.249	-0.357	-0.582	-0.092	-0.448
HCO_3	0.324	0.031	0.011	-0.094	0.020	0.278
Na	**0.794**	0.304	0.628	0.626	0.553	**0.740**
Mg	-0.186	**0.880**	0.412	0.050	0.611	0.379
K	0.071	**0.904**	0.680	0.410	**0.755**	0.625
Ca	-0.245	**0.857**	0.498	0.203	0.610	0.388
Dissolved trace elements						
Fe	-0.593	-0.571	**-0.803**	**-0.769**	**-0.813**	-0.606
Mn	-0.533	-0.534	**-0.824**	**-0.808**	-0.685	**-0.801**
Al	-0.317	-0.390	-0.522	-0.436	-0.369	-0.630
Cu	-0.240	-0.323	-0.394	-0.294	-0.254	-0.471
Pb	-0.259	-0.475	-0.402	-0.204	-0.349	-0.476
Zn	-0.446	-0.204	-0.476	-0.474	-0.263	-0.518
Cd	-0.611	0.298	-0.088	-0.234	0.106	-0.393
Ni	**-0.783**	-0.419	**-0.855**	**-0.905**	-0.684	**-0.788**
As	-0.419	**0.698**	0.332	0.103	0.474	0.090
Sb	-0.474	0.542	0.185	0.007	0.334	-0.090
Hg	**-0.690**	-0.301	**-0.696**	**-0.734**	-0.626	-0.638
Se	-0.342	-0.504	-0.633	-0.545	-0.688	-0.442
Sediment-bound trace elements						
Fe	-0.355	-0.688	**-0.842**	**-0.729**	**-0.783**	**-0.805**
Mn	0.630	-0.103	0.399	0.603	0.184	0.231
Al	-0.193	-0.191	-0.011	0.174	-0.168	-0.258
Cu	-0.100	-0.550	-0.450	-0.237	-0.458	-0.644
Pb	0.137	-0.611	-0.555	-0.432	-0.500	-0.378
Zn	0.200	-0.350	-0.006	0.223	-0.234	-0.063
Cd	0.472	-0.074	0.289	0.441	0.132	0.633
Ni	-0.359	-0.367	-0.455	-0.387	-0.548	-0.285
As	-0.223	-0.124	-0.288	-0.271	-0.093	-0.383
Sb	-0.316	-0.014	-0.129	-0.088	-0.051	-0.490
Hg	-0.550	-0.417	**-0.777**	**-0.846**	-0.688	-0.538
Se	-0.057	-0.410	-0.486	-0.386	-0.370	-0.332
Physical measurements						
Stream depth	0.493	**0.729**	0.601	0.575	**0.754**	0.613
Stream width	0.552	**0.821**	**0.721**	0.684	**0.729**	**0.894**
Canopy opening	0.523	0.089	0.416	0.495	0.188	-0.020

Contamination sources were generally at the top of sub-tributary catchments and the effects of dilution downstream leads to lower concentrations of trace elements and therefore sensitive macroinvertebrate species were able to inhabit downstream areas. Cations were positively correlated with stream order hence the positive correlation with macroinvertebrate community metrics.

4.3.4 Eel samples

The results of the eel flesh analysis (Table 4.6) indicate the mercury levels in both eels are similar and neither is elevated. The "Hikurangi Swamp" eel has twice the concentration of selenium as the "Above Puhipuhi" eel (Figure 4.13), which may indicate elevated selenium levels in the environment downstream of the Puhipuhi mine. None of the other trace elements analysed demonstrated enrichment above expected concentrations in these eels.

Table 4.6 Concentrations of trace elements in flesh of eels collected from the Puhipuhi area. All values are given as mg/kg wet weight. NZFSA limits taken from Schedule 19 of the New Zealand and Australia food standards (Food Standards Australia New Zealand 2015)

Sample	Sb	As	Cd	Cu	Pb	Hg	Ni	Se	Zn
Hikurangi Swamp eel	< 0.02	0.02	0.002	0.257	< 0.002	0.172	< 0.02	0.77	15.8
Std Dev			(0.000)	(0.040)		(0.014)		(0.12)	(5.3)
Above Puhipuhi eel	< 0.02	< 0.02	0.010	0.218	<0.002	0.192	< 0.02	0.43	15.4
Std Dev			(0.008)	(0.059)		(0.024)		(0.03)	(3.9)
NZFSA Limit		2			0.5	0.5			

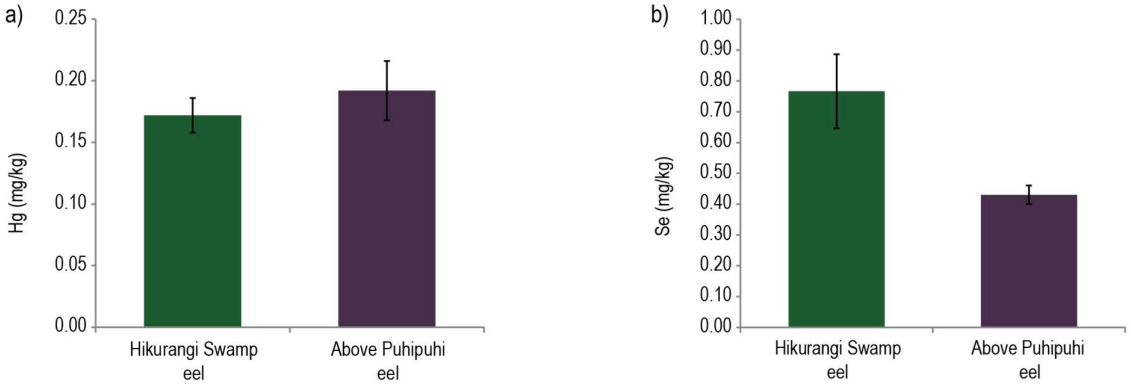

Figure 4.13 A comparison between the concentrations of Hg (a) and Se (b) in flesh samples taken from the two Puhipuhi eels.

4.4 Discussion

4.4.1 Impact of mining on the catchment

Low pH waters with elevated levels of Hg, As and other trace elements have been found in the catchment of the historic Puhipuhi mine site as well as low pH waters. Mercury and As are contaminants of significant concern as they have no known ecological benefits and Hg bioaccumulates in the food chain. Previous studies on the concentrations of these contaminants in the area have identified elevated concentrations downstream of the mine site but have not measured the potential impacts on ecology or considered how this can be remediated.

This research includes high resolution water and sediment sampling at the top of the catchment and around the mine site. Some elements, such as Hg, are highest at the ore processing site of the mine while others, such as As, are low at the mine site but are elevated in streams adjacent to the mine-affected Waikiore Stream. There are several pathways for trace elements to enter streams in the Puhipuhi area. Natural sources include weathering of sinter rock which may release Hg (cinnabar), Fe (pyrite), As (marcasite containing As) and Sb (stibnite). Anthropogenic sources include those associated with mining of rock, run off from roads lined with quarried rock, machinery at the ore processing site and vehicles on nearby roads. The variable spatial distribution of Hg and As throughout the catchment, and particularly at the headwaters of sub-tributaries suggest that there are multiple sources of Hg and As and that the source of Hg and As are different. These sources are likely to be the different sinter outcrops found within the Puhipuhi area, some of which have been disturbed by historic mining and quarrying activities while others remain undisturbed (Figure 4.14). The high concentration of sediment-bound trace elements through particulates carried into the streams from the roads that were lined with quarried rock is likely because several of the stream sampling points were close to roads (Figure 4.14).

Sites in the upper part of the catchment where concentrations of trace elements were higher showed reduced macroinvertebrate taxa richness, %EPT and a low AMDI score relative to those in the lower part of the catchment or at control sites in a nearby catchment unaffected by mining. Macroinvertebrate community indices showed strong correlations with dissolved Fe, Mn, Ni and Hg concentrations as well as with sediment-bound Fe and Hg concentrations. Control sites and sites in the lower catchment had macroinvertebrate communities dominated by beetles and mayflies whereas sites with elevated trace elements had macroinvertebrate communities comprised of worms, snails, caddisflies and chironomids in low abundance. An assessment of the flesh composition from two eels found that while the eels had similar levels of mercury, flesh from the downstream eel contained higher levels of selenium. Selenium had not been an element of concern initially and subsequent analysis of water and sediment samples for Se found it to be below the limit of detection. However, the presence of Se in cinnabar from Puhipuhi has been shown (Hampton et al. 2004). It is difficult to determine the extent of bioaccumulation of Hg and Se into the food web based on a small sample size consisting of individuals of an unknown age. It is also difficult to determine how much of the eels sampled spent in Hg contaminated waters given that the species is mobile.

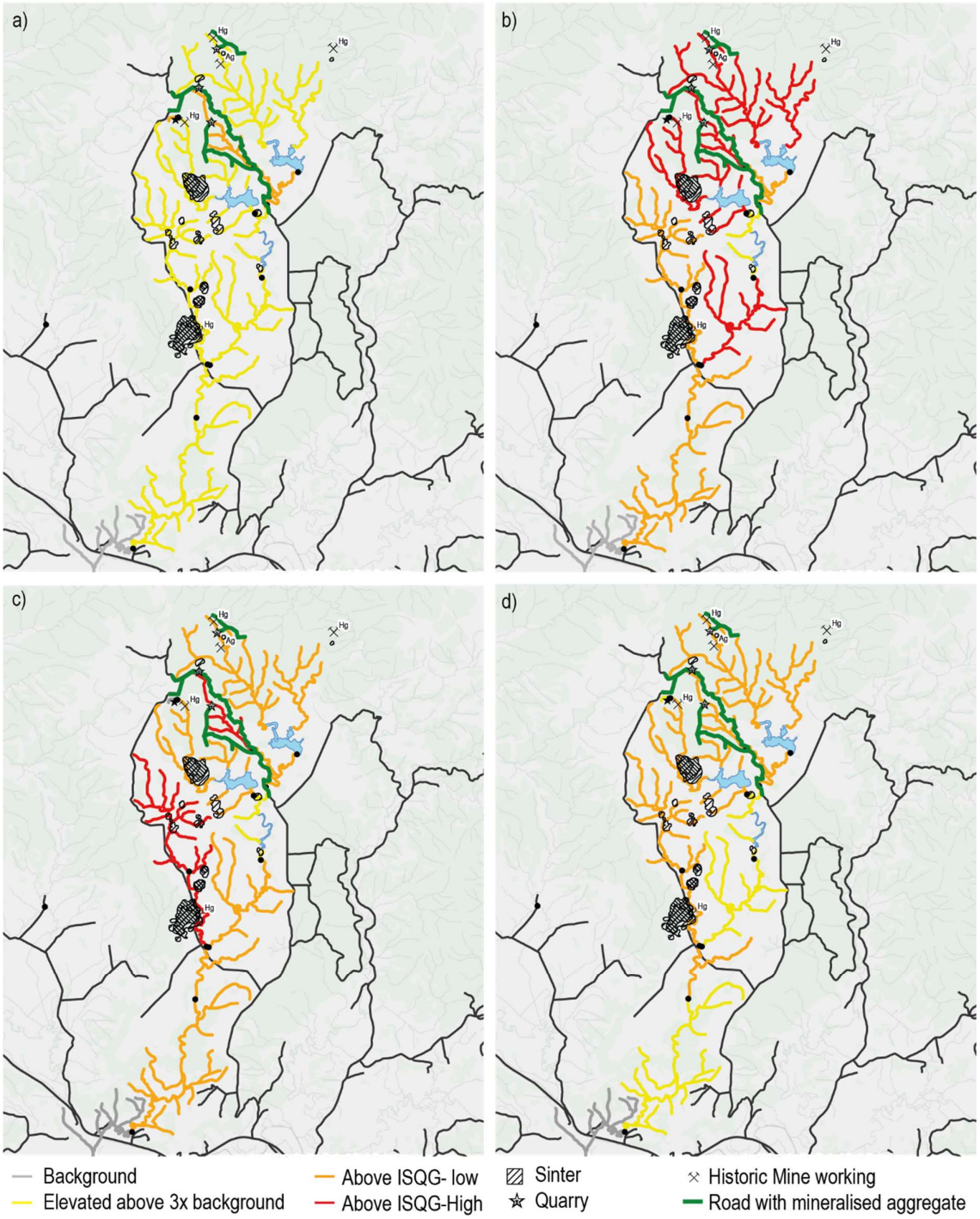

Figure 4.14 The location of mineralised sinters (White 1986, Locke et al. 1999, Hampton et al. 2004), historic mine workings (White 1986), quarries (Craw et al. 2002) and the roads where mineralised aggregate from the quarries was spread (Craw et al. 2002) overlaid on the spatial distribution maps of sediment Fe (a), Hg (b), As (c) and Sb (d).

Baseline survey conducted by Pattle Delamore Partners

In 2016, Pattle Delamore Partners (PDP) were contracted by Evolution Mining, who currently hold the permit for exploration within the Puhipuhi tenement, to carry out a more extensive environmental baseline study of the Puhipuhi area. This study consisted of sampling of groundwater, stygofauna, aquatic organisms, surface water and sediment as well as assessments of macroinvertebrates and hydrology, monitoring of noise and dust, and a physical environment survey. The work by PDP was carried out independent of this research but con-currently. As such, some of the results for Hg concentrations in surface water from this research are cited in the PDP report as these results had been communicated via personal communication though not officially published.

PDP determinations of As and Hg (as well as Cu and Zn) were similar to those of this study. Arsenic was between 1-6μg/L in ten surface water samples and <1μg/L in all other surface water samples (Pattle Delamore Partners Ltd. 2016d). Mercury was between 0.002-0.236μg/L in surface water samples, two of which exceeded the ANZECC guideline for aquatic ecosystem protection (Pattle Delamore Partners Ltd. 2016d). Aquatic ecosystem protection guidelines were exceeded at 4 sites for Cu and Zn. The source of Zn was not identified but a mineral source was ruled out. The processing plant and natural weathering of mineralised rock or soil were identified as the Hg source (Pattle Delamore Partners Ltd. 2016c).

The concentration of sediment-bound Hg was greatest at the processing plant, with concentrations of Fe and Mn also elevated at this site (Pattle Delamore Partners Ltd. 2016c). Concentrations of dissolved Hg were also elevated in a sub-tributary of Waikiore Stream which does not have a history of mining in the catchment. Therefore it was concluded that natural weathering of rock a significant source of Hg to the stream (Pattle Delamore Partners Ltd. 2016c). The concentrations of Hg in water and soil were not uniformly distributed across sub-tributary catchments and no fixed relationship between dissolved Hg and sediment-bound Hg identified. In general, however, sites with a higher concentration of dissolved Hg also had a higher concentration of sediment-bound Hg and the concentration of Hg in water and sediment decreased with distance downstream of the mine and mineralisation (Pattle Delamore Partners Ltd. 2016c). Additionally, the majority of Hg in the sediment is in an insoluble, and therefore non-bioavailable form. <0.08% of Hg in sediment was found to be present as MeHg. Concentrations of As and Sb were greatest at site PVX, on the south branch of the Pukekaikiore Stream but no relationship between Hg, As and Sb is present.

In general, sites higher in the catchment had a higher diversity and quality of macroinvertebrate species, a trend opposite to the concentration of trace elements in the water and sediment (Pattle Delamore Partners Ltd. 2016b). These results were thought to be due to the better quality habitat in forested areas as opposed to the agricultural areas downstream (Pattle Delamore Partners Ltd. 2016b). This trend is opposite to the trend observed in the research presented in this chapter.

The concentration of dissolved Hg at Puhipuhi Mine as measured by PDP was similar to other recent studies (Gionfriddo et al. 2015) and the range of Hg concentrations were higher than was measure in this study. However, downstream of the mine processing site, the concentrations measured by PDP were lower than results from this study (Table 4.7). The concentration of dissolved As measured by PDP was of a similar concentration to that found by previous studies and those measured in this research. The concentrations of sediment-bound Hg measure by PDP were similar to those previously reported and those measured in this research (Table 4.7).

Table 4.7 Concentrations of dissolved Hg and sediment-bound Hg at four sites in the Puhipuhi area. The Puhipuhi Mine site corresponds to Puhi3 in this research; Pukekaikiore Stream corresponds to Puhi4, and SH1 Bridge corresponds to Puhi1. The Tangiteroria site is further downstream from the sites sampled in this research.
This is an update on Table 4.1 with the results from this research and the PDP Baseline Survey included.

Location	Dissolved Hg (µg/L)	Sediment-bound Hg (mg/kg)	Year	Reference
Puhipuhi Mine site	0.5	28*	1972	Hoggins and Brooks (1973)
	0.118-0.240	-	2013#	Gionfriddo et al. (2015)
	<0.05-0.26	31-83	2014	Ropiha and Hansen (2015)
	0.013, 0.057	7.03, 26.0	2015, 2016	This chapter
	0.236	74.9	2016	Pattle Delamore Partners Ltd. (2016c)
Pukekaikiore Stream	0.13	4.4	1972	Hoggins and Brooks (1973)
	<0.01	-	1999#	Craw et al. (2002)
	<0.05-0.07	1.9-6.3	2014	Ropiha and Hansen (2015)
	<0.001, 0.0053	0.453, 3.29	2015, 2016	This chapter
	0.005	2.9	2016	Pattle Delamore Partners Ltd. (2016c)
SH1 Bridge	0.11	1.0	1972	Hoggins and Brooks (1973)
	<0.05	1.6-1.8	2014	Ropiha and Hansen (2015)
	<0.001, 0.051	0.135, 0.88	2015,2016	This chapter
	0.011	2.0	2016	Pattle Delamore Partners Ltd. (2016c)
Tangiteroria	-	0.2	1972	Hoggins and Brooks (1973)
	-	0.09	2016	Pattle Delamore Partners Ltd. (2016c)
Aquatic ecosystem protection†	0.06	0.15		ANZECC (2000)

* Upper-most site for which value is given in Hoggins and Brooks (1973).
# Sampling is assumed to have been carried out in the year in which the paper was received by the journal.
† Protection of 99% aquatic species guideline value used for dissolved Hg. ISQG-low guideline value used for sediment-bound Hg.

Arsenic concentrations in freshwater crayfish and eels were below detection limits. In shellfish, all total As concentrations were greater than the NZFSA maximum permissible level but it is estimated that inorganic As would be less than the maximum permissible level (Pattle Delamore Partners Ltd. 2016a). Cd concentrations in freshwater crayfish, and shellfish were below NZFSA guidelines for crustacean muscle and shellfish (Pattle Delamore Partners Ltd. 2016a). Hg concentrations in freshwater crayfish in the area downstream of the processing plant down to the SH1 bridge, and in eels just downstream of the SH1 bridge and in a separate catchment to the west, were above NZFSA guidelines (Pattle Delamore Partners Ltd. 2016a). Little correlation between water and sediment concentrations of As, Cd and Hg and tissue sample concentrations were found. This is interpreted to be due to the total concentration of As, Cd and Hg in water and sediment not reflecting the bioavailable fraction of these elements, the variable age of individuals sampled, and the mobility of eels upstream and downstream. It was

recommended that no more than 525g of eel collected from the Puhipuhi area be consumed in a month and that freshwater crayfish collected from the Puhipuhi area not be consumed (Pattle Delamore Partners Ltd. 2016a).

4.4.2 Modelling dissolved contaminants toxicity

Speciation of the water chemistry showed that the main aqueous Hg species were $HgCl_2^0$, $HgClOH^0$ and $Hg(OH)_2^0$. Although for other cationic trace elements, the free ion is the most toxic and therefore the speciation is important to determine, for mercury methylmercury is a very toxic species. Gionfriddo et al (2015) found between 0.3-1.6% of dissolved Hg was present as methylmercury. The percentage of dissolved Hg present as methylmercury was unable to be modelled because the MINTEQ database does not have data to speciate Hg into methylmercury. This is a microbially mediated process, and the presence of methylating bacteria in natural waters and sediment cannot be quantified. Dimethylmercury is in the MINTEQ database as a gas which dissociates into $Hg(OH)_2^0$ and CO_3^{2-}, or is formed as a result of the combination of the two. The saturation index of dimethylmercury was modelled to be between -250 to -260 indicating that this gas is highly unlikely to form under the present conditions.

Further to this, As and Sb are present as oxyanions, in contrast to other AMD trace elements which are usually present as cations, and are attenuated by adsorption to iron oxides at higher pH. As and Sb oxyanions desorb and are released into solution at higher pH. The potential for raising of the stream pH by addition of limestone, such as through the liming of agricultural land in the lower catchment, and releasing adsorbed As and Sb (Craw et al 2002). Arsenic and Sb do not occur as free ions so toxicity tests are using these oxyanions.

The concentrations of As, Hg and Sb in the stream water were low and only exceeded aquatic ecosystem protection guidelines for Hg in the very upper reaches of the Waikiore stream and at the ore processing site. Therefore, it is likely that a factor other than water chemistry is the main reason for the low abundance of pollution sensitive taxa at Puhipuhi.

4.4.3 Modelling sediment-bound contaminant speciation

The concentrations of sediment-bound Fe, Hg and As are high throughout the Waiariki Stream catchment and for Hg and As exceed the guidelines for the protection of aquatic life at almost all sites downstream of the mine processing area. Additionally, the metrics of stream health based on macroinvertebrate communities were strongly correlated with the concentrations of sediment-bound Fe and Hg. Stoneflies are unusually tolerant of trace elements and low pH, especially in waters rich in organic matter (Gray and Harding 2012), however no stoneflies were present in the streams at Puhipuhi. It is possible that there is not enough organic matter present in the streams to offset the impacts of low pH and high concentration of sediment-bound trace elements present in the Puhipuhi streams.

The sequential extraction results indicated that the majority of sediment-bound As and Sb was associated with HFO. Although Hg could not be analysed following the sequential extraction process, SEM imaging and elemental

scanning showed that Hg was associated with quartz veins where it is present as finely divided residual HgS. The presence of HgS-bearing particles supports the conclusion that sediment containing Hg entering streams via runoff posed more of a risk for Hg contamination than the dissolution of Hg-bearing minerals and transport of dissolved Hg to streams via run-off (Craw et al. 2002). This was supported by the fact that statistical analysis did not show a significant spatial correlation between aqueous and sediment-bound concentrations.

4.4.4 Geochemical modelling in effects assessment

The PHREEQC model was relatively reliable for predicting the dissolved speciation and therefore the toxicity and bioavailability of cationic metals and of As and Sb (oxyanions). Modelling of As and Sb adsorption to HFO was less reliable. Given that the majority of these elements are present in the sediment associated with HFO, more accurate predictions of the partitioning between solution and solid phases would be preferable. Either different values for the adsorption constants of these elements with HFO under natural conditions, or a scaling factor to limit the proportion of HFO binding sites available to these elements, could improve accuracy when predicting the attenuation of these elements. Additionally, modelling of the speciation of dissolved Hg and adsorption of Hg to HFO is unreliable. For sites where Hg contamination is of high concern and residual HgS is stable, the PHREEQC model is unsuitable for predicting Hg behaviour. Dissolved Hg speciation is therefore hampered by the role of MeHg in toxicity and by HgS stability. In order for Hg speciation prediction to be improved the rate of mercury methylation in sediment containing methylating bacteria needs to be accurately determined.

The Puhipuhi area is being investigated for future mining and this research highlights the importance of remediating mine waste in such a way that aquatic ecosystems are not impacted, targeting the different vectors through which contamination of aquatic environments can occur. Further work could be done to determine the mineralogy of the sinters around Puhipuhi and the water and sediment quality of the tributaries draining the areas where the sinter is exposed. This would confirm the hypothesis that the differences in the Hg and As concentrations in the Waiariki Stream catchment are related to the different sources of Hg and As.

4.5 Conclusion

In this research it was found that:

- High concentrations of sediment-bound As and Hg are present in the upper reaches of sub-tributaries of the Waiariki Stream indicating that sources are not limited to the ore processing site but also from other areas of exposed rock, such as sinter outcrops, former quarry sites and roads which had been sealed with quarried rock.

- Ecological assessments of aquatic organisms indicate lower %EPT, taxa richness and AMDI score occur for sites with greater Hg and As contamination. Stream health as determined by macroinvertebrate community parameters is correlated with dissolved Fe, Hg, Mn and Ni, and sediment-bound Fe and Hg as well as stream size.

- The concentration of Hg found in the flesh of eels tested was below the food safety limits for human health, however, bioaccumulation of Hg in fauna found in the Puhipuhi area may be a valid concern.

- Dissolved cationic trace elements were largely present as free metal ions and As and Sb as oxyanions, all in relatively toxic form, but at low concentrations. Hg was present as $HgCl_2^0$, $HgClOH^0$ or $Hg(OH)_2^0$. The model could not predict how much Hg was likely to be present as MeHg, the more toxic and bioaccumulative form of Hg.

- HFO is important for limiting the solubility of Cu and As but tends to overestimate adsorption (as found at Tui Mine, Chapter 3). For Sb and Hg, the degree of sorption underestimates

- The PHREEQC geochemical model is not currently reliable for modelling the effects of Hg (and perhaps Sb) released to a receiving environment

CHAPTER 5

BELLVUE MINE

Figure 5 The SRBR treatment system installed at Bellvue Mine. Photo: Jenny Webster-Brown

This chapter reports research into the water and sediment chemistry of streams draining a mine in an acid forming coal field, prior to and following remediation of mine drainage water. Remediation at this site been completed using a mussel shell sulfate-reducing bioreactor system. The speciation, toxicity and bioavailability of dissolved and sediment-bound trace elements prior to and after the treatment of mine drainage water is determined through sample analysis and geochemical modelling. The validity of a model constructed to predict changes to the chemistry of the environment receiving treated mine drainage water is also assessed.

5.1 Introduction

Bellvue mine is in the West Coast region of New Zealand, 2km north of Rapahoe and 15km north of Greymouth. AMD from Bellvue Mine used to flow from the adit down a 55m cascade and into Cannel Creek. Several small inputs including mine drainage from other mine adits, surface and sub-surface flow from waste rock piles after periods of high rainfall, and two tributaries un-impacted by mining also flow into Cannel Creek which then flows into Nine Mile Creek before flowing into the Tasman Sea (Figure 5.1).

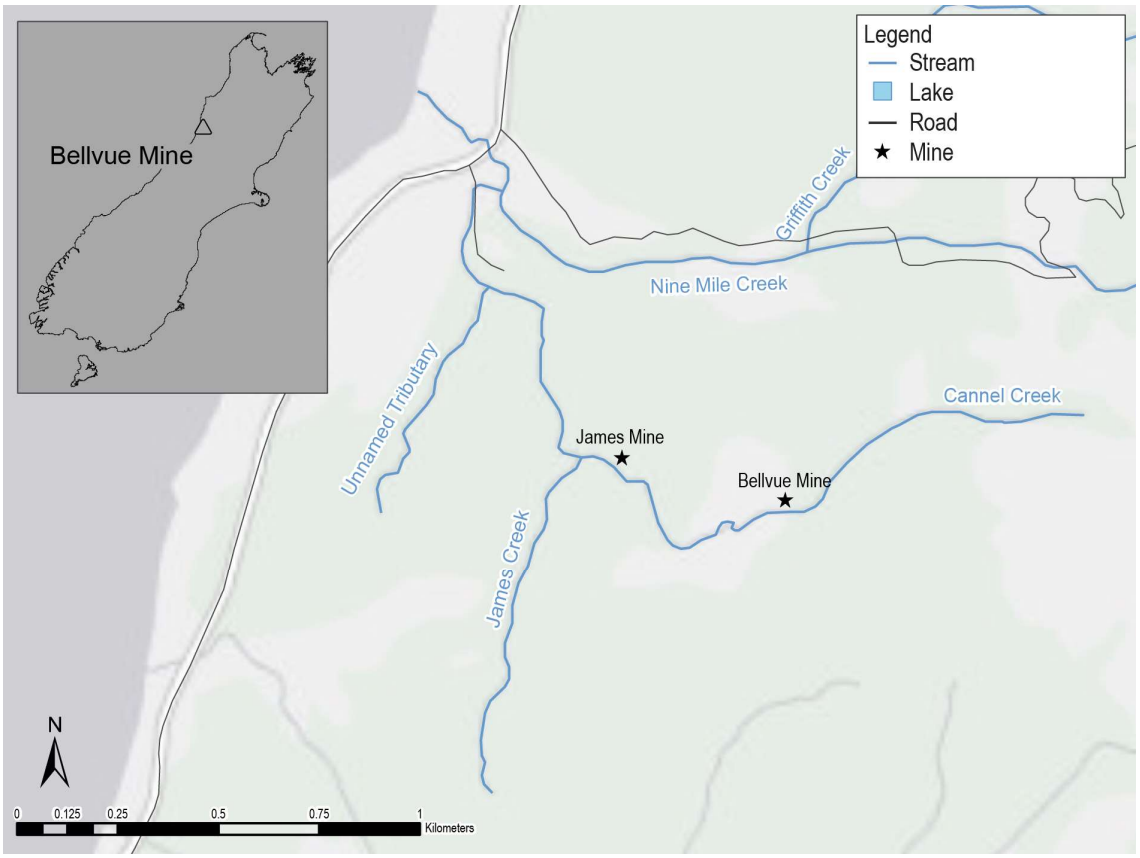

Figure 5.1 The Cannel Creek catchment including the location of Bellvue and other AMD sources, tributaries and waste rock piles.

The Bellvue mine adit is at an altitude of approximately 180masl. The mine portal has partially collapsed resulting in a small rock barrier over the base of the adit creating a pool of mine water at the entrance to the mine (Figure 5.2a). Mine drainage water exits the pool by flowing through a small pipe-like feature which runs underneath the rock barrier (West 2014). On exiting the adit, the mine drainage previously flowed down a 55m cascade and into Cannel Creek (Figure 5.2b).

Figure 5.2 The Bellvue Mine adit showing the mine pool and rock debris forming the barrier to the mine (a) and the cascade (b) which mine drainage flowed down into Cannel Creek prior to remediation. Photos: Dave Trumm

During this research project a full-scale sulfate-reducing bioreactor (SRBR) treatment system was installed at the base of the cascade to treat mine drainage water from Bellvue Mine. The mine drainage is now piped from the top of the cascade, down to the treatment system. A header system splits the flow evenly between five 30,000L plastic tanks filled with waste mussel shells (Figure 5.3; Trumm 2016a). AMD flows up through the SRBR treatment tanks and exits through pipes at the top of each tank. At the time of data collection for this research the treatment system outflow pipes discharged into a small channel and the treatment tank effluent entered Cannel Creek via overland surface flow from the channel. During this study we observed that, when the flow of AMD emanating from Bellvue Mine exceeded the capacity of the SRBR treatment system (1L/s over 5 tanks), the overflow (untreated AMD) also flowed into Cannel Creek via the channel at the base of the cascade or overland flow. Some attempts to pass the overflow through limestone-filled containers were implemented but the limestone was exhausted fairly quickly by the AMD. The change in flow path of the AMD from before and after remediation is given in Figure 5.4.

Figure 5.3 The SRBR treatment system installed at Bellvue Mine (a) and the collection pipe which transports AMD from the Bellvue Mine adit to the treatment tanks (b). Photos: Jenny Webster-Brown

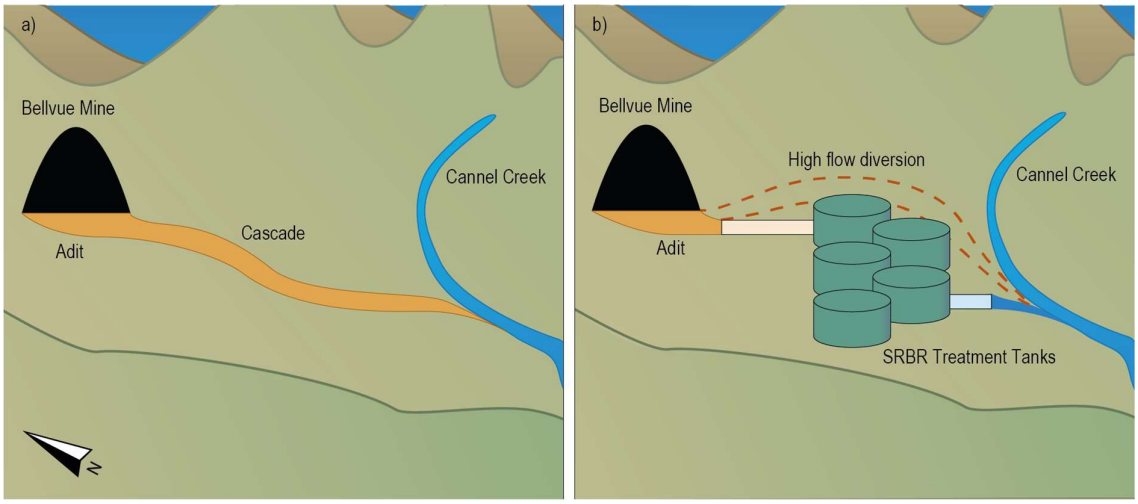

Figure 5.4 Schematic diagram of the route by which AMD from Bellvue Mine enters Cannel Creek, prior to (a) and following the installation of the treatment system (b).

5.1.1 Local geology

The basement geology in the Greymouth area is greywacke and argillite of the Greenland group overlain with coal measures of the Paparoa and Brunner groups (Gage 1952, Noble 2003, West 2014). The Paparoa coal measures (PCM; lower coal deposit) consist of shales, conglomerates, sandstones, mudstones and four coal units while the Brunner coal measures (BCM; upper coal deposit) consist of quartz sandstone, conglomerates, carbonaceous mudstones and coal seams. The Paparoa and Brunner coal measures are capped by marine sediments of the Kaiata and Island sandstone formations (Gage 1952). AMD at Bellvue is sourced from BCM rock as indicated by the acidity and concentrations of Fe and Al (Pope et al. 2006, Pope et al. 2010a)

5.1.2 History of mining at Bellvue

Mining operations at Bellvue Mine, by the Bellvue Co-operative party, were first recorded in 1927 as an extension of the James Mine (West 2014). When the James Mine workings were exhausted a new mine was opened on the other side of Cannel Creek. This is the abandoned Bellvue Mine site studied in this research. This site was mined for coal from 1941-1965 using board-and-pillar extraction method. At the surface, coal was transported to Rapahoe on an endless rope gravitational haulage system. Production ceased in 1970 (West 2014).

5.1.3 Stream flow and mine drainage water flow

Flow in Cannel Creek is described as being “flashy”, characterised by low base-flow and spikes of high flow corresponding to rainfall events (Trumm et al. 2016). Rainfall is highest in spring (227mm/month spring 2013) and lowest in summer (90mm/month summer 2013) (West 2014). Flow in Cannel Creek has been measured between 1.5 and 21.7L/s upstream of Bellvue Mine (Trumm unpublished-a data) but calculated to reach greater than 300L/s when flow, correlated with rainfall in the preceding 24hrs, is extrapolated based on historical rainfall patterns (Trumm et al. 2016). Flow of Bellvue Mine AMD is also dependent on rainfall but is much lower than that of Cannel Creek (Trumm 2016a, Trumm et al. 2016). Flow from the Bellvue Mine adit has been calculated to be in the range

of 0.041 - 30.3L/s, averaging 0.93L/s and with a median flow of 0.54L/s (Trumm 2016a, Trumm et al. 2016). Although both flows are rainfall dependent, the peak flow from Bellvue Mine has been shown to be delayed by about 24hrs relative to that of Cannel Creek (Trumm 2016a, Trumm et al. 2016)

5.1.4 Assessment of mining-related impacts at Bellvue

The existence of AMD contamination to Cannel Creek was found in 2001 as part of a survey for the West Coast Regional Council (WCRC) measuring pH and sulfate concentrations in streams and roadside drains between Westport and Greymouth (Webster and Brown 2001, Noble 2003). Streams with low pH and high concentration of sulfate, parameters indicative of ARD (as observed in Cannel Creek), were followed upstream to find the source of AMD contamination to the stream (Noble 2003). The source of AMD into Cannel Creek was identified as mine drainage from the Bellvue Mine adit (Webster and Brown 2001) and from another tributary near Bellvue Mine. The source of AMD to this second tributary was identified as James Mine by Noble (2003) but is now identified as Jubilee Mine and the adit closer to James Creek is now referred to as being James Mine. The Bellvue Mine AMD was found to have low concentrations of Mn, Cu, Pb and Cd but high concentrations of Fe, Al and Zn. Cannel Creek has intermittent Fe-oxide staining near the mine adits and complete coverage of the stream bed with sulfate-rich goethite (Webster and Brown 2001).

An assessment of dissolved As and sediment-bound As concentrations by Noble (2003) found that less As was present in coal lithologies mined at Bellvue and James Mines compared to other AMD-impacted sites in the West Coast region. Low concentrations of As (~2µg/L) were present in the water from the Bellvue Mine adit but were below detectable levels (1µg/L) in Cannel Creek itself. However, low and variable concentrations of As were observed in Cannel Creek sediments and As has accumulated in the streambed sediment (Noble 2003). Sediment-bound As concentrations were found to be proportional to sediment-bound Fe concentrations (Table 5.1; Noble 2003). Waste rock piles shortly downstream of the point where discharge from Bellvue Mine entered Cannel Creek, contribute a negligible effect on the water chemistry in Cannel Creek (Noble 2003).

Although these two pieces of research were carried out within a short time period, large differences in sediment-bound-As concentrations occurring lead to to contrasting conclusions about the source of As to Cannel Creek. Webster and Brown (2001) found very high concentrations of sediment-bound As in Cannel Creek immediately downstream of the Bellvue Mine AMD discharge point which was not observed in the mine adit sediment leading to the conclusion that As in the Cannel Creek stream bed came from a source that was not the Bellvue Mine AMD. Noble (2003) who found low concentrations of sediment-bound As in Cannel Creek immediately downstream of the Bellvue Mine AMD discharge point concluded that either all the As had been attenuated from the Bellvue Mine AMD before it entered Cannel Creek or Fe-oxide deposition, and therefore scavenging of As by freshly formed Fe-oxides, was not occurring at the time of sampling. However, this may be a reflection of the sampling process used in the two studies.

Table 5.1 Historical values of sediment-bound Fe and As in Cannel Creek (CC) and the Bellvue Mine adit.

Location	Fe (wt%)	As (mg/kg)	Ratio As:Fe	Reference
CC u/s Bellvue adit	0.92	1.35**	1.47	Noble (2003)
Bellvue Mine adit	46, 55	35.8, 49.5	0.78, 0.90	Webster and Brown (2001)
	47	24**	0.51	Noble (2003)
CC d/s Bellvue adit	23	18,600	809	Webster and Brown (2001)
	40.9	<1.0**	-	Noble (2003)
CC d/s tribs	8.16	8.16**	1.00	Noble (2003)
CC u/s 9 mile Crk	45	82.6	1.84	Webster and Brown (2001)
	11.2	13.2**	1.18	Noble (2003)
ISQG-High		70		ANZECC (2000)
ISQG-Low		20		

**It is assumed that the correct units for these values is ppm as given in the text, as opposed to ppb given in the figure accompanying these results.

A workshop lead by Trumm and Cavanagh (2006) tracked Cannel Creek upstream from its confluence with Nine Mile Creek/Griffin Creek [sic] to above the Bellvue Mine AMD discharge point. Physiochemical measurements were recorded, and samples were collected for analysis of dissolved sulfate, Fe and Al concentrations. The results of this workshop and subsequent sample analysis found 6 sources of AMD contamination to Cannel Creek. Based on the acid loads of these AMD sources, it was determined that discharge from Bellvue Mine was the most significant source of AMD to Cannel Creek (62%) and that a second adit on the true right bank of Cannel Creek (now identified at James Mine) was the next largest contribution of AMD to Cannel Creek (33%) (Trumm and Cavanagh 2006). This study recommended that water chemistry and flow data be collected from the Bellvue Mine discharge and that small scale treatment trials be carried out to determine the best method to treat the Bellvue Mine AMD (Trumm and Cavanagh 2006).

Characterisation of the aqueous geochemistry of the Bellvue Mine AMD and Cannel Creek was carried out by West (2014). The water chemistry at 6 locations around the confluence of these two waters (Bellvue Mine pool, top of cascade, middle of cascade, bottom of cascade, Cannel Creek upstream of Bellvue Mine AMD discharge point and Cannel Creek downstream of Bellvue Mine AMD discharge point) was determined through a baseline chemical survey. Flow of AMD from the Bellvue Mine adit was initially determined bi-monthly prior to the installation of a data logger being installed in the mine pool for a period of 8 months. The AMD in the mine pool had a stable pH, between 2.34-2.95, however trace element showed a seasonal variation with high concentrations in summer and low concentrations in winter. Flow of AMD from the mine adit was 0.35 ± 0.1 L/s (West 2014). The pH and trace element concentrations down the cascade were similar to those of the mine pool, however dissolved oxygen increased with distance from the mine pool. In Cannel Creek, downstream of the Bellvue Mine AMD discharge point, pH varied between 2.76 and 3.62. Seasonal trends were also present at this site. Low trace element concentrations and higher pH were present in winter and higher trace element concentrations were present in summer (West 2014).

A summary of water chemistry in Cannel Creek and the Bellvue Mine AMD between 2001 and 2013 is given in Table 5.2.

Table 5.2 Historical values of pH and concentration of aqueous sulfate, Fe, As and Zn at several points along Cannel Creek (CC) and as measured at the Bellvue Mine adit.

Location	pH	SO_4 (mg/L)	Fe (mg/L)	As (µg/L)	Zn (µg/L)	Year	Reference
CC u/s Bellvue adit	6.56	1.0				2001	Webster and Brown (2001)
	5.50-6.67	<DL		<DL		2003	Noble (2003)
	7.28	<10	0.34	<1.0		2006	Trumm and Cavanagh (2006)
	4.60-6.26	2.1-8.0	0.15-0.47		1.2-4.5	2013	West (2014)
Bellvue Mine adit	2.56	1100	97.4	<1.0	400	2001	Webster and Brown (2001)
	2.54-2.63	1108-1650		1.33-1.65		2003	Noble (2003)
	2.55		98.4	43.2		2005	Pope et al. (2006)
	2.71	900	60	<1.0		2006	Trumm and Cavanagh (2006)
	2.34-2.95	520-1280	28-210		789-520	2013	West (2014)
CC d/s Bellvue adit	3.5	165				2001	Webster and Brown (2001)
	3.30	355-400		<DL		2003	Noble (2003)
	3.30	~205	0.37	<1.0		2006	Trumm and Cavanagh (2006)
	2.76-3.62	15.1-430	0.55-26		2.4-131	2013	West (2014)
CC d/s tributaries	2.98	500		<DL		2003	Noble (2003)
	3.32	290				2006	Trumm and Cavanagh (2006)
CC u/s 9 mile Creek	3.45	120				2001	Webster and Brown (2001)
	2.90-3.28	348-420		<DL		2003	Noble (2003)
	3.3	290	0.99			2006	Trumm and Cavanagh (2006)
Aquatic ecosystem protection guideline				24 As(III) 13 As(V)	8.0		ANZECC (2000)

AMD treatment using 4 different treatment systems including a bioreactor consisting of a mixture of mussel shells, bark chips, bark mulch and garden compost, a reactor consisting of mussel shells treating anoxic AMD (MSR), a reactor consisting of mussel shells treating oxidised AMD (MSO), and an anoxic limestone drain (ALD) treating anoxic AMD was completed (West 2014). The MSR and bioreactor performed to a similar level of efficiency in removing metals and sulfate and increasing pH. The MSO performed well in removing metals and sulfate and increasing pH. However, this came at the cost of increasing hydraulic retention time through the precipitation of metal oxides clogging up pores in the substrate. The ALD performed poorly. A small increase in pH and an increase in the concentration of sulfate and several trace elements was observed, contrary to what had been intended and anticipated (West 2014).

Bellvue Mine site was selected to be a case study in achieving closure for the CMER project, to rehabilitate an abandoned mine and assess the recovery of aquatic and terrestrial ecosystems (Cavanagh et al. 2015b). A conceptual plan for a treatment system consisting of five 30,000L plastic tanks containing waste mussel shells was therefore developed (Trumm 2016a).

Flow and water chemistry of the discharge from both the Bellvue Mine adit and the James Mine adit, 550m downstream of the Bellvue Mine was monitored (Trumm et al. 2016). Using this data, a model was developed

using PHREEQC to predict how the treatment of AMD from the Bellvue Mine would affect the chemistry of stream water in Cannel Creek at the point where the Bellvue Mine AMD enters Cannel Creek, as well as downstream where the James Mine AMD and James Creek enter Cannel Creek. This modelling predicted that with the installation of the treatment system, ecologically-relevant water quality targets of pH>4.5 and trace element concentrations <1mg/L will be met for the entire length of Cannel Creek 49% of the time. However, due to the high flow of AMD, these targets will not be met for the 150m reach between James Mine and James Creek 51% of the time. Therefore, treatment of James Mine AMD by a dispersed alkaline substrate (DAS) system was investigated by Hillman (2018). Field trials were completed by Hillman between Feb-April 2018 and the DAS system was only successfully treating AMD from James Mine in the first eight weeks of the trial (Hillman *Pers comm*). A reduction in sulfate and trace element concentrations and an increase in pH downstream of the James Mine (Sites 11-18) may have occurred as a result of treatment of James Mine AMD. However due to the flow rate of James Mine being very small compared to Cannel Creek at sites Bell9 and Bell11 (<2% of Cannel Creek flow for all sampling surveys except for during June 2018 when the DAS system was not operating), a measureable change in the water chemistry of Cannel Creek downstream of James Mine was not expected to occur as a result of James Mine AMD treatment during the trials conducted.

It is important to know how the SRBR treatment system performs and how the water chemistry of Cannel Creek changes following the installation of the treatment system because this site is being used as a case study in rehabilitation of an abandoned mine site and recovery of the aquatic ecosystem. It is also vital that the model used to predict post-remediation water chemistry in Cannel Creek is tested against monitoring data to evaluate the reliability of the model and determine whether it can be used to make water chemistry predictions at similar sites in the future.

5.1.5 Aim and objectives of this research

The aim of the research described in this chapter was to assess the adequacy of the modelling used to inform the remediation methods used at this mine site, using post-remediation monitoring data. This was achieved through the following objectives;

- Characterise the water chemistry, including trace element speciation, along the length of Cannel Creek before and after the installation of the treatment system, and compare to modelled predictions for post-remediation water quality in Cannel Creek;
- Track the progress of the stream water chemistry towards ecologically-relevant targets, and to establish a baseline for the future assessment of the progress of sediment chemistry toward these targets.
- Predict the degree of trace element removal within the bioreactor treatment tanks using the PHREEQC model and compare to measured removal efficacy.

5.2 Methods

5.2.1 Study area

The abandoned Bellvue Mine was selected for this research because acid and trace element contamination of the waterways draining the site had been determined and a remediation project to treat the AMD before it was discharged to the waterway was planned. The installation of a full-scale sulfate-reducing bioreactor (SRBR) treatment system was completed within the duration of this research so samples were collected before and after installation of the treatment system. The collection of post-remediation data allowed for the assessment of modelled predictions of post-remediation water quality in Cannel Creek was also completed.

AMD water from Bellvue Mine exits through the mine pool (Bell Adit) and prior to remediation flowed down the cascade into Cannel Creek. The site Bell2 was located mid-way down the cascade. After the installation of the SRBR treatment system, AMD was piped from the mine pool to the treatment system. The treated AMD water then flowed from the treatment system into Cannel Creek via overland flow. The treated AMD water was sampled at the outlet of the pipes from the treatment tanks. The site Bell3 was located in Cannel Creek after the treated AMD entered Cannel Creek and sufficient mixing had occurred. Cannel Creek received AMD discharges from several other seepages downstream of the Bellvue Mine discharge point. These included AMD from Jubilee Mine (Bell 4), ephemeral surface flows over the waste coal piles (Bell 6a, Bell 6b and Bell7), a circum-neutral surface flow that often contained a bacteriogenic iron oxide, referred to as BIOS (Ferris 2005; Bell8) and another AMD seep (Bell 8A). The site Bell5 was located between the input from Jubilee Mine (Bell4) and the first AMD flow from the coal fields (Bell6a). The site Bell9 was located between the input from Bell8A and James Mine (Bell10). After these sites AMD water from James Mine (Bell10) entered Cannel Creek and James Creek (Bell13) flowed into Cannel Creek shortly downstream of the mine. The site Bell11 and Bell12 were located between the input from James Mine and James Creek. Downstream of James Creek, another tributary, unaffected by mining, joined Cannel Creek. However, this site was unable to be sampled in this research due to accessibility issues. The final sampling site on Cannel Creek before it flowed into Nine Mile Creek was Bell 18 (Figure 5.5).

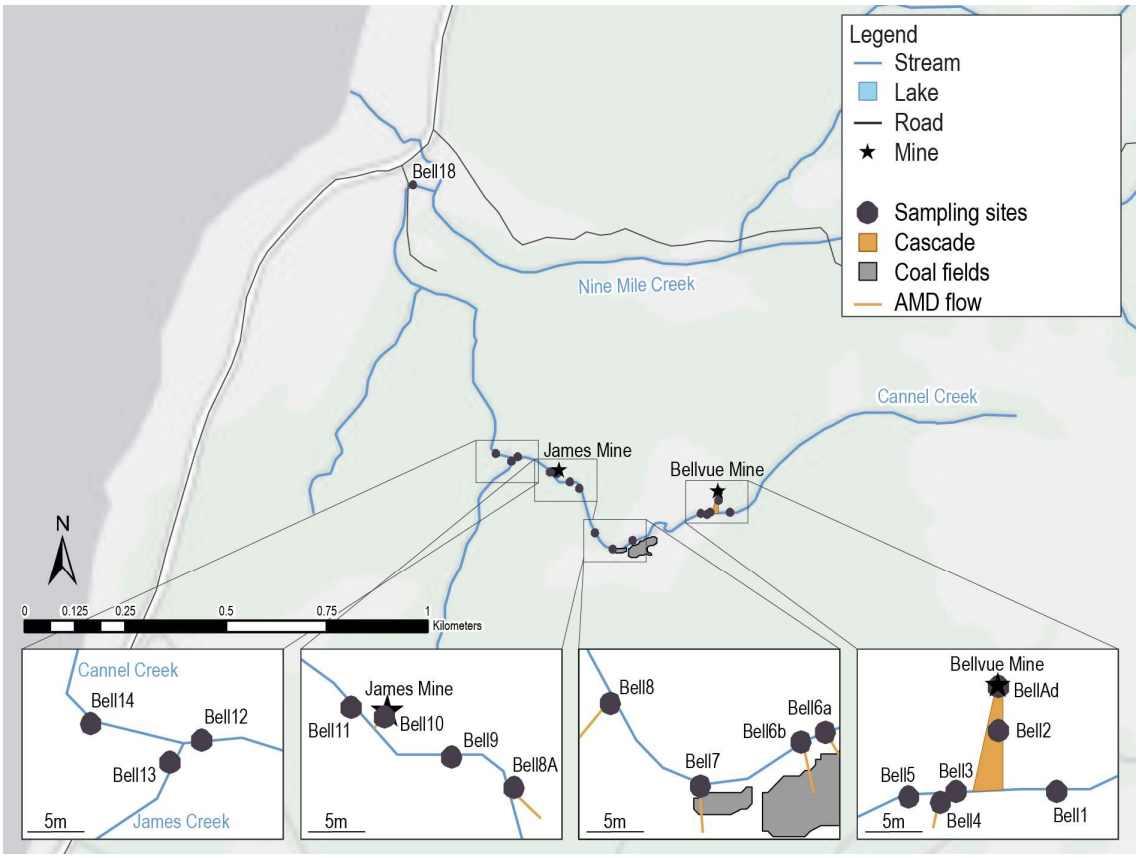

Figure 5.5 Map of the Cannel Creek catchment showing the location of the sampling sites in relation to Bellvue Mine, James Mine and James Creek.

5.2.2 Sample collection

Water samples were collected from 16 sites (Figure 5.5) within the Cannel Creek catchment including samples from the Bellvue mine pool and the James Mine adit, a sample from the middle of the cascade prior to the installation of the treatment system and at the outlet of the treatment system following the installation of the treatment system, in Cannel Creek upstream of any mining-relating impacts and in the James Creek tributary. The sampling site on Cannel Creek upstream of any mining-related impacts (Bell1) and on James Creek (Bell13) are reference sites.

Pre-remediation water samples were collected in November 2016, January 2017 and May 2017. The installation of the treatment system took place between June 2017 and December 2017. First flush samples were collected immediately following the commissioning of the treatment system. Post-remediation samples were collected bi-monthly thereafter in February 2018, April 2018 and June 2018. Surface flow at sites Bell4, Bell6 and Bell7 were ephemeral and could not be sampled in dry periods when no surface flow was present. Additional pre-remediation water chemistry data from January 2016 to April 2016 and post-remediation data from February 2018 to May 2018 was available (Trumm unpublished-a).

Sediment samples were collected where possible on the first trip. However, as large sections of the stream bed were composed of cemented Fe-oxide deposits and collection of the stream bed substrate was impossible at several sites in the lower catchment.

Water samples were collected, physiochemical parameters were measured, and stream flow was measured following the methodology outlined in Section 2.2. Flow measurements were carried out by CRL staff members, Aaron Dutton and Kerry Gordan. Flow ranged between 4.7 -64L/s at the uppermost site on Cannel Creek (Bell1) and between 14.1-31.5L/s at the lowest site on Cannel Creek (Bell18). Sampling in Feb 2018 was completed immediately following a rainfall event and flow in Cannel Creek was decreasing during the sample collection event. Therefore, the flow at Bell1 (the upper-most site on Cannel Creek) was greater than at Bell18 (the lowest site) because sampling and flow measurement occurred at the Bell1 earlier in the sample collection event than sampling and flow measurement at Bell18.

5.2.3 Sample analysis

Water

Water samples were analysed for major cations and trace elements by ICP-MS and for major anions by HPIC. Samples were analysed for dissolved inorganic carbon (DIC) by infra-red gas analysis of CO_2(g) generated on acidification of the sample, and for dissolved organic carbon (DOC) by high temperature combustion. Samples were analysed for ferrous iron, nitrate, dissolved reactive phosphorous, ammonia and sulfide by spectroscopy. These methods are described in greater detail in Section 2.3.

Sediment

Sediment samples were analysed as outlined in Section 2.4. Total sediment digests and sequential extraction of trace elements from individual mineral phases, using the method of Leleyter and Probst (1999) and Salvarredy-Aranguren et al. (2008), were carried out and the extracts analysed for trace elements by ICP-MS.

5.2.4 Geochemical modelling

Geochemical modelling of the speciation of dissolved trace elements and saturation indices of trace element-bearing minerals was carried out using the PHREEQC geochemical modelling program (Section 2.6). Additional thermodynamic data for the formation constant of schwertmannite (Eqn 5.1, Bigham et al. 1996) was added to the PHREEQC database.

$$8Fe^{3+}_{(aq)} + SO^{2-}_{4(aq)} + 14H_2O_{(l)} \rightarrow Fe_8O_8(OH)_6(SO_4)_{(s)} + 22H^{+}_{(aq)} \quad \text{(eqn 5.1)}$$

5.3 Results

5.3.1 Aqueous chemistry

pH

The pH in Cannel Creek at Bell1, upstream of any mining inputs, varied between 4.60 and 7.28 (Figure 5.6) while the pH of the mine pool of water at the adit entrance (Bell Ad) varied between 2.49 and 3.11 (Table 5.3). The pH of the Bellvue Mine AMD did not change significantly as it flowed down the cascade. The pH of AMD at the bottom of the cascade varied between 2.28 and 3.01. Prior to remediation the pH in Cannel Creek immediately downstream of the Bellvue Mine AMD discharge point varied between 2.76 and 4.30 (Figure 5.6). Following the installation of the treatment system, the effluent from the system had a pH of 7.01-7.14 and the pH in Cannel Creek immediately downstream of the treatment system discharge point from the treatment system was in the range of 4.82-6.95 (Figure 5.6). This was an increase of an average of 2.40 pH units as compared to prior to remediation.

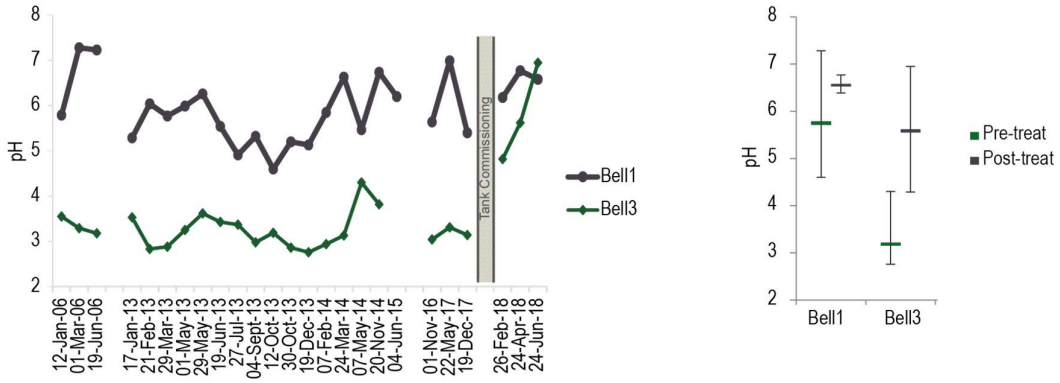

Figure 5.6 pH in Cannel Creek upstream (Bell1) and downstream (Bell3) of the Bellvue Mine AMD inflow prior to remediation, and after receiving treated effluent from the SRBR's following remediation. Values on the right-hand graph are the median values with the maximum and minimum values indicated as the range.

The small AMD flows as well as overland flow from rain events resulted in the pH of Cannel Creek increasing by 0.33 pH units between Bell3 and Bell9 prior to remediation. However, after the remedial works, the pH decreased by 0.59 pH units within this reach. Overall, the pH of Cannel Creek (at Bell9) increased by 1.48 pH units due to the installation of the treatment system. James Mine AMD (Bell10) had a pH between 2.41 - 2.66. This caused the pH of Cannel Creek to drop by only a small amount (0.18 pH units) prior to remediation. Whereas, after the remedial work, AMD input from James Mine caused the pH of Cannel Creek to increase by 1.02 pH units. Overall, the installation of the treatment system resulted in a 0.64 pH unit increase immediately downstream of James Mine. James Creek had a pH between 5.87 and 7.28. This resulted in the pH of Cannel Creek decreasing by 0.39 pH units before remediation and by 0.48 pH units following remediation. Overall the pH of Cannel Creek downstream of the confluence with James Creek increased by 1.07 pH units due to the installation of the treatment system. The

final sampling site on Cannel Creek before it flowed into Nine Mile Creek (Bell 18) had a pH between 3.3 and 5.11 prior to remediation increasing to 5.05-6.75 post-remediation. Although the installation of the treatment system only raised the pH of Cannel Creek at Bell18 by 0.36 pH units, this increase was sufficient that the pH was consistently above a pH of 5.0 at this point in the stream. The pH range of each site prior to- and following remediation (or overall for sites not influenced by the installation of the treatment system) are given in Table 5.3.

Table 5.3 The pH range of sites sampled prior to and following remediation. For sites, such as upstream and side streams where the pH was not influenced by the treatment system, the pH range for all sampling events is given in the middle column.

		pH	
Site	**Site type**	**Pre-remediation**	**Post-remediation**
Bell1	Un-impacted main channel (control)	4.60-7.28	
BellAdit	Mine adit	2.49-3.11	
Bell2	AMD Tributary	2.28-3.01	-
Tanks	Treated AMD	-	7.01-7.14
Bell3	Main channel	2.76-4.3	4.82-6.96
Bell4	AMD Tributary	2.74-3.2	
Bell5	Main channel	3.18-3.77	4.38-6.35
Bell6a	AMD Tributary	3.34-3.41	
Bell6b	AMD Tributary	3.23-4.72	
Bell7	AMD Tributary	3.27-3.75	
Bell8	AMD Tributary	5.80-6.70	
Bell8A	AMD Tributary	3.19-4.74	
Bell9	Main channel	3.19-3.94	4.30-5.70
Bell10	Mine adit	2.41-2.66	
Bell11	Main channel	3.24-3.75	4.01-4.64
Bell12	Main channel	3.11-3.81	4.26-4.91
Bell13	Un-impacted tributary (control)	5.87-7.28	
Bell14	Main channel	3.25-4.32	4.84-5.68
Bell18	Main channel	3.30-5.11	5.05-6.75

Prior to remediation the pH in Cannel Creek dropped significantly following the discharge of Bellvue Mine AMD into Cannel Creek and stayed low until the end of the stream due to additional AMD inputs. The dilution of the AMD from un-impacted tributaries was unable to make any significant improvement to the water quality of Cannel Creek. Following the installation of the treatment system, the pH of Cannel Creek decreased slowly over the course of the stream due to small AMD inputs, particularly that of James Mine. However, the un-impacted tributaries were able to improve the water quality in the lower reaches of Cannel Creek such that the final sampling site was consistently above pH 5.0.

Dissolved trace elements

The range of concentrations measured at points along Cannel Creek, in Bellvue Mine AMD, SRBR tank effluent, James Mine AMD, and James Creek prior to and following the installation of the SRBR treatment system are summarised in Table 5.4 for Fe, Al, Zn and Ni. Dissolved and total As concentrations were <1µg/L for all sites

except for Bell10 (up to 1.46µg/L) for all sampling events. However, a relatively high dissolved As concentration was recorded during the first flush samples when the SRBR treatment tanks were commissioned (44-131µg/L).

Table 5.4 Dissolved trace element concentrations at sites along Cannel Creek, AMD discharges and a circum-neutral tributary both prior to and following the installation of an SRBR treatment system to treat AMD from Bellvue Mine before discharging into Cannel Creek. Bell1, BellAdit, Bell10 and Bell13 are given as combined "pre- and post- remediation" values as these sites were outside of the main stream channel affected by the installation of the treatment system.

Site	Time frame	Fe (mg/L)	Al (mg/L)	Zn (µg/L)	Ni (µg/L)
Bell1	Pre- and Post-remed	0.18-0.55	0.08-0.27	1.38-7.30	0.47-0.90
BellAdit	Pre- and Post-remed	2.4-210	19.2-67	195-520	63.0-187
Bell2	Pre-remed	35.0-140	25.0-72.0	220-530	84-193
Tanks	Post-remed	0.06-12.1	0.01-0.62	0.17-70.4	0.23-24.4
Bell3	Pre-remed	0.37-33	0.55-26	29.5-103	9.67-57.0
	Post-remed	0.26-1.53	0.11-2.79	4.66-31.8	1.67-10.5
Bell5	Pre-remed	2.02-5.77	2.76-6.00	25.3-68.4	8.22-21.0
	Post-remed	0.03-1.05	0.01-1.05	8.88-19.5	3.68-6.48
Bell9	Pre-remed	1.69-5.76	1.61-5.77	17.3-58.3	6.40-18.2
	Post-remed	1.31-1.41	0.06-1.71	12.0-29.5	5.37-10.2
Bell10	Pre-and Post-remed	16.5-169	122-231	960-1510	412-660
Bell11	Pre-remed	3.3-8.98	4.3-12.0	36.0-105	14.6-35.9
	Post-remed	1.23-3.39	2.40-4.54	40.9-81.1	15.2-27.2
Bell12	Pre-remed	8.75-9.08	10.1-12.6	15.5-98.9	34.1-35.0
	Post-remed	2.00-3.00	3.34-5.24	47.2-79.7	15.4-26.3
Bell13	Pre- and Post-remed	0.27-0.51	0.05-0.17	<0.05-1.79	0.42-1.31
Bell14	Pre-remed	2.10-5.33	3.30-9.23	60.9-79.8	26.7-28.3
	Post-remed	1.17-3.86	0.39-4.31	31.1-66.7	12.6-21.9
Bell18	Pre-remed	1.01-2.07	1.98-6.11	23.0-59.5	9.70-21.1
	Post-remed	0.37-1.38	0.01-1.97	28.9-45.4	10.1-16.1

Dissolved trace element concentrations were low in Cannel Creek, upstream of any mining influences (Bell1) but the mine pool (BellAd) had very high concentrations of trace elements. Prior to remediation, the average concentration of trace elements in the Bellvue Mine AMD increased slightly at the bottom of the cascade (Bell2). Following remediation, the concentration of trace elements in the treatment tank effluent was much lower than that of the mine pool. Prior to remediation, the concentration of trace elements in Cannel Creek immediately downstream of the Bellvue Mine AMD discharge point (Bell3) were variable (Figure 5.7). Following remediation, the concentration of Fe and Al decreased by >90% (Figure 5.7a). Zn and Ni concentrations decreased initially but spiked in April before decreasing again (Figure 5.7b). This meant that the average concentration decrease was 66% for Zn and 81% for Ni. The average post-remediation concentrations at Bell3 were higher than the ANZECC 95% ecosystem protection guideline for Al, Zn and Ni, however, even the upstream "control" site (Bell1) is higher than the ANZECC guideline value for Al reflecting the naturally high Al concentrations found in West Coast streams.

High concentrations of As (up to 130µg/L) in the treatment tank effluent were measured in the first flush samples although the concentration of dissolved As had been near to or below detection limits in previous samples of both

the Bellvue Mine AMD and in Cannel Creek. These high concentrations of As in the treatment tank effluent were not present in any subsequent sampling survey.

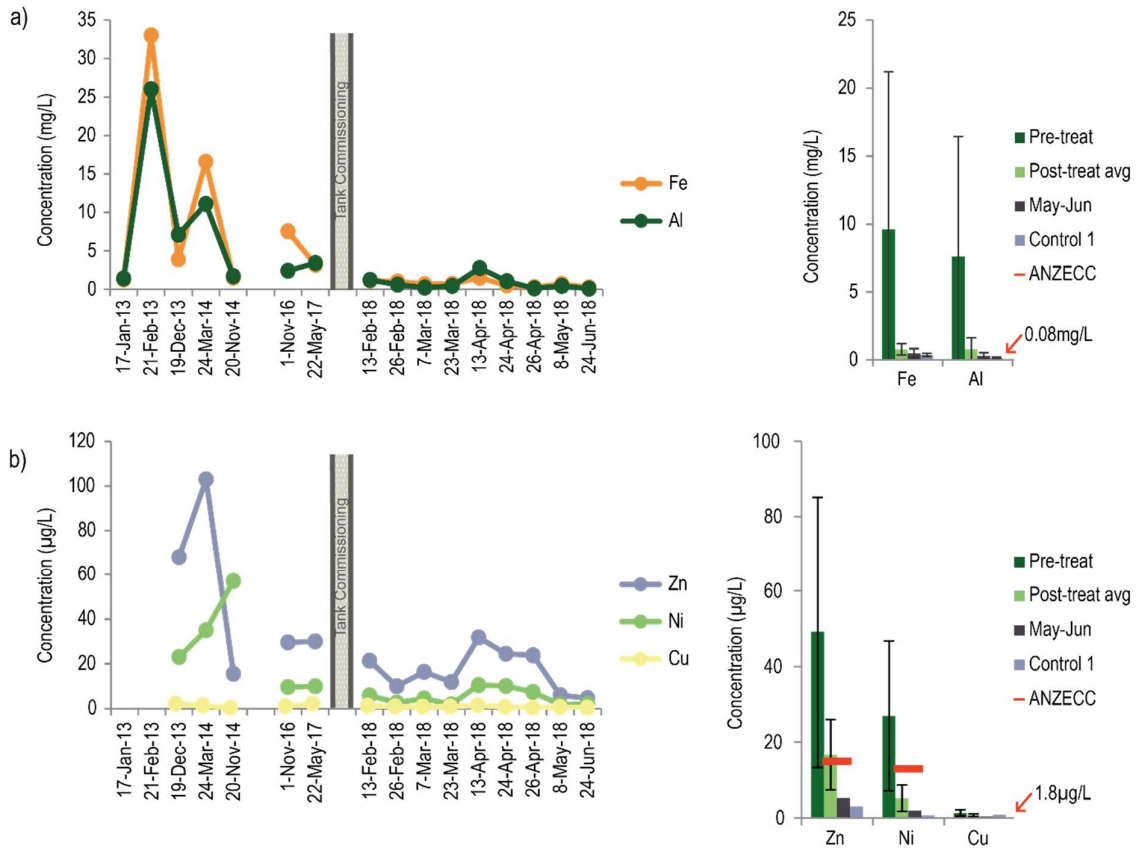

Figure 5.7 Water chemistry changes in Cannel Creek immediately downstream of the Bellvue Mine AMD inflow (Bell-3) for dissolved a) Fe and Al and b) Zn, Ni and Cu. The post-treatment average includes all results from Feb 2018 to Jun 2018 inclusive whereas "May-Jun" only includes the results for the May 2018 and June 2018 sampling events. Control 1 includes all results for the Bell1 site. The "ANZECC" line shows the ANZECC (2000) guideline for the protection of 90% of aquatic species as applied to severely impacted ecosystems.

The concentration of trace elements in Cannel Creek increases slightly downstream as it receives AMD inflow from Jubilee Mine (Bell4), surface and sub-surface flow from the waste rock piles (Bell6-8) and an AMD seep (Bell8A). This is consistent both prior to and following the installation of the treatment system. Between Bell9 and Bell11, Cannel Creek receives AMD discharge from James Mine. James Mine AMD contains extremely high concentrations of trace elements and causes a dramatic increase in trace element concentrations in Cannel Creek downstream of the discharge point. However, the effect of treating the AMD from Bellvue Mine and reducing trace element concentration in Cannel Creek is noticeable in the change in concentration of trace elements at Bell11 (Figure 5.8).

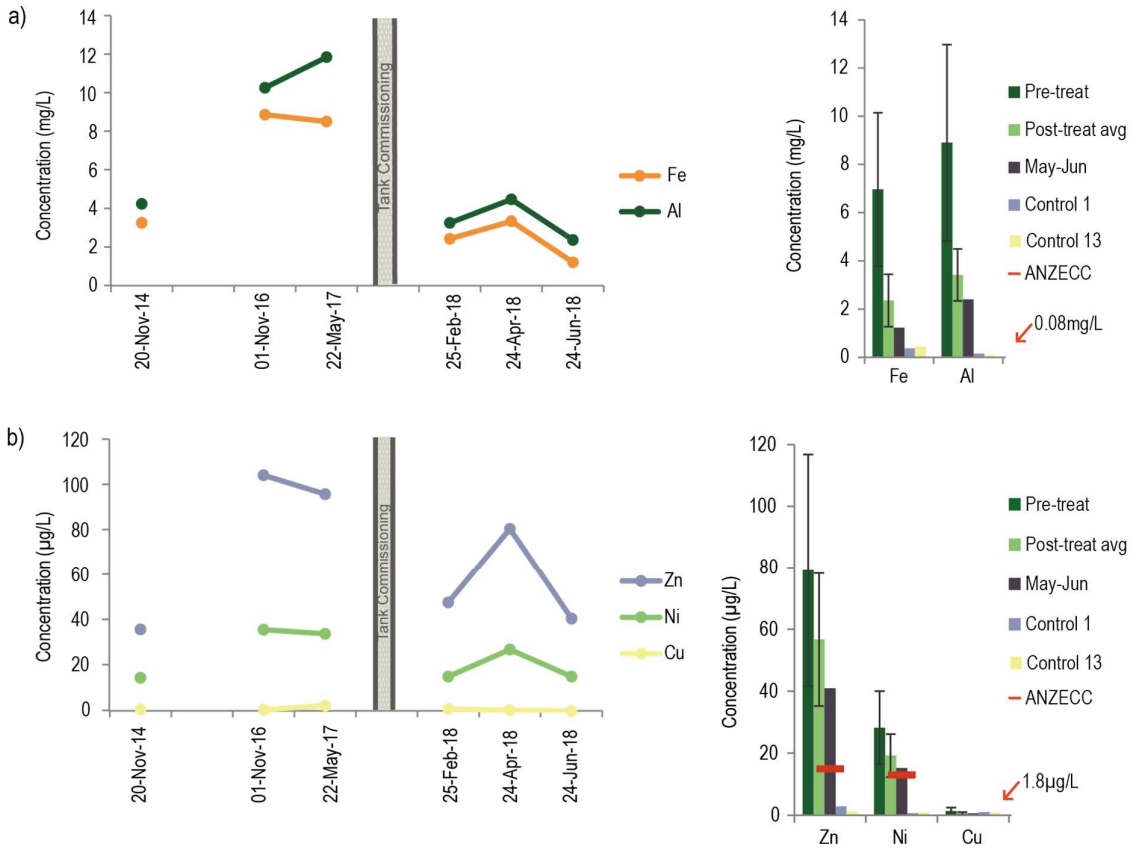

Figure 5.8 Water chemistry changes in Cannel Creek, downstream of the James Mine AMD inflow (Bell11) for a)Fe and Al, and b) Zn, Ni and Cu. The post-treatment average includes all results from Feb 2018 to Jun 2018 inclusive whereas "May-Jun" only includes the results for the June 2018 sampling events. Control 1 includes all results for the Bell1 site. Control 13 includes all results for the bell13 sampling site. The "ANZECC" line shows the ANZECC (2000) guideline for the protection of 90% of aquatic species as applied to severely impacted ecosystems.

After the James Mine AMD input, Cannel Creek is joined by James Creek, a tributary un-impacted by mining, which reduces the concentration of trace elements in Cannel Creek through dilution (Figure 5.9). However, due to the influx of trace elements from James Mine, the concentrations of Al, Zn and Ni still exceeded the ANZECC guidelines for the protection of 95% of aquatic species.

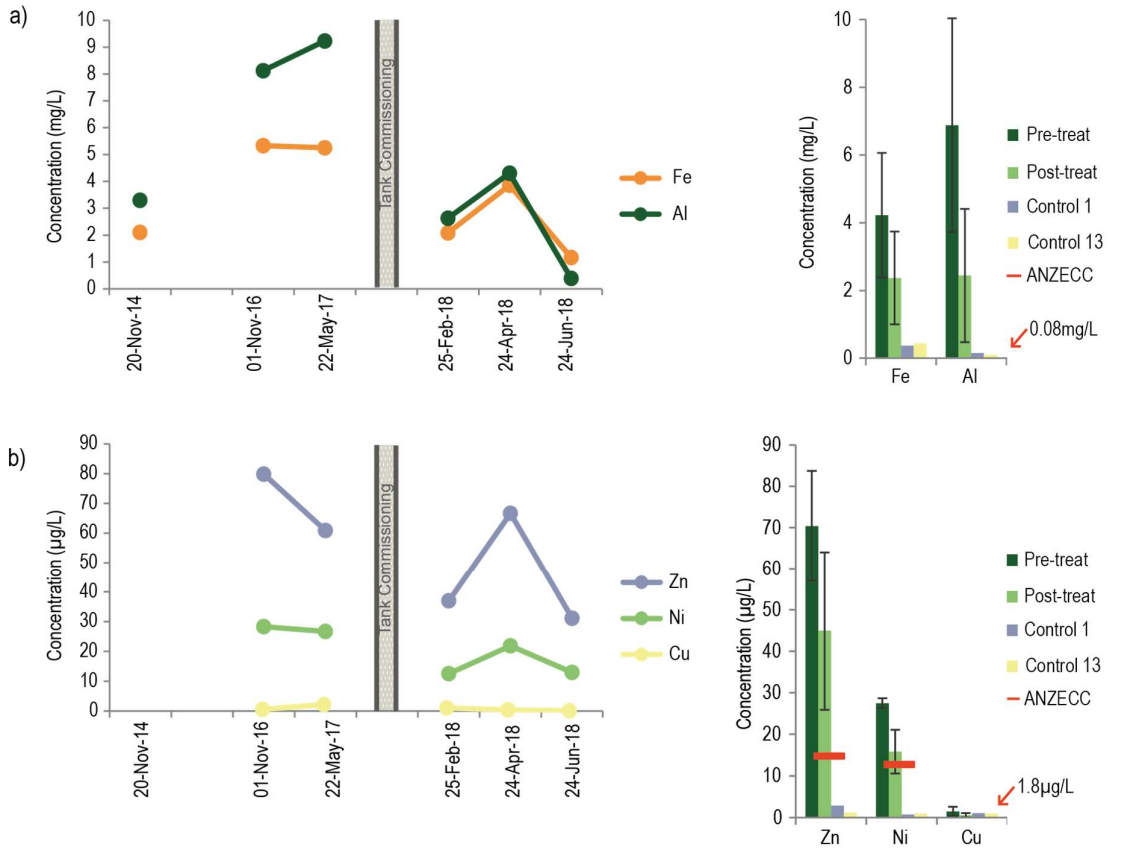

Figure 5.9 Water chemistry changes in Cannel Creek, downstream of the confluence with James Creek (Bell14) for a) Fe and Al, and b) Zn, Ni and Cu. The post-treatment average includes all results from Feb 2018 to Jun 2018. Control 1 includes all results for the Bell1 site. Control 13 includes all results for the bell13 sampling site. The "ANZECC" line shows the ANZECC (2000) guideline for the protection of 90% of aquatic species as applied to severely impacted ecosystems.

Cannel Creek is joined by another unnamed tributary, un-affected by mining which further dilutes the AMD and reduces the concentration of trace elements in the stream water. However, the average concentration of Al, Zn and Ni was still above the ANZECC 95% aquatic ecosystem protection guideline values for these sites. The trend indicated in trace element concentration is downward and it is anticipated that the water chemistry in Cannel Creek will be below the ANZECC (2000) guidelines in the near future.

Samples were passed through filters with pore sizes 0.45µm, 0.22µm and 0.10µm but the smaller pore sizes did not have a significant impact on the concentration of dissolved trace elements passing through the filter (Table A7).

Other dissolved constituents

With the exception of BellAdit and Bell10 during the April 2018 sampling (23.0mg/L and 2.86mg/L respectively), all samples had a nitrate concentration <1.00mg/L and most samples were below the limit of detection (Tables A1-

A6). All samples had a phosphate concentration <0.10mg/L and most samples were below the limit of detection (Tables A1-A6). Most samples had an ammonia concentration <0.5mg/L. Bell10 had a consistently high ammonia concentration (0.38-2.04mg/L). As had been indicated by results of West (2014), there was a very high concentration of ammonia in the first flush samples collected from the treatment system (188 - 630mg/L). However, ammonia concentration in the treatment system effluent decreased over the following months such that NH_4^+ concentrations in the treatment system effluent was 2.97mg/L and around 1.0mg/L for subsequent sampling rounds. The high ammonia concentration did not have a major impact on the chemistry of Cannel Creek. Ammonia concentrations in Cannel Creek immediately following the treatment tank discharge point did not show an increase in concentration for the sample collection events after the initial first flush (Tables A1-A6).

Sulfide was less than the limit of detection (0.03mg/L) for most samples. Only in the effluent from the treatment system during the first flush was sulfide present at a significant concentration (0.06-0.22mg/L). There was a strong smell of hydrogen sulfide during this sampling round and the February 2018 sampling round. However, very little aqueous sulfide was observed in February 2018. Sulfate was highest in the James Mine AMD (Bell10) followed by the Bellvue Mine AMD (BellAd, Bell2 and Tanks). There was no significant decrease in the concentration of sulfate entering Cannel Creek from Bellvue Mine following the installation of the SRBR treatment system (Table A1-A6).

The concentration of DIC varied between <0.01 and 100mg/L for most samples. DIC concentrations were typically higher in the mine adit waters as compared to the main stream and decreased downstream. High concentrations of DIC were also measured in the SRBR tank effluent (Tanks, 417-346mg/L) and in the circum-neutral drainage containing BIOS floc (Bell8, 81.9-104mg/L). DOC concentrations ranged between 1.06 and 15.7mg/L and were typically higher at the control sites and Bell8.

Speciation of aqueous constituents

The speciation of dissolved trace elements was initially modelled for the unimpacted, circum-neutral sites (Bell1 and Bell13) using a pE of 12, as is typical for fully oxygenated waters, the sites in the main stem of Cannel Creek using a pE of 10, and the AMD discharges using a pE of 8 as they had a low dissolved oxygen concentration indicating reducing conditions. Under these conditions the main divalent trace elements, Mn, Zn, Ni, Cu, Pb and Cd were mainly present in the free ion form (>70%) and the most common complex was with sulfate. Significant proportions of Al were present as Al^{3+} in the low pH samples. Modelling also predicted that all the Fe at the sites with pH<4.5 was mostly present as Fe^{2+} (>85%) and only in the sites with pH >4.5 was Fe present as Fe(III) in the form of $Fe(OH)_2^+$. This doesn't appear to be correct, from our knowledge of Fe redox chemistry and so refinement of pE conditions was completed.

Modelling of dissolved trace element speciation using the redox pairs for which data was available (NH_4^+/NO_3^- and O^{2-}/O_2) to determine pE was completed. These models did not change the speciation of the main divalent trace elements; these elements still were mainly present in their free ion form, but it did change the speciation of Fe and

Al. In the model with the nitrogen redox pair determining the pE of the waters, the low pH sites contained a large proportion (50-80%) of Fe as Fe^{2+}, with a small proportion of Fe present as Fe^{3+}, and the most common complex being with sulfate. The sites with a pH >4.5 were predicted to have a small proportion of Fe present as Fe^{2+} (20-30%) with the large majority being present as $Fe(OH)_2^+$. Using the oxygen redox pair to determine solution pE resulted in the low pH solutions being modelled to have a small proportion of Fe present as Fe^{3+} (<20%), no solutions containing Fe^{2+}, and the main complexes shifting from $FeSO_4^+$ to $FeOH_2^+$ to $Fe(OH)_2^+$ as the pH increased. The higher pH (>4.5) solutions were predicted to consist of Fe mainly present as $Fe(OH)_2^+$ with small proportions (<5%) of $Fe(OH)_3^0$ being present. Al was predicted to be 30-65% Al^{3+} and the remaining Al as $AlSO_4^+$ at the low pH sites and 15-30% Al^{3+} and the remaining Al as $AlOH^{2+}$ and $Al(OH)_2^+$ and the higher pH sites.

Analysis of Fe^{2+} (Figure 5.10) and S^{2-} in subsequent sampling surveys allowed for the modelling of iron speciation using the Fe^{2+}/Fe^{3+} and S^{2-}/SO_4^{2-} redox pairs. A summary of the range of pE values calculated using the various redox pairs is given in Table 5.5. The Fe and N redox pairs gave the most sensible speciation for dissolved Fe. This is supported by findings of Nordstrom et al. (1979) that the Fe redox pair exerts the most influence on redox chemistry in AMD systems. The similar pE values calculated using the N redox pair is supported by the findings of Washington et al. (2004)

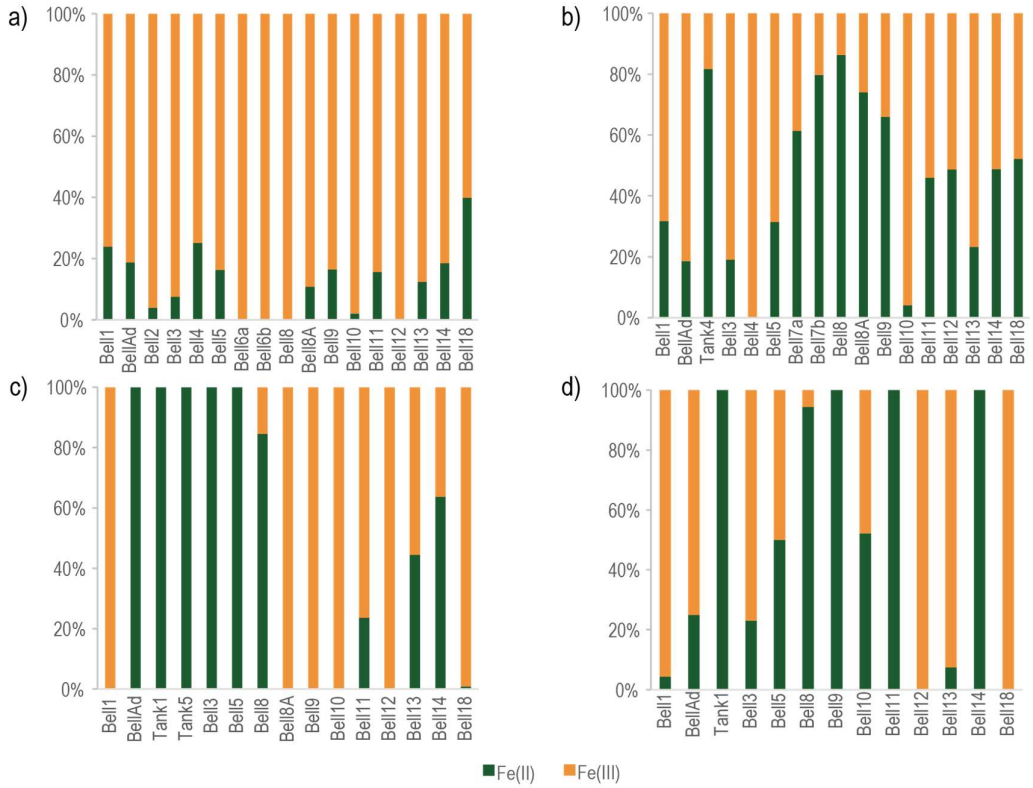

Figure 5.10 Measured speciation of Fe for May 2017(a), February 2018(b), April 2018(c) and June 2018(d). Fe(II) measurements were completed on site at the time of sampling. Fe(III) measurements were calculated by subtracting the Fe(II) concentration from the dissolved Fe concentration.

Table 5.5 The pE values as determined by the four different redox pairs for which both constituents was measured.

Date	pE (Fe^{2+}/Fe^{3+})	pE (NH_4^+/NO_3^-)	pE (O^{2-}/O_2)	pE (S^{2-}/SO_4^{2-})
Nov 2016		8.4-12.3	15.9-19.1	
May 2017	5.84-13.7	6.95-12.3	14.7-19.1	
Feb 2018	4.65-13.2	6.52-12.4	14.2-19.1	-3.06-2.65
Apr 2018	5.49-12.0	6.28-12.6	13.9-18.9	-3.19-2.58
Jun 2018	6.15-12.6	6.69-12.2	14.6-18.9	-3.05-2.51

The speciation of Zn and Ni in Cannel Creek was only affected by the installation of the SRBR treatment system at the two sites immediately downstream of the treatment system discharge point (Bell3 and Bell5). Bell9 was far enough downstream that the speciation of these elements did not change significantly following the installation of the treatment system. At sites Bell3 and Bell5, a decrease in Zn^{2+} was offset by an increase in $Zn(HS)_2^0$ while a decrease in Ni^{2+} was due to an increase in $NiCO_3^0$. However, this decrease in Zn^{2+} and Ni^{2+} did not occur immediately after the installation of the treatment system, it occurred over the following six months. The speciation of Fe was highly variable and no significant changes between pre-remediation and post-remediation data occured. As well as the dissolved concentration of Al decreasing, the proportion of Al as Al^{3+} also decreased in Cannel Creek following the installation of the SRBR treatment system. This was most notable at sites Bell3, Bell5 and Bell18. The decrease in the proportion of Al^{3+} was accompanied by increases in the proportion of Al as $AlOH^{2+}$ and $Al(OH)_2^+$.

Any decrease in the toxicity of Zn and Ni is caused by a decrease in the dissolved concentration of these elements entering Cannel Creek, not by complexation of these elements. A decrease in the dissolved concentration of Fe entering Cannel Creek may result in less Fe-rich minerals forming in Cannel Creek because Fe released from the treatment system as Fe^{2+} and can be transported a significant length downstream. This may also have the effect of providing less surfaces to which cationic trace elements can adsorb to and be attenuated. The decrease in dissolved Al and Al^{3+} decreases the toxicity of Al but there is likely to be an increase in Al-rich precipitates forming in Cannel Creek due to the hydrolysis and complexation of Al with the hydroxyl ion, OH^-.

5.3.2 Sediment chemistry

The sediment chemistry for sites where sufficient quantities of material could be collected from is shown in Table 5.6. Little Fe is present in the sediment upstream of the Bellvue AMD discharge point (Bell1), however concentrations of some trace elements are relatively high as compared to downstream of the AMD discharge point. Although the concentration of sediment-bound Fe in the adit mine pool (BellAd) and the cascade (Bell2) is low, the Fe concentration increases to >40% in Cannel Creek below the Bellvue AMD discharge point, indicative of pure Fe (oxy)hydroxide minerals. The sediment-bound Fe concentration of James Creek (Bell13) is moderate, although most elements had the highest concentration at this site.

Table 5.6 Sediment chemistry at sites along Cannel Creek prior to remediation (November 2016) as well as the low and high interim sediment quality guidelines (ISQG) (ANZECC 2000). Values which exceed the ISQG-low guidelines are denoted in bold and values which exceed the ISQG-high guidelines are denoted in red.

Site	Fe (%)	Al (%)	Cu (mg/kg)	Pb (mg/kg)	Zn (mg/kg)	As (mg/kg)	Ni (mg/kg)	Co (mg/kg)
Bell1	3.4	1.4	4.7	11.2	79.2	10.8	17.6	15.0
BellAd	23.6	0.7	3.6	5.5	17.5	**42.9**	3.5	1.4
Bell2	17.7	0.5	10.3	9.5	16.7	**49.5**	3.2	1.5
Bell3	40.0	0.1	13.5	6.1	11.4	**38.0**	1.1	0.5
Bell8A	44.6	0.2	1.1	0.9	5.3	4.6	2.6	1.1
Bell9	22.6	0.7	16.8	8.0	29.7	**32.5**	6.7	2.2
Bell10	46.9	0.1	5.7	1.3	30.5	**23.8**	1.9	1.1
Bell12	42.8	0.3	2.0	2.0	3.2	**4.6**	0.9	0.4
Bell13	24.9	2.6	25.7	**55.1**	**245.7**	**76.9**	**50.1**	30.9
ISQG-high			270	220	410	70	52	
ISQG-low			60	50	200	20	21	

During the sequential chemical extraction process, the majority of Fe, Cu and As was extracted from the "Fe-oxides" fraction (Figure 5.11a, e and f). Less than 10% of As was extracted from non-Fe-oxide-bound fractions. In general, the proportion of Al, Zn and Ni extracted from the "residual and sulfides" fraction decreased downstream as the proportion of these elements extracted from the "Fe-oxides" and "exchangeable" fractions increased (Figure 5.11b, c and d). At Bell2 and Bell10, the Bellvue and James Mine adits, moderate amounts of Al were extracted from the "exchangeable" fraction. Significant amounts of Zn and Ni were also extracted in the "exchangeable" fraction (up to 45% Zn and up to 90%Ni), particularly at the low pH sites (Bell 2, Bell8A and Bell10). The proportion of Cu extracted from the "Organic matter" fraction increased with distance downstream of the Bellvue Mine adit. (Figure 5.11e)

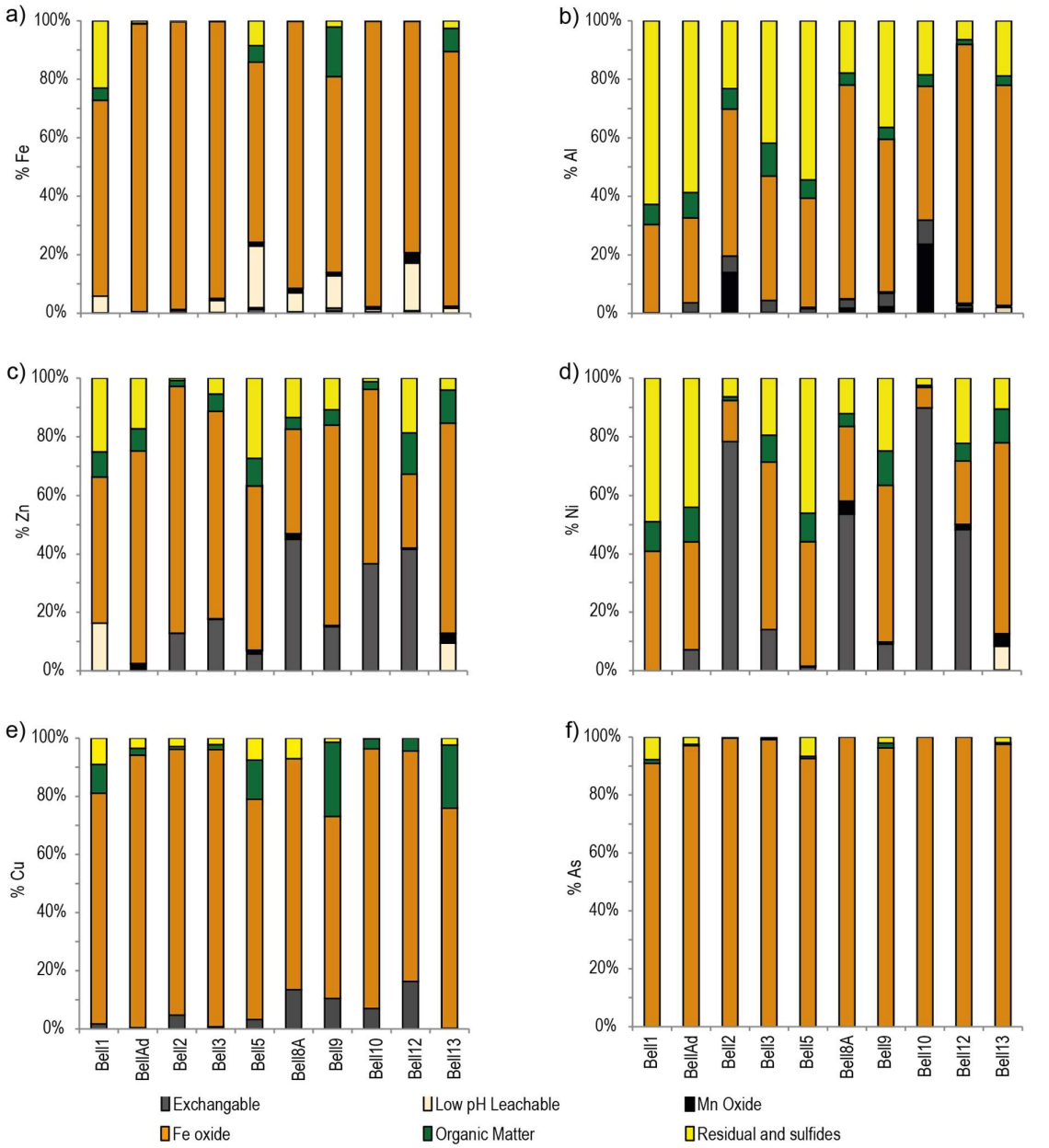

Figure 5.11 Speciation of sediment-bound trace elements a) Fe, b) Al, c) Zn, d) Ni, e) As and f) Pb, as determined by sequential extraction of trace elements from specific mineral phases.

Precipitation of mineral phases

Trace element-bearing mineral phases are summarised in Table 5.7. Prior to remediation, schwertmannite was predicted to be thermodynamically stable at all sites except for Bell4 and Bell12 in Nov 2016 and Bell6a in May 2017. Ferrihydrite [$Fe(OH)_3$] was predicted to be thermodynamically stable at sites with pH>4.5 under modelling conditions in Nov 2016 and at sites with pH>3.4 in May 2017. Al-oxides such as, basaluminite, boehmite and gibbsite were predicted to be stable at the sites with pH>4.5 in Nov 2016 and at sites with pH>3.4 in May 2017. Mineral phases containing other trace elements, besides Fe and Al, were undersaturated in all mine drainages and

in Cannel Creek prior to remediation. The sites where $Fe(OH)_3$ and Al-oxides were predicted to form were those with a higher pH namely the control sites, the circum-neutral tributary with BIOS and the lowest site on Cannel Creek. The saturation index of schwertmannite was positive at most sites, at several sites it was somewhat high (~20) indicating that kinetic or geochemical controls may be preventing precipitation. These sites where the saturation index of schwertmannite was high were also the sites for which ferrihydrite had a positive saturation index. The precipitation of ferrihydrite may prevent precipitation of schwertmannite if it is kinetically favoured.

Table 5.7 Sites where the saturation index of Al-, Fe- and Mn-oxides, sulfides and carbonates are predicted to have a positive saturation index.

	Nov 2016	May 2017	Feb 2018	Apr 2018	Jun 2018
Al					
Basuluminite	Where pH>4.5	Where pH>3.4	Where pH>4.5	Where pH>4.5	Where pH>4.5
Boehmite	Where pH>4.5	Where pH>3.4	Where pH>4.5	Where pH>4.5	Where pH>4.5
Gibbsite	Where pH>4.5	Where pH>3.4	Where pH>4.5	Where pH>4.5	Where pH>4.5
$Al(OH)_3$			All except control sites		
Ca					
Aragonite			Tanks	Tanks	Tanks
Calcite			Tanks	Tanks	Tanks
Fe					
Ferrihydrite	Where pH>4.5	Where pH>3.4	Where pH>4.0	Where pH>4.0	Where pH>4.5
Schwertmannite	All except Bell4 and Bell12	All except Bell6a	All sites	Where pH>4.5	At all sites with measurable Fe^{3+}
Mn					
Birnessite			Where pH>4.0 & When S^{2-} not present		
When S^{2-} included in model:					
Chalcopyrite			All sites with S^{2-} present	All sites with S^{2-} present	All sites with Fe^{2+} and S^{2-}
Galena			Where pH>4.35	Where pH>5.0	-
Greenokite			Where pH>4.0	Where pH>4.0	All sites with S^{2-} Cd and pH>3.0
Pyrite			All sites with S^{2-} present	All sites with S^{2-} present	All sites with Fe^{2+} and S^{2-}
Sphalerite			Where pH>4.0	Where pH>4.2	All sites with S^{2-} Zn and pH>4.0

Following the installation of the SRBR treatment system schwertmannite had positive saturation index at all sites. Gibbsite, basaluminite and boehmite had positive saturation index at sites with pH>4.5 while $Fe(OH)_3$ had a positive saturation index at sites with pH>4.0. Amorphous $Al(OH)_3$ had positive saturation index at the control sites (Bell1 and Bell13).

When S^{2-} was included in the model at the concentration less than the detection limit (0.02) several metal sulfides, such as chalcopyrite [$CuFeS_2$], galena [PbS], greenokite [CdS], pyrite [FeS_2] and sphalerite [ZnS] had positive

saturation indices at various sites including the control sites. Therefore, S^{2-} was only included in the model for the sites and sampling surveys where dissolved oxygen concentrations were low and when sulfide gas could be detected by olfactory observations. This resulted in sulfides of Fe, Zn, Cu, Pb and Cd being predicted to form in the SRBR tank effluent and therefore in the SRBR tanks themselves. When S^{2-} was excluded from the model at all other sites several Mn-oxides had positive saturation indices in the lower reaches of Cannel Creek and are therefore predicted to form in these lower reaches.

The increase in the pH of Cannel Creek stream water results in a pH>4.5 for most sites, except for Bell9-Bell12. This allows for the saturation index of $Fe(OH)_3$ and Al-oxides to be reached. Schwertmannite has a positive saturation index for any site where Fe(III) was present however, due to the reducing nature of the treatment system most of the Fe released from the treatment system was in the reduced form and did not have time to completely oxidise to Fe(III) in the time it takes to be transported to the confluence of Cannel Creek with Nine Mile Creek (Bell18; Figure 5.11).

Schwertmannite was predicted to precipitate at most sites with only a few exceptions prior to and following treatment of Bellvue Mine AMD. However ferrihydrite was predicted to precipitate at sites which had a pH>4.0 so for these sites ferrihydrite formation is likely to be preferred over schwertmannite formation because it forms first when pH is lower. Al-oxides such as basaluminite, boehmite and gibbsite were predicted to precipitate at sites which had a pH>4.5 at several sites in the main channel of Cannel Creek following treatment of Bellvue Mine AMD due to the pH increase.

Modelling of trace element adsorption to HFO

Prior to remediation the pH in Cannel Creek downstream of the Bellvue Mine AMD discharge point was low (2.6-5.1) and was below the pH where adsorption of cationic trace elements to HFO is favoured. Additionally, very little suspended particulate Fe (and therefore HFO) was measured in these low pH waters. Therefore, very little adsorption of these trace elements to HFO was possible (Figure 5.12). Although As could adsorb at low pH, the adsorption of cationic trace elements was only predicted to occur at sites Bell1, Bell8 and Bell13 and Bell18 when the pH was high enough to favour adsorption. Only the concentrations of dissolved Cu, Pb and As were predicted to decrease by a significant proportion because of adsorption at these sites. The concentration of dissolved Zn and Ni was not predicted to decrease significantly because of adsorption to HFO even at the higher pH sites.

Following the installation of the treatment system, variable amounts of Cu was predicted to adsorb at sites depending on the concentration of Cu, the amount of HFO available at the site and the pH of the site (Figure 5.13). Adsorption of Cu was most common at the control sites, the sites immediately downstream of the treatment system, in the treatment tank effluent and at the site furthest downstream. Adsorption of Zn and Ni to HFO was negligible in February 2018 but increased to 45% Zn and 18% Ni at Bell18 in June 2018 but between 1-10% for most other sites. Moderate quantities of particulate HFO present, especially at Bell11, Bell14 and Bell18 could lead to greater

quantities of trace elements adsorbing after the installation of the treatment system. However, the pH was not high enough at Bell11 and Bell14 for adsorption of Ni and Zn to be significant even when large quantities of HFO were present. The concentrations of Cd and Pb were below detection limits for the post-remediation sample collection events.

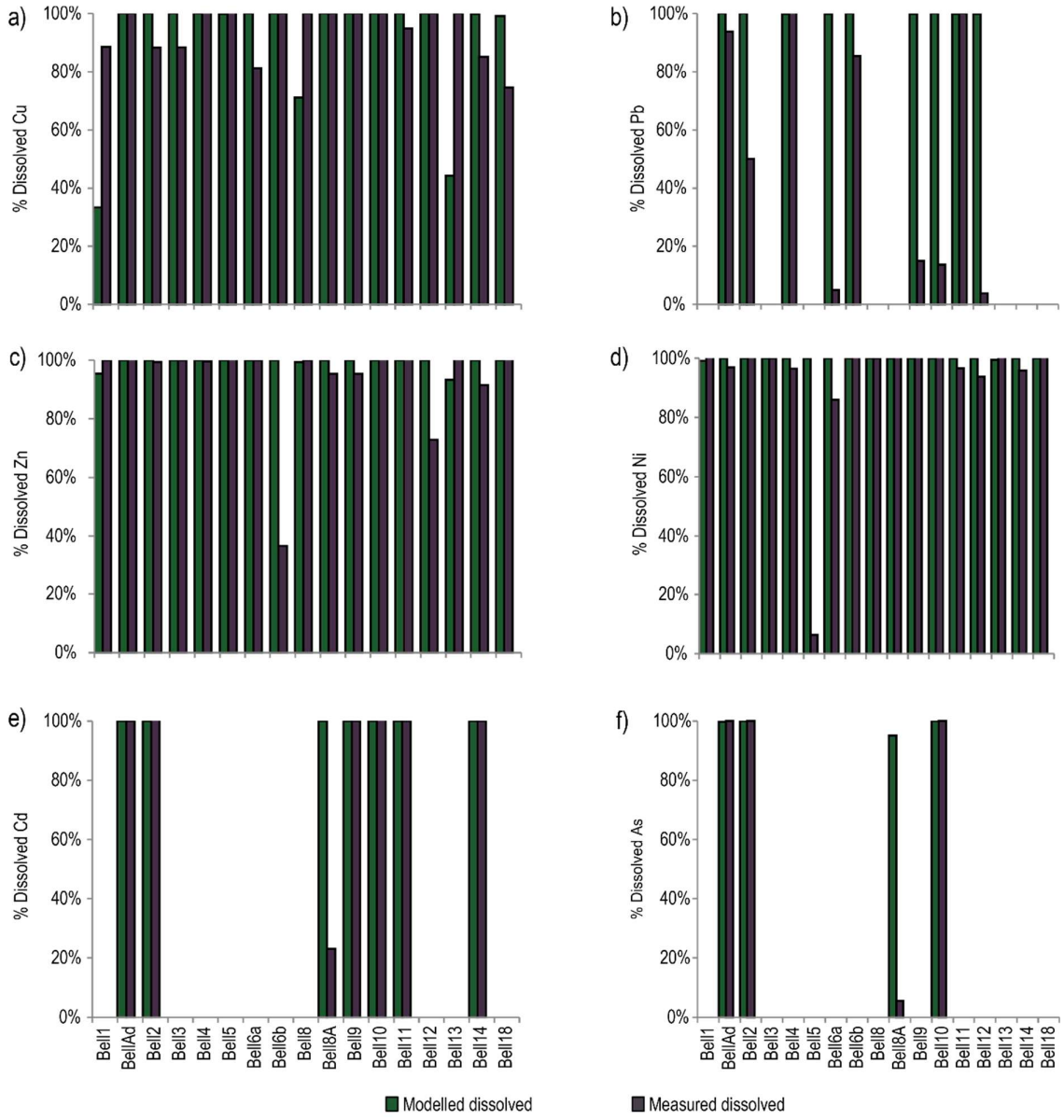

Figure 5.12 Adsorption of Cu (a), Pb (b), Zn (c), Ni (d), Cd (e) and As (f) to HFO for the pre-remediation stream conditions as measured in May 2017

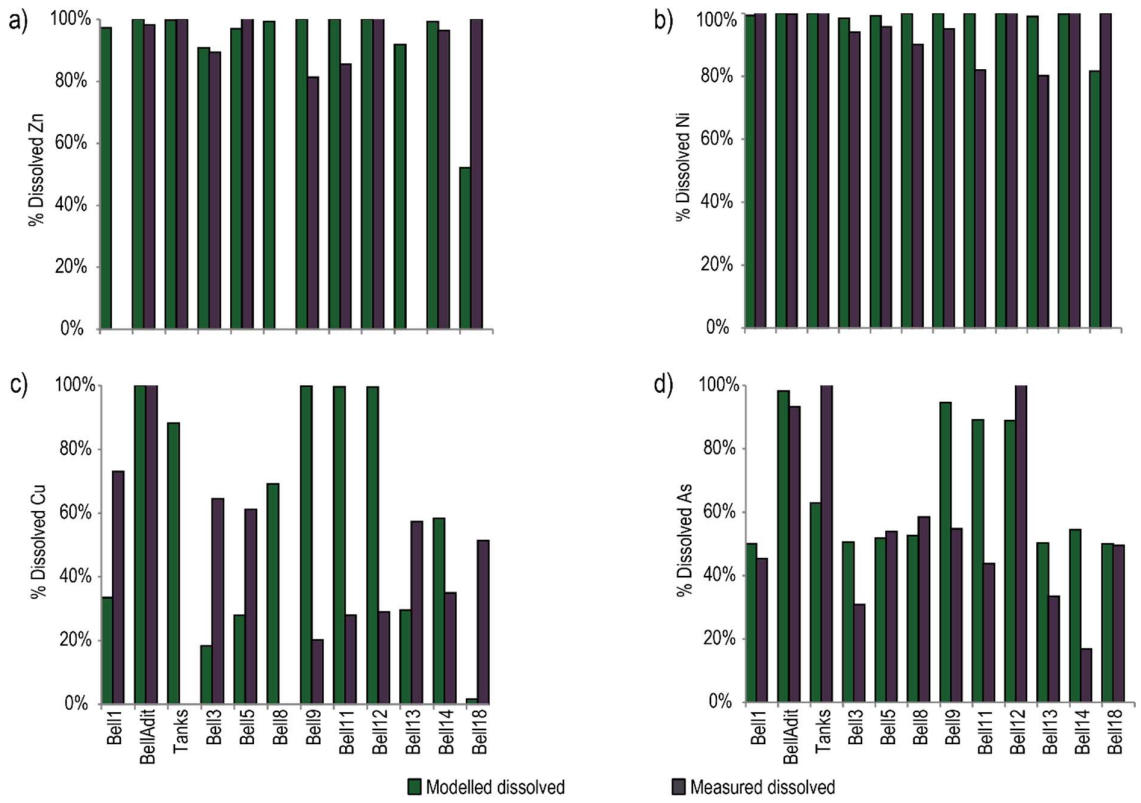

Figure 5.13 Adsorption of Zn (a), Ni (b), Cu (c) and As (d) to HFO for the post-remediation stream conditions as measured in June 2018

5.3.3 Assessment of simple mixing model

The simple mixing model developed by Trumm et al. (2016) to predict pH and concentrations of Fe and Al in Cannel Creek prior to and following the installation of the treatment system was based on the non-synchronous flow pattern of the mine AMD and Cannel Creek. It made predictions of water chemistry at six times within a typical 3 day rainfall event and six locations along Cannel Creek (upstream and downstream of the treatment system discharge point, upstream and downstream of the James Mine AMD discharge point and upstream and downstream of the confluence with James Creek). It also modelled the scenario where precipitation of Fe- and Al-bearing phases occurred up to the point of saturation of schwertmannite and gibbsite and where no precipitation of Fe- or Al-bearing phases occurred. This gave a maximum and minimum concentration range for Fe and Al concentrations.

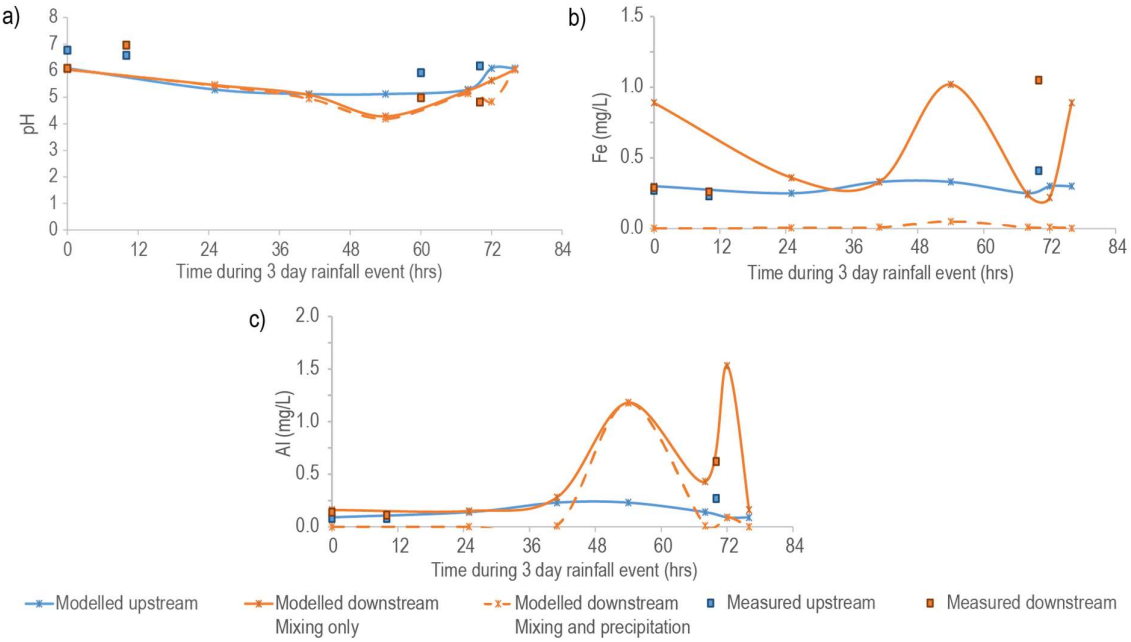

Figure 5.14 Measured pH (a), concentration of Fe (b) and concentration of Al (c) in Cannel Creek upstream and downstream of the treated Bellvue Mine AMD discharge point as compared to the modelled predictions for pH, Fe concentration and Al concentration of Trumm et al. (2016)

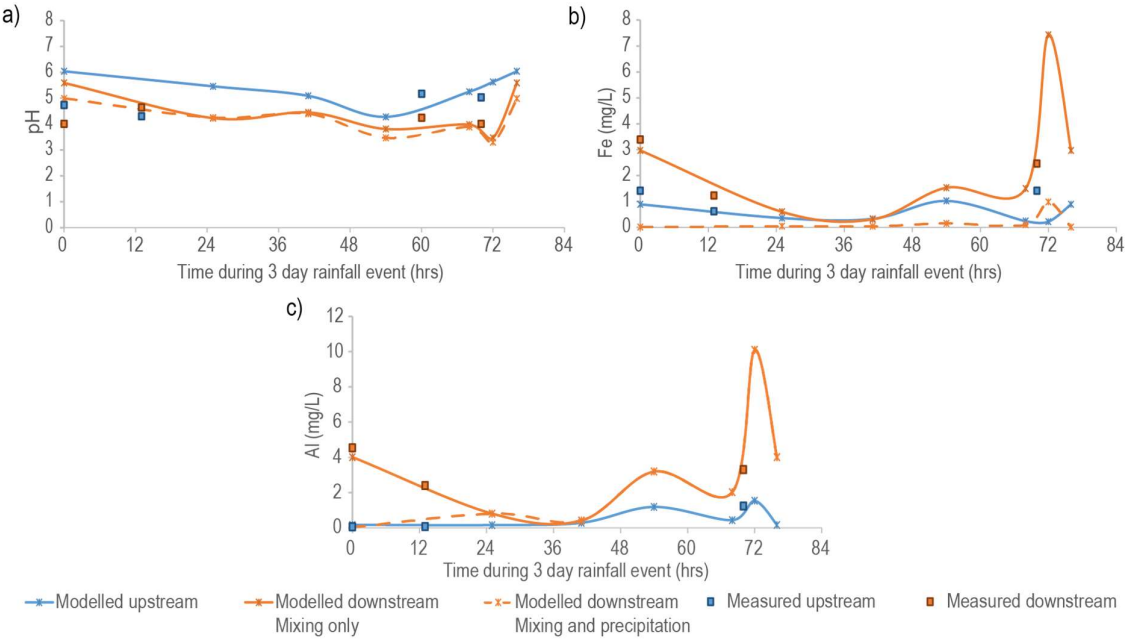

Figure 5.15 Measured pH (a), concentration of Fe (b) and concentration of Al (c) in Cannel Creek upstream and downstream of the James Mine AMD inflow point as compared to the modelled predictions for pH, Fe concentration and Al concentration of Trumm et al. (2016).

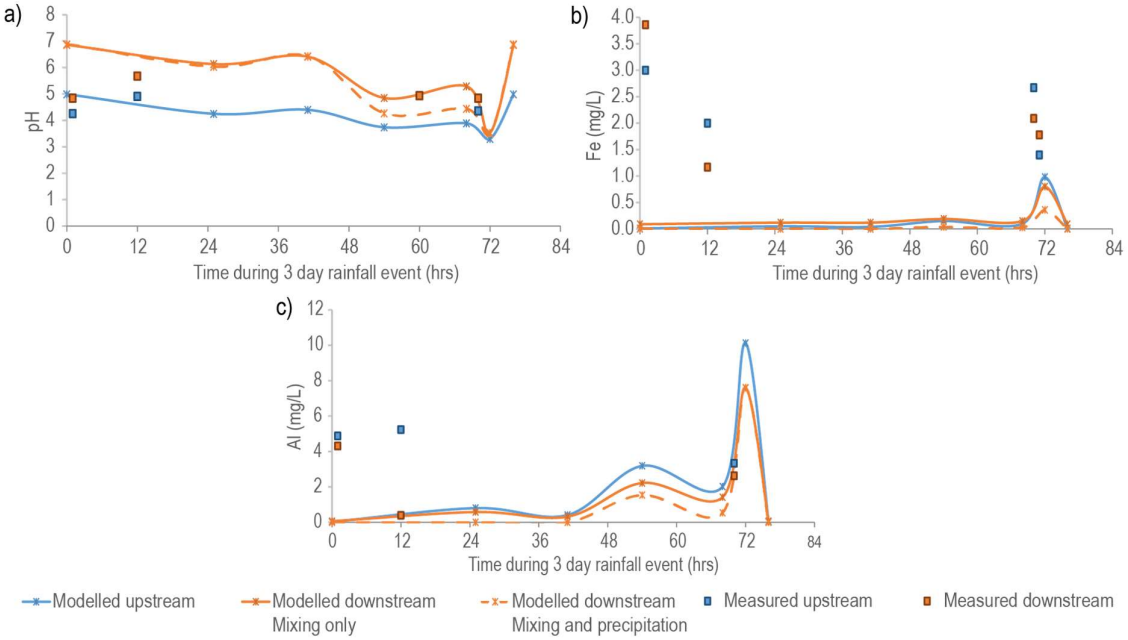

Figure 5.16 Measured pH (a), concentration of Fe (b) and concentration of Al (c) in Cannel Creek upstream and downstream of the confluence with James Creek as compared to the modelled predictions for pH, Fe concentration and Al concentration of Trumm et al. (2016).

For the upper-most site, Cannel Creek immediately downstream of the treated AMD discharge point (Bell3), the measured concentrations of Fe and Al were within the range predicted while pH was generally higher than predicted (Figure 5.14). At the middle site, Cannel Creek immediately downstream of the James Mine inflow point (Bell11), pH was variable but fairly close to the predicted value. Measured Fe and Al concentrations were close to the predicted scenario where no precipitation of Fe- and Al- bearing phases occurred (Figure 5.15). For the furthest downstream site, Cannel Creek downstream of the confluence with James Creek (Bell14), pH was lower than predicted for pre-rainfall and start-of-rainfall conditions but accurately predicted for end-of-rainfall conditions (Figure 5.16). However, Fe and Al concentrations were higher than predicted, particularly for the pre-rainfall and start of rainfall conditions. Al concentration was accurately predicted for end-pf-rainfall conditions.

5.4 Discussion

5.4.1 Water and sediment chemistry improvements

Following the installation of the SRBR treatment system, there has been a significant decrease (>90%) in the concentration of Fe and Al in Cannel Creek immediately downstream of where the Bellvue Mine AMD entered Cannel Creek (Bell3). The concentration of Zn and Ni at site Bell3 decreased initially following the installation of the SRBR treatment system but increased again in April 2018. This increase is thought to have been due to an algal growth in the tanks preventing proper functioning of the treatment system. After the algal growth was removed from the tanks proper functioning of the tanks recommenced and a reduction in Zn and Ni concentrations were

observed in subsequent months. Although the concentration of Al, Zn and Ni still exceeded ecologically relevant guidelines for water chemistry, the trend observed indicated that these guideline values would be met at some point within the near future (Figures .5.7-5.9)

However, the treatment system has an operating limit of 1L/s AMD able to pass through each of the tanks in order to properly treat the AMD. At high flow when this limit was exceeded the excess AMD bypassed these tanks and entered Cannel Creek untreated. It was predicted that the concentration of trace elements in Cannel Creek will therefore spike during high rainfall events. The data collected in this research was non-continuous data and was manually collected during times of low to moderate flow. Therefore, data on the periods of very high flow where significant volumes of AMD would bypass the treatment system are not included in the post-remediation data set. However, such high flows are only expected to occur 9% of the time.

Slightly less sediment-bound Fe but similar amounts of sediment-bound As was present in the sediment of the Bellvue Mine adit as compared to Webster and Brown (2001) and Noble (2003). Similar concentrations of sediment-bound Fe to Noble (2003) were found in Cannel Creek downstream of the Bellvue Mine AMD discharge point. The concentration of sediment-bound As in Cannel Creek downstream of the discharge point was between that of Webster and Brown (2001) and Noble (2003) was found although these two studies found very different amounts of sediment-bound As at this site.

5.4.2 Arsenic

Upstream source of Arsenic

Low concentrations of dissolved As were found in this research as well as that of Webster and Brown (2001), however, highly variable concentrations of sediment-bound As were found by Noble (2003), Webster and Brown (2001) and in this research. This was particularly so in the mine pool of the Bellvue Mine adit and in Cannel Creek downstream of the Bellvue Mine AMD discharge point.

Webster and Brown (2001) found very high concentrations of sediment-bound As in Cannel Creek downstream of the Bellvue Mine AMD discharge point but as the concentration of dissolved As in the Bellvue Mine AMD as well as sediment-bound As in the Bellvue Mine adit was lower than in Cannel Creek, it was concluded that Bellvue Mine was not the source of As in Cannel Creek. However, Noble (2003) found very low concentrations of As in the sediment of Cannel Creek immediately downstream of the Bellvue Mine AMD discharge point, lower than those observed in the Bellvue Mine adit. In this research, similar concentrations of As were found in the Bellvue Mine adit to that of previous research and an intermediate concentration of sediment-bound As was found in Cannel Creek immediately downstream of the Bellvue Mine AMD discharge point. As this downstream concentration was higher than at the site upstream of the Bellvue Mine AMD discharge point, this would indicate that the Bellvue Mine

was the source of As to Cannel Creek and that the very low quantities of dissolved As in the AMD are quickly scavenged by freshly formed Fe-rich precipitates and deposited on the streambed of Cannel Creek.

Arsenic in the SRBR Treatment system

A large flux of dissolved As in the SRBR treatment tank effluent first flush was observed in this research (Table A3). This was concerning at first as the dissolved concentration of As had previously been very low (at or below detection limits). However, the high concentration of dissolved As in the treatment system effluent did not continue and was not observed in any subsequent sampling surveys.

A possible explanation for this flux of As is that Fe-rich precipitates were formed on encountering the mussel shells in the SRBR treatment tanks and adsorption of As onto the freshly formed Fe-rich precipitates occurred. Then reductive dissolution of the freshly formed Fe-rich precipitates followed once the SRB began to colonise the tanks. This resulted in the re-release of adsorbed As into the solution. Due to the availability of Fe(III) under reducing conditions in the presence of SRB this was reduced to Fe(II) and attenuated through the formation of FeS or FeS_2, without any accompanying attenuation of As, ie as FeAsS. An autopsy of the precipitates formed in the SRBR treatment tanks is required to confirm whether FeAsS formed in the treatment tanks or not.

If this explanation is the case, then the reduced solution emanating from the treatment system to Cannel Creek may have resulted in the reductive dissolution of Fe-rich precipitates from the bed of Cannel Creek and thus the release of adsorbed trace elements, such as As, Zn, Ni, Cu and Pb, to Cannel Creek.

Sediment-bound Arsenic in James Creek

The very high sediment-bound As concentration in James Creek indicates that the source of As may not be mine related. The sequential extraction process found that this As was associated with Fe-rich precipitates which would indicate that it has adsorbed to a secondary mineral as opposed to being residual FeAsS associated with geologic formations in the area. The dissolution of coal associated-FeAsS and the subsequent formation of Fe-rich precipitates and adsorption of As to Fe-rich precipitates may still have been a natural attenuation process given the abundance of coal in the area, either naturally exposed through geologic processes or during excavation works to form roads and railways to service the James and Bellvue Mines. It was beyond the scope of this project to determine whether the adsorption of As to Fe-rich precipitates in James Creek was a historic process or was still occurring at this time this research was undertaken.

5.4.3 The reliability of the models used pre-remediation

Speciation of trace elements

PHREEQC was useful in being able to calculate the pE of the stream waters based on the different redox pairs available. However, the change in speciation and saturation indices of trace element-bearing sulfides due to the inclusion of measured concentrations of S^{2-} gave concerning results about toxic sulfides in Cannel Creek. Either

the detection limit of sulfide analysis was too high or the method was not accurate enough so even the inclusion of values that were below the detection limit resulted in the prediction of complexes and metal sulfides at sites where these were not thought to be present, such as the control sites and those too far downstream of the treatment system for sulfide minerals to be forming.

Assessment of the model predicting post-remediation water chemistry

It was predicted by PHREEQC that ferrihydrite and/or schwertmannite would precipitate in Cannel Creek, and particulate matter with the characteristic orange-rust colour was observed in the samples. The model that did not take into account the formation of Fe-oxide (or Al-oxide) precipitates was a more accurate prediction of water chemistry that the model which did include the formation of Fe-oxide (and Al-oxide) precipitates. Particulate-Fe concentrations were greatest in the effluent of the treatment tanks and at the sites furthest downstream, but no statistically significant difference between pre-remediation and post-remediation particulate-Fe concentrations was observed. The concentration of dissolved Fe did not decrease between the sites Bell11 and Bell12 either by a significant amount, or by the amount predicted by modelling the precipitation of ferrihydrite and schwertmannite.

5.5 Conclusion

In this research it was found that:

- The installation of the SRBR treatment system at Bellvue Mine caused an increase to the pH of Cannel Creek downstream of Bellvue Mine and a decrease in dissolved Fe, Al, Zn and Ni entering Cannel Creek from the Bellvue Mine adit. The pH in Cannel Creek immediately downstream of the Bellvue Mine AMD discharge point increased by 2.4 pH units. After remediation the concentration of dissolved Fe, Al and Ni entering Cannel Creek from Bellvue Mine was 80% lower than the average pre-remediation concentration at the site immediately downstream of the Bellvue Mine AMD discharge point. The concentration of dissolved Zn in Cannel Creek was 66% lower than before remediation.

- The speciation of trace elements was only affected by the installation of the SRBR treatment system at the two sites in Cannel Creek immediately downstream of the treatment system discharge point but above the waste coal piles. At these sites Fe speciation was variable and no overall trends in speciation occurred. Significant proportions of Fe^{2+} were expected to enter Cannel Creek from both the untreated and treated Bellvue Mine AMD. The concentration and proportions of Zn^{2+}, Ni^{2+} and Al^{3+} decreased with corresponding increases in the proportions of $Zn(HS)_2^0$, $NiCO_3^0$, $AlOH^{2+}$ and $Al(OH)_2^+$ The change in speciation of Fe, Al, Zn and Ni is not expected to significantly alter the toxicity of these elements or enhance their capacity to attenuate other trace elements.

- Characterisation of the sediment chemistry of sites along Cannel Creek indicate that downstream of the Bellvue Mine AMD discharge point the stream bed chemistry consisted of ~40% Fe with low concentrations of Al, Cu, Pb, Zn and Ni but higher concentrations of As, exceeding sediment quality

guidelines. Sediment-bound Cu, Pb, Zn, Ni and As was highest at Bell13 which is unimpacted by mining. Trace elements at this site were found to be associated with Fe-oxides while, at the main channel sites, moderate amounts of Zn and Ni were found to be associated with the sediment and were released into deionised water. Moderate amounts of Al, Zn and Ni were also found to be associated with residual and sulfide phases.

- The saturation indices of trace element-bearing minerals indicated that schwertmannite would precipitate at most sites both prior to and following treatment of Bellvue Mine AMD. Ferrihydrite was predicted to precipitate at sites which had a pH>4.0 so for these sites ferrihydrite formation is likely to occur before schwertmannite formation. Al-oxides such as basaluminite, boehmite and gibbsite were predicted to precipitate at sites which had a pH>4.5. Therefore Al-oxide precipitation was predicted to occur at several sites in the main channel of Cannel Creek following treatment of Bellvue Mine AMD due to the pH increase.

- Modelling of the adsorption of trace elements to particulate Fe-oxides (hydrous ferric oxide, HFO) showed that very little adsorption was predicted to occur prior to remediation due to the low pH of the stream water. However, following remediation, the pH of Cannel Creek increased sufficiently such that adsorption of Cu and Pb were favoured and due to the formation of large amounts of particulate Fe-oxide in the lower sections of Cannel Creek, up to 45% dissolved Zn and 18% dissolved Ni were predicted to be attenuated by adsorption to HFO.

- Measured post-remediation water chemistry was compared to a model developed by Trumm et al. (2016) which predicted water chemistry in Cannel Creek following remediation. It was found that the simple mixing model, which did not allow for precipitation of Fe-oxides or Al-oxides, accurately predicted concentrations of dissolved Fe and Al in the sections of Cannel Creek upstream of the confluence with James Creek. The modelled water chemistry deviated from the measured water chemistry around the confluence of Cannel Creek with James Creek because the model used the upstream predictions of water chemistry which took precipitation of Fe- and Al-oxides into account to predict downstream water chemistry.

- PHREEQC was useful in being able to predict the changes in water chemistry that would occur in Cannel Creek following the installation of the SRBR bioreactor but only when the precipitation of Fe- and Al-oxides were not taken into account. Because PHREEQC models solutions at equilibrium Fe- and Al-oxides are modelled to precipitate. However, because the stream is fast flowing, precipitation of these mineral phases occurs as they are being transported downstream. Therefore, the decrease in trace elements due to precipitation and adsorption predicted at a certain site in fact occurs over a length of the stream.

CHAPTER 6

SYNTHESIS AND CONCLUSIONS

Figure 6 An AMD seep which enters Cannel Creek downstream of the coal fields but upstream of James Mine; sampling site Bell8A.

This chapter brings together the findings from the previous chapters and identifies the situations which can be reliably modelled with the geochemical modelling program, PHREEQC, and the situations which cannot, at present, be reliably modelled with PHREEQC.

6.1 Introduction

In this thesis, the state of water and sediment chemistry in the streams draining three mine sites at various stages within the remediation process were investigated and the trace element attenuation processes occurring in the streams were modelled in PHREEQC. For the sites where remedial works had been carried out, the enhanced trace element attenuation processes expected to occur through the techniques employed in the remedial works were modelled with PHREEQC and the results assessed against measured data. For Tui Mine, the attenuation of trace elements through the addition of limestone was modelled for Tui Mine. For Puhipuhi Mine, the presence of trace elements, their sources and fate was assessed. For Bellvue Mine, the attenuation of trace elements through the formation of sulfides in the SRBR treatment tanks and formation of ferrihydrite and schwertmannite in Cannel Creek downstream of the treated AMD discharge point were modelled and a pre-remediation model assessed.

The evaluation of the PHREEQC model through a comparison between the predicted water quality results and those measured in the streams shows the conditions under which PHREEQC modelling is reliable and can be used successfully to optimise mine site remediation. It also shows the situations where PHREEQC cannot reliably predict water chemistry outcomes for a particular attenuation process, with the current technology and geochemical knowledge. In these situations, using PHREEQC to model a remediation project and the related trace element attenuation processes could be misleading.

6.2 Situations reliably modelled by PHREEQC

6.2.1 Dissolved speciation of cationic trace elements

The speciation of dissolved cationic trace elements was reliably modelled for Cu, Pb, Zn and Cd at Tui Mine (Figure 3.3), for Cu, Zn and Ni at Puhipuhi Mine (Figure 4.5) and for Mn, Cu, Pb, Zn, Cd and Ni at Bellvue Mine. The reliability of dissolved speciation modelling at Tui Mine was supported by the relationship between the free ion concentration and macroinvertebrate taxa richness (Figure 3.4). There is no reason to believe that the speciation of dissolved trace elements at Puhipuhi Mine was not reliable because where sites had a pH≤7, the majority of Cu, Zn and Ni was predicted to be present in the free ion form as expected (Figure 4.5). The presence of these trace elements as free ions, the form most toxic to aquatic species is matched the low abundance of macroinvertebrates, and particularly those of the sensitive EPT taxa.

At Bellvue Mine Mn, Cu, Zn and Ni were predicted to be mainly present in the free ion form, except for those sites with a pH>7 where large proportions of Cu present as $Cu(OH)_2^0$ and $CuCO_3^0$ and Ni present as $NiCO_3^0$. However, the sites which were closest to the mine adits and therefore had the lowest pH had the lowest proportion of Mn present as Mn^{2+} and Zn present as Zn^{2+} because these sites had high concentrations of SO_4^{2-} and high proportions of $MnSO_4^0$ and $ZnSO_4^0$. These proportions did not change significantly for these trace elements with changing redox conditions.

Zn^{2+} and Ni^{2+} concentrations in Cannel Creek at Bellvue Mine are significantly greater than the ANZECC (2000) guidelines for the protection of 95% of aquatic species (as applied to moderately disturbed systems) and the protection of 90% of aquatic species (as applied to severely disturbed systems). This is consistent with the depauperate macroinvertebrate community reported in Cannel Creek (Hogsden and Harding 2012). It can be assumed, therefore, that dissolved speciation modelling and determination of the concentration of free metal ions can be a reliable indicator of toxicity of Cu, Pb, Zn, Cd and Ni in the AMD environments of the type studied.

6.2.2 Formation of mineral precipitates

Fe (oxy)hydroxides and Mn oxides at Tui Mine, Fe (oxy)hydroxides at Puhipuhi Mine and Fe (oxy)hydroxides, Fe (oxy)hydroxysulfates, Al (oxy)hydroxides and Al(oxy)hydroxysulfates at Bellvue Mine were predicted to form in the mine drainage where saturation indices for these minerals were exceeded. The formation of these mineral precipitates was confirmed by both SEM-EDS and sequential extraction of the sediments collected from the respective sites. Additionally, SEM-EDS and the predictions of PHREEQC were able to show that carbonate minerals were not forming *in situ* in Tui Mine drainage even though the results of the sequential extraction had indicated that significant quantities of Cu, Pb Zn and Cd were extracted into the sequential extraction step that targets "carbonate" minerals. This fraction is more likely to represent metals leaching from oxide surfaces under low pH conditions. No trace element-bearing mineral phases were predicted to form *in situ* in the mine drainages. As such, residual minerals, such as the ZnS particle observed under SEM-EDS analysis of sediment collected from Tui Mine drainage, are predicted to dissolve under the current conditions.

6.2.3 Adsorption of Cu, Zn, Cd and Ni to HFO

The amount of Cu, Zn, Cd and Ni predicted by PHREEQC to adsorb to HFO was compared to the amount of Cu, Zn, Cd and Ni measured to be in the suspended particulate matter fraction (the fraction removed from solution by filtration; Figure 6.1). It was assumed that freshly-formed Fe-rich precipitates that were suspended in solution presented the largest surface area for cation (Cu, Zn, Cd and Ni) adsorption, and had the characteristics of HFO as determined by Dzomback and Morel (1990).

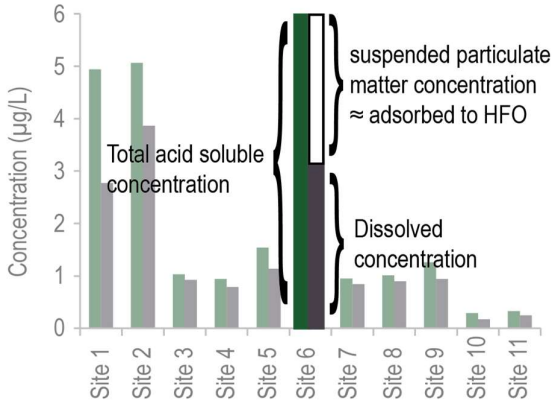

Figure 6.1 The relationship between the total acid soluble concentration, the dissolved concentration and the suspended particulate matter (assumed to be adsorbed to HFO) concentration.

At Tui Mine the adsorption of Cu, Zn, Cd and Ni to HFO was reliably predicted by PHREEQC. The percentage of these elements modelled to be in the dissolved form was within 20% of the percentage measured to be dissolved in the stream waters (Figure 3.7).

At Puhipuhi Mine, the adsorption of Zn and Ni to HFO was reliably predicted by PHREEQC (Figure 4.10). A large disagreement between the predicted and measured adsorption of Zn (92% predicted cf. 13% measured) occurred at the Puhi7 site, which was a control site. A larger disagreement between the modelled and measured adsorption of Cu to HFO occurred for the Puhipuhi Mine samples than for the Tui Mine samples. Cu adsorption was slightly underestimated (though still within a 20% margin of error) at Tui Mine but adsorption of Cu was greatly overestimated at Puhipuhi Mine. Additional binding surfaces, such as organic matter, clays and older less reactive Fe (oxy)hydroxides, were considered. However, given the abundance of fresh Fe (oxy)hydroxides at these sites, adsorption to HFO must be the dominant factor influencing adsorption. When considering adsorption of Cu to HFO differences in the reliability of the PHREEQC model may be due to the lower pH values measured at Puhipuhi Mine, in contrast to Tui Mine. The Tui Mine sites had a pH>6.8 for the November 2015 sampling event whereas the Puhipuhi Mine sites had pH values in the range of 4.18-7.03 for the January 2016 sampling event (control sites excluded). This would mean that the Puhipuhi Mine sites were in the pH range corresponding to greatest change in Cu adsorption. For example, as shown in Figure 6.2 (apart from Tuna1 and Tui1, had much lower concentrations of total, dissolved and particulate Fe than the Puhipuhi Mine sites). The Tui Mine sites had a higher pH and were therefore at the higher adsorption end of the adsorption edge. Additionally, the concentration of available HFO binding sites would have been a large influence on Cu adsorption to HFO.

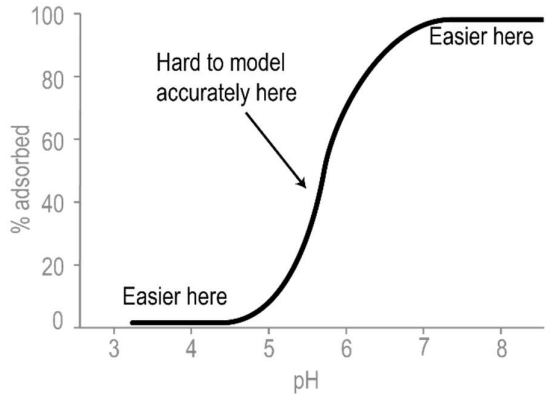

Figure 6.2 A typical adsorption edge for a cationic species on a negatively charged absorptive surface, showing a shallow gradient at low pH (0% adsorption) and at high pH (100% adsorption) but with a steep gradient at moderate pH. Modelling of adsorption may be less accurate when the solution is within the pH range that corresponding to greatest change on the adsorption edge.

At Bellvue Mine, Cu, Zn and Ni adsorption to HFO were reliably predicted by PHREEQC prior to remediation (Figure 5.12). However, there was again disagreement between the predicted and measured adsorption of Cu at circum-neutral pH sites prior to remediation. Most other low pH sites had only minor Cu adsorption. Following remediation, adsorption of Zn and Ni were still reliably predicted by PHREEQC, even though the pH was coincident with the adsorption edge. The adsorption of Cu was less reliably predicted.

These results show that precise measurements of pH and determination of particulate Fe concentrations are required to accurately predict adsorption of Cu to HFO, because the pH range of greatest change in the Cu adsorption edge is within a critical range for AMD-affected streams. This may not be practical for a natural system where fluctuating pH and Fe concentrations may occur both spatially and temporally. However, general agreement for other cationic trace elements shows that PHREEQC can still be a useful tool for predicting adsorption of these elements. This is also a consideration when predicting the conditions under which leaching of trace elements from streambed sediment may occur, as was investigated though the laboratory experiments using Tui Mine sediment in Section 3.2.5.

6.3 Situations not reliably modelled by PHREEQC

6.3.1 Dissolved speciation of Fe when the redox conditions are uncertain

The speciation of Fe was reliant on the redox conditions at the site. When modelling dissolved Fe speciation at Bellvue Mine, where a range of redox conditions were present, it was important that a representative ORP or reliable redox pair was used to set pE (or Eh) in PHREEQC. The remediation technique used at this mine involved a dramatic change in the redox conditions from those of the AMD emanating from the mine adit, to the SRBR system and to those in Cannel Creek water. Using a different redox pair to determine pE resulted in significantly different results when speciating dissolved Fe, and this would have follow-on consequences for how much HFO formed downstream or how much FeS_2 formed in the SRBR treatment tank. The most reliable redox pair for determining pE in AMD systems including at Bellvue Mine was the Fe^{2+}/Fe^{3+} pair as found by Nordstrom et al. (1979). The NH_4^+/NO_3^- redox pair also gives similar values of Eh as the Fe^{2+}/Fe^{3+} redox pair, as shown by Washington et al. (2004) and this study.

6.3.2 Speciation of dissolved Hg

The speciation of Hg is, important as although different forms of Hg can be toxic, Hg in the form of MeHg is toxic as well as bioaccumulative and therefore knowing how much of this species is present is important when determining the ecotoxicity of Hg in a system. At present, the PHREEQC model has limited ability to model the methylation of Hg to form methylmercury. In this research thermodynamic data from the MINTEQv4 database was inserted into the WATEQ4f in order to carry out Hg speciation modelling, but this did not include thermodynamic data for MeHg. Methylation of mercury is a bacterially-mediated process that occurs in the sediment under reducing conditions. Although Dong et al. (2010) compiled the reaction constants for Hg^{2+} and CH_3Hg^+ of Powell et al. (2005) and Smith et al. (2004) to speciate dissolved Hg, there is no reaction constant for the conversion of Hg^{2+} to CH_3Hg^+. Additionally, for this reaction to be modelled in PHREEQC, the concentrations of the constituent components must be known. Therefore, the concentration of dissolved methane present in the sediment porewater would be required in order for the methylation of mercury to be calculated by PHREEQC as a complexation reaction.

6.3.3 Adsorption of As to HFO

At Tui Mine and Puhipuhi Mine predictions of the adsorption of As adsorption to HFO were overestimated (Figure 3.7 and Figure 4.10). Modelling of As adsorption to HFO was not completed at Bellvue Mine, as dissolved As concentrations were below the detection limit. The disagreement between the modelled and measured percentage adsorption of As to HFO has been reported previously by Webster-Brown and Lane (2005) who found that the best way to accurately predict the percentage adsorption of geothermal As to HFO in the Waikato River, was to assume that only 5% of the HFO was available to adsorb As at any given site. A similar approach would likely model As adsorption in AMD environments, but site specific testing would be required to determine the percentage of HFO available to As for binding.

6.3.4 Adsorption of Pb to HFO

At Tui Mine predictions of the adsorption of Pb to HFO were underestimated (Figure 3.7). Modelling of Pb adsorption for Puhipuhi Mine and Bellvue Mine was not completed as the dissolved concentrations of Pb were close to or below the detection limit for these sites. The disagreement between the modelled and measured percentage adsorption of Pb to HFO may be due to the pH range of the sites being in the range of greatest change in the Pb adsorption edge (Figure 3.9) as was discussed for Cu in Section 6.2.

6.3.5 Where residual sulfides are present

The presence of residual primary sulfide minerals in the mine drainage may also influence water chemistry as these minerals dissolve. At Tui Mine small amounts of Fe, Mn, Zn and Cu were extracted from the sulfiide and residual fraction during the sequential extraction process (Figure 3.6). In addition to this, a ZnS particle was observed by SEM-EDS analysis of the sediment sample from Tuna1 (Figure 3.5). At Puhipuhi Mine moderate amounts of Zn and Cu and significant amounts of Ni were present in the sulfide and residual fraction of the sequential extraction process (Figure 4.9). Also, HgS dispersed through quartz particles were observed by SEM-EDS analysis of the sediment sample from Puhi3 (Figure 4.7.1 and Figure 4.7.2).At Bellvue Mine small amounts of Fe, As and Pb and moderate amounts of Al and Ni were extracted from the sulfide and residual fraction of the sequential extraction process (Figure 5.14). The presence of residual sulfides in the sediment was especially significant at Bell13, which was actually designated as a control site, but had the highest concentration of trace elements (Al, Cu, Pb, Zn, Ni and As; Table 5.3). The presence of residual sulfide minerals is not often considered when modelling post-mining water quality. These sulfides would have been transported downstream in the water column at an early stage, making up a component of the particulate-bound trace element concentration. As long as they are sulfide minerals they would not be contributing to poor ecological health as they are considered to be non-bioavailable.

However, they may be contributing, to poor water quality in the overlying water column (Section 3.3.2) by oxidising and dissolving, albeit at slow rates. Although the amounts of residual sulfides encountered in this study were a small component of the sediment, in other systems where active mining is occurring or mining has ceased more

recently, they may comprise a larger proportion of the sediment-bound trace elements and contribute to poor water quality. Because sulfide concentrations are below detection levels in oxygenated AMD streams, the sulfides will be predicted to dissolve using PHREEQC modelling, but the rate of this dissolution will not be clear using thermodynamic equilibrium modelling.

6.3.6 Attenuation of dissolved Fe by formation of Fe-rich precipitates

At all three sites investigated in this research, the formation of Fe-rich precipitates (ferrihydrite or schwertmannite), was predicted by PHREEQC and confirmed by visual assessment of the site, SEM-EDS analysis of sediment and the results of the sequential extraction process. However, the degree to which dissolved Fe is attenuated by the formation of Fe-rich oxide precipitates is not reliably predicted in PHREEQC and depending on the modelled results can lead to inaccurate predictions of water quality.

At Tui Mine, the concentration of dissolved Fe was predicted to decrease from 22.1µg/L to 1.03µg/L (Figure 3.9) when $Fe(OH)_3$ was allowed to precipitate if the saturation index exceeded 0.0. Similarly, at Bellvue Mine, the concentration of dissolved Fe in Cannel Creek was predicted to decrease from 2.97mg/L to 0.01mg/L, between downstream of the influx of James Mine AMD and upstream of the confluence of James Creek with Cannel Creek, as a result formation of schwertmannite (Figure 5.15) when the stream was under baseflow conditions. However, the measured concentrations of dissolved Fe did not show this decrease in concentration, remaining around 2.5mg/L. The assumption that this stretch of stream was precipitating and depositing ferrihydrite and schwertmannite would therefore lead to a much lower concentration of dissolved Fe being predicted at the site furthest downstream than was actually measured. This may have implications for the concentrations of dissolved Fe chosen for remediation targets. Additionally, consecutively filtering a sample through smaller filters (0.45µm, 0.22µm and 0.10µm) at Bellvue Mine did not result in a lower concentration of dissolved Fe. The majority of particulate Fe is therefore relatively coarse and removed from solution by filtering through a 0.45µm filter. Therefore, the difference between measured and modelled concentration is not due to colloidal Fe in the 0.1-0.45µm range.

6.3.7 Formation of Mn oxides and adsorption of trace elements to HMO

At Tui Mine, Mn and to a lesser extent Zn, Pb and Cd, were extracted from the “bound to Mn-oxides” fraction of the sequential extraction process (Figure 3.6). Additionally, a crust showing a strong association between Mn and Zn was observed on a particle analysed by SEM-EDS (Figure 3.5). However, particulate-bound Mn was not present in the water samples (Table 3.3.2) and Mn oxides were not predicted by the PHREEQC model to form until the solution was raised to a pH>8.5 (Figure 3.9). Christenson et al. (2019) showed that Mn oxides can form when Mn-oxidising bacteria is present and Davies and Morgan (1989) showed that Fe (oxy)hydroxides can act as a surface catalyst for Mn oxide formation. However, the inclusion of Mn oxides (hydrous manganese oxide or HMO) as a binding surface with the adsorption constants and surface characteristics described by Tonkin et al. (2004) did not improve the accuracy of trace element adsorption to particulate matter surfaces, due to the lack of particulate Mn

in the Tui Mine samples. So, while SEM-EDS results indicated that Mn oxides in the sediment may be a significant binding phase for Zn, Pb and Cd, the formation of Mn oxides could not be reliably predicted by PHREEQC. The adsorption of Cu, Pb, Zn and Cd onto Mn oxide surfaces was also poorly modelled with PHREEQC.

6.3.8 Systems with micro-organisms

In Section 1.1, it was noted that the oxidation of iron sulfide in natural waters can be bacterially mediated by microorganisms. In fact, microbially mediated oxidation of pyrite occurs at a much faster rate than abiotic oxidation. (Singer and Stumm 1970, Nordstrom and Alpers 1999). However, the impact of microorganisms on the rate of pyrite oxidation is not accounted for in the pyrite oxidation equations (Equations 1.1-1.4). In Sections 1.2.2 and 6.3.7, the potential for the precipitation of Fe (Bigham and Nordstrom 2000) and Mn (Christenson et al. 2019) metal oxides and (oxy)hydroxides in natural waters to be microbially mediated is discussed. Although formation of these precipitates may be kinetically inhibited, the micro-environments created by micro-organisms can lead to conditions favourable for the formation of mineral precipitates that are unable to form in the macro-environment (Nordstrom and Alpers 1999, Bigham and Nordstrom 2000).

In addition to oxidation reactions and precipitation of minerals in oxygenated systems, the reduction of iron and sulfur can also be bacterially mediated as occurs in sulfate reducing treatment systems discussed in Section 1.3.3 and Chapter 5, and in the methylation of mercury discussed in Sections 4.4 and 6.3.2. Again, the microbially-mediated component of these reactions is not included in the equations describing these reactions and is therefore not included in PHREEQC code or a geochemical model based on PHREEQC code.

Although micro-organisms are ubiquitous in natural AMD systems and play an important role in iron, sulfur and mercury cycling, the lack of inclusion of their influence on oxidation, reduction and precipitation reactions results in their exclusion from geochemical models based on codified reactions.

6.4 Recommendations for further research

It is recommended that further research be carried out to improve the ability of models based on the PHREEQC program to predict the extent to which sediment quality affects the water quality in AMD-affected streams.

- Research could include what mineralogical settings create downstream conditions where sediment quality is of high importance and must be considered when undertaking mine remediation projects. A section of this research could also look at how best to take residual sulfides into account when modelling evolution of post-mining or post-remediation water chemistry.

- Further work could also be done to better speciate dissolved Hg and determine a way to calculate the proportion of Hg present as MeHg because this portion of Hg is of highest environmental concern due to its ability to bioaccumulate in biota.

- Further work needs to be done to determine adsorption constants for the adsorption of As to HFO that can be used reliably when modelling natural stream waters.

- Further work could also be done using models based on the PHREEQC program to predict the formation of mineral precipitates in the SRBR treatment system, to better predict effluent quality.

References

Akcil, A. and Koldas, S. (2006). "Acid Mine Drainage (AMD): causes, treatment and case studies." Journal of Cleaner Production **14**(12): 1139-1145.

Alford, É. R., Pilon-Smits, E. A. and Paschke, M. W. (2010). "Metallophytes—a view from the rhizosphere." Plant and Soil **337**(1-2): 33-50.

ANZECC (2000). Australian and New Zealand Guidelines for Freshwater and Marine Water Quality, Australian and New Zealand Environment Conservation Council. Canberra.

ATSDR, U. (1999). "Toxicological profile for mercury." Atlanta: Agency for Toxic Substances and Disease Registry, US Department of Health and Human Services.

Bäckström, M. and Sartz, L. (2011). "Mixing of acid rock drainage with alkaline ash leachates—fate and immobilisation of trace elements." Water, Air, & Soil Pollution **222**(1-4): 377-389.

Bacon, J. R. and Davidson, C. M. (2008). "Is there a future for sequential chemical extraction?" Analyst **133**(1): 25-46.

Baker, A., Ernst, W., van der Ent, A., Malaisse, F. and Ginocchio, R. (2010). "Metallophytes: the unique biological resource, its ecology and conservational status in Europe, central Africa and Latin America." Ecology of industrial pollution: 7-40.

Balistrieri, L. S., Box, S. E. and Tonkin, J. W. (2003). "Modeling precipitation and sorption of elements during mixing of river water and porewater in the Coeur d'Alene River basin." Environmental Science and Technology **37**(20): 4694-4701.

Balistrieri, L. S., Seal Ii, R. R., Piatak, N. M. and Paul, B. (2007). "Assessing the concentration, speciation, and toxicity of dissolved metals during mixing of acid-mine drainage and ambient river water downstream of the Elizabeth Copper Mine, Vermont, USA." Applied Geochemistry **22**(5): 930-952.

Banks, D., Younger, P. L., Arnesen, R. T., Iversen, E. R. and Banks, S. B. (1997). "Mine-water chemistry: The good, the bad and the ugly." Environmental Geology **32**(3): 157-174.

Barker, S. L., Kim, J. P., Craw, D., Frew, R. D. and Hunter, K. A. (2004). "Processes affecting the chemical composition of Blue Lake, an alluvial gold-mine pit lake in New Zealand." Marine and Freshwater Research **55**(2): 201-211.

Barnden, A. R. and Harding, J. S. (2005). "Shredders and leaf breakdown in streams polluted by coal mining in the South Island, New Zealand."

Barry, J., Duff, S. and MacFarlan, D. (1994). "Coal resources of New Zealand, Resource information report 16." Energy and Resources Division, Ministry of Commerce, New Zealand.

Batley, G. E., Apte, S. C. and Stauber, J. L. (2004). "Speciation and bioavailability of trace metals in water: progress since 1982." Australian Journal of Chemistry **57**(10): 903-919.

Batty, L. C. (2003). "Wetland plants-More than just a pretty face?" Land Contamination and Reclamation **11**(2): 173-180.

Batty, L. C., Auladell, M., Sadler, J. and Hallberg, K. (2010). "The impacts of metalliferous drainage on aquatic communities in streams and rivers." Ecology of industrial pollution: 70-100.

Benjamin, M. M. and Leckie, J. O. (1981). "Multiple-site adsorption of Cd, Cu, Zn, and Pb on amorphous iron oxyhydroxide." Journal of Colloid And Interface Science **79**(1): 209-221.

Bigham, J. and Nordstrom, D. K. (2000). "Iron and aluminum hydroxysulfates from acid sulfate waters." Reviews in mineralogy and geochemistry **40**(1): 351-403.

Bigham, J., Schwertmann, U., Traina, S., Winland, R. and Wolf, M. (1996). "Schwertmannite and the chemical modeling of iron in acid sulfate waters." Geochimica et Cosmochimica Acta **60**(12): 2111-2121.

Black, A., Clemens, A. and Trumm, D. (2004a). An insight into the direction of environmental management in New Zealand's coal industry. AusIMM New Zealand Branch 37th Annual Conference**:** 15-22, AusIMM. Nelson, New Zealand.

Black, A., Craw, D., Youngson, J. H. and Karubaba, J. (2004b). "Natural recovery rates of a river system impacted by mine tailing discharge: Shag River, East Otago, New Zealand." Journal of Geochemical Exploration **84**(1): 21-34.

Blowes, D. W., Ptacek, C. J., Jambor, J. L. and Weisener, C. G. (2003). "The Geochemistry of Acid Mine Drainage". Treatise on Geochemistry. **9:** 149-204.

Bogue, S. B., Webster-Brown, J. G. and Brown, K. L. (2002). The Influence of Mining on Sediment Geochemistry of the Waitekauri Catchment, Waihi, New Zealand. AusIMM New Zealand Branch 35th Annual Conference, AusIMM. Auckland, New Zealand.

Boothroyd, I., Goldstone, A., Fitzpatrick, M. and MacGillivray (2005). "Criteria for the protection of aquatic ecological values at Golden Cross Mine: A case study". Metal Contaminants in New Zealand. T. A. Moore, A. Black, J. A. Centeno, J. S. Harding and D. Trumm**:** 359-374. Resolutionz Press, Christchurch, New Zealand.

Bowell, R. J., Alpers, C. N., Jamieson, H. E., Nordstrom, D. K. and Majzlan, J. (2014). "The environmental geochemistry of arsenic—an overview—." Reviews in Mineralogy and Geochemistry **79**(1): 1-16.

Brathwaite, R. and Christie, A. (1996). Geology of the Waihi Area. Institute of Geological & Nuclear Sciences Limited.

Bray, J. P., Broady, P. A., Niyogi, D. K. and Harding, J. S. (2009). "Periphyton communities in New Zealand streams impacted by acid mine drainage." Marine and Freshwater Research **59**(12): 1084-1091.

Brooks, R. R., Lee, J., Reeves, R. D. and Jaffré, T. (1977). "Detection of nickeliferous rocks by analysis of herbarium specimens of indicator plants." Journal of Geochemical Exploration **7**: 49-57.

Brown, J. G., Bassett, R. L. and Glynn, P. D. (1998). "Analysis and simulation of reactive transport of metal contaminants in ground water in Pinal Creek Basin, Arizona." Journal of Hydrology **209**(1-4): 225-250.

Brown, P. L. and Markich, S. J. (2000). "Evaluation of the free ion activity model of metal-organism interaction: extension of the conceptual model." Aquatic Toxicology **51**(2): 177-194.

Bryan, G., Langston, W., Hummerstone, L., Burt, G. and Ho, Y. (1983). "An assessment of the gastropod, Littorina littorea, as an indicator of heavy-metal contamination in United Kingdom estuaries." Journal of the Marine Biological Association of the United Kingdom **63**(2): 327-345.

Butcher, M. (2010). The Puhipuhi Mercury Mine, History and Site Description, Department of Conservation. Wellington.

Byrne, P., Wood, P. J. and Reid, I. (2012). "The impairment of river systems by metal mine contamination: a review including remediation options." Critical Reviews in Environmental Science and Technology **42**(19): 2017-2077.

Camargo, J. (1995). "Effect of body size on the intraspecific tolerance of aquatic insects to low pH: A laboratory study." Bulletin of environmental contamination and toxicology **54**(3): 403-408.

Campbell, P. G. C. (1995). "Interactions between trace metals and aquatic organisms: a critique of the free-ion activity model". Metal speciation and bioavailability in aquatic systems. A. Tessier and D. R. Turner**:** 45-102. John Wiley & Sons Ltd, New York, USA.

Canadian Council of Ministers for the Environment (2003). Canadian Water Quality Guidelines for the Protection of Aquatic Life. Inorganic mercury and methlymercury**:** 6, Canadian Council of Ministers for the Environment,. Winnipeg, Canada.

Carlson, L., Bigham, J. M., Schwertmann, U., Kyek, A. and Wagner, F. (2002). "Scavenging of As from acid mine drainage by schwertmannite and ferrihydrite: A comparison with synthetic analogues." Environmental Science and Technology **36**(8): 1712-1719.

Caspers, H., Mackereth, F. J. H., Heron, J. and Talling, J. F. (1979). Water Analysis: Some Revised Methods for Limnologists. Ambleside Freshwater Biological Association Scientific, Far Sawrey.

Cavanagh, J. E., Pope, J., Harding, J. S., Trumm, D., Craw, D., Simcock, R. and Ross, C. (2015a). New Zealand Minerals Sector Environmental Framework, A User's Guide**:** 145, Landcare Research, CRL Energy, University of Canterbury and University of Otago. Christchurch, New Zealand.

Cavanagh, J. E., Pope, J., Simcock, R., Harding, J. S., Trumm, D., Craw, D., Weber, P., Webster-brown, J., Eppink, F. and Simon, K. (2018a). Mine Environment Life-cycle Guide: Epithermal gold mines**:** 173. New Zealand.

Cavanagh, J. E., Pope, J., Simcock, R., Harding, J. S., Trumm, D., Craw, D., Weber, P., Webster-Brown, J., Eppink, F. and Simon, K. (2018b). Mine Environment Life-cycle Guide: Mesothermal (orogenic) gold mines**:** 169. Christchurch, New Zealand.

Cavanagh, J. E., Pope, J., Simcock, R., Harding, J. S., Trumm, D., Craw, D., Weber, P., Webster-brown, J., Eppink, F. and Simon, K. (2018c). Mine Environment Life-cycle Guide: Potentially acid-forming and non-acid-forming coal mines**:** 174. Christchurch, New Zealand.

Cavanagh, J. E., Pope, L., Harding, J. S., Trumm, D., Craw, D., Simcock, R., Webster-Brown, J., Weber, P., Simon, K. and Eppink, F. (2015b). Onshore NZ Minerals Sector Environmental Research – Mine Environment Life Cycle Guide. 2015 AusIMM New Zealand Branch Annual Conference, AusIMM. Dunedin, NZ.

CCME (1999). Canadian Environmental Quality Guidelines. C. C. o. M. f. t. Environment, Canadian Council of Ministers for the Environment. Canada.

Chakoumakos, C., Russo, R. C. and Thurston, R. V. (1979). "Toxicity of copper to cutthroat trout (Salmo clarki) under different conditions of alkalinity, pH, and hardness." Environmental Science & Technology **13**(2): 213-219.

Christenson, H., Pope, J., Craw, D., Johns, J. and Newman, N. (2017). Characterisation of arsenic geochemistry in mine tailings from a mesothermal Au deposit. 2017 AusIMM New Zealand Branch Conference, AusIMM. Christchurch, New Zealand.

Christenson, H., Pope, J., Trumm, D., Newman, N., Blanco, I., Kerr, G., Young, M. and Uster, B. (2019). "Manganese and trace element removal from New Zealand coal mine drainage using limestone leaching beds." New Zealand Journal of Geology and Geophysics: 1-12.

Christie, A. B. and Brathwaite, R. L. (2003). "Hydrothermal alteration in metasedimentary rock-hosted orogenic gold deposits, Reefton goldfield, South Island, New Zealand." Mineralium deposita **38**(1): 87-107.

Christie, T. and Brathwaite, B. (1995). "Mineral commodity report 8—Mercury." New Zealand Mining **17**: 34-39.

Ciszewski, D., Kubsik, U. and Aleksander-Kwaterczak, U. (2012). "Long-term dispersal of heavy metals in a catchment affected by historic lead and zinc mining." Journal of Soils and Sediments **12**(9): 1445-1462.

Clements, W. H., Vieira, N. K. and Church, S. E. (2010). "Quantifying restoration success and recovery in a metal-polluted stream: a 17-year assessment of physicochemical and biological responses." Journal of Applied Ecology **47**(4): 899-910.

Coffey, B. (2009). Tui Mine Remedial Works - Instream Ecological Baseline Monitoring**:** 23. Whangamata, New Zealand.

Comber, S., Merrington, G., Sturdy, L., Delbeke, K. and Van Assche, F. (2008). "Copper and zinc water quality standards under the EU Water Framework Directive: The use of a tiered approach to estimate the levels of failure." Science of the Total Environment **403**(1-3): 12-22.

Cooke, J. A. and Johnson, M. S. (2002). "Ecological restoration of land with particular reference to the mining of metals and industrial minerals: A review of theory and practice." Environmental Reviews **10**(1): 41-71.

Cravotta, C. A., Brightbill, R. A. and Langland, M. J. (2010). "Abandoned mine drainage in the Swatara Creek Basin, Southern Anthracite Coalfield, Pennsylvania, USA: 1. Stream water quality trends coinciding with the return of fish." Mine Water and the Environment **29**(3): 176-199.

Cravotta, C. A. and Trahan, M. K. (1999). "Limestone drains to increase pH and remove dissolved metals from acidic mine drainage." Applied geochemistry **14**(5): 581-606.

Craw, D. (2005). "Potential anthropogenic mobilisation of mercury and arsenic from soils on mineralised rocks, Northland, New Zealand." Journal of environmental management **74**(3): 283-292.

Craw, D., Brown, K. and Webster-Brown, J. (2005). "Metals derived from gold mining and geothermal sources". Metal Contaminants in New Zealand. Resolutionz Press, Christchurch. T. A. Moore, A. Black, J. A. Centeno, J. S. Harding and D. Trumm**:** 231-246. Resolutionz Press, Christchurch, New Zealand.

Craw, D., Chappell, D. and Black, A. (2002). "Surface run-off from mineralised road aggregate, Puhipuhi, Northland, New Zealand." New Zealand Journal of Marine and Freshwater Research **36**(1): 105-116.

Craw, D., Chappell, D. and Reay, A. (2000a). "Environmental mercury and arsenic sources in fossil hydrothermal systems, Northland, New Zealand." Environmental Geology **39**(8): 875-887.

Craw, D., Chappell, D., Reay, A. and Walls, D. (2000b). "Mobilisation and attenuation of arsenic around gold mines, east Otago, New Zealand." New Zealand Journal of Geology and Geophysics **43**(3): 373-383.

Craw, D. and Chappell, D. A. (2000). "Metal redistribution in historic mine wastes, Coromandel Peninsula, New Zealand." New Zealand Journal of Geology and Geophysics **43**(2): 187-198.

Craw, D., Mulliner, T., Haffert, L., Paulsen, H. K., Peake, B. and Pope, J. (2008). "Stratigraphic controls on water quality at coal mines in southern New Zealand." New Zealand Journal of Geology and Geophysics **51**(1): 59-72.

Craw, D. and Rufaut, C. (2017). "Geochemical and mineralogical controls on mine tailings rehabilitation and vegetation, Otago Schist, New Zealand." New Zealand Journal of Geology and Geophysics **60**(3): 176-187.

Craw, D., Rufaut, C., Haffert, L. and Paterson, L. (2007a). "Plant colonization and arsenic uptake on high arsenic mine wastes, New Zealand." Water, air, and soil pollution **179**(1-4): 351-364.

Craw, D., Rufaut, C., Haffert, L. and Todd, A. (2006). "Mobilisation and attenuation of boron during coal mine rehabilitation, Wangaloa, New Zealand." Science of the total environment **368**(2-3): 444-455.

Craw, D., Rufaut, C. G., Hammit, S., Clearwater, S. G. and Smith, C. M. (2007b). "Geological controls on natural ecosystem recovery on mine waste in southern New Zealand." Environmental Geology **51**(8): 1389-1400.

Crombie, F. M., Weber, P. A., Lindsay, P., Thomas, D. G., Rutter, G. A., Shi, P., P., R. and Pizey, M. H. (2011). Passive Treatment of Acid Mine Drainage using Waste Mussel Shell, Stockton Coal Mine, New Zealand. 7th Australian Workshop on Acid and Metalliferous Drainage. L. C. Bell and B. Braddock**:** 393-405, JK Tech. Darwin, Australia.

Davey, H. and Van Moort, J. (1986). "Current mercury deposition at Ngawha Springs, New Zealand." Applied geochemistry **1**(1): 75-93.

David, C. P. C. (2003). "Establishing the impact of acid mine drainage through metal bioaccumulation and taxa richness of benthic insects in a tropical Asian stream (The Philippines)." Environmental Toxicology and Chemistry **22**(12): 2952-2959.

Davies, S. H. R. and Morgan, J. J. (1989). "Manganese(II) oxidation kinetics on metal oxide surfaces." Journal of Colloid and Interface Science **129**(1): 63-77.

de Schamphelaere, K. A. and Janssen, C. R. (2002). "A biotic ligand model predicting acute copper toxicity for Daphnia magna: the effects of calcium, magnesium, sodium, potassium, and pH." Environmental science & technology **36**(1): 48-54.

Della Puppa, L., Komárek, M., Bordas, F., Bollinger, J.-C. and Joussein, E. (2013). "Adsorption of copper, cadmium, lead and zinc onto a synthetic manganese oxide." Journal of colloid and interface science **399**: 99-106.

Denny, P. (1980). "Solute movement in submerged angiosperms." Biological Reviews **55**(1): 65-92.

Di Toro, D. M., Allen, H. E., Bergman, H. L., Meyer, J. S., Paquin, P. R. and Santore, R. C. (2001). "Biotic ligand model of the acute toxicity of metals. 1. Technical basis." Environmental Toxicology and Chemistry **20**(10): 2383-2396.

Dold, B. (2017). "Acid rock drainage prediction: A critical review." Journal of Geochemical Exploration **172**: 120-132.

Dong, W., Liang, L., Brooks, S., Southworth, G. and Gu, B. (2010). "Roles of dissolved organic matter in the speciation of mercury and methylmercury in a contaminated ecosystem in Oak Ridge, Tennessee." Environmental Chemistry **7**(1): 94-102.

Doshi, S. M. (2006). "Bioremediation of acid mine drainage using sulfate-reducing bacteria." US Environmental Protection Agency, Office of Solid Waste and Emergency Response and Office of Superfund Remediation and Technology Innovation **65**.

Durance, P. M. J., Hill, M. P., Turnbull, R. E., Morgenstern, R. and Rattenbury, M. S. (2018). Nickel and cobalt mineral potential in New Zealand. Australasian Institute of Mining and Metallurgy 51st New Zealand

Branch Annual Conference, Tauranga, New Zealand, Australasian Institute of Mining and Metallurgy, New Zealand Branch.

Dvorak, D. H., Hedin, R. S., Edenborn, H. M. and McIntire, P. E. (1992). "Treatment of metal-contaminated water using bacterial sulfate reduction: Results from pilot-scale reactors." Biotechnology and bioengineering **40**(5): 609-616.

Dzomback, D. A. and Morel, F. M. M. (1990). Surface complexation modeling: hydrous ferric oxide. John Wiley & Sons, Inc., United States of America.

Eaton, A. D., Clesceri, L. S., Greenberg, A. E. and Franson, M. A. H. (2005). Standard methods for the examination of water and wastewater. American Public Health Association, Water Pollution Control Federation, Water Environment Federation.

Edbrooke, S. W. and Brook, F. J. (2009). Geology of the Whangarei area : scale 1:250 000, Institute of Geological & Nuclear Sciences.

Ellis, A. and Mahon, W. (1964). "Natural hydrothermal systems and experimental hot-water/rock interactions." Geochimica et Cosmochimica Acta **28**(8): 1323-1357.

Ellis, A. and Mahon, W. (1967). "Natural hydrothermal systems and experimental hot water/rock interactions (Part II)." Geochimica et Cosmochimica Acta **31**(4): 519-538.

Espana, J. S., Pamo, E. L., Santofimia, E., Aduvire, O., Reyes, J. and Barettino, D. (2005). "Acid mine drainage in the Iberian Pyrite Belt (Odiel river watershed, Huelva, SW Spain): geochemistry, mineralogy and environmental implications." Applied geochemistry **20**(7): 1320-1356.

Evangelou, V. P. (1995). Pyrite Oxidation and its Control. CRC Press, Boca Raton, USA.

Evolution Mining (2016). Exploration at Puhipuihi**:** 5, Evolution Mining. Sydney, Australia.

Fairgray, M., Mackenzie, E. and Webster-Brown, J. (2017a). The impact of historical mining activity on aquatic macroinvertebrates at Puhipuhi, Northland, New Zealand. Integrating Multiple Aquatic Values (IMAV), Hamilton, New Zealand, New Zealand Freshwater Sciences Society (NZFSS).

Fairgray, M., Mackenzie, E. and Webster-Brown, J. (2017b). The impact of historical mining activity on aquatic macroinvertebrates at Puhipuhi, Northland, New Zealand. The International Society for Environmental Biogeochemistry (ISEB) 23rd International Symposium, Palm Cove, Australia.

Fairgray, M., Pope, J., Trumm, D. and Webster-Brown, J. (2018a). Changes to the water chemistry of Cannel Creek following remedial work of Bellvue Mine Waterways Postgraduate Student Conference, Lincoln, New Zealand, Waterways Centre for Freshwater Management.

Fairgray, M., Pope, J., Trumm, D. and Webster-Brown, J. (2018b). The use of redox pairs to model bioreactor processes in the treatment of acid mine drainage. Goldschmidt, Boston, USA, Geochemical Society and European Association of Geochemistry.

Fairgray, M., Pope, J., Trumm, D., Webster-Brown, J. and Harding, J. (2018c). Changes to the water chemistry of Cannel Creek following remedial work of Bellvue Mine New Zealand Freshwater Sciences Society Annual Conference, Nelson, New Zealand, New Zealand Freshwater Sciences Society.

Fairgray, M., Pope, J., Trumm, D. and Webster, J. (2018d). Water chemistry changes in Cannel Creek following remedial work of Bellvue Mine AMD. 2018 AusIMM New Zealand Branch Annual Conference, Tauranga, New Zealand, AusIMM.

Fairgray, M. and Webster-Brown, J. (2016a). Spatial distribution and bioavailability of Mercury and other toxic trace elements in the Puhipuhi catchment, Northland. New Zealand Freshwater Sciences Society (NZFSS) Annual Conference - Freshwaters On The Edge, Invercargill, New Zealand, New Zealand Freshwater Sciences Society.

Fairgray, M. and Webster-Brown, J. (2016b). Spatial distribution and bioavailability of Mercury and other toxic trace elements in the Puhipuhi catchment, Northland. Waterways Postgraduate Student Conference, Lincoln, New Zealand, Waterways Centre for Freshwater Management.

Fairgray, M. and Webster-Brown, J. (2017a). The Fate of Toxic Trace Elements at Tui Mine. Waterways Postgraduate Student Conference, Lincoln, New Zealand.

Fairgray, M. and Webster-Brown, J. (2017b). Release of toxic trace elements from contaminated stream sediment at Tui Mine, Te Aroha, New Zealand. 2017 AusIMM New Zealand Branch Conference**:** 8, AusIMM. Christchurch, New Zealand.

Fairgray, M., Webster-Brown, J., Harding, J. and Waters, A. S. (2016). Geochemical Modelling of Metal Toxicity in the Tui Mine Catchment, Te Aroha, NZ. 2016 Australian Intitute of Minerals and Mining New Zealand Branch Annual Conference**:** 9. Wellington, New Zealand.

Farag, A., Woodward, D., Goldstein, J., Brumbaugh, W. and Meyer, J. (1998). "Concentrations of metals associated with mining waste in sediments, biofilm, benthic macroinvertebrates, and fish from the Coeur d'Alene River Basin, Idaho." Archives of Environmental Contamination and Toxicology **34**(2): 119-127.

Ferris, F. (2005). "Biogeochemical properties of bacteriogenic iron oxides." Geomicrobiology Journal **22**(3-4): 79-85.

Filella, M., Belzile, N. and Chen, Y.-W. (2002). "Antimony in the environment: a review focused on natural waters: II. Relevant solution chemistry." Earth-Science Reviews **59**(1-4): 265-285.

Filipek, L. H., Chao, T. and Carpenter, R. (1981). "Factors affecting the partitioning of Cu, Zn and Pb in boulder coatings and stream sediments in the vicinity of a polymetallic sulfide deposit." Chemical Geology **33**(1-4): 45-64.

Food Standards Australia New Zealand (2015). Australia New Zealand Food Standards Code. Shedule 19 - Maximum levels of contaminants and natural toxicants, Food Standards Australia New Zealand. Wellington, New Zealand.

Freitas, R. M., Perilli, T. A. and Ladeira, A. C. Q. (2013). "Oxidative precipitation of manganese from acid mine drainage by potassium permanganate." Journal of Chemistry **2013**.

Freund, J. G. and Petty, J. T. (2007). "Response of fish and macroinvertebrate bioassessment indices to water chemistry in a mined Appalachian watershed." Environmental Management **39**(5): 707-720.

Fromm, P. O. (1980). "A review of some physiological and toxicological responses of freshwater fish to acid stress." Environmental Biology of Fishes **5**(1): 79-93.

Gage, M. (1952). The Greymouth Coalfield. New Zealand Geological Survey**:** 240, Department of Scientific and Industrial Research. Wellington, New Zealand.

Gerhardt, A. (1992). "Effects of subacute doses of iron (Fe) on Leptophlebia marginata (Insecta: Ephemeroptera)." Freshwater Biology **27**(1): 79-84.

Gerhardt, A. (1993). "Review of impact of heavy metals on stream invertebrates with special emphasis on acid conditions." Water, Air, and Soil Pollution **66**(3-4): 289-314.

Gerhardt, A., Janssens de Bisthoven, L. and Soares, A. M. V. M. (2004). "Macroinvertebrate response to acid mine drainage: community metrics and on-line behavioural toxicity bioassay." Environmental Pollution **130**(2): 263-274.

Ghaly, M., El-Dars, F. M., Hegazy, M. and Rahman, R. A. (2016). "Evaluation of synthetic Birnessite utilization as a sorbent for cobalt and strontium removal from aqueous solution." Chemical Engineering Journal **284**: 1373-1385.

Gholinejad, M., Karimi, B. and Mansouri, F. (2014). "Synthesis and characterization of magnetic copper ferrite nanoparticles and their catalytic performance in one-pot odorless carbon-sulfur bond formation reactions." Journal of Molecular Catalysis A: Chemical **386**: 20-27.

Gionfriddo, C. M., Ogorek, J. M., Butcher, M., Krabbenhoft, D. P. and Moreau, J. W. (2015). "Mercury distribution and mobility at the abandoned Puhipuhi mercury mine, Northland, New Zealand." New Zealand Journal of Geology and Geophysics **58**(1): 78-87.

Goldberg, S. and Johnston, C. T. (2001). "Mechanisms of arsenic adsorption on amorphous oxides evaluated using macroscopic measurements, vibrational spectroscopy, and surface complexation modeling." Journal of colloid and Interface Science **234**(1): 204-216.

Goodyear, K. and McNeill, S. (1999). "Bioaccumulation of heavy metals by aquatic macro-invertebrates of different feeding guilds: a review." Science of the Total Environment **229**(1-2): 1-19.

Gore, D. B., Preston, N. J. and Fryirs, K. A. (2007). "Post-rehabilitation environmental hazard of Cu, Zn, As and Pb at the derelict Conrad Mine, eastern Australia." Environmental Pollution **148**(2): 491-500.

Gray, D. and Harding, J. (2012). "Acid Mine Drainage Index (AMDI): a benthic invertebrate biotic index for assessing coal mining impacts in New Zealand streams." New Zealand Journal of Marine and Freshwater Research **46**(3): 335-352.

Gregersen, R. G. (2016). The Response of Stream Ecosystem Function to Acid Mine Drainage Remediation. MSc Unpublished Thesis, University of Auckland.

Gunn, J., Sarrazin-Delay, C., Wesolek, B., Stasko, A. and Szkokan-Emilson, E. (2010). "Delayed recovery of benthic macroinvertebrate communities in Junction Creek, Sudbury, Ontario, after the diversion of acid mine drainage." Human and Ecological Risk Assessment **16**(4): 901-912.

Gusek, J. J. (2002). "Sulfate-reducing bioreactor design and operating issues: is this the passive treatment technology for your mine drainage." National Association of Abandoned Mine Land Programs, Park City, Utah.

Haffert, L. and Craw, D. (2008). "Processes of attenuation of dissolved arsenic downstream from historic gold mine sites, New Zealand." Science of The Total Environment **405**(1): 286-300.

Haffert, L., Craw, D. and Pope, J. (2010). "Climatic and compositional controls on secondary arsenic mineral formation in high-arsenic mine wastes, South Island, New Zealand." New Zealand Journal of Geology and Geophysics **53**(2-3): 91-101.

Haines, T. A. and Baker, J. P. (1986). "Evidence of fish population responses to acidification in the eastern United States." Water, air, and soil pollution **31**(3-4): 605-629.

Hampton, W., White, G., Hoskin, P., Browne, P. and Rodgers, K. (2004). "Cinnabar, livingstonite, stibnite and pyrite in Pliocene silica sinter from Northland, New Zealand." Mineralogical Magazine **68**(1): 191-198.

Harding, J. and Boothroyd, I. (2004). Impacts of mining. Freshwaters of New Zealand. J. S. Harding, P. Mosley, C. Pearson and B. Sorrell**:** 36.31-36.10, The Caxton Press. Christchurch, New Zealand.

Harding, J. and Simon, K. (, in prep). "The response of water chemistry and benthic stream communities to remediation of the Tui metal mine." New Zealand journal of marine and freshwater research.

Harvey, S. A. and Webster-Brown, J. G. (2003). Environmentally and publicly acceptable options for remediation at Tui Mine site, Te Aroha AusIMM New Zealand Branch 36th Annual Conference, AusIMM. Greymouth, New Zealand.

Hassler, C. S., Slaveykova, V. I. and Wilkinson, K. J. (2004). "Some fundamental (and often overlooked) considerations underlying the free ion activity and biotic ligand models." Environmental Toxicology and Chemistry **23**(2): 283-291.

Havas, M. and Advokaat, E. (1995). "Can sodium regulation be used to predict the relative acid-sensitivity of various life-stages and different species of aquatic fauna?" Water, air, and soil pollution **85**(2): 865-870.

Hedin, R. S. and Watzlaf, G. R. (1994). "The effects of anoxic limestone drains on mine water chemistry." US Bureau of Mines Special Publication SP A **6**: 185-194.

Hedin, R. S., Watzlaf, G. R. and Nairn, R. W. (1994). "Passive treatment of acid mine drainage with limestone." Journal of Environmental Quality **23**(6): 1338-1345.

Hem, J. D. (1963). "Chemical equilibria affecting the behavior of manganese in natural water." Hydrological Sciences Journal **8**(3): 30-37.

Hendy, C. H. (1981). "The Tui Mine - After the miners have left." New Zealand Environment(29): 3.

Henley, R. W., Truesdell, A., Barton, P. and Whitney, J. (1985). Fluid-mineral equilibria in hydrothermal systems. Society of Economic Geologists, Chelsea, MI.

Hewlett, L., Craw, D. and Black, A. (2005). "Comparison of arsenic and trace metal contents of discharges from adjacent coal and gold mines, Reefton, New Zealand." Marine and Freshwater Research **56**(7): 983-995.

Hickey, C. W. and Clements, W. H. (1998). "Effects of heavy metals on benthic macroinvertebrate communities in New Zealand streams." Environmental Toxicology and Chemistry **17**(11): 2338-2346.

Hiller, E., Petrák, M., Tóth, R., Lalinská-Voleková, B., Jurkovič, Ľ., Kučerová, G., Radková, A., Šottník, P. and Vozár, J. (2013). "Geochemical and mineralogical characterization of a neutral, low-sulfide/high-carbonate tailings impoundment, Markušovce, eastern Slovakia." Environmental Science and Pollution Research **20**(11): 7627-7642.

Hillman, C. (2018). Quantifying and treating contaminant discharges from the James Mine on New Zealand's West Coast. MSc Unpublished Thesis, University of Canterbury.

Hobbins, J. (2018). Recent exploration results from the Puhipuhi epithermal camp. 2018 AusIMM New Zealand Branch Annual Conference, AusIMM. Tauranga, New Zealand.

Hoggins, F. E. and Brooks, R. R. (1973). "Natural dispersion of mercury from Puhipuhi, northland, New Zealand." New Zealand journal of marine and freshwater research **7**(1-2): 125-132.

Hogsden, K. L. (2013). Structure and function of food webs in acid mine drainage streams. PhD Unpublished PhD Thesis, University of Canterbury.

Hogsden, K. L. and Harding, J. S. (2011). "Consequences of acid mine drainage for the structure and function of benthic stream communities: a review." Freshwater Science **31**(1): 108-120.

Hogsden, K. L. and Harding, J. S. (2012). "Anthropogenic and natural sources of acidity and metals and their influence on the structure of stream food webs." Environmental pollution **162**: 466-474.

Hughes, M. F. (2002). "Arsenic toxicity and potential mechanisms of action." Toxicology letters **133**(1): 1-16.

Iavazzo, P., Ducci, D., Adamo, P., Trifuoggi, M., Migliozzi, A. and Boni, M. (2012). "Impact of past mining activity on the quality of water and soil in the High Moulouya Valley (Morocco)." Water, Air, and Soil Pollution **223**(2): 573-589.

Jacob, D., Soldati, A., Wirth, R., Huth, J., Wehrmeister, U. and Hofmeister, W. (2008). "Nanostructure, composition and mechanisms of bivalve shell growth." Geochimica et Cosmochimica Acta **72**(22): 5401-5415.

Jage, C., Zipper, C. and Noble, R. (2001). "Factors affecting alkalinity generation by successive alkalinity-producing systems." Journal of environmental Quality **30**(3): 1015-1022.

James, T. I. (2003). Water quality of streams draining various coal measures in the North-Central West Coast. AusIMM New Zealand Branch 36th Annual Conference AusIMM. Greymouth, New Zealand.

Jennette, K. W. (1981). "The role of metals in carcinogenesis: biochemistry and metabolism." Environmental health perspectives **40**: 233-252.

Johnson, D. B. and Hallberg, K. B. (2005). "Acid mine drainage remediation options: A review." Science of the Total Environment **338**(1-2 SPEC. ISS.): 3-14.

Karthikeyan, K. G., Elliott, H. A. and Cannon, F. S. (1997). "Adsorption and Coprecipitation of Copper with the Hydrous Oxides of Iron and Aluminum." Environmental Science & Technology **31**(10): 2721-2725.

Kepler, D. A. and McCleary, E. C. (1994). "Successive alkalinity-producing systems (SAPS) for the treatment of acidic mine drainage." Bureau of Mines Special Publication SP 06B-94 **1**: 185-194.

King, J. K., Harmon, S. M., Fu, T. T. and Gladden, J. B. (2002). "Mercury removal, methylmercury formation, and sulfate-reducing bacteria profiles in wetland mesocosms." Chemosphere **46**(6): 859-870.

Kolta, G. A., El-Tawil, S. Z., Ibrahim, A. A. and Felix, N. S. (1981). "Kinetics and mechanism of copper ferrite formation." Thermochimica Acta **43**(3): 279-287.

Kosta, L., Byrne, A. R. and Zelenko, V. (1975). "Correlation between selenium and mercury in man following exposure to inorganic mercury." Nature **254**(5497): 238-239.

Kovács, E., Tamás, J., Frančišković-Bilinski, S., Omanović, D., Bilinski, H. and Pižeta, I. (2012). "Geochemical study of surface water and sediment at the abandoned Pb-Zn mining site at Gyongyosorosz, Hungary." J Fresenius Environ Bull **21**: 1212-1218.

Kumpiene, J., Lagerkvist, A. and Maurice, C. (2008). "Stabilization of As, Cr, Cu, Pb and Zn in soil using amendments–a review." Waste management **28**(1): 215-225.

Lachmar, T. E., Burk, N. I. and Kolesar, P. T. (2006). "Groundwater contribution of metals from an abandoned mine to the North Fork of the American Fork River, Utah." Water, air, and soil pollution **173**(1-4): 103-120.

Lander, L., Reuther, R., (2004). "Speciation, Mobility and Bioavailability of Metals". Metals in Society and in the Environment. **8**. Kluwer Academic Publishers, Dordrecht.

Langer, E. R., Davis, M. R. and Ross, C. W. (1999). Rehabilitation of lowland indigenous forest after mining in Westland. Department of Conservation Wellington, Wellington, New Zealand.

Langley, S., Gault, A. G., Ibrahim, A., Takahashi, Y., Renaud, R., Fortin, D., Clark, I. D. and Ferris, F. G. (2009). "Sorption of strontium onto bacteriogenic iron oxides." Environmental science & technology **43**(4): 1008-1014.

Leleyter, L. and Probst, J.-L. (1999). "A new sequential extraction procedure for the speciation of particulate trace elements in river sediments." International Journal of Environmental Analytical Chemistry **73**(2): 109-128.

Leonard, G. S., Begg, J. G. and Wilson, C. N. J. (2010). Geology of the Rotorua area : scale 1:250,000**:** 1:250,000 geological map, Institute of Geological & Nuclear Sciences

Letterman, R. D. and Mitsch, W. J. (1978). "Impact of mine drainage on a mountain stream in Pennsylvania." Environmental Pollution (1970) **17**(1): 53-73.

Li, Y., Chen, C., Li, B., Sun, J., Wang, J., Gao, Y., Zhao, Y. and Chai, Z. (2006). "Elimination efficiency of different reagents for the memory effect of mercury using ICP-MS." Journal of Analytical Atomic Spectrometry **21**(1): 94-96.

Lindsay, M. B. J., Condon, P. D., Jambor, J. L., Lear, K. G., Blowes, D. W. and Ptacek, C. J. (2009). "Mineralogical, geochemical, and microbial investigation of a sulfide-rich tailings deposit characterized by neutral drainage." Applied Geochemistry **24**(12): 2212-2221.

Lindsay, M. B. J., Moncur, M. C., Bain, J. G., Jambor, J. L., Ptacek, C. J. and Blowes, D. W. (2015). "Geochemical and mineralogical aspects of sulfide mine tailings." Applied Geochemistry **57**: 157-177.

Livingston, M. E. (1987). Preliminary studies on the effects of past mining on the aquatic environment, Coromandel Peninsula, Ministry of Works.

Locke, C. A., Johnson, S. A., Cassidy, J. and Mauk, J. L. (1999). "Geophysical exploration of the Puhipuhi epithermal area, Northland, New Zealand." Journal of Geochemical Exploration **65**(2): 91-109.

Lottermoser, B. G. (2003). Mine Wastes. Springer, Germany.

Lottermoser, B. G., Ashley, P. M. and Lawie, D. C. (1999). "Environmental geochemistry of the Gulf Creek copper mine area, north-eastern New South Wales, Australia." Environmental Geology **39**(1): 61-74.

Lu, P., Nuhfer, N. T., Kelly, S., Li, Q., Konishi, H., Elswick, E. and Zhu, C. (2011). "Lead coprecipitation with iron oxyhydroxide nano-particles." Geochimica et Cosmochimica Acta **75**(16): 4547-4561.

Mackenzie, A. (2010). Characterization of drainage chemistry in Fanny Creek catchment and optimal passive AMD treatment options for Fanny Creek. MSc Unpublished MSc Thesis, University of Canterbury.

Madambi, K. and Moore, J. (2013). Technical Report for the REEFTON PROJECT**:** 133. Melbourne, Australia.

Malloch, K. R., Craw, D. and Trumm, D. (2017). "Arsenic mineralogy and distribution at the historic Alexander gold mine, Reefton goldfield, New Zealand." New Zealand Journal of Geology and Geophysics **60**(2): 129-144.

Malmström, M. E., Berglund, S. and Jarsjö, J. (2008). "Combined effects of spatially variable flow and mineralogy on the attenuation of acid mine drainage in groundwater." Applied Geochemistry **23**(6): 1419-1436.

Malmström, M. E., Destouni, G. and Martinet, P. (2004). "Modeling Expected Solute Concentration in Randomly Heterogeneous Flow Systems with Multicomponent Reactions." Environmental Science and Technology **38**(9): 2673-2679.

Markich, S. J. and Brown, P. L. (1999). Thermochemical Data (log K) for Environmentally-Relevant Elements, ANSTO. Australia.

Mays, P. and Edwards, G. (2001). "Comparison of heavy metal accumulation in a natural wetland and constructed wetlands receiving acid mine drainage." Ecological engineering **16**(4): 487-500.

McCauley, C. A. (2011). Assessment of passive treatment and biogeochemical reactors for ameliorating acid mine drainage at Stockton coal mine. PhD Unpublished PhD Thesis, University of Canterbury.

McCauley, C. A., O'Sullivan, A. D., Weber, P. A. and Trumm, D. A. (2008). Development of Passive Treatment Systems for Treating Acid Mine Drainage at Stockton Mine. AusIMM New Zealand Branch Annual Conference**:** 10, AusIMM. Auckland, New Zealand.

McKenzie, R. M. (1980). "The adsorption of lead and other heavy metals on oxides of manganese and iron." Australian Journal of Soil Research **18**(1): 61-73.

McLachlan, C. and Craw, D. (2018). "Environmental mineralogy and geochemistry of processing residues at Prohibition historic gold mine site, Waiuta, Westland, New Zealand." New Zealand Journal of Geology and Geophysics **61**(2): 180-194.

McLean, G. (2016). Puhipuhi Epithermal System, Taupo Volcanic Zone. 2016 AusIMM New Zealand Branch Annual Conference, AusIMM. Wellington, New Zealand.

Mendez, M. O. and Maier, R. M. (2007). "Phytostabilization of mine tailings in arid and semiarid environments—an emerging remediation technology." Environmental health perspectives **116**(3): 278-283.

Milham, L. and Craw, D. (2009). "Two-stage structural development of a Paleozoic auriferous shear zone at the Globe-Progress deposit, Reefton, New Zealand." New Zealand Journal of Geology and Geophysics **52**(3): 247-259.

Ministry of Health (1995). Standards for potable water. M. o. Health, Ministry of Health. Wellington, New Zealand.

Ministry of Health (2000). Drinking Water Standards for New Zealand. Ministry of Health, Ministry of Health,. Wellington, New Zealand.

Ministry of Heath (2008). Drinking Water Standards for New Zealand 2005 (revised 2008), Ministry of Health. Wellington.

Moreira-Santos, M., Donato, C., Lopes, I. and Ribeiro, R. (2008). "Avoidance tests with small fish: Determination of the median avoidance concentration and of the lowest-observed-effect gradient." Environmental Toxicology and Chemistry: An International Journal **27**(7): 1576-1582.

Morgenstern, R., Turnbull, R. E., Hill, M. P., Durance, P. M. J. and Rattenbury, M. S. (2018). Rare earth element mineral potential in New Zealand: a mineral systems approach. Australasian Institute of Mining and Metallurgy 51st New Zealand Branch Annual Conference, Tauranga, New Zealand, Australasian Institute of Mining and Metallurgy, New Zealand Branch.

Morrell, W. J. (1997). An Assessment of the Revegetation Potential of Base-Metal Tailings from the Tui Mine, Te Aroha, New Zealand Unpublished PhD Thesis, Massey University, NZ.

Morrison, R., Brooks, R., Reeves, R. and Malaisse, F. (1979). "Copper and cobalt uptake by metallophytes from Zaïre." Plant and Soil **53**(4): 535-539.

Navarro, A., Cardellach, E. and Corbella, M. (2011). "Immobilization of Cu, Pb and Zn in mine-contaminated soils using reactive materials." Journal of Hazardous Materials **186**(2-3): 1576-1585.

Navarro, A. and Martínez, F. (2010). "The use of soil-flushing to remediate metal contamination in a smelting slag dumping area: Column and pilot-scale experiments." Engineering Geology **115**(1-2): 16-27.

Neculita, C. M., Zagury, G. J. and Bussière, B. (2007). "Passive treatment of acid mine drainage in bioreactors using sulfate-reducing bacteria: Critical review and research needs." Journal of Environmental Quality **36**(1): 1-16.

Nemati, M., Harrison, S., Hansford, G. and Webb, C. (1998). "Biological oxidation of ferrous sulphate by Thiobacillus ferrooxidans: a review on the kinetic aspects." Biochemical engineering journal **1**(3): 171-190.

Niyogi, S. and Wood, C. M. (2004). "Biotic ligand model, a flexible tool for developing site-specific water quality guidelines for metals." Environmental Science & Technology **38**(23): 6177-6192.

Noble, C. (2003). The Source and Fate of Arsenic in Selected West Coast Catchments, South Island, New Zealand. MSc Unpublished Thesis, University of Auckland.

Nordstrom, D. K. (1982). "Aqueous pyrite oxidation and the consequent formation of secondary iron minerals". Acid Sulfate Weathering. Kittrick JA, Fanning DS and H. LR. **10:** 37-56. Soil Science Society of America.

Nordstrom, D. K. (1999). "Some Fundamentals of Aqueous Geochemistry". The environmental geochemistry of mineral deposits: Case studies and research topics. G. S. Plumlee and M. J. Logsdon. **6A:** 117-123. Society of Economic Geologists, Littleton, CO, USA.

Nordstrom, D. K. and Alpers, C. N. (1999). "Geochemistry of acid mine waters". Reviews in Economic Geology. G. S. Plumlee and M. J. Logsdon. **6:** 133-160. Society of Economic Geologists, Littleton, CO, USA.

Nordstrom, D. K., Blowes, D. W. and Ptacek, C. J. (2015). "Hydrogeochemistry and microbiology of mine drainage: an update." Applied Geochemistry **57**: 3-16.

Nordstrom, D. K., Jenne, E. A. and Ball, J. W. (1979). "Redox equilibria of iron in acid mine waters." Chemical modeling in aqueous systems **93**: 51-80.

Northland Regional Council. (2016). "River and Rainfall Data." Retrieved 23/11/2015, 2015, from http://www.nrc.govt.nz/Environment/River-and-rainfall-data/River-and-Rainfall-Data/.

Nylander, M. and Weiner, J. (1991). "Mercury and selenium concentrations and their interrelations in organs from dental staff and the general population." British Journal of Industrial Medicine **48**(11): 729-734.

NZPAM. (2017). "Regional coal resources." Retrieved 23/03/19, from https://www.nzpam.govt.nz/our-industry/nz-minerals/minerals-data/coal/regional-coal-resources/.

O'Halloran, K., Cavanagh, J. A. and Harding, J. S. (2008). "Response of a New Zealand mayfly (Deleatidium spp.) to acid mine drainage: implications for mine remediation." Environmental Toxicology and Chemistry **27**(5): 1135-1140.

OceanaGold (2017). 2017 Fact Book.

Otte, M., Kearns, C. and Doyle, M. (1995). "Accumulation of arsenic and zinc in the rhizosphere of wetland plants." Bulletin of Environmental Contamination and Toxicology **55**(1): 154-161.

Otte, M. L. and Jacob, D. L. (2006). "Constructed wetlands for phytoremediation: rhizofiltration, phytostabilisation and phytoextraction". Phytoremediation Rhizoremediation**:** 57-67. Springer.

Pang, L. (1995). "Contamination of groundwater in the Te Aroha area by heavy metals from an abandoned mine." Journal oí Hydrology (NZ) Vol **33**(1).

Paquin, P. R., Gorsuch, J. W., Apte, S., Batley, G. E., Bowles, K. C., Campbell, P. G., Delos, C. G., Di Toro, D. M., Dwyer, R. L. and Galvez, F. (2002). "The biotic ligand model: a historical overview." Comparative Biochemistry and Physiology Part C: Toxicology & Pharmacology **133**(1-2): 3-35.

Park, S. M., Yoo, J. C., Ji, S. W., Yang, J. S. and Baek, K. (2013). "Selective recovery of Cu, Zn, and Ni from acid mine drainage." Environmental Geochemistry and Health **35**(6): 735-743.

Parkhurst, D. L. and Appelo, C. A. J. (2013). "Description of Input and Examples for PHREEQC. Version 3--A Computer Program for Speciation, Batch-Reaction, One-Dimensional Transport, and Inverse Geochemical Calculations". U.S. Geological Survey Techniques and Methods Book 6**:** 497. U.S. Geological Survey, Reston, WV, USA.

Parks, J. M., Johs, A., Podar, M., Bridou, R., Hurt, R. A., Smith, S. D., Tomanicek, S. J., Qian, Y., Brown, S. D. and Brandt, C. C. (2013). "The genetic basis for bacterial mercury methylation." Science **339**(6125): 1332-1335.

Pattle Delamore Partners Ltd. (2016a). Baseline Environmental Monitoring, Program 2: Aquatic Organisms Sampling - Exploration Permit #51985 at Puhipuhi, Northland. Auckland, New Zealand.

Pattle Delamore Partners Ltd. (2016b). Baseline Environmental Monitoring, Program 2: Macroinvertebrate Assessment - Exploration Permit #51985 at Puhipuhi, Northland. Auckland, New Zealand.

Pattle Delamore Partners Ltd. (2016c). Baseline Environmental Monitoring, Program 2: Surface Water and Sediment Sampling - Exploration Permit #51985 at Puhipuhi, Northland. Auckland, New Zealand.

Pattle Delamore Partners Ltd. (2016d). Baseline Environmental Monitoring, Program 2: Surface Water Sampling - Exploration Permit #51985 at Puhipuhi, Northland**:** 73. Auckland, New Zealand.

Paulson, A. J. and Balistrieri, L. (1999). "Modeling removal of Cd, Cu, Pb, and Zn in acidic groundwater during neutralization by ambient surface waters and groundwaters." Environmental Science & Technology **33**(21): 3850-3856.

PDP (2010). Tui Remedial Works: Baseline Monitoring**:** 307. Auckland, New Zealand.

PDP (2013). Tui Mine: Post Remediation Ecological Monitoring 2013. Auckland, New Zealand.

PDP (2014). Tui Mine Monitoring Report 2013 - Water Quality Monitoring (After Rehabilitation of Tui Mine). Auckland.

PDP (2016). Tui Mine Monitoring Report 2015 - Water Quality Monitoring (After Rehabilitation of Tui Mine)**:** 276. Auckland, New Zealand.

Pérez-López, R., Quispe, D., Castillo, J. and Nieto, J. M. (2011). "Acid neutralization by dissolution of alkaline paper mill wastes and implications for treatment of sulfide-mine drainage." American Mineralogist **96**(5-6): 781-791.

Plumlee, G. S. (1999). "The Environmental Geology of Mineral Deposits". The Environmental Geochemistry of Mineral Deposits, Part A: Processes, Techniques and Health Issues. G. S. Plumlee and L. M. J. **6**. Society of Economic Geologists, Inc., Littleton, CO.

Plumlee, G. S., Smith, K. S., Montour, M. R., Ficklin, W. H. and Mosier, E. L. (1999). "The environmental geology of mineral deposits". The environmental geochemistry of mineral deposits, Part B, case studies and research topics. L. H. Filipek and G. S. Plumlee. **6B:** 71-116. Society of Economic Geology.

Pope, J., Newman, N. and Craw, D. (2006). Coal mine drainage geochemistry, West Coast, South Island - a preliminary water quality hazard model. AusIMM New Zealand Branch Annual Conference, AusIMM. Waihi.

Pope, J., Newman, N., Craw, D., Trumm, D. and Rait, R. (2010a). "Factors that influence coal mine drainage chemistry West Coast, South Island, New Zealand." New Zealand Journal of Geology and Geophysics **53**(2-3): 115-128.

Pope, J., Weber, P., Mackenzie, A., Newman, N. and Rait, R. (2010b). "Correlation of acid base accounting characteristics with the Geology of commonly mined coal measures, West Coast and Southland, New Zealand." New Zealand Journal of Geology and Geophysics **53**(2-3): 153-166.

Powell, J. D. (1988). "Origin and influence of coal mine drainage on streams of the United States." Environmental Geology and Water Sciences **11**(2): 141-152.

Powell, K. J., Brown, P. L., Byrne, R. H., Gajda, T., Hefter, G., Sjöberg, S. and Wanner, H. (2005). "Chemical speciation of environmentally significant heavy metals with inorganic ligands. Part 1: The Hg2+–Cl–, OH–, CO32–, SO42–, and PO43–aqueous systems (IUPAC Technical Report)." Pure and applied chemistry **77**(4): 739-800.

Rait, R., Trumm, D., Pope, J., Craw, D., Newman, N. and MacKenzie, H. (2010). "Adsorption of arsenic by iron rich precipitates from two coal mine drainage sites on the West Coast of New Zealand." New Zealand Journal of Geology and Geophysics **53**(2-3): 177-193.

Ranville, J. F. and Schmiermund, R. L. (1998). "An overview of environmental colloids." Perspectives in Environmental Chemistry, edited by: Macalady, DL, Oxford University Press, New York, USA: 25-56.

Rattenbury, M. S. and Stewart, M. (2000). "Structural setting of the Globe-Progress and Blackwater gold mines, Reefton goldfield, New Zealand." New Zealand Journal of Geology and Geophysics **43**(3): 435-445.

Regoli, F. and Principato, G. (1995). "Glutathione, glutathione-dependent and antioxidant enzymes in mussel, Mytilus galloprovincialis, exposed to metals under field and laboratory conditions: implications for the use of biochemical biomarkers." Aquatic Toxicology **31**(2): 143-164.

Robertson, T., Waugh, G. D. and Mol, J. (1975). "Mercury levels in New Zealand snapper Chrysophrys auratus." New Zealand journal of marine and freshwater research **9**(3): 265-272.

Robles-Arenas, V. and Candela, L. (2010). "Hydrological conceptual model characterisation of an abandoned mine site in semiarid climate: the Sierra de Cartagena-La Unión (SE Spain)." Geologica acta **8**(3): 235-248.

Ropiha, R. and Hansen, K. (2015). Puhipuhi Water and Sediment Heavy Metal Testing Program 2013-2014**:** 199-213, Northland Regional Council. Whangarei, New Zealand.

Ross, C., Simcock, R., Williams, P., Toft, R., Flynn, S., Birchfield, R. and Comesky, P. (2000). Salvage and direct transfer for accelerating restoration of native ecosystems on mine sites in New Zealand. . AusIMM New Zealand Branch 33rd Annual Conference**:** 97-104, AusIMM. Wellington, New Zealand.

Rötting, T. S., Thomas, R. C., Ayora, C. and Carrera, J. (2008). "Passive treatment of acid mine drainage with high metal concentrations using dispersed alkaline substrate." Journal of Environmental Quality **37**(5): 1741-1751.

Rufaut, C., Craw, D. and Foley, A. (2015). "Mitigation of acid mine drainage via a revegetation programme in a closed coal mine in Southern New Zealand." Mine Water and the Environment **34**(4): 464-477.

Rumsby, A. J. (1996). Environmental Geochemistry of Sulphide Mine Wastes, Tui Mine, Mt Te Aroha. MSc Unpublished MSc Thesis, University of Waikato.

Rytuba, J. J. (2000). "Mercury mine drainage and processes that control its environmental impact." Science of the Total Environment **260**(1-3): 57-71.

Saaltink, M. W., Batlle, F., Ayora, C., Carrera, J. and Olivella, S. (2004). "RETRASO, a code for modeling reactive transport in saturated and unsaturated porous media." Geologica acta **2**(3): 0235-0251.

Sabti, H., Hossain, M. M., Brooks, R. R. and Stewart, R. B. (2000). "The current environmental impact of base-metal mining at the Tui Mine, Te Aroha, New Zealand." Journal of the Royal Society of New Zealand **30**(2): 197-207.

Safran, A. (20177). Heavy Metal Bioaccumulation & Toxicity in Response to Acid Mine Drainage Remediation of The Tui Mine. MSc Unpublished MSc Thesis, University of Auckland.

Salomons, W. (1995). "Environmental impact of metals derived from mining activities: processes, predictions, prevention." Journal of Geochemical exploration **52**(1-2): 5-23.

Salvarredy-Aranguren, M. M., Probst, A., Roulet, M. and Isaure, M.-P. (2008). "Contamination of surface waters by mining wastes in the Milluni Valley (Cordillera Real, Bolivia): Mineralogical and hydrological influences." Applied Geochemistry **23**(5): 1299-1324.

Santore, R. C., Di Toro, D. M., Paquin, P. R., Allen, H. E. and Meyer, J. S. (2001). "Biotic ligand model of the acute toxicity of metals. 2. Application to acute copper toxicity in freshwater fish and Daphnia." Environmental Toxicology and Chemistry **20**(10): 2397-2402.

Santore, R. C., Mathew, R., Paquin, P. R. and DiToro, D. (2002). "Application of the biotic ligand model to predicting zinc toxicity to rainbow trout, fathead minnow, and Daphnia magna." Comparative Biochemistry and Physiology Part C: Toxicology & Pharmacology **133**(1-2): 271-285.

Sapsford, D., Florence, K., Pope, J. and Trumm, D. (2015). Passive Removal of Iron from AMD Using VFRs. 10th International Conference on Acid Rock Drainage & IMWA Annual Conference, IMWA. Santiago, Chile.

Saria, L., Shimaoka, T. and Miyawaki, K. (2006). "Leaching of heavy metals in acid mine drainage." Waste management & research **24**(2): 134-140.

Sharplin, R. E. P. (2008). Environmental Geochemistry after Partial Site Remediation at Tui Mine, New Zealand Unpublished MSc. Thesis, University of Auckland, NZ.

Sheoran, A. S. and Sheoran, V. (2006). "Heavy metal removal mechanism of acid mine drainage in wetlands: A critical review." Minerals Engineering **19**(2): 105-116.

Silverman, M. P. (1967). "Mechanism of bacterial pyrite oxidation." Journal of Bacteriology **94**(4): 1046-1051.

Simcock, R., Ross, C. and Pizey, M. (2004). Rehabilitation of alluvial gold and open-cast coal mines: 1904 to 2004. AusIMM New Zealand Branch 37th Annual Conference**:** 77-82, AusIMM. Nelson, New Zealand.

Simcock, R., Toft, R., Ross, C. and Flynn, S. (1999). A case study of the cost and effectiveness of a new technology for accelerating rehabilitation of native ecosystems. 24th Annual Minerals Council of Australia Environmental Workshop, Townsville, Australia, Dickson, Minerals Council of Australia.

Simkiss, K. and Taylor, M. (1995). "Transport of metals across membranes." Metal speciation and bioavailability in aquatic systems **3**: 1-44.

Simpson, S. L. and Batley, G. E. (2007). "Predicting metal toxicity in sediments: a critique of current approaches." Integrated Environmental Assessment and Management **3**(1): 18-31.

Singer, P. C. and Stumm, W. (1970). "Acidic Mine Drainage: The Rate-Determining Step." Science **167**(3921): 1121-1123.

Skousen, J. (1998). Overview of Passive Systems for Treating Acid Mine Drainage**:** 21, West Virginia University.

Skousen, J., Lilly, R. and Hilton, T. (1993). "Special chemicals for treating acid mine drainage." Green Lands **23**(3): 34-41.

Skousen, J., Zipper, C. E., Rose, A., Ziemkiewicz, P. F., Nairn, R., McDonald, L. M. and Kleinmann, R. L. (2016). "Review of Passive Systems for Acid Mine Drainage Treatment." Mine Water and the Environment: 1-21.

Smedley, P. L. and Kinniburgh, D. (2002). "A review of the source, behaviour and distribution of arsenic in natural waters." Applied geochemistry **17**(5): 517-568.

Smith, K. S. (1999). "Metal sorption on mineral surfaces: an overview with examples relating to mineral deposits." The Environmental Geochemistry of Mineral Deposits. Part B: Case Studies and Research Topics **6**: 161-182.

Smith, K. S., Balistrieri, L. S. and Todd, A. S. (2015). "Using biotic ligand models to predict metal toxicity in mineralized systems." Applied Geochemistry **57**: 55-72.

Smith, K. S. and Huyck, H. L. (1999). "An overview of the abundance, relative mobility, bioavailability, and human toxicity of metals." The environmental geochemistry of mineral deposits **6**: 29-70.

Smith, R., Martell, A. and Motekaitis, R. (2004). "NIST standard reference database 46." NIST Critically Selected Stability Constants of Metal Complexes Database Ver **2**.

Sobolewski, A. (1996). "Metal species indicate the potential of constructed wetlands for long-term treatment of metal mine drainage." Ecological Engineering **6**(4): 259-271.

Sobolewski, A. (1999). "A review of processes responsible for metal removal in wetlands treating contaminated mine drainage." International journal of phytoremediation **1**(1): 19-51.

Sperling, M. (2010). "PACS-2 - Marine Sediment Reference Materials for Trace Metals and other Constituents." Retrieved 19/06/2018, from http://www.speciation.net/Database/Materials/National-Research-Council-of-Canada-NRC--CNRC/PACS2--Marine-Sediment-Reference-Materials-for-Trace-Metals-and-other-Constituents-;i45.

Stark, J. D., Boothroyd, I. K., Harding, J. S., Maxted, J. R. and Scarsbrook, M. R. (2001). Protocols for sampling macroinvertebrates in wadeable streams. New Zealand Macroinvertebrate Working Group Report No. 1., Ministry for the Environment, . Wellington.

Stumm, W. (1992). Chemistry of the solid-water interface: processes at the mineral-water and particle-water interface in natural systems. John Wiley & Son Inc.

Sundar, S. and Chakravarty, J. (2010). "Antimony toxicity." International journal of environmental research and public health **7**(12): 4267-4277.

Swedlund, P. J. and Webster, J. G. (2001). "Cu and Zn ternary surface complex formation with SO 4 on ferrihydrite and schwertmannite." Applied Geochemistry **16**(5): 503-511.

Swedlund, P. J., Webster, J. G. and Miskelly, G. M. (2003). "The effect of SO4 on the ferrihydrite adsorption of Co, Pb and Cd: Ternary complexes and site heterogeneity." Applied Geochemistry **18**(11): 1671-1689.

Tay, K. A. (1980). Geochemistry and environmental impact of the discharge of heavy metals from the Tui Mine and its tailings Unpublished Msc Thesis, University of Waikato, NZ.

Temple, K. L. and Colmer, A. R. (1951). "The autotrophic oxidation of iron by a new bacterium, thiobacillus ferrooxidans." Journal of bacteriology **62**(5): 605-611.

To Bangthanh, T., Nordstrom, D. K., Cunningham, K. M., Ball, J. W. and McCleskey, R. B. (1999). "New method for the direct determination of dissolved Fe (III) concentration in acid mine waters." Environmental Science & Technology **33**(5): 807-813.

Tonkin, J. W. (2002). Metal partitioning in the aqueous environment:field, laboratory, and modeling studies, Unpublished Ph. D. Thesis, University of Washington.

Tonkin, J. W., Balistrieri, L. S. and Murray, J. W. (2002). "Modeling metal removal onto natural particles formed during mixing of acid rock drainage with ambient surface water." Environmental Science & Technology **36**(3): 484-492.

Tonkin, J. W., Balistrieri, L. S. and Murray, J. W. (2004). "Modeling sorption of divalent metal cations on hydrous manganese oxide using the diffuse double layer model." Applied Geochemistry **19**(1): 29-53.

Trumm, D. (2007). Selection of passive AMD treatment systems – flow charts for New Zealand conditions. AusIMM New Zealand Branch 40th Annual Conference**:** 23-27, AusIMM. Christchurch, New Zealand.

Trumm, D. (2008). Selection of active treatment systems for acid mine drainage. AusIMM New Zealand Branch 41st Annual Conference**:** 563-576, AusIMM. Wellington, New Zealand.

Trumm, D. (2010a). "Selection of active and passive treatment systems for AMD—flow charts for New Zealand conditions." New Zealand journal of geology and geophysics **53**(2-3): 195-210.

Trumm, D. (2010b). "Selection of active and passive treatment systems for AMD in New Zealand - Flow charts for New Zealand conditions." New Zealand Journal of Geology and Geophysics **53**(2-3): 16.

Trumm, D. (2016a). Bellvue Mine - Conceptual AMD Remediation Plan**:** 27, CRL Energy Ltd. Christchurch, New Zealand.

Trumm, D. (2016b). Proposal: Waihi Gold Tailings Drainage Treatment Trials**:** 22. Christchurch, New Zealand.

Trumm, D. (unpublished-a). Bellvue ALL DATA. M. Fairgray, CRL Energy. Christchurch, New Zealand.

Trumm, D. (unpublished-b). Bellvue Data. M. Fairgray, CRL Energy. Christchurch, New Zealand.

Trumm, D., Ball, J., Pope, J. and Weisener, C. (2015a). Passive Treatment of ARD Using Mussel Shells - Part III: Technology Improvement and Future Direction. 10th International Conference on Acid rock Drainage & IMWA Annual Conference, IMWA.

Trumm, D., Black, A., Cavanagh, J., Harding, J., de Joux, A., Moore, T. A. and O'Halloran, K. (2003). Developing assessment methods and remediation protocols for New Zealand sites impacted by Acid Mine Drainage (AMD). Sixth International Conference on Acid Rock Drainage, Cairns, Australia.

Trumm, D., Black, A., Gordon, K., Cavanagh, J., O'Halloran, K. and De Joux, A. (2005a). "Acid Mine Drainage Assessment and Remediation at an Abandoned West Coast Coal Mine". Metal Contaminants in New Zealand. T. A. Moore, A. Black, J. A. Centeno, J. S. Harding and D. A. Trumm**:** 317-340. Resolutionz Press, Christchurch, New Zealand.

Trumm, D. and Cavanagh, J. E. (2006). Investigation of Remediation of Acid-Mine-Impacted Waters at Cannel Creek**:** 17, Landcare Research New Zealand Ltd. New Zealand.

Trumm, D., Lindsay, P. and Watts, M. (2007). Acid Mine Drainage Treatment at Herbert Stream, Stockton. AusIMM New Zealand Branch 40th Annual Conference, AusIMM. Christchurch, New Zealand.

Trumm, D. and Pope, J. (2015). "Passive Treatment of Neutral Mine Drainage at a Metal Mine in New Zealand Using an Oxidizing System and Slag Leaching Bed." Mine Water and the Environment **34**(4): 430-441.

Trumm, D., Pope, J., West, R. and Weber, P. (2016). Bellvue Mine AMD - Downstream geochemistry and proposed treatment. 2016 AusIMM New Zealand Branch Annual Conference**:** 11, AusIMM. Wellington, New Zealand.

Trumm, D., Sapsford, D., Rubio, I. and Pope, J. (2015b). Application of vertical flow reactors in New Zealand for removal of iron from AMD, AusIMM. AusIMM New Zealand Branch Annual Conference.

Trumm, D., Watts, M., Pope, J. and Lindsay, P. (2008). "Using pilot trials to test geochemical treatment of acid mine drainage on Stockton Plateau." New Zealand Journal of Geology and Geophysics **51**(3): 175-186.

Trumm, D. A., Watts, M. and Gunn, P. (2005b). Use of small-scale passive systems for treatment of acid mine drainage. AusIMM New Zealand Branch 38th Annual Conference, AusIMM. Auckland, New Zealand.

Trumm, D. A., Watts, M. and Gunn, P. (2006). AMD Treatment in New Zealand – Use of Small-scale Passive Systems. 7th International Conference on Acid Rock Drainage (ICARD). R. I. Barnhisel**:** 26-30, American Society of Mining and Reclaimation (ASMR). St, Louis, MO.

Turner, D. R., Whitfield, M. and Dickson, A. G. (1981). "The equilibrium speciation of dissolved components in freshwater and seawater at 25°C and 1 atm. Pressure." Geochim. Cosmochim. Acta **45**: 855-881.

U.S. EPA (2001). Mercury Update: Impact on Fish Advisories. EPA Fact Sheet EPA-823-F-01-001, Environmental Protection Agency, Office of Water. Washington DC, USA.

Uster, B. (2015). The use of waste mussel shell in sulfate-reducing bioreactors treating mine-influenced waters. PhD Unpublished PhD Thesis, University of Canterbury.

Uster, B., O'Sullivan, A. D., Ko, S. Y., Evans, A., Pope, J., Trumm, D. and Caruso, B. (2015). "The use of mussel shells in upward-flow sulfate-reducing bioreactors treating acid mine drainage." Mine Water and the Environment **34**(4): 442-454.

Wagemann, R. and Barica, J. (1979). "Speciation and rate of loss of copper from lakewater with implications to toxicity." Water Research **13**(6): 515-523.

Wang, N., Ingersoll, C. G., Ivey, C. D., Hardesty, D. K., May, T. W., Augspurger, T., Roberts, A. D., Van Genderen, E. and Barnhart, M. C. (2010). "Sensitivity of early life stages of freshwater mussels (Unionidae) to acute and chronic toxicity of lead, cadmium, and zinc in water." Environmental Toxicology and Chemistry **29**(9): 2053-2063.

Ward, C. R., Li, Z. and French, D. (2005). "Geological Sources of Metals in Coal and Coal Products". Metal Contaminants in New Zealand. T. A. Moore, A. Black, J. A. Centeno, J. S. Harding and D. A. Trumm**:** 49-79. Resolutionz Press, Christchurch.

Ward, N., Brooks, R. and Reeves, R. (1976). "Copper, cadmium, lead and zinc in soils, stream sediments, waters and natural vegetation around the Tui Mine, Te Aroha, New Zealand." New Zealand Journal of Sciences **19**: 81-89.

Ward, N., Brooks, R. and Roberts, E. (1977). "Contamination of a pasture by a New Zealand base-metal mine." New Zealand Journal of Science **20**: 413-419.

Warren, L. A. and Haack, E. A. (2001). "Biogeochemical controls on metal behaviour in freshwater environments." Earth-Science Reviews **54**(4): 261-320.

Warrender, R., Pearce, N. J. G., Perkins, W. T., Florence, K. M., Brown, A. R., Sapsford, D. J., Bowell, R. J. and Dey, M. (2011). "Field Trials of Low-cost Reactive Media for the Passive Treatment of Circum-neutral Metal Mine Drainage in Mid-Wales, UK." Mine Water and the Environment **30**(2): 82-89.

Washington, J. W., Endale, D. M., Samarkina, L. P. and Chappell, K. E. (2004). "Kinetic control of oxidation state at thermodynamically buffered potentials in subsurface waters." Geochimica et cosmochimica acta **68**(23): 4831-4842.

Waters, A. S. and Webster-Brown, J. G. (2013). "Assessing aluminium toxicity in streams affected by acid mine drainage." Water Science and Technology **67**(8): 1764-1772.

Watten, B. J., Sibrell, P. L. and Schwartz, M. F. (2005). "Acid neutralization within limestone sand reactors receiving coal mine drainage." Environmental Pollution **137**(2): 295-304.

Watzlaf, G. R., Schroeder, K. T., Kleinmann, R. L., Kairies, C. L. and Nairn, R. W. (2004). "The passive treatment of coal mine drainage." United States Department of Energy National Energy Technology Laboratory Internal Publication.

Weber, P., Weisener, C. G., DiLoreto, Z. and Pizey, M. (2015). Passive Treatment of ARD Using Mussel Shells – Part I: System Development and Geochemical Processes. 10th International Conference on Acid Rock Drainage (ICARD) and IMWA Annual Conference, IMWA. Santiago, Chile.

Webster-Brown, J. and Craw, D. (2005). "Examples of Trace Metal Mobility Around Historic and Modern Metals Mines". Metal Contaminants in New Zealand. T. A. Moore, A. Black, J. A. Centeno, J. S. Harding and D. Trumm**:** 213-230. Resolutionz Press, Christchurch, New Zealand.

Webster-Brown, J. G. and Lane, V. (2005). "Modeling seasonal arsenic behavior in the Waikato River, New Zealand". ACS symposium series. **915:** 253-266. Oxford University Press.

Webster, J. and Brown, K. (2001). Results of West Coast ARD Sampling**:** 16, GEOKEM Geochemical Consulting. Auckland, New Zealand.

Webster, J. G. (1995). "Chemical processes affecting trace metal transport in the Waihou river and estuary, New Zealand." New Zealand Journal of Marine and Freshwater Research **29**(4): 539-553.

Webster, J. G., Swedlund, P. J. and Webster, K. S. (1998). "Trace metal adsorption onto an acid mine drainage iron (III) oxy hydroxy sulfate." Environmental Science & Technology **32**(10): 1361-1368.

West, R. A. (2014). Trialling small-scale passive systems for treatment of acid mine drainage: A case study from Bellvue Mine, WestCoast, New Zealand. MWRM Unpublished Thesis, University of Canterbury.

Whelan, K. D. (2007). Plants for Constructed Mine Wetlands in New Zealand: A Case Study at Golden Cross Mine. MSc Unpublished Thesis, University of Auckland.

White, G. P. (1986). "Puhipuhi mercury deposit". Monograph Series on Mineral Deposits. R. W. Henley, J. W. Hedenquist and P. J. Roberts. **26**. Gebruder Borntraeger, Berlin-Stuttgart.

White, S. (2006). Wetland Use in Acid Mine Drainage Remediation**:** 10, Iowa State University.

Wilson, N., Craw, D. and Hunter, K. (2004a). "Antimony distribution and environmental mobility at an historic antimony smelter site, New Zealand." Environmental Pollution **129**(2): 257-266.

Wilson, N., Craw, D. and Hunter, K. (2004b). "Contributions of discharges from a historic antimony mine to metalloid content of river waters, Marlborough, New Zealand." Journal of Geochemical Exploration **84**(3): 127-139.

Winterbourn, M. J., Gregson, K. L. D. and Dolphin, C. H. (2006). "Guide to the Aquatic Insects of New Zealand." Bulletin of the Entomological Society of New Zealand **14**.

Wodzicki, A. and Weissberg, B. G. (1970). "Structural control of base metal mineralisation at the Tui Mine, Te Aroha, New Zealand." New Zealand Journal of Geology and Geophysics **13**(3): 610-630.

World Health Organisation (1971). International Standards for Drinking Water 3rd Ed., World Health Organization. Geneva.

Younger, P., Banwart, S. and Hedin, R. (2002). Mine Water: hydrology, pollution, remediation. Klumer Academic Publishers, Dordrecht.

Yu, J.-Y., Heo, B., Choi, I.-K., Cho, J.-P. and Chang, H.-W. (1999). "Apparent solubilities of schwertmannite and ferrihydrite in natural stream waters polluted by mine drainage." Geochimica et Cosmochimica Acta **63**(19-20): 3407-3416.

Ziemkiewicz, P. F., Skousen, J. G., Brant, D. L., Sterner, P. L. and Lovett, R. J. (1997). "Acid mine drainage treatment with armored limestone in open limestone channels." Journal of Environmental Quality **26**(4): 1017-1024.

Zipper, C. E., Skousen, J. G. and Jage, C. R. (2014). "Passive treatment of acid-mine drainage". Acid Mine Drainage, and Acid Sulfate Soils: Causes Assessment, Prediction, Prevention, and Remediation. J. A. Jacobs, J. H. Lehr and S. M. Testa**:** 339-353. John Wiley & Sons, Inc.

Appendix

Water chemistry; Bellvue Mine

Table A1. Chemistry of Cannel Creek and inputs in November 2016. For trace metals, the dissolved fraction (<0.45um) is shown, and concentrations denoted in bold are above ANZECC (2000) aquatic ecosystem guidelines for the protection of 95% aquatic species, as shown at the base of the table. A.S.= Acid soluble

NB. DOC, NH_4^+ and DRP sampled Jan2017

a) Physicochemical parameters and nutrients

Site	Flow (L/s)	pH	Temp (°C)	DO (mg/L)	Cond (µS/cm)	DOC (mg/L)	NH_4^+ (mg/L)	DRP (mg/L)
Bell1	4.78	5.64	10.0	10.4	52.5	7.32	0.05	<0.01
BellAd	0.62	2.62	13.1	0.6	1460	1.06	0.70	<0.01
Bell2	0.47	2.62	12.3	11.1	1380	6.18	0.46	<0.01
Bell3	nm	3.04	10.2	8.84	380	3.27	0.28	<0.01
Bell4	0.03	3.07	11.6	10.0	364	nm	nm	nm
Bell5	4.3	3.22	10.1	9.99	333	3.42	0.16	<0.01
Bell7	0.02	3.65	12.1	0.41	150	nm	nm	nm
Bell8	0.05	5.80	11.2	2.44	144	5.45	0.13	<0.01
Bell8A	0.01	3.19	11.5	6.88	1290	2.46	1.32	0.02
Bell9	7.5	3.50	10.5	10.0	283	3.02	0.15	<0.01
Bell10	0.15	2.46	13.7	1.32	3250	7.25	1.96	0.07
Bell11	9.1	3.24	10.8	10.4	456	4.72	0.88	<0.01
Bell12	9.0	3.32	10.9	10.5	442	nm	nm	nm
Bell13	1.7	5.87	10.7	8.34	140	11.7	0.04	<0.01
Bell14	10.7	3.73	10.9	9.32	3.38	3.18	0.80	<0.01
Bell18	14.1	4.52	10.8	8.86	265	2.30	0.59	<0.01

b) Major ions

Site	Cl^- (mg/L)	NO_3^- (mg/L)	SO_4^{2-} (mg/L)	HCO_3^- (mg/L)	Na^+ (mg/L)	Mg^{2+} (mg/L)	K^+ (mg/L)	Ca^{2+} (mg/L)
Bell1	12.1	0.10	2.30	91.8	6.80	1.45	0.46	2.90
BellAd	15.2	0.06	470	13.4	10.9	23.9	1.29	70.1
Bell2	14.9	0.08	467	3.50	10.8	24.6	1.25	70.7
Bell3	13.9	0.13	106	12.1	8.74	3.58	1.07	13.3
Bell4	14.7	0.16	93.0	3.52	9.04	3.61	0.86	11.4
Bell5	12.6	0.17	125	9.48	7.19	6.04	0.60	15.8
Bell7	12.9	0.09	34.2	46.3	7.39	1.25	0.71	4.30
Bell8	11.1	0.09	13.0	98.8	7.72	2.47	0.56	26.9
Bell8A	12.4	0.13	533	36.3	11.3	85.5	2.19	127
Bell9	12.4	0.19	118	17.6	7.33	6.95	0.63	18.2
Bell10	17.9	0.12	1010	98.8	17.1	150	2.12	247
Bell11	12.3	0.16	194	8.58	7.60	12.2	0.68	25.8
Bell12	12.5	0.18	192	7.36	7.89	12.4	0.72	28.3
Bell13	16.9	0.34	11.5	63.2	10.4	2.59	0.72	21.8
Bell14	13.9	0.17	158	15.2	8.98	10.9	0.76	28.4
Bell18	15.8	0.16	128	4.98	9.85	8.90	0.75	25.0

c) Trace elements

Site	Fe (mg/L)		Mn (mg/L)		Al (mg/L)		Cu (µg/L)		Pb (µg/L)	
	Dissolved	A. S.	Dissolved	A. S.	Dissolved	A. S.	Dissolved	A. S.	Dissolved	A. S.
Bell1	0.348	0.608	0.011	0.014	0.095	0.143	0.27	0.30	<0.05	0.09
BellAd	82.6	83.5	0.927	0.974	38.8	41.7	1.15	1.28	0.17	0.19
Bell2	65.9	64.4	0.945	0.938	40.2	40.3	1.31	1.25	0.28	0.26
Bell3	7.57	7.48	0.296	0.280	2.42	2.37	0.92	0.82	0.70	0.70
Bell4	1.17	1.28	0.321	0.339	3.04	3.23	2.15	2.18	1.36	1.41
Bell5	5.77	6.46	0.183	0.193	6.00	6.38	0.67	0.73	0.15	0.20
Bell7	5.30	5.41	0.086	0.087	0.330	0.340	0.13	0.12	0.22	0.23
Bell8	0.148	1.45	0.014	0.018	0.018	0.033	0.11	0.09	<0.05	0.02
Bell8A	24.5	22.9	1.88	1.93	29.6	30.3	0.13	0.31	0.15	0.32
Bell9	4.89	5.81	0.181	0.179	4.76	4.85	0.55	0.56	0.16	0.16
Bell10	149	149	6.54	6.46	164	164	2.86	2.96	0.18	0.20
Bell11	8.98	10.6	0.407	0.400	10.4	10.6	0.69	0.70	0.18	0.20
Bell12	8.75	9.89	0.404	0.414	10.1	10.2	0.69	0.68	0.19	0.22
Bell13	0.508	0.674	0.019	0.020	0.080	107	0.27	0.30	0.10	0.12
Bell14	5.33	10.3	0.335	0.335	8.12	8.38	0.63	0.71	0.13	0.23
Bell18	2.07	3.96	0.258	0.260	5.68	6.18	0.45	0.53	0.05	0.11
ANZECC	-			*1.90*		*0.055*		*1.4*		*3.4*

Site	Zn (µg/L)		Cd (µg/L)		Ni (µg/L)		As (µg/L)	
	Dissolved	A. S.	Dissolved	A. S.	Dissolved	A. S.	Dissolved	A. S.
Bell1	2.27	1.89	<0.05	<0.05	0.56	0.61	0.14	0.16
BellAd	430	442	0.31	0.31	142	147.	0.68	0.70
Bell2	429	412.	0.30	0.29	141	138	0.69	0.68
Bell3	29.5	27.3	<0.05	<0.05	9.67	9.20	0.88	0.99
Bell4	31.7	33.5	0.05	0.05	11.2	11.7	0.09	0.10
Bell5	68.4	70.4	0.05	0.05	21.0	21.8	0.17	0.22
Bell7	13.2	11.7	<0.05	<0.05	2.12	2.12	0.36	0.41
Bell8	<0.75	0.43	<0.05	<0.05	0.40	0.37	0.15	0.23
Bell8A	435	430	0.31	0.30	199	194	0.50	0.50
Bell9	58.6	57.9	<0.05	<0.05	18.2	18.1	0.16	0.26
Bell10	1140	1120	0.70	0.70	511	499	1.12	1.13
Bell11	105	103	0.07	0.07	35.9	36.0	0.19	0.35
Bell12	98.9	99.8	0.07	0.06	35.0	35.6	0.18	0.29
Bell13	1.19	0.91	<0.05	<0.05	0.64	0.66	0.24	0.27
Bell14	79.8	81.6	0.05	0.05	28.3	28.2	0.15	0.38
Bell18	59.5	59.3	<0.05	<0.05	21.1	21.3	0.12	0.21
ANZECC		*8.0*		*0.2*		*11*		*24/13*

Table A2. Chemistry of Cannel Creek and inputs in May 2017. For trace elements, the ANZECC (2000) aquatic ecosystem guidelines for the protection of 95% aquatic species are shown at the base of the table. A.S.= Acid soluble

a) Physicochemical parameters and nutrients

Site	Flow (L/s)	pH	Temp (°C)	DO (mg/L)	Cond (µS/cm)	DOC (mg/L)	NH_4^+ (mg/L)	DRP (mg/L)	Fe^{2+} (mg/L)
Bell1	7.8	6.99	8.61	11.09	51	6.95	<0.01	<0.01	0.11
BellAd	0.95	2.69	13.15	1.14	1470	3.06	0.29	<0.01	11.24
Bell2	0.90	2.67	12.24	10.61	1420	2.18	0.39	<0.01	2.41
Bell3	7.1	3.31	9.14	11.23	355	5.53	0.08	<0.01	0.24
Bell4	0.17	3.18	9.54	11.94	313	nm	<0.01	<0.01	0.89
Bell5		3.71	9.71	11.69	170	2.85	0.03	<0.01	0.33
Bell6a	0.10	3.34	11.41	7.08	207	nm	<0.01	<0.01	nm
Bell6b	0.14	4.72	11.72	10.81	93	nm	<0.01	<0.01	nm
Bell8	0.16	6.43	10.01	4.43	120	4.34	0.04	<0.01	1.02
Bell8A	0.02	3.36	10.26	9.27	1120		0.47	0.011	2.25
Bell9	11.0	3.60	8.06	11.98	260	2.67	0.06	<0.01	0.95
Bell10	0.13	2.55	13.79	4.07	3270	3.48	1.64	0.022	2.74
Bell11	11.7	3.37	8.00	12.07	382	2.86	0.19	<0.01	1.35
Bell12	19.1	3.45	7.94	12.25	368	nm	0.19	<0.01	nm
Bell13	2.7	7.28	9.24	9.30	115	4.60	<0.01	<0.01	0.06
Bell14	16.4	3.81	8.17	11.95	279	2.99	0.15	<0.01	0.97
Bell18	17.9	4.87	7.66	13.39	190	3.02	0.11	<0.01	0.61

b) Major ions

Site	Cl^- (mg/L)	NO_3^- (mg/L)	SO_4^{2-} (mg/L)	HCO_3^- (mg/L)	Na^+ (mg/L)	Mg^{2+} (mg/L)	K^+ (mg/L)	Ca^{2+} (mg/L)
Bell1	10.6	0.25	2.24	15.2	6.81	1.31	0.50	3.29
BellAd	11.9	0.23	642	50.7	11.2	23.2	1.23	67.0
Bell2	15.9	0.39	712	3.52	11.3	25.7	1.19	68.6
Bell3	10.8	0.31	22.1	11.2	7.31	1.54	0.53	4.10
Bell4	14.2	0.32	79.5	9.56	9.33	3.05	1.02	11.0
Bell5	12.4	0.32	52.4	8.11	7.26	3.20	0.54	7.57
Bell6a	12.1	0.29	25.3	6.44	8.83	1.46	0.86	6.92
Bell6b	8.79	0.67	32.3	32.2	6.27	0.80	0.70	2.51
Bell8	8.84	0.28	10.7	104	6.61	1.81	0.44	22.8
Bell8A	13.9	0.91	771	25.0	11.4	78.7	2.02	124
Bell9	11.0	0.64	116	12.0	7.69	7.14	0.69	18.1
Bell10	20.7	0.24	2380	44.4	18.0	153	2.11	235
Bell11	11.3	0.34	190	8.43	8.51	14.1	0.76	28.9
Bell12	11.4	0.32	200	8.44	8.76	14.0	0.76	27.5
Bell13	14.3	0.39	10.8	58.2	10.7	2.45	0.77	20.4
Bell14	12.1	0.37	156	13.4	9.16	11.8	0.76	27.2
Bell18	14.0	0.44	110	6.91	10.5	8.90	0.79	24.0

c) Trace elements

Site	Fe (mg/L)		Mn (mg/L)		Al (mg/L)		Cu (µg/L)		Pb (µg/L)	
	Dissolved	A. S.	Dissolved	A. S.	Dissolved	A. S.	Dissolved	A. S.	Dissolved	A. S.
Bell1	0.46	0.718	0.012	0.012	0.17	0.204	2.32	2.62	<0.05	<0.05
BellAd	59.7	59.9	0.713	0.751	44.9	45.9	3.69	2.82	0.15	0.16
Bell2	60.5	60.3	0.849	0.854	54.4	53.4	3.10	3.51	<0.05	0.06
Bell3	3.19	1.140	0.079	0.028	3.44	0.565	2.13	2.41	<0.05	<0.05
Bell4	3.54	3.88	0.158	0.160	1.82	1.92	3.06	2.93	0.79	0.75
Bell5	2.02	3.10	0.074	0.080	2.76	3.00	2.62	2.41	<0.05	<0.05
Bell6a	1.55	1.91	0.049	0.058	0.18	0.229	1.63	2.01	<0.05	0.08
Bell6b	1.35	1.32	0.056	0.052	0.38	0.364	2.28	1.96	0.41	0.48
Bell8	1.52	1.66	0.018	0.020	0.06	0.066	2.20	1.35	<0.05	<0.05
Bell8A	20.9	24.1	1.69	1.61	30.6	29.5	1.66	0.31	<0.05	<0.05
Bell9	5.76	6.37	0.169	0.169	5.77	5.79	3.09	0.92	<0.05	<0.05
Bell10	136	118	7.05	6.07	231	200	6.15	3.99	0.11	0.08
Bell11	8.62	10.3	0.369	0.398	12.0	12.4	2.59	2.73	0.11	0.11
Bell12	9.08	10.2	0.404	0.397	12.6	12.7	3.38	1.17	<0.05	<0.05
Bell13	0.48	0.678	0.014	0.017	0.17	0.188	2.66	2.12	<0.05	<0.05
Bell14	5.25	8.17	0.310	0.317	9.23	9.70	2.23	2.62	<0.05	<0.05
Bell18	1.53	4.29	0.229	0.224	6.11	6.64	1.85	2.48	<0.05	<0.05
ANZECC	-			*1.9*		*0.055*		*1.4*		*3.4*

Site	Zn (µg/L)		Cd (µg/L)		Ni (µg/L)		As (µg/L)		Co (µg/L)	
	Dissolved	A. S.	Dissolved	A. S.	Dissolved	A. S.	Dissolved	A. S.	Dissolved	A. S.
Bell1	1.81	1.42	<0.05	<0.05	0.65	0.63	<0.05	<0.05	0.18	0.19
BellAd	322	317	0.12	<0.05	103	107	0.19	0.10	40.7	41.68
Bell2	353	355	0.17	0.16	121	121	0.27	0.19	46.9	47.52
Bell3	30.0	4.82	<0.05	<0.05	9.99	1.65	<0.05	<0.05	3.78	0.64
Bell4	20.7	20.8	<0.05	<0.05	7.05	7.31	<0.05	<0.05	2.95	3.20
Bell5	25.3	23.7	<0.05	<0.05	8.22	12.9	<0.05	<0.05	3.38	3.53
Bell6a	9.91	7.88	<0.05	<0.05	1.47	1.71	<0.05	<0.05	0.54	0.71
Bell6b	8.83	24.1	<0.05	<0.05	2.03	1.84	<0.05	<0.05	0.58	0.53
Bell8	<0.75	0.38	<0.05	<0.05	0.29	0.24	<0.05	<0.05	<0.05	0.08
Bell8A	314	330	<0.05	0.13	142	137	0.05	0.09	71.2	68.09
Bell9	51.4	53.9	<0.05	<0.05	17.9	17.4	<0.05	<0.05	7.42	7.33
Bell10	1320	1230	0.95	0.94	559	486	1.54	1.20	284	244.69
Bell11	96.5	92.6	0.05	<0.05	34.1	35.3	<0.05	<0.05	15.4	16.49
Bell12	75.5	104	<0.05	<0.05	34.1	36.4	<0.05	<0.05	16.5	16.85
Bell13	1.79	1.66	<0.05	<0.05	0.74	0.70	<0.05	<0.05	0.11	0.13
Bell14	60.9	66.6	<0.05	<0.05	26.7	27.8	<0.05	<0.05	12.4	12.92
Bell18	50.0	49.1	<0.05	<0.05	19.7	19.3	<0.05	<0.05	9.35	8.80
ANZECC		8.0		0.2		11		13/24		

Table A3. Chemistry of Cannel Creek and inputs in Dec 2017. For trace elements, the ANZECC (2000) aquatic ecosystem guidelines for the protection of 95% aquatic species are shown at the base of the table.

a) Physicochemical parameters and nutrients

Site	Flow (L/s)	pH	Temp (°C)	DO (mg/L)	Cond (µS/cm)	DOC (mg/L)	NH_4^+ (mg/L)	DRP (mg/L)	Fe^{2+} (mg/L)	S^{2-} (mg/L)
Bell1							<0.01	<0.01		<0.03
Tank2	0.06	7.3					176	0.72		0.06
Tank3	0.07						613	3.21		0.22
Tank5	0.09	7.8					630	2.48		0.18

b) Major ions

Site	Cl^- (mg/L)	NO_3^- (mg/L)	SO_4^{2-} (mg/L)	HCO_3^- (mg/L)	Na^+ (mg/L)	Mg^{2+} (mg/L)	K^+ (mg/L)	Ca^{2+} (mg/L)
Bell1	11.8	0.36	2.94					
Tank2	268	0.49	994					
Tank3	373	1.10	782					
Tank5	316	15.1	745					

c) Trace elements (dissolved)

Site	Fe (mg/L)	Mn (mg/L)	Al (mg/L)	Cu (µg/L)	Pb (µg/L)	Zn (µg/L)	Cd (µg/L)	Ni (µg/L)	As (ug/L)	Co (µg/L)
Bell1										
Tank2	2.22	0.38	0.05	2.29	0.85	9.95	0.19	5.55	44.2	3.33
Tank3	0.24	0.23	0.15	1.86	0.68	16.9	0.21	5.84	118	1.30
Tank5	0.46	0.15	0.19	3.16	0.75	13.9	0.22	6.21	131	1.64
ANZECC	-	*1.9*	*0.055*	*1.4*	*3.4*	*8.0*	*0.2*	*11*		*ngv*

Table A4. Chemistry of Cannel Creek and inputs in Feb 2018. For trace elements, the ANZECC (2000) aquatic ecosystem guidelines for the protection of 95% aquatic species are shown at the base of the table. A.S.= Acid soluble

a) Physicochemical parameters and nutrients

Site		pH	Temp (°C)	Cond (µS/cm)	DO (mg/L)	DOC (mg/L)	NH_4^+ (mg/L)	DRP (mg/L)	Ferrous Iron (mg/L)	Sulfide (mg/L)
Bell1	64.0	6.18	14.6	42.2	9.83	15.7	0.02	<0.01	0.13	<0.03
BellAd	3.34	2.49	13.8	1260	5.60	3.01	0.22	<0.01	4.50	<0.03
Tank 4	0.19	7.01	17.1	1300	3.14		2.97	0.147	0.85	0.03
Bell3	55.0	4.82	14.8	434	7.51	14.9	0.11	<0.01	0.20	0.03
Bell4	0.76	3.05	14.9	362	9.25		0.03	<0.01	nm	0.03
Bell5	51.2	4.38	14.9	140	8.93	4.10	0.15	<0.01	0.33	0.03
Bell7a	1.36	3.23	17.2	240	5.39		0.01	<0.01	0.73	<0.03
Bell7b	0.24	3.27	16.9	238	0.63		0.04	<0.01	3.50	<0.03
Bell8	0.47	6.29	14.6	134	3.82	12.5	0.14	<0.01	0.50	<0.03
Bell8A	0.75	4.13	14.1	255	9.72	6.76	0.17	<0.01	1.68	<0.03
Bell9	12.5	5.03	14.1	220	9.31	3.80	0.14	<0.01	0.93	<0.03
Bell10	0.24	2.51	14.6	2940	5.28		2.04	0.056	3.70	<0.03
Bell11	19.9	4.01	13.8	275	8.55	6.05	0.24	<0.01	1.13	<0.03
Bell12	25.6	4.36	13.7	266	9.87		0.24	<0.01	1.30	<0.03
Bell13	6.7	6.59	13.9	112	7.87		0.03	<0.01	0.10	<0.03
Bell14	32.3	4.84	13.7	223	9.77		0.18	<0.01	1.02	<0.03
Bell18	31.5	5.05	14.2	202	10.03		0.16	<0.01	0.72	<0.03

b) Major ions

Site	Cl^- (mg/L)	NO_3^- (mg/L)	SO_4^{2-} (mg/L)	HCO_3^- (mg/L)	Na^+ (mg/L)	Mg^{2+} (mg/L)	K^+ (mg/L)	Ca^{2+} (mg/L)
Bell1	2.79	0.10	2.27	<0.01	5.97	0.81	0.37	1.48
BellAd	4.70	0.08	186	25.7	8.42	14.2	0.85	42.9
Tank4	8.03	0.09	451	417	13.4	16.7	0.95	313
Bell3	5.39	0.18	25.0	4.75	5.73	1.41	0.36	11.3
Bell4	7.12	0.11	45.7	<0.0	8.23	2.73	0.75	9.74
Bell5	11.2	0.23	48.4	1.91	5.90	2.30	0.39	13.8
Bell7a	4.65	0.32	13.4	21.5	6.41	1.00	0.51	4.17
Bell7b	4.37	0.08	21.2	45.3	6.72	1.28	0.50	5.68
Bell8	7.53	0.11	36.5	81.9	6.42	1.58	0.37	22.2
Bell8A	28.4	3.68	117	<0.01	6.85	6.02	0.54	27.9
Bell9	12.4	0.83	86.2	2.30	7.01	4.03	0.51	25.7
Bell10	19.7	0.17	2260	29.7	14.2	107	1.84	205
Bell11	12.7	0.27	126	1.18	6.43	5.36	0.50	28.4
Bell12	12.7	0.27	128	0.05	6.55	5.56	0.53	30.2
Bell13	18.3	0.12	10.9	30.8	8.77	1.50	0.53	12.8
Bell14	14.0	0.24	100	1.95	7.65	4.98	0.56	26.6
Bell18	16.5	0.22	78.6	<0.01	8.93	4.42	0.58	22.8

c) Trace elements

Site	Fe (mg/L)		Mn (mg/L)		Al (mg/L)		Cu (µg/L)		Pb (µg/L)	
	Dissolved	A. S.	Dissolved	A. S.	Dissolved	A. S.	Dissolved	A. S.	Dissolved	A. S.
Bell1	0.41	0.41	0.02	0.02	0.27	0.33	0.56	0.57	0.17	0.10
BellAd	24.3	23.8	0.41	0.41	19.7	21.6	1.50	1.61	0.17	0.22
Tank4	1.04	0.84	0.52	0.49	0.02	0.00	<0.05	0.02	0.04	0.05
Bell3	1.05	0.37	0.05	0.04	0.62	0.26	0.79	0.65	0.17	0.11
Bell4	2.16	1.92	0.09	0.09	1.51	1.49	2.10	1.94	1.53	1.38
Bell5	1.05	0.48	0.07	0.06	1.05	0.61	1.13	0.72	0.25	0.17
Bell7a	1.19	1.02	0.07	0.06	0.17	0.15	0.82	0.70	0.35	0.27
Bell7b	4.39	4.14	0.09	0.08	0.58	0.57	0.47	0.47	0.52	0.44
Bell8	0.58	0.53	0.02	0.01	0.05	0.03	0.26	0.20	0.05	0.05
Bell8A	2.27	1.58	0.18	0.16	2.14	1.93	1.01	0.93	0.29	0.19
Bell9	1.41	0.80	0.12	0.11	1.23	0.32	1.00	0.74	0.22	0.09
Bell10	89.5	90.1	5.86	5.92	122	128	2.60	2.71	0.31	0.34
Bell11	2.46	1.78	0.20	0.19	3.30	2.61	1.05	0.91	0.31	0.23
Bell12	2.67	1.44	0.21	0.20	3.34	2.77	1.02	1.08	0.32	1.62
Bell13	0.43	0.30	0.01	0.01	0.12	0.07	0.42	0.40	0.24	0.12
Bell14	2.09	1.04	0.17	0.16	2.63	1.62	1.07	0.71	0.27	0.12
Bell18	1.38	0.60	0.14	0.13	1.67	0.29	0.68	0.46	0.19	0.07
ANZECC	-			*1.9*		*0.055*		*1.4*		*3.4*

Site	Zn (µg/L)		Cd (µg/L)		Ni (µg/L)		As (µg/L)		Co (µg/L)	
	Dissolved	A. S.	Dissolved	A. S.	Dissolved	A. S.	Dissolved	A. S.	Dissolved	A. S.
Bell1	2.71	3.14	<0.05	<0.05	0.81	0.95	0.16	0.48	0.23	0.24
BellAd	205	197	0.17	0.18	63.0	63.8	0.52	0.76	21.7	21.4
Tank4	0.17	0.22	<0.05	<0.05	0.57	0.41	0.40	0.50	0.21	0.20
Bell3	9.93	8.69	<0.05	<0.05	2.65	2.30	0.28	0.29	0.93	0.82
Bell4	31.0	29.3	<0.05	0.05	8.66	8.36	0.39	0.26	3.20	3.15
Bell5	17.3	15.1	<0.05	<0.05	5.42	4.75	0.27	0.25	2.04	1.88
Bell7a	11.0	9.82	<0.05	<0.05	2.29	1.85	0.15	0.20	0.72	0.69
Bell7b	12.7	12.2	<0.05	<0.05	4.08	3.38	0.28	0.26	1.05	0.96
Bell8	1.27	0.81	<0.05	<0.05	0.46	0.69	0.35	0.35	0.10	0.08
Bell8A	41.4	38.5	<0.05	<0.05	13.7	13.5	0.29	0.23	6.14	5.68
Bell9	24.9	23.9	<0.05	<0.05	8.13	8.09	0.35	0.24	3.51	3.29
Bell10	1250	1250	0.65	0.71	412	426	1.41	1.43	185	191
Bell11	48.0	45.7	0.05	0.05	15.2	14.6	0.27	0.28	6.48	6.10
Bell12	47.2	56.3	<0.05	0.06	15.4	14.0	0.25	0.22	6.50	6.17
Bell13	1.27	1.32	<0.05	<0.05	1.31	0.73	0.28	0.27	0.11	0.08
Bell14	37.0	36.6	<0.05	<0.05	12.6	12.1	0.28	0.23	4.92	5.07
Bell18	30.1	31.1	<0.05	0.09	10.1	9.32	0.26	0.17	4.05	3.93
ANZECC		*8.0*		*0.2*		*11*		*13/24*		

Table A5. Chemistry of Cannel Creek and inputs in Apr 2018. For trace elements, the ANZECC (200) aquatic ecosystem guidelines for the protection of 95% aquatic species are shown at the base of the table. A.S.= Acid soluble

a) Physicochemical parameters and nutrients

Site	Flow (L/s)	pH	Temp (°C)	DO (mg/L)	Cond (µS/cm)	DOC (mg/L)	NH_4^+ (mg/L)	DRP (mg/L)	Fe^{2+} (mg/L)
Bell1	4.70	6.77	11.6	10.5	68.3	5.28	<0.01	0.10	<0.01
BellAd	1.03	2.61	13.9	6.71	1680	2.61	0.09	0.16	2.55
Tank1	0.13	7.28	13.5	0.18	1470	2.24	1.10	0.19	1.34
Tank5	0.13	6.80	13.9	0.18	1480	4.64	0.85	0.10	1.70
Bell3	6.20	5.62	11.8	9.95	287	3.16	0.21	0.11	0.32
Bell5	7.00	5.52	11.8	9.96	331	2.83	0.18	0.10	0.49
Bell8	0.03	6.70	11.7	3.46	182	4.65	0.02	0.10	0.22
Bell8A	0.45	4.74	11.0	10.9	374	-	0.16	0.10	-
Bell9	7.30	5.70	11.1	10.8	333	2.37	0.16	0.10	-
Bell10	0.12	2.66	14.5	5.50	3990	3.23	1.24	0.10	-
Bell11	7.6	4.01	10.9	10.7	533	2.27	0.23	0.10	0.80
Bell12	8.9	4.26	10.9	10.9	522	-	0.31	0.10	-
Bell13	1.6	6.23	11.3	9.14	192	5.52	0.01	0.10	0.16
Bell14	10.5	4.84	11.0	10.7	429		0.26	0.09	2.46
Bell18	15.3	5.05	11.8	10.6	350	2.37	0.13	0.10	0.01

b) Major ions

Site	Cl^- (mg/L)	NO_3^- (mg/L)	SO_4^{2-} (mg/L)	HCO_3^- (mg/L)	Na^+ (mg/L)	Mg^{2+} (mg/L)	K^+ (mg/L)	Ca^{2+} (mg/L)
Bell1	10.2	0.13	1.75	7.24	4.98	0.93	0.38	2.60
BellAd	26.8	23.0	764	16.5	6.26	11.7	1.30	36.5
Tank1	12.4	0.03	379	344	8.26	12.0	0.79	230
Tank5	3.77	0.03	270	348	8.80	12.9	0.85	246
Bell3	25.5	0.22	184	40.4	6.02	4.05	0.52	31.6
Bell5	12.9	0.31	17.8	22.0	6.26	5.40	0.52	31.0
Bell8	7.41	0.32	87.4	101	5.32	2.01	0.55	19.0
Bell8A	17.7	0.10	191	<5	6.96	10.0	0.67	34.6
Bell9	12.9	0.36	134	7.01	6.46	6.87	0.59	30.0
Bell10	25.2	2.86	3510	37.4	13.2	139	1.86	175
Bell11	12.9	0.53	190	5.13	6.02	11.6	0.62	34.0
Bell12	7.82	0.42	100	1.82	5.98	11.5	0.59	32.8
Bell13	10.2	0.46	9.33	59.1	8.12	2.48	0.68	17.0
Bell14	8.43	0.64	89.8	7.39	6.93	11.0	0.65	32.8
Bell18	2.73	0.35	19.2	<5	8.33	7.74	0.65	25.9

c) Trace elements

Site	Fe (mg/L)		Mn (mg/L)		Al (mg/L)		Cu (µg/L)		Pb (µg/L)	
	Dissolved	A. S.	Dissolved	A. S.	Dissolved	A. S.	Dissolved	A. S.	Dissolved	A. S.
Bell1	0.27	0.47	0.01	0.009	0.08	0.095	3.90**	0.76	0.05	0.12
BellAd	2.36	22.9	0.43	0.428	19.2	18.8	0.97	2.08	0.07	0.19
Tank1	0.91	0.94	0.50	0.458	0.01	0.018	<0.05	<0.05	<0.05	<0.05
Tank5	1.16	1.36	0.48	0.488	0.03	0.023	<0.05	<0.05	<0.05	<0.05
Bell3	0.29	1.45	0.10	0.128	0.14	1.75	0.27	0.88	<0.05	0.22
Bell5	0.03	1.26	0.08	0.143	0.01	1.52	<0.05	0.55	<0.05	0.23
Bell8	0.26	0.57	0.01	0.015	0.01	0.016	0.12	0.32	<0.05	0.07
Bell8A	1.98	2.75	0.18	0.238	0.96	2.20	0.29	0.50	<0.05	0.25
Bell9	1.41	1.91	0.14	0.162	0.06	1.21	0.19	0.49	<0.05	0.22
Bell10	16.5	12.4	5.89	6.559	127	138	2.73	3.15	0.21	0.32
Bell11	3.39	4.19	0.32	0.374	4.54	5.95	0.51	0.64	0.07	0.26
Bell12	3.00	4.81	0.32	0.370	4.88	5.84	0.51	0.60	0.07	0.19
Bell13	0.36	0.54	0.02	0.021	0.05	0.07	0.21	0.35	<0.05	0.21
Bell14	3.86	4.02	0.27	0.327	4.31	5.17	0.47	0.63	0.14	0.23
Bell18	1.14	2.16	0.20	0.217	0.95	2.83	0.25	0.50	<0.05	0.18
ANZECC				*1.9*		*0.055*		*1.4*		*3.4*

Site	Zn (µg/L)		Cd (µg/L)		Ni (µg/L)		As (µg/L)		Co (µg/L)	
	Dissolved	A. S.	Dissolved	A. S.	Dissolved	A. S.	Dissolved	A. S.	Dissolved	A. S.
Bell1	4.70	1.13	<0.05	<0.05	0.90	1.00	0.12	0.14	0.15	0.15
BellAd	231	234	0.20	0.25	70.2	69.7	0.32	0.26	22.6	23.1
Tank1	<0.05	<0.05	<0.05	<0.05	0.82	0.64	0.12	0.12	0.51	0.52
Tank5	<0.05	<0.05	<0.05	<0.05	0.72	0.75	0.13	0.11	1.16	1.11
Bell3	23.8	27.3	<0.05	0.08	7.47	8.22	0.11	0.29	2.45	2.48
Bell5	19.5	29.3	<0.05	0.08	6.48	9.85	0.06	0.48	2.21	3.24
Bell8	0.55	1.84	<0.05	0.07	0.25	1.01	0.16	0.45	0.09	<0.05
Bell8A	41.9	48.8	0.06	0.08	14.4	17.7	0.18	0.46	5.99	6.87
Bell9	29.5	30.2	<0.05	0.05	10.2	10.7	0.19	0.46	3.79	3.91
Bell10	1510	1520	0.96	0.92	503	539	1.06	1.46	222	232
Bell11	81.1	85.7	0.07	0.09	27.2	28.4	0.35	0.46	11.4	11.6
Bell12	79.7	80.3	0.08	0.08	26.3	28.1	0.25	0.34	11.1	11.4
Bell13	0.48	2.23	<0.05	<0.05	0.96	1.17	0.16	0.25	0.14	<0.05
Bell14	66.7	77.0	0.08	0.07	21.9	24.9	0.32	0.31	9.22	9.91
Bell18	45.4	45.5	0.05	0.08	16.1	16.3	0.12	0.25	6.90	6.55
ANZECC		*8.0*		*0.2*		*11*		*13/24*		

Table A6. Chemistry of Cannel Creek and inputs in June 2018. For trace elements, the ANZECC (2000) aquatic ecosystem guidelines for the protection of 95% aquatic species are shown at the base of the table. A.S.= Acid soluble

a) Physicochemical parameters and nutrients

Site	Flow (L/s)	pH	Temp (°C)	DO (mg/L)	Cond (µS/cm)	Flow (L/s)	DOC (mg/L)	NH_4^+ (mg/L)	DRP (mg/L)	Fe^{2+} (mg/L)	S^{2-} (mg/L)
Bell1	7.5	6.58	8.5	10.49	71.6	7.5	1.45	0.01	<0.01	0.01	<0.03
BellAd	0.52	3.11	12.5	4.71	1670	0.52	2.14	0.24	<0.01	9.40	<0.03
Tank1	0.17	7.14	11.1	4.65	1530	0.17	6.21	1.02	<0.01	0.83	0.03
Bell3	7.1	6.95	8.7	9.90	229	7.1	4.09	0.09	<0.01	0.06	0.03
Bell5	7.4	6.35	8.8	9.96	251	7.4	4.38	0.09	<0.01	0.11	0.03
Bell8	0.05	6.24	9.1	3.97	218	0.05	3.69	0.04	<0.01	0.67	<0.03
Bell9	20.6	4.30	9.5	-	287	20.6	4.96	0.09	<0.01	0.76	<0.03
Bell10	6	2.65	13.3	-	3980	6.0	2.17	0.38	<0.01	>16.5	<0.03
Bell11	23.1	4.64	9.0	-	441	23.1	2.22	0.18	<0.01	1.31	<0.03
Bell12	14.2	4.91	9.0	-	442	14.2	-	0.22	<0.01	-	<0.03
Bell13	7.5	7.00	9.9	-	159	7.5	5.10	0.01	<0.01	0.02	<0.03
Bell14	21.7	5.68	9.3	-	332	21.7	2.00	0.15	<0.01	1.27	<0.03
Bell18	-	6.75	9.6	-	273	-	-	0.09	<0.01	-	-

b) Major ions

Site	Cl^- (mg/L)	NO_3^- (mg/L)	SO_4^{2-} (mg/L)	HCO_3^- (mg/L)	Na^+ (mg/L)	Mg^{2+} (mg/L)	K^+ (mg/L)	Ca^{2+} (mg/L)
Bell1	13.8	0.17	2.46		7.24	1.54	0.64	3.37
BellAd	17.7	0.13	607		10.4	20.7	1.36	56.5
Tank1	17.6	0.14	541		14.3	22.3	1.33	332
Bell3	12.9	0.38	64.7		7.68	3.40	0.65	28.5
Bell5	14.0	0.36	72.5		7.99	4.47	0.64	31.1
Bell8	8.11	0.14	26.3		7.55	2.74	0.45	31.1
Bell9	13.7	0.39	93.0		7.97	5.91	0.74	33.4
Bell10	21.1	0.14	2590		18.4	153	2.24	233
Bell11	11.7	0.34	148		8.22	11.1	0.73	43.9
Bell12	13.4	0.34	174		8.80	12.5	0.80	47.2
Bell13	14.0	0.24	10.3		10.1	2.23	0.72	17.2
Bell14	9.01	0.25	57.8		9.15	8.42	0.74	35.7
Bell18	7.64	0.21	31.8		10.9	6.35	0.85	27.7

c) Trace elements

Site	Fe (mg/L)		Mn (mg/L)		Al (mg/L)		Cu (µg/L)		Pb (µg/L)	
	Dissolved	A. S.	Dissolved	A. S.	Dissolved	A. S.	Dissolved	A. S.	Dissolved	A. S.
Bell1	0.23	0.55	0.01	0.03	0.08	0.13	0.18	0.25	<0.05	<0.05
BellAd	37.7	38.7	0.65	0.66	35.0	33.8	1.04	0.95	<0.05	<0.05
Tank1	0.44	0.50	0.70	0.70	0.01	0.01	<0.05	0.00	<0.05	<0.05
Bell3	0.26	0.76	0.08	0.08	0.11	0.50	0.20	0.31	<0.05	<0.05
Bell5	0.22	0.96	0.11	0.10	0.07	0.88	0.22	0.36	<0.05	<0.05
Bell8	0.71	0.89	0.02	0.02	0.01	0.02	<0.05	0.00	<0.05	<0.05
Bell9	0.62	1.71	0.13	0.14	0.07	1.37	0.10	0.49	<0.05	<0.05
Bell10	**77.1	31.6	6.70	6.71	177	170	2.65	2.77	<0.05	0.06
Bell11	1.23	4.17	0.27	0.30	2.40	5.31	0.18	0.64	<0.05	<0.05
Bell12	2.00	5.12	0.37	0.35	5.24	5.87	0.31	1.07	<0.05	<0.05
Bell13	0.27	0.52	0.01	0.02	0.07	0.11	0.16	0.28	<0.05	<0.05
Bell14	1.17	3.81	0.21	0.22	0.39	3.84	0.13	0.37	<0.05	<0.05
Bell18	0.37	8.25	0.22	0.16	0.01	7.45	0.45	0.88	<0.05	<0.05
ANZECC				*1.9*		*0.055*		*1.4*		*3.4*

Site	Zn (µg/L)		Cd (µg/L)		Ni (µg/L)		As (µg/L)		Co (µg/L)	
	Dissolved	A. S.	Dissolved	A. S.	Dissolved	A. S.	Dissolved	A. S.	Dissolved	A. S.
Bell1	<0.05	<0.05	<0.05	<0.05	0.53	0.52	0.10	0.11	0.18	0.46
BellAd	306	312	0.19	0.17	97.5	97.8	0.29	0.31	35.0	34.7
Tank1	49.6	<0.05	<0.05	<0.05	0.81	0.71	0.07	0.04	2.59	2.42
Bell3	4.66	5.22	<0.05	<0.05	2.15	2.29	0.06	0.11	1.04	0.83
Bell5	8.88	7.76	<0.05	<0.05	3.68	3.85	0.09	0.09	1.74	1.73
Bell8	<0.05	<0.05	<0.05	<0.05	0.17	0.19	0.13	0.12	0.04	0.05
Bell9	9.72	11.95	<0.05	<0.05	5.10	5.37	0.09	0.15	2.32	2.45
Bell10	1370	1380	1.00	0.68	504	510	0.95	1.09	237	241
Bell11	40.9	47.8	0.05	<0.05	15.2	18.8	0.11	0.23	7.66	8.27
Bell12	58.6	56.2	0.11	0.11	22.5	21.3	0.20	0.15	10.6	9.59
Bell13	<0.05	<0.05	<0.05	<0.05	0.42	0.52	0.14	0.22	0.09	0.13
Bell14	31.1	32.3	<0.05	<0.05	13.0	12.9	0.06	0.20	6.04	6.05
Bell18	28.9	21.0	<0.05	<0.05	12.9	8.79	0.29	0.29	5.96	4.17
ANZECC		*8.0*		*0.2*		*11*		*13/24*		

Table A7 Concentration of trace elements through various filter sizes

Site and filter pore size	Fe (mg/L)	Mn (mg/L)	Al (mg/L)	Cu (µg/L)	Pb (µg/L)	Zn (µg/L)	Cd (µg/L)	Ni (µg/L)	As (µg/L)
Bell3 0.22µm	0.159	0.076	0.093	0.17	<0.05	4.05	<0.05	2.16	<0.05
Bell3 0.1 µm	0.187	0.076	0.104	0.26	<0.05	3.81	<0.05	2.48	0.09
Bell5 0.22µm	0.187	0.097	0.067	0.18	<0.05	6.28	<0.05	3.51	0.05
Bell5 0.1 µm	0.209	0.095	0.070	0.26	<0.05	5.94	<0.05	3.35	0.06
Bell14 0.22µm	1.072	0.219	0.293	0.11	<0.05	33.20	<0.05	13.3	0.08
Bell14 0.1 µm	1.07	0.212	0.191	0.15	<0.05	31.18	<0.05	12.8	0.07
BellAd 0.22 µm	40.2	0.666	34.6	0.93	<0.05	318.01	<0.05	97.9	0.39